Crack widths in HSC

A study into crack width prediction methods for slender HSC balconies

S.P. Hildering

Technische Universiteit Delft

TU Delft

Pieters BOUWTECHNIEK

Crack widths in HSC

A study into crack width prediction methods for slender HSC balconies

by

S.P. Hildering

to obtain the degree of Master of Science
at the Delft University of Technology.

To be defended publicly on Thursday January 11th, 2018 at 03:45 PM.

Student number:	4159438	
E-mail:	sven.hildering@gmail.com	
Graduation date:	Thursday January 11th, 2018	
Thesis committee:	Prof. dr. ir. D.A. Hordijk,	TU Delft, Chairman
	Ir. R. Van Nalta,	Pieters Bouwtechniek
	Ir. P. Lagendijk,	TU Delft
	Dr. ir. M. Lukovic,	TU Delft
	Dr. ir. M.A.N. Hendriks	TU Delft
	Ir. L.J.M. Houben	TU Delft

Cover image: Picture of the connection of a UHPFRC balcony engineered by Pieters Bouwtechniek Delft

TU Delft

Pieters BOUWTECHNIEK

Summary

Pieters Bouwtechniek Delft and Hi-Con Denmark cooperatively designed slender balconies in ultra-high performance fibre reinforced concrete (UHPFRC). For a variety of reasons other engineering firms tend to recreate these slender balconies in high strength concrete (HSC). However, engineers from Hi-Con and Pieters Bouwtechniek have their doubts on the validity of these reproductions in terms of cracking behaviour. This doubt is initiated by the high slenderness of the balconies, the big concrete cover for HSC and the difference in material characteristics which combined might lead to unforeseen cracking behaviour. This doubt results in the research question *'To which extent gives the analytical Eurocode 2 crack width prediction method an insight in the cracking behaviour of slender high strength concrete cantilevering balconies?'*

The research is step wisely conducted starting with a simple fully clamped cantilevering slab. For this slab the cross sectional height, reinforcement diameter and reinforcement spacing are varied to investigate their influence on analytical crack width predictions. First for all variants an analytical design and analysis process is executed, followed by a numerical analysis with DIANA FEA and a comparison of the results. The most important observation from this set of balcony slabs is that for a cross sectional height of 120 mm or smaller reinforcement bars are located outside the effective area. In the crack width prediction method proposed by article 7.3.4 in Eurocode 2 crack widths are predicted with an effective area b*$h_{c,eff}$. In case reinforcement is located outside this area, the hidden tensile member is unreinforced and the reliability of the method becomes unsure. Furthermore, a big discrepancy between the predictions of the different analytical models is observed, indicating an unreliability of these methods.

The fully clamped balcony is transformed towards a balcony with an in-plane ridge to assess the influence of a geometric disturbance on the analytical crack width prediction. The balcony is analytically designed according to rules and legislations from Eurocode 2 and numerically analysed with DIANA FEA. From the numerical analysis significantly bigger crack widths emerged compared to the analytical analysis, which were induced by peak stress concentrations resulting from the geometric disturbance. These peak stress concentrations are analytically not taken into account, resulting in the difference between the analytical and numerical analysis.

The last step is designing a Hi-Con shaped balcony with an out-of-plane ridge to find out whether a reproduction in HSC obeys the rules and legislations prescribed by Eurocode 2 and whether this actually leads to a structurally sound design in terms of cracking and deflection. Moreover, this balcony design is used to verify observations from the balcony with an in-plane ridge. It is observed that in light of detailing rules it appeared impossible to create an identical reproduction, but the concept could be reproduced in a less slender way. Furthermore, once more the analytical design results are compared with numerically obtained results. From this comparison it was observed that because the top of the slab is now kept constant, no peak stress concentrations occur and analytically predicted crack widths are bigger. In the ridge peak stress concentrations do occur. However, it has been found that because the ridge is less slender compared to the in-plane ridge and has a smaller concrete cover the effects are less pronounced and numerical crack widths remain limited.

When summarizing, it appears that specific care should be taken when analytically predicting crack widths in slender balconies because it might appear that the reinforcement is not located in the effective area. Furthermore, the more slender the structures become, the bigger the influence of a geometric disturbance can be, increasing the risk of an underestimation of the occurring crack widths because peak stress concentrations are analytically not accounted for.

For future research it is advised to investigate the influence of the reinforcement located outside the effective area on the reliability of analytical predictions of crack widths. In addition, the emergence of the discrepancy between the analytical methods is interesting to examine since it provides information on which method is suitable for which case. Furthermore, the ultimate capacity of the reproduced balcony should be analysed to assess the moment of failure and the failure mode. To finalize it is recommended to conduct laboratory testing for verification of the numerical models.

Preface

Dear reader,

I feel proud to present to you my thesis report as a partial fulfilment of the requirements to obtain the degree of Master of Science in Civil Engineering at the Delft University of Technology.

Within this report a twofold research product is presented. Pieters Bouwtechniek Delft and Hi-Con Denmark cooperatively designed balconies in ultra-high performance fibre reinforced concrete, which obtained a proof of concept by extensive research. Nowadays their balconies become more and more commonly applied. However, they have noticed a trend towards similarly shaped balconies executed in high strength concrete, about which they doubt the integrity in terms of cracking behaviour. The main part of this thesis aims to find out to which extent crack width prediction methods give an insight in the cracking behaviour of slender high strength concrete cantilevering balconies.

Prior to the research into the cracking behaviour of these balconies, a study, in cooperation with Stufib, into the connection and design of prefab concrete balconies has been conducted. This study has led to a report containing points of attention, tools and methods for the design and execution process of a prefabricated concrete balcony. The aim is that Stufib can eventually use this report as the backbone of an actual Stufib publication when the required modifications are appended. The report is called *Bevestigen van prefab betonnen balkons* and is separately attached to this report.

Besides the regular feelings induced by working on a thesis, a lot has happened the past year. While reflecting on this period the only remaining feeling is extreme gratitude towards everyone who provided me with the strength I needed and supported me in any possible way. Nonetheless, I would like to express my gratitude in particular to a number of people. For starters my graduation committee, Dick Hordijk, Rogier van Nalta, Paul Lagendijk, Mladena Lukovic and Max Hendriks. I would like to express my thankfulness for their guidance, advice, commentary and assistance whenever I was in need. Furthermore I would like to thank Chantal Frissen for providing me with support regarding DIANA FEA. I am very thankful for the opportunity Pieters Bouwtechniek Delft has offered me. I have had a very pleasant time working in their office. In addition to that I would like to thank all colleagues at Pieters Bouwtechniek Delft for always being interested in what I was working on and their willingness to assist when I asked for it. To finalize, I would like to express my sincerest gratitude towards my family and friends for listening to me and supporting me unconditionally.

I wish you a pleasant read.

S.P. (Sven) Hildering
Delft, January 2018

Outline of the report

The core of this report is subdivided in five parts: I, II, III, IV and V.

In **part I**, Introduction, the project initiation is explained and theoretically substantiated by assessing material characteristics and behaviour. Combining the origin of the project with the theoretical substantiation a main research question accompanied by a set of sub-questions is formulated. Part I is finalized with a general and coarse description of the method of approach for this research.

Part II, simple cantilever slab, starts off with a more explicit method of approach specifically for part II, followed by the development of a Maple TA script for making iterative design and check executions of a fully clamped cantilevering slab more easy. The script is verified with results from Technsoft Liggers in chapter 7 followed by an overview of the build up of finite element models in DIANA FEA. In the last chapter of part II, chapter 9, the analytical results from the script are compared to the numerically obtained results from the models in DIANA FEA.

Part III introduces a geometrical disturbance in the slab from part II, resulting in a balcony with an in-plane ridge. Part III starts off with a more specific method of approach followed by chapter 11 in which the process around designing and checking the balcony with an in-plane ridge is treated. Again a DIANA FEA model is developed, which is discussed in chapter 12, and the analytical and numerical results are compared in the sub-sequential chapter. **Part IV** has the same structure as part III, but a more sophisticated balcony design is assessed.

The core of this report is finalized with **Part V** in which all results are merged into conclusions and recommendations. In chapter 18 first a concluding text is written per part before summarizing it all by answering the main and sub- research questions. Part V ends with recommendations for future research on this topic.

As mentioned before a design and check script is developed in part II. Step wisely this script is converted to a script suitable for part III and IV. In part II the origin of the script is described where in part III and IV only the specific developments and the thoughts behind it are treated to prevent duplicate information.

The report *Bevestigen van prefab betonnen balkons*, elaborating on points of attention, tips and tricks for the design, connection and construction of a concrete prefab balcony has been attached as a separate report. That report has been developed as part of this total research. The idea behind it is explained in the flow scheme on the next page (figure 1).

In case a reference to a Eurocode is made, the following edition of the document is meant:

Code	Name	Citation in bibliography
Eurocode 0	NEN-EN 1990+A1+A1/C2	[20]
	NEN-EN 1990+A1+A1/C2 NB	[21]
Eurocode 1	NEN-EN 1991-1-1+C1	[22]
	NEN-EN 1991-1-1+C1 NB	[23]
Eurocode 2	NEN-EN 1992-1-1+C2	[24]
	NEN-EN 1992-1-1+C2 NB	[25]

During this research several software programs are utilized. For DIANA FEA release 10.1 is employed. The scripts are developed in Maple TA 2016.2 and the verification is performed with Technosoft Liggers V6.24d.

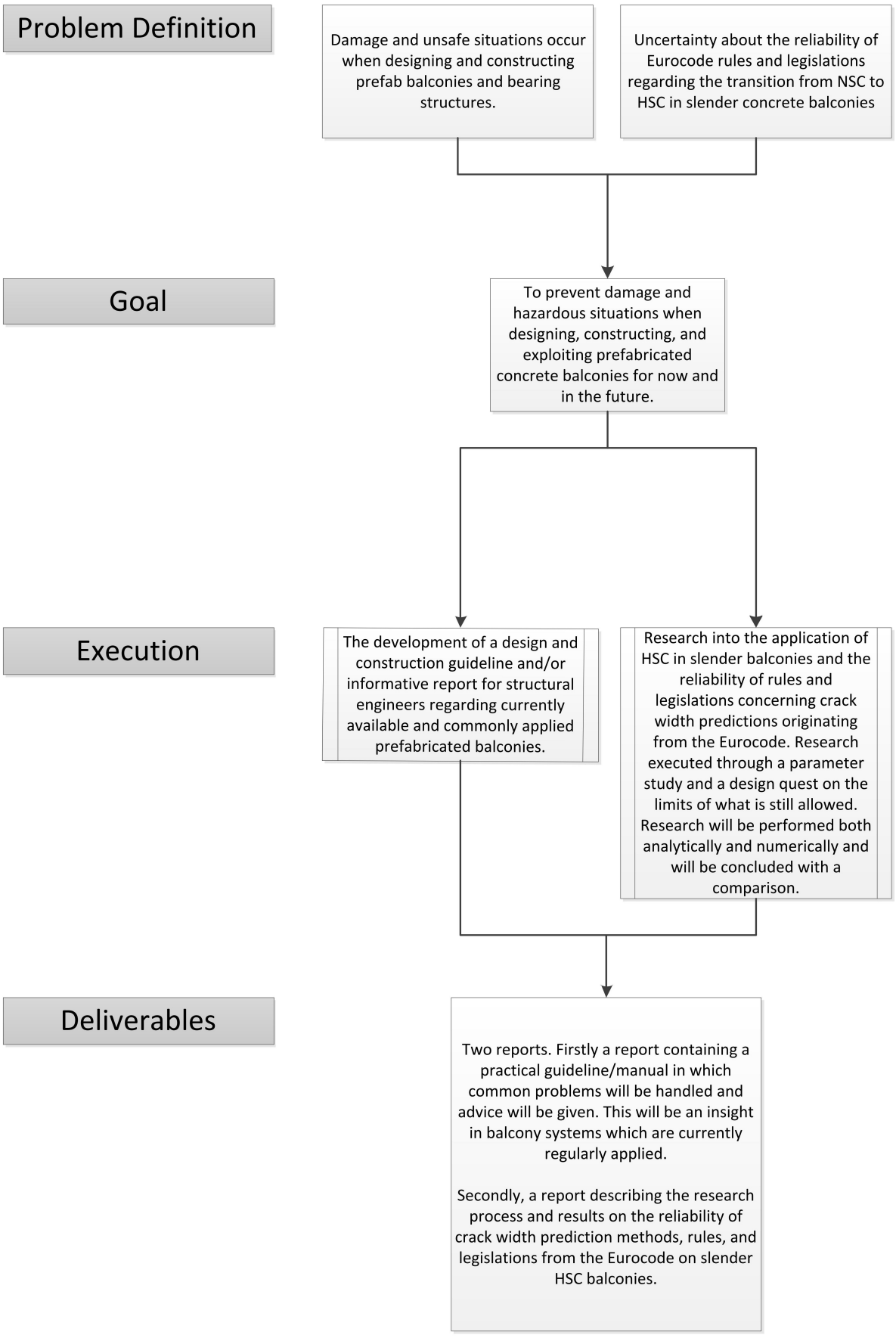

Figure 1: General overview describing the problem definition, goal, execution, and deliverables for this report and *Bevestigen van prefab betonnen balkons* together as the total product for this master's thesis.

Contents

List of Figures

List of Tables

I

Introduction

1 Initiation

In collaboration with Hi-Con, Pieters Bouwtechniek Delft designs slender balconies in ultra-high performance fibre reinforced concrete, like in figure 1.1. For a variety of reasons other engineering firms tend to recreate these slender balconies in high strength concrete.

Figure 1.1: Balcony executed in ultra high performance fibre reinforced concrete, designed by Pieters Bouwtechniek.

Engineers from both Hi-Con and Pieters Bouwtechniek Delft have their doubts on the validity of these 'copied' balcony designs. The hypothesis is that due to the relatively high slenderness and differences in material characteristics, methods proposed by Eurocode 2 do not correctly predict cracking behaviour. In case the hypothesis is correct, the following problems might occur:

- Unforeseen crack widths could lead to a reduced durability of the element, possibly leading to future brittle failure.
- Potentially big crack widths reduce cross-sectional stiffness, negatively influencing the deformation under the loading and the dynamic behaviour of the balcony.
- Big crack widths are undesirable in terms of aesthetics.

The substantiation of this hypothesis finds its origin in the difference in material characteristics, fracture mechanics, strain behaviour and durability of the concrete. All of these matters will be further elaborated in chapter 2.

2

Material characteristics & behaviour

For being able to theoretically substantiate the hypothesis on which this research is based, an understanding of material behaviour is of importance. This chapter will first introduce some differences between the materials normal strength concrete (NSC), high strength concrete (HSC), and ultra high performance fibre reinforced concrete (UHPFRC) before going more into depth on the fracture mechanics, durability and strain behaviour.

2.1. Material characteristics

Concrete basically consists of a mixture of fine and coarse aggregates bound together by hardened cement, often combined with reinforcement. By changing the composition of the concrete mixture, in terms of adding even finer aggregates and admixtures, the properties of the concrete over time can be adjusted. For example the higher concrete grades (≥ HSC) usually possess a more homogeneous structure with a lower porosity and permeability because of the properties of its constituents (more fine) [18], see figure 2.1.

Due to a higher homogeneity; strength, stiffness, and durability increase. The counterpart of a higher grade is a lower water/cement-factor and more fine particles, resulting in a decreased workability. However, this workability issue can be overcome with the addition of a (super)plasticizer, resulting in a concrete mixture with a higher final grade.

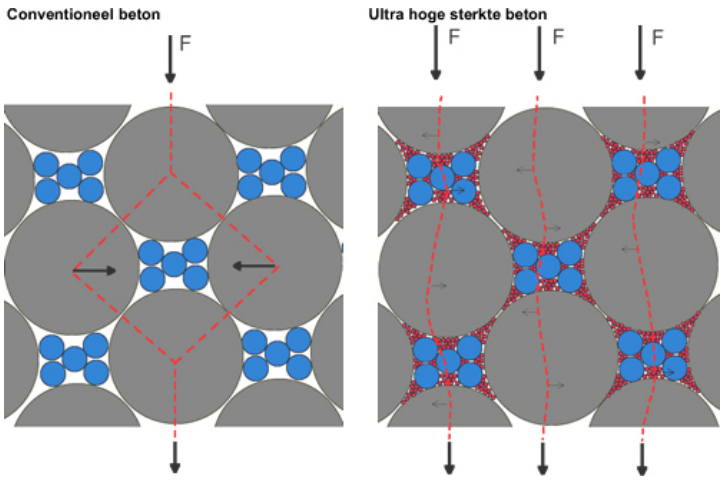

Figure 2.1: Mechanics of NSC and HSC, related to density and homogeneity of concrete mixture, source: [9].

There are a lot of different concrete types, which, for this research, are subdivided in the categories presented in table 2.1. Within these categories, variations are possible by combining materials. Relevant for this research is the combination of ultra high strength concrete and (stainless) steel fibres. When adding stainless steel

	Concrete class	wcf
Normal strength concrete	≤ C50/60	≥ 0,40
High strength concrete	≤ C90/105	0,30-0,35
Ultra high strength concrete	> C90/105	0,12-0,30

Table 2.1: Overview of general concrete types.

fibres to the ultra high strength concrete, the ultra high performance fibre reinforced concrete is obtained (UHPFRC). This concrete type has several advantages over NSC and HSC:

- Higher strength;
- Higher stiffness;
- Higher ductility;
- Lower permeability and porosity and thus a higher durability;
- Finer crack pattern;
- Smaller crack width.

Nevertheless, UHPFRC has its disadvantages as well, mainly in the field of the application process. Whereas NSC and HSC are covered in Eurocode 2, about which consensus in the building industry has been achieved, UHPFRC is not. This might be a motivation for engineering firms to apply HSC instead of UHPFRC.

2.2. Fracture mechanics

Another difference between concrete types relevant for this research is the difference in fracture mechanics. Fracture mechanics studies the initiation and propagation of cracks in concrete in terms of energy requirement. For NSC, the required energy to propagate a crack is influenced by several parameters, e.g. aggregate size, water/cement-factor and the age of concrete. The same holds for higher concrete grades, however, the influence of the aggregate type seems to affect the fracture energy more than the aggregate size [18]. According to Hansen et al. [16], that phenomenon is initiated by the change of the path of the crack.

Interfacial Transition Zone

The interfactial transition zone (ITZ) is the interface between the cement matrix and the aggregate. This interface has a different microstructure than the actual cement matrix because during casting a water/cement-ratio gradient develops near aggregates [26].

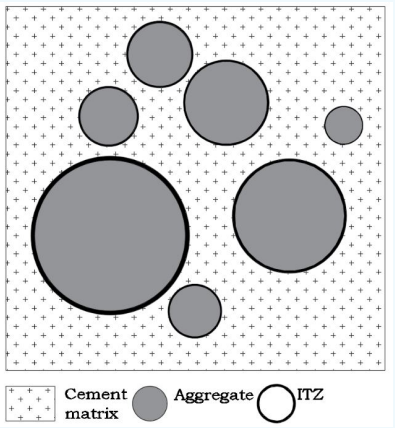

Figure 2.2: Schematization of ITZ.

The change of the crack path occurs because of a change in porosity of the concrete and a change of the properties of the aggregates. A schematization of the flow of forces through concrete is depicted in figure 2.1. It is clear that the splitting forces reduce for a decreasing porosity, the forces are more gradually transferred between the elements within the concrete. Because higher concrete grades are produced with a lower water/cement-factor, the porosity is lower and a shift of the weakest link in the concrete takes place. Where in conventional concrete the interfacial transition zone (ITZ, see box and figure 2.2) is the weakest link, for HSC and higher grades the aggregates are.

Figure 2.3 gives an insight in how, from left to right, NSC, UHSC, and UHPFRC crack. In NSC, cracks follow the edges of the aggregates because the aggregates and the cement matrix are stronger than the ITZ. For HSC, because

of the decreased porosity and change of flow of forces, the aggregate becomes the weakest link, and cracks will go through it. Now, when adding steel fibres to the concrete mixture, these fibres cut off the paths of the cracks. Because the energy needed to elongate the fibre is higher than the required energy to crack the concrete surface on another place, the crack will not propagate and the final crack pattern of UHPFRC will be more fine than for NSC and (U)HSC. Since cracking of the concrete happens through a different mechanism, the application of a crack width prediction method based on conventional concrete is doubtful.

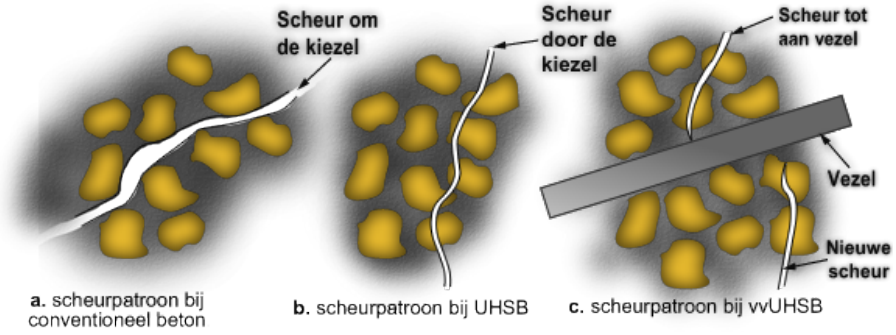

Figure 2.3: Cracking through NSC, UHSC and UHPFRC, source: [9].

2.3. Durability

For durability reasons concrete balconies in The Netherlands designed according to Eurocode 2, possessing governing environmental class XD3, have to have a concrete cover at the top side of the balcony slab of at least 30 mm, stated in chapter 4 in Eurocode 2. The purpose of this cover is to protect the concrete from environmental influences. The most important influence is the risk of de-icing salts which the user of the balcony might apply to reduce or prevent ice forming on the balcony surface. The concrete cover prevents the salts from entering the concrete through existing cracks and reaching the reinforcement bars. When the salt reaches the reinforcement, it degenerates the passivation layer and induces corrosion. During the corrosion process the cross-sectional area of the reinforcement bar reduces which can potentially lead to a brittle failure of the balcony.

From research executed by Hi-Con and Pieters Bouwtechniek it appeared that UHPFRC-elements lack the need of a high concrete cover due to the high density of the concrete and the fine crack pattern. Because the concrete cover may be smaller, the cross section and the reinforcement bars are more efficient, resulting in a higher capacity and/or less needed reinforcement. This issue will be handled in more detail in paragraph 2.4.

Besides the more beneficial concrete cover, higher grade concretes possess the ability of self-healing. They contain a larger amount of unbounded cement particles which are activated by moisture entering the concrete through the small cracks. The newly hydrated cement thus closes the cracks again up to a certain amount. The higher the concrete grade, the higher the amount of unbounded cement and thus the better the self-healing ability.

2.4. Stress and strain

As mentioned in paragraph 2.3, elements without fibre reinforcement need a higher concrete cover for durability reasons. This higher cover influences strains in the outer fibre of the element. In figure 2.4 three schematizations of concrete elements are depicted. They are all loaded under the same bending moment and the dimensions of the cross sections of the UHPFRC and the HSC elements are equal. It has been chosen to apply the same cross sections for these two grades since that is exactly what is pursued in practice with the remake of balconies. The NSC-cross section has been depicted to contemplate all concrete types in this visualization.

Easy to notice is that d, the distance between the outer compressive fibre and the reinforcement, decreases with an increasing concrete cover. Subsequently the height of the compression zone x_e and the internal lever arm z decrease. The bending moment is balanced by the normal forces in the concrete and the reinforcing

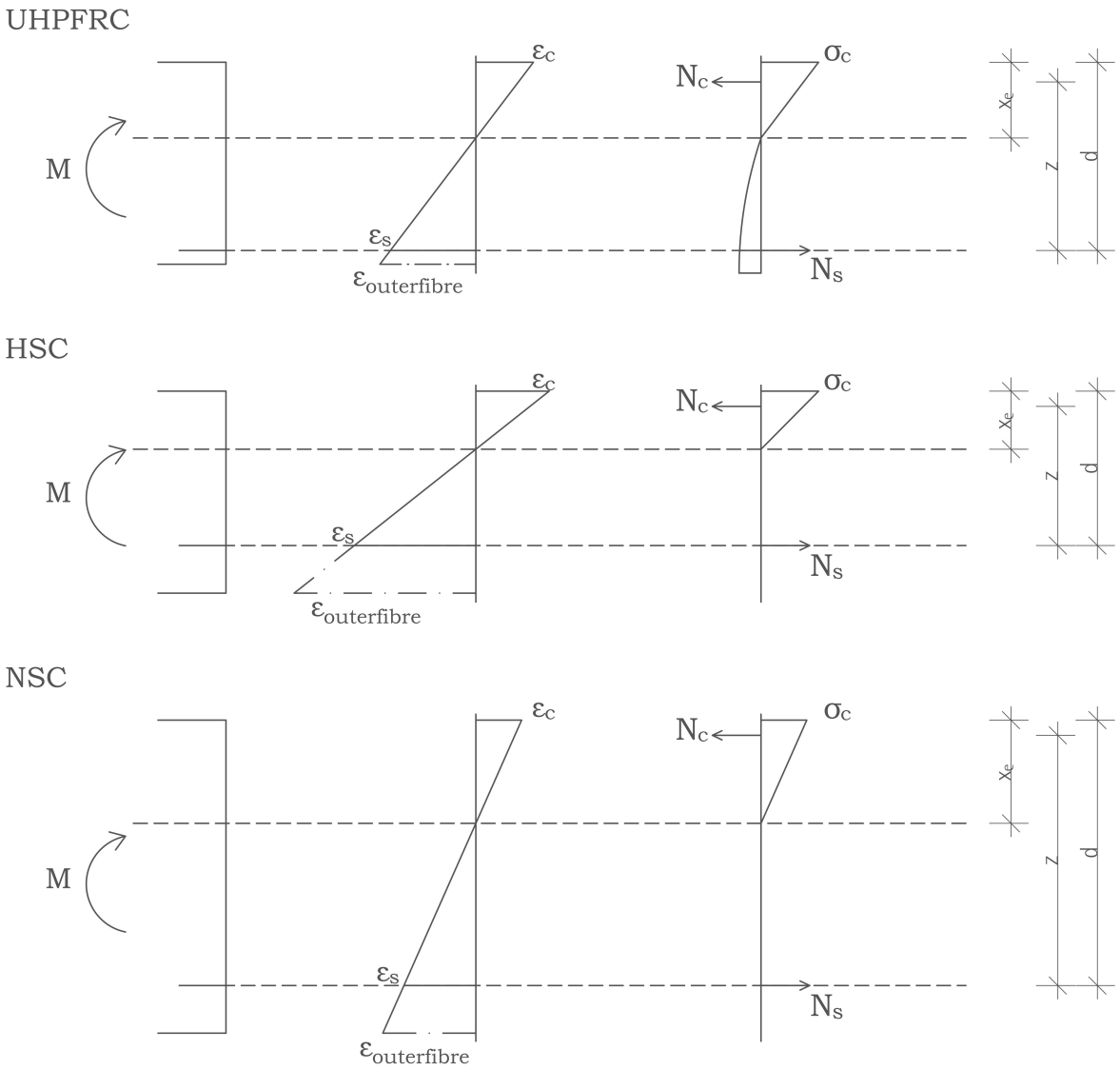

Figure 2.4: Strain and Stress diagrams for different concrete elements loaded under equal bending moment.

steel in the following manner:

$$M = N_s * z = N_c * z \quad [1] \tag{2.1}$$

When comparing the UHPFRC and the HSC-elements; with a decreasing internal lever arm for the HSC-element the normal forces should increase to reach an equilibrium with the bending moment. The normal force is the product of the area, the strain and the modulus of elasticity. When transitioning from UHPFRC to HSC, the decreases of the internal lever arm and the modulus of elasticity of the concrete should result in an (absolute) bigger strain for both the tension and compression zone to reach equilibrium.

The increased strain in the tension zone, and thus in the reinforcing steel, potentially initiates wider and more cracks. Easiest solution seems to be increasing the amount of reinforcement, were it not for the fact that the cross sections of these slender balconies are relatively small and more reinforcement might not be possible. On the compressive side of the cross section; with increasing compressive stresses, the risk of concrete crushing and brittle failure increases as well.

[1] For the sake of simplification, tensile capacity of the UHPFRC is left out of consideration. When taken into account, it would emphasize the effect even more.

A last difference between UHPFRC and HSC is about brittleness. In the graph in figure 2.5 it has been visualized that the horizontal branch of the HSC stress-strain graphs are shorter, which indicates less ductility. The reason behind the increased brittleness is that the cement matrix tends to become less tough. This happens because initially formed micro cracks behave more unstable. The micro cracks grow rapidly into a macro crack which might initiate failure [18], [27]. One of the purposes of the fibres in UHPFRC is overcoming this brittleness and creating a ductile concrete product. Since HSC elements do not possess fibres, they most likely will behave brittle.

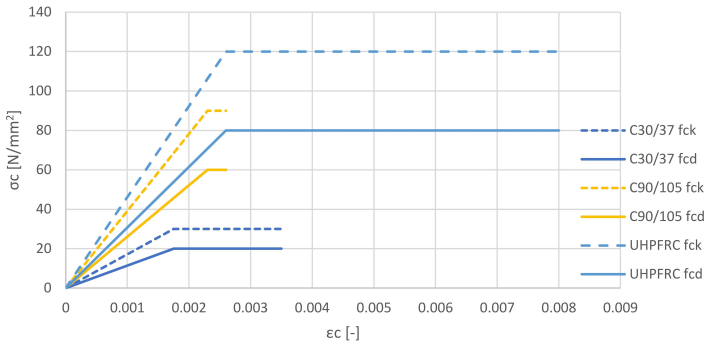

Figure 2.5: Stress-strain relationship for NSC, HSC and UHPFRC for either the characteristic compressive strength and the design compressive strength. The values of NSC and HSC are based on the Eurocode 2 material characteristics for a bi-linear stress-strain relationship.

2.5. Summary

In practice the balconies in HSC are applied and approved according to Eurocode 2. However, differences in material properties, fracture mechanics, durability, and stress and strain behaviour between all concrete types, and specifically between HSC and UHPFRC, feed the idea that crack width prediction methods in Eurocode 2 might underestimate the actual crack widths. Unforeseen big crack widths reduce durability and increase the risk of troubles regarding the serviceability limit state.

3

Research questions

In addition to the theoretical substantiation of the previous paragraphs, an article published by DIANA FEA,[31], states that 'checks in design codes are mainly based on the forces and bending moments in the cross-section of the structure, and are unreliable for relatively thin plate-shaped structures'. Furthermore in [10] it is stated that with increasing experimental crack widths it appeared that the accuracy of the model proposed by article 7.3.4 in Eurocode 2 became less and less accurate. Combining these statements with the substantiation, the following main research question is drawn up:

To which extent gives the analytical Eurocode 2 crack width prediction method an insight in the cracking behaviour of slender high strength concrete cantilevering balconies?

To systematically work towards a conclusion on this research question four sub-questions have been formulated:

- What is the influence of slab height, reinforcement diameter and reinforcement spacing on the reliability of analytical crack width predictions in slender high strength concrete cantilevering balconies?
- What is the influence of geometrical disturbances on the reliability of analytical crack width predictions in slender high strength concrete cantilevering balconies?
- Is it analytically possible to recreate a durable Hi-Con balcony in high strength concrete while applying currently prescribed methods, taking into account all rules and legislations from Eurocode 2?
- Is it possible to recreate a durable Hi-Con balcony in high strength concrete while obeying all rules and legislations from Eurocode 2?

4

General research method

This chapter describes in a coarse way the method of approach to find answers on the research questions. A more elaborate and specific method of approach is described at the start of parts II, III and IV of this report.

4.1. General approach

To find out whether the crack width prediction method in article 7.3.4 of Eurocode 2 does provide a proper insight in cracking behaviour of slender balconies in HSC it has been chosen to work stepwisely from a coarse balcony design, figure 4.1, up to a sophisticated Hi-Con balcony design, figure 4.3. For starters a script will be developed which allows the user to easily alter geometric properties of a simple fully clamped balcony (figure 4.1) and perform design checks on these balconies. The results then will be compared with the results of structural non-linear analysis executed with DIANA FEA and might lead to a conclusion on the influence of slab height, reinforcement diameter and reinforcement spacing on the Eurocode 2 crack width predictions.

The first script will be transformed towards a script for analytically designing and checking a cantilevering balcony with an in-plane ridge, as in figure 4.2, to discover the influence of geometric cross sectional disturbances. The research will be finalized by redesigning a Hi-Con shaped balcony in C90/105 to find out whether this is even possible following rules and legislations and determine whether this results in an acceptable design in terms of durability and serviceability. A schematization of this last variant is presented in figure 4.3.

4.2. Balcony geometries

The first coarse balcony design, depicted in figure 4.1, is a simple cantilevering fully clamped slab loaded on its own weight and a point load of variable magnitude. The slab has a length of 1575 mm and a width of 1300 mm. It has been decided to keep the length and width constant for the different designs to remain compatible with already existing formwork from Hi-Con for potential future laboratory testing.

In two steps the simple cantilevering slab will be transformed to a more realistic balcony design. The first step is adding a ridge to create a local support, resulting in the balcony schematized in figure 4.2. In the analysis now the disturbed regions play a role in crack width predictions.

The last step is converting the ridged balcony to the most sophisticated design, see figure 4.3. The idea behind this design originates from engineering work by Hi-Con and Pieters Bouwtechniek Delft. The slender balcony is supported by a higher ridge, which results in a complex flow of forces and possibly undesirable behaviour and big crack widths.

4.3. Analysis

As mentioned in the General approach paragraph, the first analysis will start with the development of a script. This script for the simple fully clamped balcony will be used as a basis and will be stepwisely converted to a more sophisticated script that supports the second and third balcony design as well. Within the script four crack width prediction methods are incorporated for the sake of verification. After the manual designing and

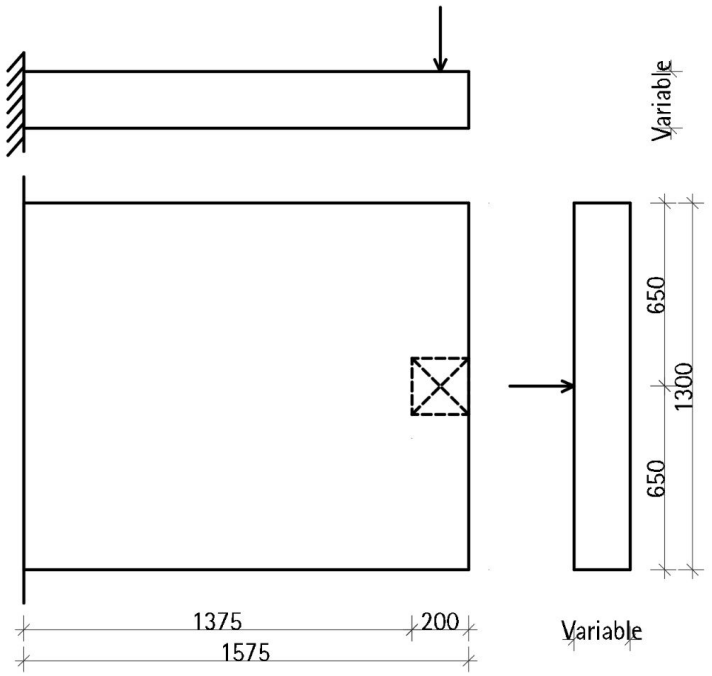

Figure 4.1: Schematic drawing of simple fully clamped cantilever balcony.

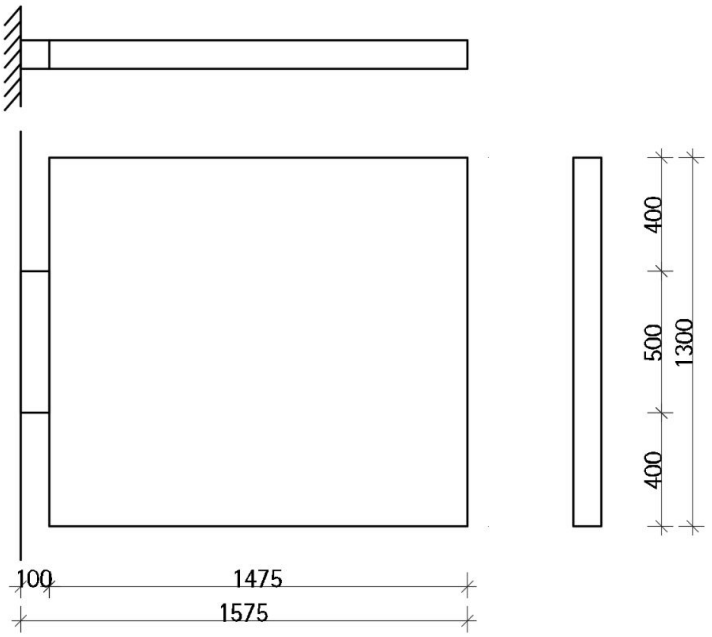

Figure 4.2: Schematic drawing of cantilever balcony with ridge connection.

checking process, the balconies will be modelled in DIANA FEA and a structural non-linear analysis will be executed to study whether the crack widths predicted by the several methods are realistic and what the influences of cross sectional height, reinforcement diameter and reinforcement spacing are on the reliability of the crack width predictions.

By developing the script towards a compatible tool for designing and checking the more realistic balcony designs, it should become possible to find an answer on the sub-questions about disturbed regions and the possibility of designing a slender balcony in HSC.

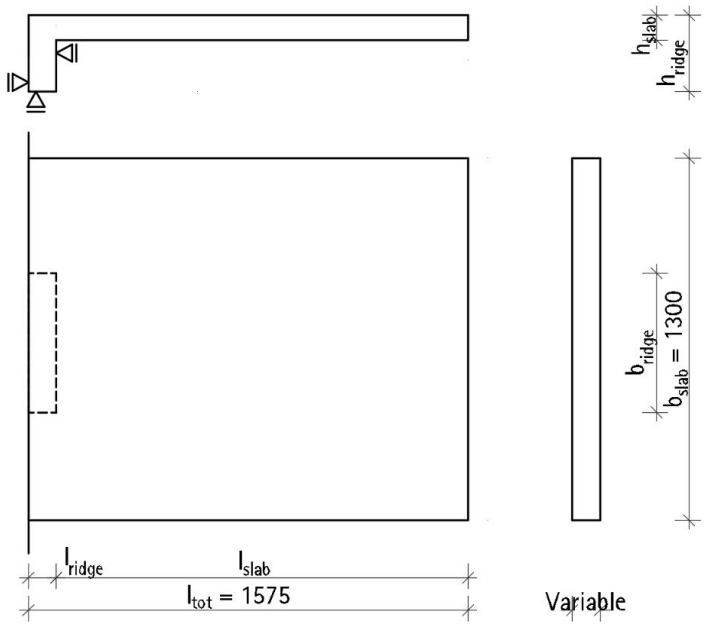

Figure 4.3: Schematic drawing of Hi-Con designed cantilever balcony.

4.4. Crack width models

In the script for the first simple balcony design, crack widths will be predicted according to Eurocode 2, the American building code ACI 318, the Egyptian building code and the method described in *Concrete Structures under Imposed Thermal and Shrinkage Deformations - Theory and Practice* [33]. Eurocode 2 presents two methods, article 7.3.3 and 7.3.4. For this research only article 7.3.4 will be taken into account since article 7.3.3 is a crack width control method based on prefabricated tables containing experimentally obtained values. For these values a lot of assumptions are made, reducing the reliability of the final outcome of the crack width analysis for a different case than in the experiments [2].

II

Fully clamped cantilever slab

5

Method

For a first indication of the influence of several parameters on the Eurocode 2 crack width prediction methods for slender, high strength concrete balconies, a parameter sensitivity analysis will be performed. A simple fully clamped cantilevering slab, figure 5.1, will be examined. The results should lead to a conclusion on the first sub-question. The analysis will be executed in an iterative way by varying three parameters:

- The thickness of the slab will be varied from 200 mm to 80 mm in steps of 20 mm, resulting in seven different cross sectional heights. The lower boundary is dictated by the definition of a plate stated in article 9.3 in Eurocode 2.
- Three reinforcement diameters regarding the main longitudinal reinforcement will be applied; 12, 10, and 8 mm.
- Five reinforcement spacings regarding the main longitudinal reinforcement will be considered; 150, 120, 100, 80, and 60 mm.

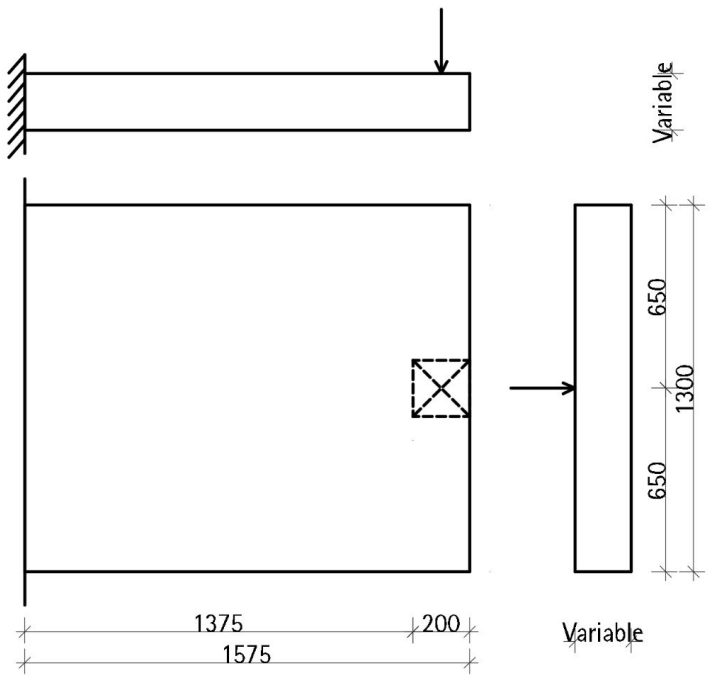

Figure 5.1: Schematic drawing of simple fully clamped cantilever balcony.

Varying these three parameters leads to a set of 105 variants (7x3x5). Each of these 105 variants will be loaded under its own weight and a point load at 1475 mm from the support. The magnitude of this point load will

be determined by the demand that the moment following from the characteristic load combination has to exceed the cracking moment with 10%. The 10% value has been chosen for three reasons. Firstly, to be able to compare results a common denominator is required which has been found in a predefined exceedance of the cracking moment. Secondly, it guarantees that every member is cracked. And thirdly, it limits the variants where this point load will lead to an exceedance of the bending moment resistance in the fundamental load combination.

For each of the 105 variants, four crack width prediction models will be applied. The method described in article 7.3.4 of Eurocode 2, the American building code ACI 318 method, the method described in *Concrete structures under Imposed Thermal and Shrinkage Deformation* [33] and a method described in the Egyptian Code. It has been chosen to include the Egyptian code to broaden the range of methods with a less common one.

At the point where all 105 variants are dimensioned and loaded and all crack widths are predicted, the variants will be modelled in DIANA FEA. The crack width predictions produced by DIANA FEA will be compared to the analytical results and a conclusion will be drawn on the influence of element height, reinforcement diameter, and reinforcement spacing on the reliability of analytical crack width prediction for slender slabs in C90/105 concrete.

For both the numerical Eurocode 2 crack width prediction method as well as the method DIANA FEA applies, background information is presented in appendix A

6

Development of Script

This chapter elaborates on the emergence of the script starting with the structural starting points, followed by the executed checks and the crack width prediction methods. The complete script can be found in appendix B. It is advised to read this chapter accompanied by the script.

6.1. Structural starting points

The first sections in the script allow the user to alter geometric conditions, material properties of concrete and reinforcement, loads, reinforcement configuration and concrete cover. It has been decided to keep the length and width of the slab constant for compatibility reasons as has been explained in paragraph 4.2. For the sake of this research the concrete grade has been set on C90/105 to approach the limit of Eurocode 2 with a maximum grain size of 16 mm. The material characteristics follow from table 3.1 in Eurocode 2. The concrete cover has been determined according to chapter 4 of Eurocode 2 and has been set on 30 mm based on environmental class XD3 for a prefabricated element. XD3 is governing because of the risk of the application of de-icing salts on a balcony surface. The environmental class leads to a maximum allowable crack width of 0.2 mm for the top surface. The steel grade for the reinforcement is chosen to be B500b.

The consequence class and the design working life are determined according to Eurocode 0 and are based on a balcony attached to a normal house. The building category followed from Eurocode 1.

Consequence class:	CC2
Design working life:	50 years
Building category:	A - Balcony

From Eurocode 0 the load combinations could be determined for the Ultimate Limit State, resulting in the combinations presented in table 6.1. The Serviceability Limit State load combination are displayed in table 6.2.

Permanent		Leading variable action	Accompanying variable actions	
Unfavourable	Favourable		Main	Others
1,35 $G_{k,j,sup}$	0,9 $G_{k,inf}$		1,5 $\psi_{0,1}$ $Q_{k,1}$	1,5 $\psi_{0,i}$ $Q_{k,i}$ (i>1)
1,2 $G_{k,j,sup}$	0,9 $G_{k,inf}$	1,5 $Q_{k,1}$		1,5 $\psi_{0,i}$ $Q_{k,i}$ (i>1)

Table 6.1: Equations 6.10a and 6.10b from Eurocode 0 and the Dutch national annex.

6.2. Cracking moment

The cracking moment is determined through the use of the mean tensile strength of the concrete. Since the balcony is loaded under pure bending, the cracking moment is determined with f_{ctm} instead of $f_{ctm,fl}$ [6].

$$M_{cr} = f_{ctm} * W_c = f_{ctm} * \frac{1}{6} bh^2 \tag{6.1}$$

Combination	Permanent		Accompanying variable actions	
	Unfavourable	Favourable	Main	Other
Characteristic	$G_{k,j,sup}$	$G_{k,j,inf}$	$Q_{k,1}$	$\psi_{0,i}Q_{k,i}$
Frequent	$G_{k,j,sup}$	$G_{k,j,inf}$	$\psi_{1,1}$ $Q_{k,1}$	$\psi_{2,i}Q_{k,i}$
Quasi-Static	$G_{k,j,sup}$	$G_{k,j,inf}$	$\psi_{2,1}$ $Q_{k,1}$	$\psi_{2,i}Q_{k,i}$

Table 6.2: Equations 6.14a up to 6.14b from Eurocode 0 and the Dutch national annex.

6.3. Bending moment resistance

For each variant the bending moment resistance is determined through the ultimate height of the concrete compressive zone and the internal lever arm. The internal lever arm is obtained by subtracting βx_u from d, so the first step is to determine x_u. The height of the ultimate compressive zone is determined by the demand that the steel has to yield when the concrete reaches its ultimate strain ε_{cu3}. With the use of the image on the right in figure 6.1, the following equations lead to x_u.

$$N_s = N_c \tag{6.2}$$

$$N_s = A_s * f_{yd} \tag{6.3}$$

$$N_c = \alpha * x_u * b * f_{cd} \quad with \quad \alpha = \frac{1}{2}\frac{\varepsilon_{c3}}{\varepsilon_{cu3}} + \left(1 - \frac{\varepsilon_{c3}}{\varepsilon_{cu3}}\right) \tag{6.4}$$

$$\left(\frac{1}{2}\frac{\varepsilon_{c3}}{\varepsilon_{cu3}} + \left(1 - \frac{\varepsilon_{c3}}{\varepsilon_{cu3}}\right)\right) * xu * b * f_{cd} = A_s * f_{yd} \tag{6.5}$$

$$x_u = \frac{A_s * f_{yd}}{\left(\frac{1}{2}\frac{\varepsilon_{c3}}{\varepsilon_{cu3}} + \left(1 - \frac{\varepsilon_{c3}}{\varepsilon_{cu3}}\right)\right) * b * f_{cd}} \tag{6.6}$$

Within these calculations α is a shape factor describing the shape of the compressive zone as a ratio of a (fictitious) square compressive zone. For complete linear behaviour this factor would be 0.5 since the ultimate stress diagram is a triangle. For NSC α is 0.75 since ε_{cu3}=3.5‰and ε_{c3}=1.75‰, which results in a bilinear diagram with a kink halfway x_u. Now for HSC ε_{cu3}=2.6‰and ε_{c3}=2.3‰, resulting in $\alpha \approx 0.56$.

Since for C90/105 there is less ductile behaviour, the square top part of the ultimate stress graph is smaller and thus the value of β decreases. Whereas β equals 0.39 for NSC, for C90/105 this is reduced to 0.3373. This new β can be found by calculating the centre of gravity of the concrete compressive zone at its ultimate capacity. βx_u is determined in equation B.6 in appendix B.

When βx_u is known, the bending moment resistance can be found by multiplying the steel area with the design yield strenght and the internal lever arm. The complete method of determining the bending moment resistance can be found in appendix B.

$$M_{Rd} = A_s * f_{yd} * (d - \beta x_u) = N_s * z \tag{6.7}$$

6.4. Shear resistance

The script checks the shear resistance according to the requirements described in paragraph 6.2 in Eurocode 2. For starters, since this research covers slabs up to a height of 200 mm, shear reinforcement is not allowed according to article 9.3.2(1) in Eurocode 2. The complete method of determining the shear resistance can be found in the script in appendix B.

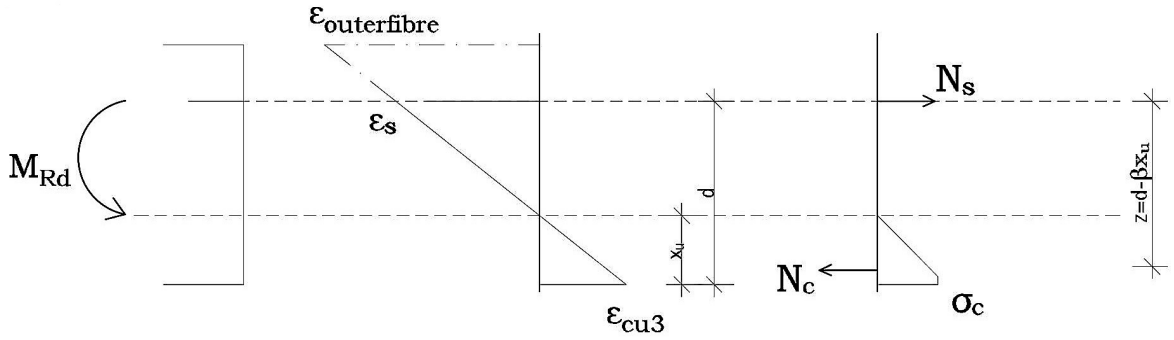

Figure 6.1: Determination of bending moment resistance.

6.5. Crack width models

The coming sections describe the analytical crack width prediction methods used in the script. Before these models are introduced a small introduction into the background of cracking behaviour is treated. For the models, first the method proposed in article 7.3.4 in Eurocode 2, which has the same background as the method described in the FIB Model Code [14], is described, followed by the method introduced in *Concrete Structures under Imposed Thermal and Shrinkage Deformations - Theory and Practice* [33]. To be able to compare results and broaden the perspective, also the methods from the American Building Standard ACI 318 and the less commonly known and applied Egyptian code are used.

Background of cracking

A concrete member loaded in bending is likely to crack at a certain moment. Cracking happens following several stages, depicted in figure 6.2. Following the graph, the first stage from M=0 to M=M_{cr} is the structural linear elastic stage at which the concrete is assumed to be uncracked. When the bending moment reaches a certain value M_{cr}, cracks start to occur. This phase is depicted by the pointy part in the graph and is called the crack formation stage.

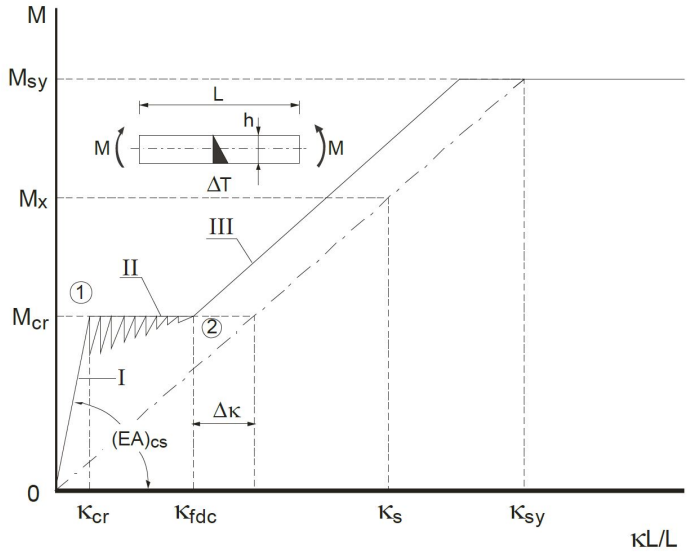

Figure 6.2: M-κ-diagram of a reinforced concrete member loaded in bending, source: [33].

During the crack formation stage, the crack pattern develops until there is no space left for new cracks. There is a limitation to the number of cracks formed in the crack formation stage because of an upper and lower boundary of the crack spacing. This phenomenon can be explained by the help of figure 6.3. Cracks are separated by a space with a lower boundary l_t and an upper boundary of $2l_t$. l_t is the transfer length and is mainly dictated by reinforcement properties. Figure 6.3 depicts stresses in the concrete and reinforcement steel at

the location of a crack. In the first image (a), it can be seen that at the location of a single crack the concrete stress drops to zero whereas the steel takes over and thus undergoes an increase in tensile stress. It can also be seen that the member needs a distance l_t to return to the pre-cracking stress distribution. The crack spacing can not become smaller than l_t because the concrete cannot reach its tensile capacity in less than a distance l_t and cannot become higher than $2\,l_t$ because the concrete will then already have reached its tensile capacity.

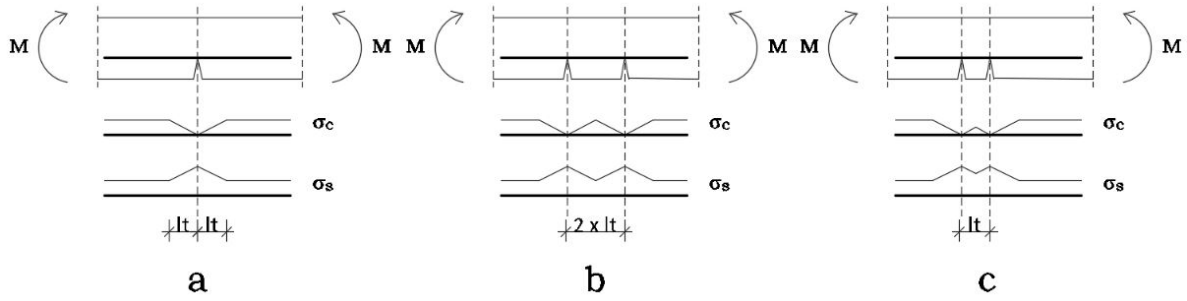

Figure 6.3: Stresses in concrete and reinforcement at the location of a crack.

The third stage is the stabilized cracking stage. In this stage all cracks are present, the only development of the cracks is the widening. This stage continues until the reinforcement yields or the concrete is crushed and the member fails. This research focuses on the stabilized cracking stage, thus with a loading exceeding M_{cr}.

Eurocode 2 and FIB Model Code

The Eurocode and Model Code method utilize the difference between the average steel strain and average concrete strain. To calculate the crack width, use is being made of a so called hidden tensile member around the reinforcing steel. This hidden tensile member is assumed to be an effective tensile stress area. The upper limit value of the crack width can be calculated by:

$$w_k = s_{r,max}(\varepsilon_{sm} - \varepsilon_{cm}) \tag{6.8}$$

where

$$s_{r,max} = k_3 c + k_1 k_2 k_4 \frac{\phi}{\rho_{p,eff}} \tag{6.9}$$

$$\varepsilon_{sm} - \varepsilon_{cm} = \frac{\sigma_s - k_t \frac{f_{ct,eff}}{\rho_{p,eff}}(1 + \alpha_e \rho_{p,eff})}{E_s} \geq 0.6 \frac{\sigma_s}{E_s} \tag{6.10}$$

In the equations the subscript eff relates to the dimensions of the hidden tensile member.

k_t is a factor depending on the duration of loading. For long term loading k_t equals 0.4 whereas for short term it equals 0.6. For this research, since it is pursued to remain compatible with future laboratory testing a factor of 0.6, short term loading, has been used. In case long term effects are assessed the decrease of k_t results in an increase in the steel strain difference and thus in the predicted crack width. This effect is induced by for example creep.

In appendix A a background assessment on the Eurocode 2 method is presented in which it is found that this method is based on two conservative assumptions, namely:

1. The crack width prediction is determined with the maximum crack spacing, resulting in an upper limit of the crack width;
2. It is assumed that the increase in steel strain after cracking is concentrated completely within an existing crack.

Concrete Structures under Imposed Thermal and Shrinkage Deformations

The advantage of this method, described in [33], is that crack width and crack spacing can be expressed as a function of the steel stress directly after cracking and the actual steel stress, which means the effective

height of the hidden tensile member does not have to be determined. The crack width can be found by firstly determining the average crack width in the crack formation stage.

$$w_{m0} = 2 * \left(\frac{0.4 * \phi}{f_{cm,cube} * E_s} * \left(\frac{\sigma_{cr}}{\rho_l} \right)^2 * \left(1 + \alpha_e \rho_l\right) \right)^{0.85} \tag{6.11}$$

The mean crack spacing in the stabilized cracking stage can be determined with the knowledge that the crack spacing is limited between l_t and $2l_t$.

$$l_t = 1.2 * w_{m0} * \frac{E_s}{\sigma_{s,cr}} \tag{6.12}$$

$$l_m = \frac{l_t + 2l_t}{2} = 1.8 * w_{m0} * \frac{E_s}{\sigma_{s,cr}} \tag{6.13}$$

In the stabilized cracking stage, the mean crack width can also be determined by the use of the strain difference:

$$w_{mv} = \frac{l_m}{E_s} * \left(\sigma_s - 0.5\sigma_{s,cr}\right) \tag{6.14}$$

Now, to check whether the crack width criterion is met, an upper limit value (95% fractile) of the occurring crack width should be determined. To make the transition from the mean value to an upper limit value, scatter of the cracks and the type of loading should be taken into account.

$$w_k = w_{mv} * \gamma_s * \gamma_\infty \tag{6.15}$$

For a fully developed crack pattern, the factor for scatter, γ_s, is 1.7, whereas for a not fully developed crack pattern γ_s=1.5. γ_∞ represents a factor for the loading type. For a short term instantaneous loading, this factor is 1.

$$w_k = \gamma_s * w_{mv} = 1.7 * w_{mv} \tag{6.16}$$

Egyptian Code

The Egyptian building code states that the crack width can be determined by multiplying the average stabilized crack spacing (S_{rm}), the mean steel strain induced by the loading of the member (ε_{sm}), and a coefficient to convert the mean average crack width to an upper limit value.

β_1 is a value accounting for the bond properties between the concrete and the reinforcing steel and is assumed to be 0.8 for bars with a profile. β_2 takes loading duration into account and is 1 for non-repetitive short term loading. β is a factor determined by the factor that induces the cracking. For cracking induced by bending β equals 1.7.

$$\varepsilon_{sm} = \frac{\sigma_s}{E_s} * \left(1 - \beta_1 \beta_2 \left(\frac{\sigma_{s,cr}}{\sigma_s} \right)^2 \right) \tag{6.17}$$

$$S_{rm} = 50 + \frac{0.25 k_1 k_2 \phi}{\rho_{eff}} \tag{6.18}$$

$$W_k = \beta * \varepsilon_{sm} S_{rm} \tag{6.19}$$

American standard ACI 318

The ACI 318 does make use of an effective area but takes into account the specific location of the reinforcement by use of the factor β. A_0 is according to Allam et al. [1], the area of concrete surrounding each reinforcing bar. A_0 is determined with the help of parameter A_e and d_c. d_c is the distance between the centroid of the reinforcement bars to the outer tensile fibre and A_e then is somewhat similar to the effective area as it's known from the Eurocode.

$$\beta = \frac{h - x_u}{d - x_u} \tag{6.20}$$

$$d_c = h - d \tag{6.21}$$

$$A_e = 2 * d_c * b \tag{6.22}$$

$$A_0 = \frac{A_e}{n_b} \tag{6.23}$$

$$w_{max} = 0.011 * \beta * \sigma_s * (d_c * A_0)^{1/3} * 10^{-3} \tag{6.24}$$

7

Verification of script

The results from the script discussed in the previous chapter have been compared with results generated with Technosoft Liggers V6 to verify the script's ability to predict crack widths according to article 7.3.4 of Eurocode 2. This has been exectued for several variants. In this report only the verification results for a slab with a height of 160 mm, reinforcement ⌀12-80 and a point load with a magnitude of 16.5 kN are presented. In this chapter only snapshots of the full output of the script and Technosoft liggers are present, the full output can be found in appendix C.

Figure 7.1 gives the outcome of the script for the just described balcony slab. According to the Eurocode 2 method the predicted crack width is 0.041 mm, which is confirmed by the output of Technosoft Liggers in figure 7.2. Technosoft uses the same crack width prediction method thus it can be concluded that the developed script predicts crack widths correctly according to article 7.3.4 in Eurocode 2. Also bending moment and shear force resistances are compared and do correspond. The full script and Technosoft output can be found in appendix C.

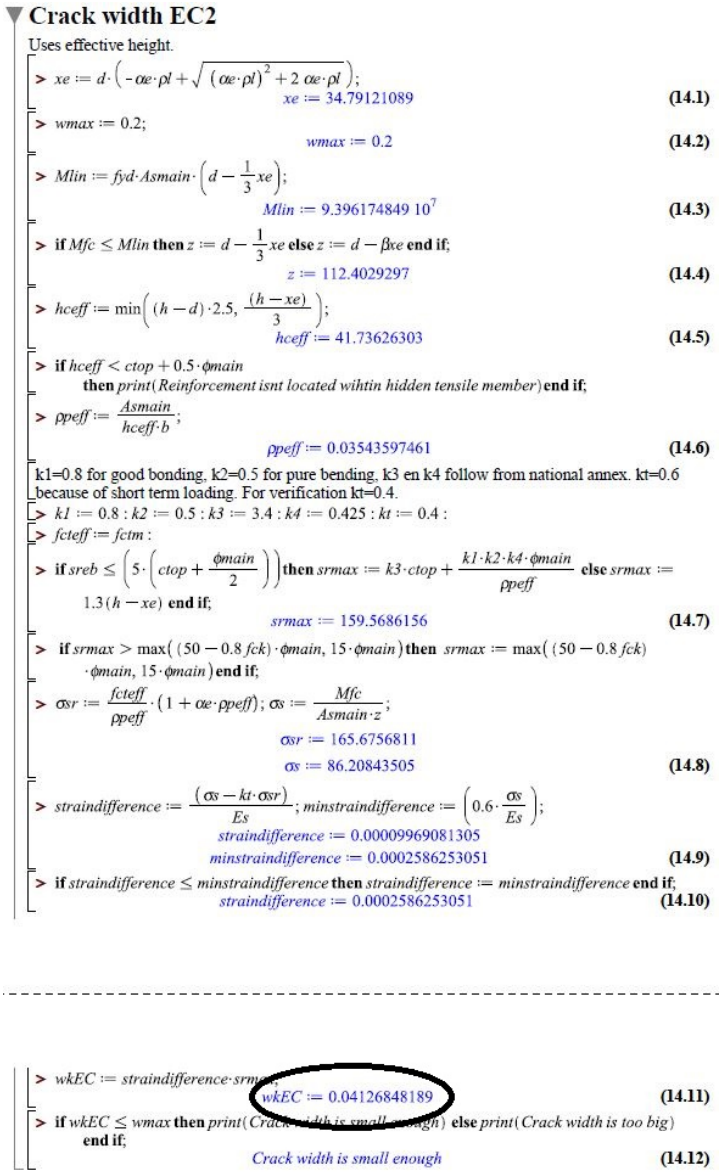

Figure 7.1: Crack width prediction according to Eurocode 2 article 7.3.4 for slab with h=160 mm, reinforcement ⌀10-80 mm, and a point load of 22 kN.

Scheurvorming volgens artikel 7.3.4 Ligger:1

Geb.	Pos. [mm]	Zijde	$M_{E;freq}$ [kNm]	$s_{r,max}$ [mm]	$\varepsilon_{sm}-\varepsilon_{cm}$ [‰]	w_k [mm]	k_x	w_{max} [mm]	U.C.	Opm.
1	S1+0	Bov	18.63	159	0.259	0.041	1.00	0.200	0.21	
1	S1+150	Bov	18.25	159	0.253	0.040	1.00	0.200	0.20	
1	S1+300	Bov	15.86	159	0.220	0.035	1.00	0.200	0.18	
1	S1+439	Bov	13.75	159	0.191	0.030	1.00	0.200	0.15	

Figure 7.2: Crack width prediction by Technosoft Liggers for same slab as described in figure 7.1.

8

Numerical analysis DIANA FEA

The variants that have been analysed in the previous paragraphs are modelled in DIANA FEA 10.1 and numerically analysed as well to determine up to which extent the three parameters influence the crack width predictions in the previous paragraph. This chapter elaborates respectively on geometry, meshing, boundary conditions, loading, material models, the numerical analysis and the interpretation of the results.

8.1. Geometry

To limit calculation time for this part of the research it has been chosen to perform a 2D analysis where the load is spread over the full width of the slab. Since the slab is fully clamped this is possible. By the time the load arrives at the connection, it will be spread over the full width.

All balconies are modelled as 2D sheets. For each balcony the reinforcement is modelled as a line with properties representing the total amount of reinforcement bars in the slab. A visualization of the modelled geometry is presented in figure 8.2

8.2. Meshing

The mesh size has been determined by performing a mesh refinement study for the highest cross section. During this study after each analysis the mesh size is halved and a new analysis is executed. When the difference in the results of analysis i and i+1 is less than 1%, the mesh refinement study is completed.

According to the report of Rijkswaterstaat on Nonlinear finite element analysis [17], the maximum element size of a 2D model is limited by the following demand: Maximum element size = $min\left(\frac{l}{50}, \frac{b}{50}\right) = min\left(\frac{1575}{50}, \frac{1300}{50}\right) = 26mm$. For this model the governing mesh size has been determined to be 10 mm.

The concrete is modelled with CQ16M elements. This is an 8 node quadrilateral isoparametric plane stress element. Since the reinforcement is modeled as embedded reinforcement (see paragraph 8.5 and appendix D for an explanation), the reinforcement doesn't have any own degrees of freedom.

Calculation time

From the lectures of CIE5148 Computational modelling of structures at TU Delft it can be learned that the calculation time/costs of a 2D and a 3D model can be expressed in the dimensions.
The number of equations n for the 2D model are proportional to d^2 and for the 3D model to d^3. The bandwidth b from these models is d and d^2 respectively.
Now, the calculation costs can be determined by $n*b^2$ resulting in computation costs directly proportional to d^4 and d^7.

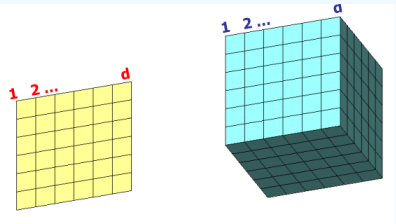

Figure 8.1: 2D and 3D calculation time from lectures CIE5148 at TU Delft.

8.3. Boundary conditions

The balconies are all cantilevering, thus require a fixed/clamped support. In practice, these supports are never completely stiff but in Diana they can be. An infinitely stiff connection is undesirable because, under the influence of deformations described by the Poisson's ratio, it might introduce stresses which in reality will not occur. Furthermore an infinitely stiff connection might induce singularities.

Singularity

A singularity is a point (can be multiple) where analysis results tend to approach an infinite value. Singularities can for example be induced by sharp corners, completely stiff boundary conditions, and point loads. When decreasing mesh size, which should increase the reliability of the results, this singularity effect is emphasized even more.

To solve this matter, over the full height only supports fixing translations in x-direction (horizontally) are applied. Only one support fixing translations in y-direction (vertically) is modelled at the bottom of the slab. The restraints are depicted in figure 8.2.

8.4. Loading

Loading on the slab exists out of dead weight and a point load.
The point load is spread over a width of 200 mm at the end of the cantilever to prevent singularity. The centre of gravity of the force is still 100 mm from the edge.

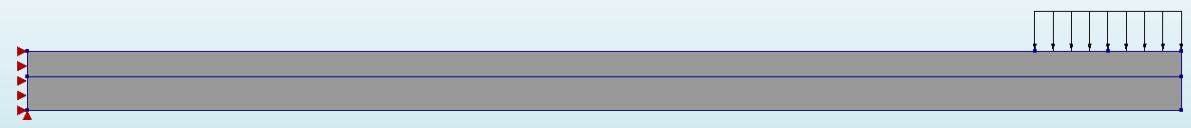

Figure 8.2: Visualization of geometry in DIANA FEA, including boundary conditions and representation of point load.

8.5. Material models

The material models applied in the numerical model have been generated following the advices from ir. C. Frissen, employee at DIANA FEA, the document *Guidelines for Nonlinear Finite Element Analaysis of Concrete Structures* [17] from Rijkswaterstaat and material characteristics from Eurocode 2 and FIB model code 2010 [14].

Table 8.1 presents all input parameters for the concrete model. An elaboration on parameters that request an explanation is attached in appendix D.

Table 8.2 presents the in DIANA FEA modelled material characteristics for the reinforcement. The influence of modelling bond-slip between the reinforcement and concrete has been investigated. The model characteristics are elaborated in appendix D. Eventually bond-slip has been left out of the analysis for two reasons. Firstly, the influence appeared to be minimal for the investigated alternatives. Secondly, as is stated in [13], with the determination of the shear stiffness DSSX and the normal stiffness DSNY a lot of uncertainty is incorporated. Ignoring bond-slip might lead to an underestimation of crack widths compared to the reality, see also appendix A. However, this is accepted because the determination of the bond-slip parameters leads to insecurities as well.

8.6. Numerical analysis

According to table 7.1N in Eurocode 2 crack widths are predicted by using the frequent load combination in case environmental class XD3 is governing. Furthermore, the stage the concrete is in (cracked or uncracked) is determined through comparing the bending moment following from the characteristic load combination with the analytical cracking moment. In some cases this results in a bending moment following from the frequent load combination being smaller than the analytical cracking moment. When trying to predict crack widths with DIANA FEA for the frequent load combination the member then remains uncracked, although

it should be cracked since the bending moment following from the characteristic load combination does exceed the analytical cracking moment.

To prepare an approach on how to load the structure in Diana and prevent that problem from occurring, the essence of load combinations is relevant. The characteristic load combination is assumed to occur maximum once during the design service life of the structure, as can be seen in figure 8.3, whereas the frequent load combination occurs more often. This means that predicting the crack width with the characteristic load combination is too conservative, but the residual stiffness after the characteristic load combination has occurred actually is required. Particularly because the stiffness is reduced irreversibly when the value of the characteristic load combination has occurred during the life time of the structure.

So, to use the lowest stiffness of the member during the design working life without overestimating crack widths, the member will first be loaded under the characteristic load combination before it will be partially unloaded to arrive at the loading value of the frequent load combination.

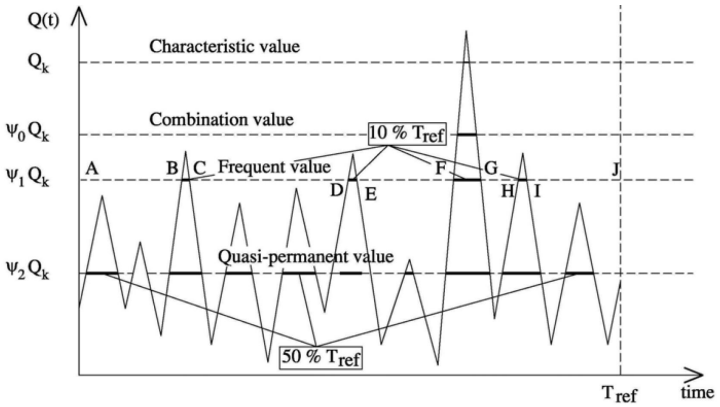

Figure 8.3: Visualization of loading developing, depicting the occurrence of load combinations over time, source [10].

This process has been numerically modelled by working with three execute blocks:

1. Step wise addition of dead weight: 10 x 0.1*G = G
2. Step wise addition of point load: 7 x -0.1*Q + 30 x 0.01*Q = G+ Q
3. Stepwise unloading of point load: 10 x -0.05*Q = G + Q - 0.5 Q = G + 0.5 Q

Table 8.3 presents the numerical characteristics of the analysis. An elaboration on how this approach emerged can be found in appendix D.

8.7. Interpretation

If not specified particularly, DIANA FEA considers concrete to be a homogeneous material. In reality concrete is not and this inhomogeneous character is one of the reasons in practice cracks localize. Unfortunately an unambiguous and relatively easy method for modelling inhomogeneous concrete is currently not available (see appendix A) thus it has been decided to follow the advice from [17] in addition to the results directly obtained from DIANA FEA. This guideline advices to predict crack widths by taking the mean steel strain in the cracked area following from the non-linear structural analysis and multiply it with the analytically determined maximum crack spacing $s_{r,max}$. In this research the conservative choice to use the maximum steel strain in the cracked area instead of the mean strain has been made for two reasons. Firstly the cracked regions are in general small thus the average strain will not be much smaller than the maximum strain. Secondly it appeared to be difficult to extract several steel strains over a certain area and compute an average.

This method does however influence the reliability of the results. Since in the numerical prediction of crack widths again an analytical Eurocode 2 method is incorporated, containing empirically determined parameters, the hybrid prediction of crack widths is not independent of the Eurocode. Whether the determination of the maximum crack spacing is suitable for slender HSC cross sections should be investigated in a future research.

Concrete & Masonry C90/105	Category	Value
Linear material properties	Young's modulus	43630.5 N/mm^2
	Poisson's ratio	0.15
	Mass density	2500 kg/m^3
Total strain based crack model	Crack orientation	Rotating
	Crack bandwidth specification	Rots
Tensile behaviour	Tensile curve	Hordijk
	Tensile Strength	5.05 N/mm^2
	Fracture energy	0.166 N/mm^2
	Residual strength	0.1 N/mm^2
	Poisson's ratio reduction	Damage based
Compressive behaviour	Compression curve	Parabolic stress strain diagram with softening branch
	Compressive strength	98 N/mm^2
	Compressive fracture energy	$G_c = G_f * 250 = 41.66$ N/m
	Reduction due to lateral cracking	Vechhio & Collins [34] $\beta_\sigma^{min} = 0.4$
	Stress confinement	No increase

Table 8.1: Concrete material properties DIANA FEA numerical model.

Steel reinforcement	Category	Value
B500	Steel Model	Uniaxial nonlinear elasticity
	Young's modulus	200 000 N/mm^2
	Yield stress	438.8 N/mm^2
	$E_{har} = 0.02 * E_s$	4000 N/mm^2

Table 8.2: Steel reinforcement material properties DIANA FEA numerical model.

Load class	Category	Value
Dead weight	Integration Scheme	Secant (Quasi-Newton) BFGS Previous iteration
	Load steps	0.1(10)
	Line search	yes
	Convergence criteria	Displacement & Force both 0.01
Point load	Integration Scheme	Secant (Quasi-Newton) BFGS Previous iteration
	Load steps	0.1(7) 0.01(30)
	Line search	yes
	Convergence criteria	Displacement & Force both 0.01
-0.5 x Point Load	Integration Scheme	Newton Raphson Regular Linear
	Load steps	0.1(10)
	Line search	yes
	Convergence criteria	Displacement & Force both 0.01

Table 8.3: Characteristics of numerical analysis.

9 Results

In this chapter first the results from the analytical analysis will be treated, followed by the results from the finite element analysis. This chapter will be concluded by a comparison of the results of the analytical and numerical methods. The complete table of the results, accompanied by visualizations of these results, can be found in appendix E.

9.1. Analytical analysis

Visualizing the results in table E.1 and ignoring the DIANA FEA results for a moment, it becomes clear that there is a (big) discrepancy between the crack width predictions following from the different methods, up to a factor five between the lowest and highest predicted crack width for a single variant. Later in this paragraph this discrepancy is analysed.

From the graphs in appendix E it can be observed that a decreasing cross sectional height results in a smaller difference between the methods except for the American Code. Decreasing the reinforcement diameter increases the differences between the predictions and decreasing the reinforcement spacing results in a slight decrease. However, this tells nothing about the reliability of the Eurocode 2 method.

In addition, for the different heights it can be observed that:

1. h=200: Van Breugel most pessimistic. American Code and Egyption Code almost similar;
2. h=180: Van Breugel most pessimistic. For smaller diameter American Code and Egyption code almost similar;
3. h=160: Van Breugel most pessimistic, closely followed by American Code. For smaller diameter American code and Egyption code almost similar;
4. h=140: American Code most pessimistic. With decreasing bar diameter all but the Eurocode method find more or less similar results;
5. h=120: American Code most pessimistic. With decreasing bar diameter all but the Eurocode method find more or less similar results;
6. h=100: American Code most pessimistic. For a diameter of 12 and 10 mm Eurocode, Van Breugel and Egyptian code produce more or less similar results, for diameter 8 mm again there appears a difference in results where the Eurocode is most optimistic;
7. h=80: American Code most pessimistic, the other three produce more or less similar results. The difference increases a little with decreasing bar diameter.

Since it is unknown which method describes reality for which case, the obtained information is insufficient for concluding anything on the reliability of crack width predictions. However, an interesting influence of the height of the slab is observed in the prediction of the crack widths according to methods utilizing the effective height. These methods make use of the so-called hidden tensile member with a height $h_{c,eff}$. For the variants with a cross section equal to or lower than 120 mm the problem arises that the reinforcement is not located in the hidden tensile member but lies higher, see figure 9.1. What happens then is that the effective reinforcement ratio, determined through equation 9.1, in essence equals zero because there is no reinforcement present in the effective area, and the crack width prediction should fail.

$$\rho_{eff} = \frac{A_s}{h_{c,eff} * b} \tag{9.1}$$

However, for example software like Technosoft does still produce crack width predictions which in essence do not particularly make sense any more. These low cross sections fall out of the applicable range for the crack width prediction method proposed by Eurocode 2.

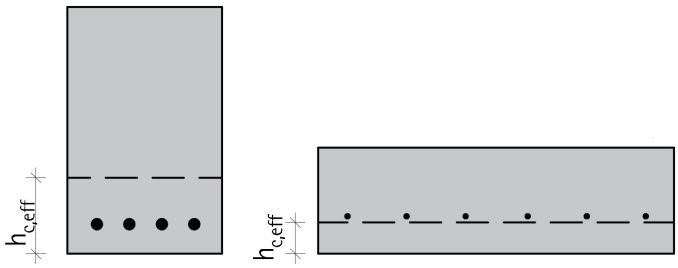

Figure 9.1: Left: Visualization of reinforcement localized inside of the effective height of the hidden tensile member. Right: Visualization of reinforcement localized outside of the effective height of the hidden tensile member.

Discrepancy

The methods proposed by the Eurocode and the Egyption code are quite similar and both make use of the effective height. This can be observed in the results either since for most configurations they predict the smallest crack widths. The difference between these two however is still relatively big and is most likely induced by the experimentally determined parameters in the equations.

The American code is the only code which explicitly takes into account the vertical location of the reinforcement and does not take into account the steel stress at the onset of cracking. It can be observed that for slab heights equal or smaller than 120 mm the American code predicts crack widths significantly bigger compared to the others. This is also the moment that the reinforcement is not located in the hidden tensile member any more.

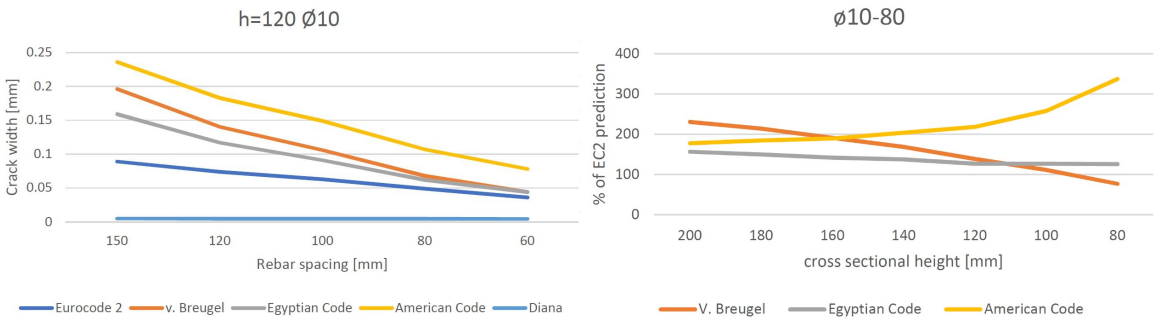

Figure 9.2: Left: Visualization of crack width predictions for the different methods for a slab with a height of 120 mm and reinforcement diameter ⌀10 and a varying reinforcement spacing. Right: Visualization of the percentual values of a method compared to the Eurocode 2 prediction. The 100% level indicates an equal value of the Eurocode 2 method and the plotted method. It can be observed that for decreasing height the American prediction diverges from the Eurocode 2 prediction.

9.2. Numerical analysis

In all graphs in appendix E the crack widths determined with DIANA FEA seem almost non-existent, see for example figure 9.2. This occurs since the numerically predicted crack widths appear to be very small. The

results are counter intuitive and do not stroke with the hypothesis. However, a great effort has been invested in the optimization of the model by consulting specialists like ir. Chantal Frissen, employee at DIANA FEA bv., and dr. ir. Max Hendriks, specialized in numerical analysis of structures. This fact has resulted in the acceptance of the results, despite the fact that it is acknowledged that these results are most likely not realistic. In the last part of this chapter an explanation of these results is proposed.

During the research for several alternatives force-displacement-diagrams up to failure have been produced. These diagrams show some interesting results. For one of the alternatives figure 9.3 presents a force-displacement diagram. Some observations:

- The numerically determined capacity of the slabs is higher than analytically determined. This can be contributed to the fact that when analytically determining the cross sectional bending moment resistance the concrete tensile capacity is left out of consideration (N_s=N_c). This is conservative since the uncracked concrete around (and below) the cracks will contribute to the equilibrium and thus there is a possibility of redistribution of forces/stresses.
- Because the influence of the tensile capacity is completely neglected in the analytical determination of the capacity, steel strains and stresses are higher compared to the numerical analysis, resulting in bigger analytical crack width predictions.
- It is observed in the numerical results that crack widths remain small until, just before failure, a limited amount (very few) of the cracks propagate and instantly lead to failure.

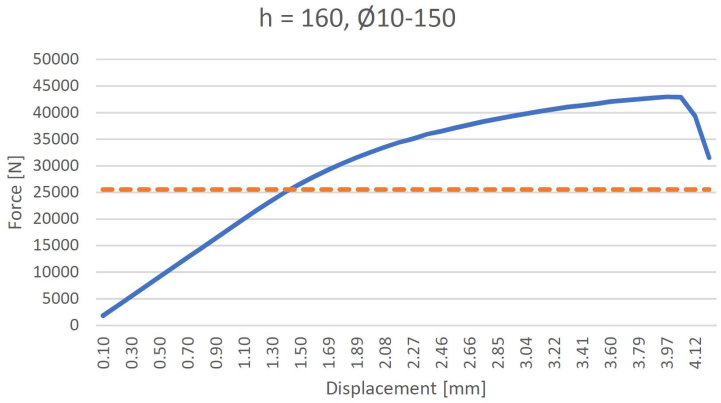

Figure 9.3: Force-Displacement diagram of fully clamped balcony, h = 160 mm, ⌀10-150. The orange dotted line indicates the force related to the analytical bending moment capacity.

9.3. Comparison

The comparison of the results is difficult. Even more difficult is distinguishing the influence of the slab height, reinforcement diameter and reinforcement spacing on the reliability of the crack width prediction method proposed by Eurocode 2. The crack widths that follow from the numerical analysis are that much smaller than the analytically determined values that a clear distinction cannot be made.

As mentioned in paragraph 8.7 the analytically determined crack spacing is used to convert the numerically found steel strain to a crack width. This means that still the numerically found crack widths are dependent on the Eurocode 2 method. This method is partially build up of empirically determined values. Currently it is not known if these values are valid for high strength concretes and thus the utilization of this expression leads to an unreliability. The crack spacing for example is limited by $s_{r,max}$ which depends, amongst some other parameters, on the characteristic compressive strength of the concrete. Whether this relation describes the behaviour of HSC correctly, is unknown.

Remark

The big dataset required 2D modelling to limit calculation time which resulted in a too homogeneous boundary condition (fully clamped). Combining this homogeneous boundary condition with the homogeneous geometry (no geometric disturbances) and the homogeneously modelled concrete, the model is a too simple

schematization of reality. In practice the disturbances/inhomogeneities in material properties, geometries, and boundary conditions result in localization of cracks (appendix A), which in these models did not happen. This might have resulted in the unrealistically fine crack patterns and the inability of discovering the influence of reinforcement spacing and reinforcement diameter on the reliability of analytical crack width predictions.

III

Cantilever slab with in-plane ridge connection

10

Method

With the knowledge gained in the previous chapters, the research will now focus on a specific balcony design. This balcony will have a constant thickness, will be connected with a clamped ridge, and will be loaded and checked in accordance with rules and legislations from Eurocode 2 and its Dutch national annex to determine the influence of a geometric disturbance on the reliability of analytical crack width predictions. The main geometry (figure 10.1), except the thickness, is dictated by already existing formwork from Hi-Con, to remain compatible with potential future laboratory testing.

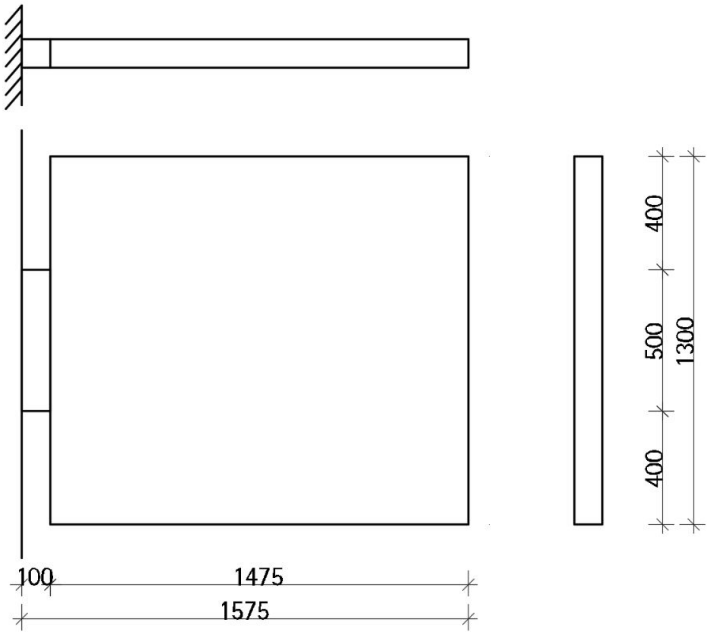

Figure 10.1: Schematization of main geometric characteristics of balcony design supported by an in-plane clamped ridge.

During the design of this balcony it will be tried to approach the limit of the thickness for which the design is still allowed and possible, and check how well the rules and legislations apply to this C90/105 slender cantilevering slab. The designing and checking will once more be manually and analytically executed with a script. As a basis the same script as in Part II will be used and further developed. For the reason that the limit in slenderness will be be searched for, the designing process will become an iterative one where parameters need constant fine tuning to find a design on the edge of what is possible. This iterative work justifies the labour which should be invested in developing a script.

The script will be developed in such a way that besides capacity and design checks, it calculates crack widths, the first eigen frequency and deflections for serviceability limit state demands. Since it is still the goal to

check the reliability of the Eurocode 2 method on slender HSC elements, the complete balcony design will be modelled in DIANA FEA afterwards and results will again be compared.

11

Design

This chapter elaborates on the design and checking of the balcony slab from figure 10.1 in a comparable way as chapter 6. The script from chapter 6 (and appendix B) has been used as a basis for the development of the script for this part of the research. To prevent duplicate information, this chapter will only elaborate on additions and changes compared to the previous script. The full script can be found in appendix F. It is advised to read this chapter accompanied by the script. During the design process it has been pursued that all relevant demands, rules and legislations from the Eurocodes have been met.

11.1. Structural starting points

As has been explained in chapter 10, the research now focuses on a balcony as slender as possible, executed in a C90/105 concrete grade. Nonetheless this focus is an extension of the research started in part II of this report and thus mainly possesses the same structural starting points like consequence class, design working life, building category, load combinations, etc. The ones that are different, or require more attention, are treated specifically.

Loading

For the design of this balcony in terms of loading now the Eurocode demands have been followed. Table 6.2 in the Dutch national annex of Eurocode 1 presents prescribed live loads for a balcony in building category A. There are two options: a surface load of 2.5 kN/m^2 or a line load Q, 100 mm from a free edge, with a magnitude of 5 kN/m for the length of 1 m. For a length of 1575 mm and a width of 1300 mm, the latter appears to be governing.

Furthermore the slab is loaded by its own weight G, assumed to be 25 kN/m^3, and a line load at the edge of the cantilever, g, which represents the weight of a balustrade. In this research only a balustrade at the end of the cantilever has been taken into account. Figure 11.1 shows the load configuration in longitudinal direction.

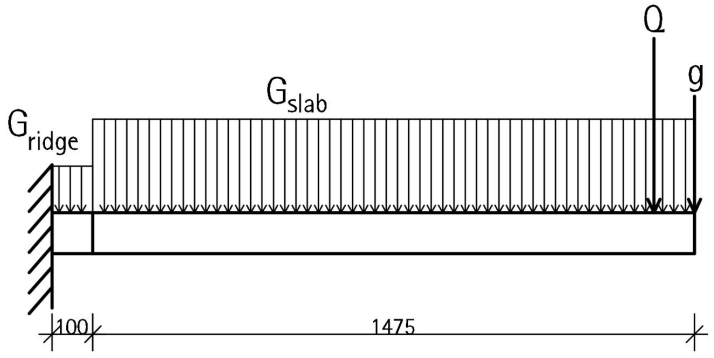

Figure 11.1: Load configuration for the design of the balcony.

Environmental class

For this design not only the environmental class of the top face is relevant. Table 11.1 treats the determination of the different concrete covers. For the ridge the reduction for plate geometry is not allowed since it does not fit in the definition of a plate (art. 9.3(1) in Eurocode 2).

Face	Governing environmental class	Reductions	Structural class	Concrete cover
Top face slab	XD3		S4	
		Concrete grade ≥ C45/55	-1	
		Element with plate geometry	-1	
		Specific quality control	-1 +	
			S1	25+5 = 30 mm
Top face ridge	XD3		S4	
		Concrete grade ≥ C45/55	-1	
		Specific quality control	-1 +	
			S2	30+5 = 35 mm
Other faces slab	XC3		S4	
		Concrete grade ≥ C45/55	-1	
		Element with plate geometry	-1	
		Specific quality control	-1 +	
			S1	10+5 = 15 mm
Other faces ridge	XC3		S4	
		Concrete grade ≥ C45/55	-1	
		Specific quality control	-1 +	
			S2	15+5 = 20 mm

Table 11.1: Determination of concrete covers.

11.2. Bending moment resistance

The bending moment resistance is determined in a similar way as in chapter 6 and appendix B. This method has been applied on both the slab and the ridge. In an iterative way cross-sectional dimensions and reinforcement configurations are tweaked until both the ridge and the slab can withstand the loading following from the fundamental load combination.

Since for the ridge reinforcement bars with a bigger diameter were required to obtain a sufficient ultimate resistance and fulfil detailing demands, for the slab an equivalent reinforcement height, d, has to be determined. This has been carried out by using the vertical coordinate of the centre of gravity of all the longitudinal reinforcement bars in the top of the slab together.

The influence of the load bearing structure to which in reality the balcony would be attached is neglected in this part of the research. This results in the fact that the protruding reinforcement in the ridge will not be sufficient in case the concrete grade of the load bearing structure is lower than C90/105.

11.3. Shear resistance

For the slab the same method as in part II, described in paragraph 6.2 in Eurocode 2, has been used to determine the shear resistance. For the ridge an additional design step has been performed. At the interface of the ridge and the load bearing structure in practice there will be a difference in concrete strength. This results in a decrease in the reliability of the shear resistance determination on this interface. For this reason it has been chosen to apply curved reinforcement bars through the connection, see figure 11.2.

The reinforcement area required to resist this shear force on the interface surface has been determined through equation 11.1.

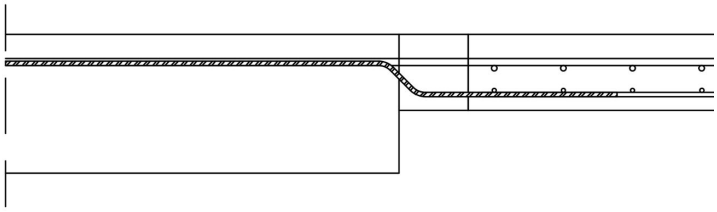

Figure 11.2: Example of reinforcement for shear in balcony-floor-connection.

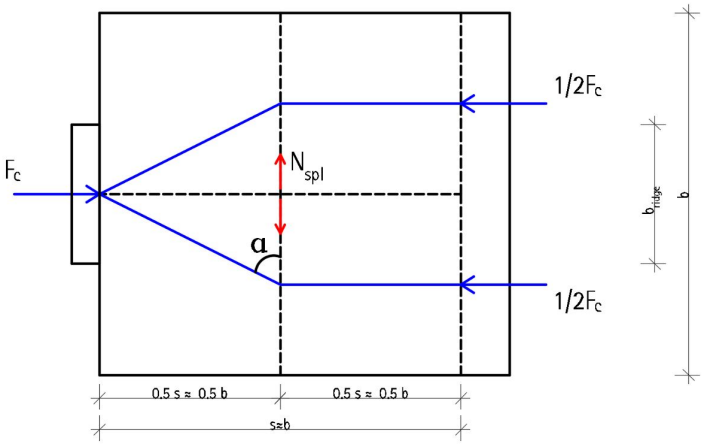

Figure 11.3: Visualization of disturbed region and the accompanying tensile splitting force in bottom side of slab due to compressive force from support. This schematization is conservative, as is assessed in appendix G, and is applied because the width over which the tensile splitting force is spread is unknown.

$$A_{s,shear,req} = \frac{V_{Ed} * \sqrt{2}}{0.9 * f_{yd}} \tag{11.1}$$

11.4. Disturbed region

Because the slab is now connected to the load bearing structure through the application of a ridge, all forces from the slab have to be channelled from the full width to the width of the ridge. This change in cross-sectional width induces that the St.-Venant's principle becomes relevant. This principle states that there is a certain length required to spread a load and obtain a uniform load distribution in case a change in cross section has occurred. This length, called the disturbance length, is equal to the maximum width across which the load has to be spread. A visualization of the disturbed region in the bottom side of the balcony slab is depicted in figure 11.3. The same phenomenon occurs in the top side of the balcony but in opposite way. The supporting force is a tensile force, which results in a compressive normal force perpendicular to the line of work of the supporting force.

In the visualization the compressive force is modelled as a single point load. This is a conservative choice, in reality this force is spread over the full width of the ridge. A sensitivity analysis of this effect is presented in appendix G. This conservative choice has been used to level out an optimistic assumption that the tensile splitting force is spread over 1 m. Making an assumption was necessary since no unambiguous information about the spreading of the tensile splitting force has been obtained. It has been assumed that the tensile splitting force will be taken up by the bottom cross reinforcement. The capacity of the reinforcement has been checked as well.

11.5. Stiffness

For determining the eigen frequency and the deflection of the cracked balcony, an equivalent stiffness for both the ridge and the slab has to be found. The method described in GTB 2013 [29] and the Cement article *Doorbuiging in de GTB* [8] has been applied. This method enables the user to find four stiffness coefficients, a cracked and an uncracked one for t=0 and for t=∞, taking into account the creep factor and loading ratio's.

Depending on the loading ratios ($\lambda, \mu_1, \mu_2, \mu_3$) the state of the concrete of the balcony can be determined (always non cracked, cracked for frequent combination, always cracked), which leads to a fictitious stiffness representing the state of the concrete.

11.6. Eigen frequency

In the serviceability limit state, article A1.4.4 from Eurocode 0 demands that, when it might be possible that people jump or dance on the 'floor', a first eigen frequency of at least 5 Hz should be obtained. In chapter 10 and appendix D of the report *Bevestigen van prefab betonnen balkons* (separately attached report), developed as part of this master thesis, a method to simply determine the first eigen frequency of a cantilevering beam/slab analytically is derived and presented.

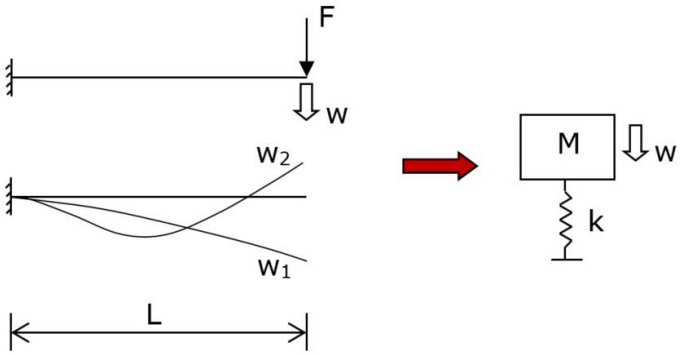

Figure 11.4: Visualization of the transfer from the cantilever into a single-mass-spring-system.

To find the first eigen frequency, the balcony is transformed into a single-mass-spring-system, see figure 11.4, which is loaded with an equivalent load. This equivalent load is a combination of all forces working on the sturcture and can be found through the equations in figure 11.5.

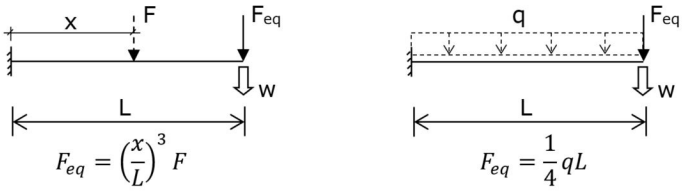

Figure 11.5: Equations to determine equivalent force for single-mass-spring-system of cantilever.

Now by using the stiffness determined with the method described in the previous paragraph, the deflection due to the equivalent point load can be found. Dividing the equivalent force by this deflection leads to a stiffness for the single-mass-spring-system. From this stiffness and the equivalent load, the first eigen frequency can be found through the equations below.

$$k = \frac{F_{eq}}{w_{Feq,\infty}} [N/m] \tag{11.2}$$

$$\omega_n = \sqrt{\frac{k}{m}} \quad with \quad m = \frac{F_{eq}}{g} [kg] \tag{11.3}$$

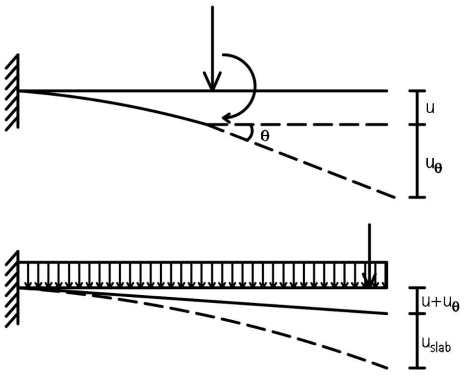

Figure 11.6: Top figure: Schematization of influence 'kwispeleffect' on total deflection. Bottom figure: Schematization of determination of total deflection.

$$f_n = \frac{\omega_n}{2\pi}[Hz] \tag{11.4}$$

11.7. Deflection

The deflection has been determined using the loads, the fictitious stiffness, and the so called vergeetmenietjes. The maximum deflection of the balcony consists in this simplified case of three parts. The deflection of the ridge, the rotation of the ridge multiplied by the length of the slab and the deflection of the slab itself. For the analysis several cross sections are used. For the determination of the stiffness a creep coefficient of 0.9 is used, in accordance with Eurocode 2.

Figure 11.6 roughly schematizes the effect of the ridge on the total deflection of the balcony. In the top figure the area left of the point load represents the ridge and the area to the right the slab. To be able to visualize the effect the dimensionsal ratio between the slab and the ridge are not correct in the top figure. The point load represents the shear force from the slab and the bending moment is the same moment as is transferred from the slab to the ridge. It can be seen that the point load and moment induce a deflection u and a rotation θ. θ results in a deflection u_θ at the end of the balcony.

The bottom figure shows how the total deflection is calculated. The influence of the ridge, the so called 'kwispeleffect', is considered to be an initial deflection to which the deflection of the slab is added to end up with the total deflection.

The influence of the deformation of the connection and the load bearing structure are neglected in this calculation since it does not fit in the scope of this research. The influence of these elements is described in the separately attached report *Bevestigen van prefab betonnen balkons*.

11.8. Bending moment resistance cross direction

In the same way the bending moment resistance in the main span is determined for the slab and ridge, the cross bending moment resistance of the slab is determined for a width of 1 m. The result of this bending moment resistance then is compared with the bending moment in cross direction following from the fundamental load combination on the schematization in figure 11.7.

11.9. Crack width

The final check in the script involves the crack width prediction according to the method presented in article 7.3.4 in Eurocode 2, which is also applied in part II of this report. The crack width is predicted for the frequent load combination in the main direction for both the slab and the ridge.

Because of the presence of cross reinforcement in the slab, according to article 7.3.4(4) the maximum crack spacing is determined through equation 11.5.

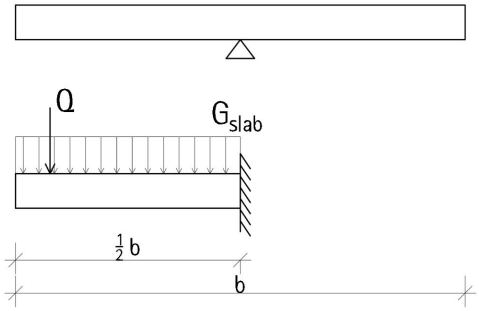

Figure 11.7: Mechanical scheme for determination of cross bending moment. The supporting forces from the ridge are neglected as a conservative approach.

$$s_{r,max} = \frac{1}{\frac{cos\theta}{s_{r,max,y}} + \frac{sin\theta}{s_{r,max,x}}} \tag{11.5}$$

In which θ represents the angle between the reinforcement bars.

11.10. Detailing

Most of the relevant detailing rules in chapter 8 and 9 of Eurocode 2 are taken into account. However, for example edge reinforcement at the edges of the slab is neglected. It is assumed this choice does not affect the results of this research.

11.11. Design result

The iterative procedure, of which some steps are treated in the previous paragraphs and of which the full script can be found in appendix F, has lead to the following design and design results. Bigger visualizations of the design can be found in appendix H.

Geometry

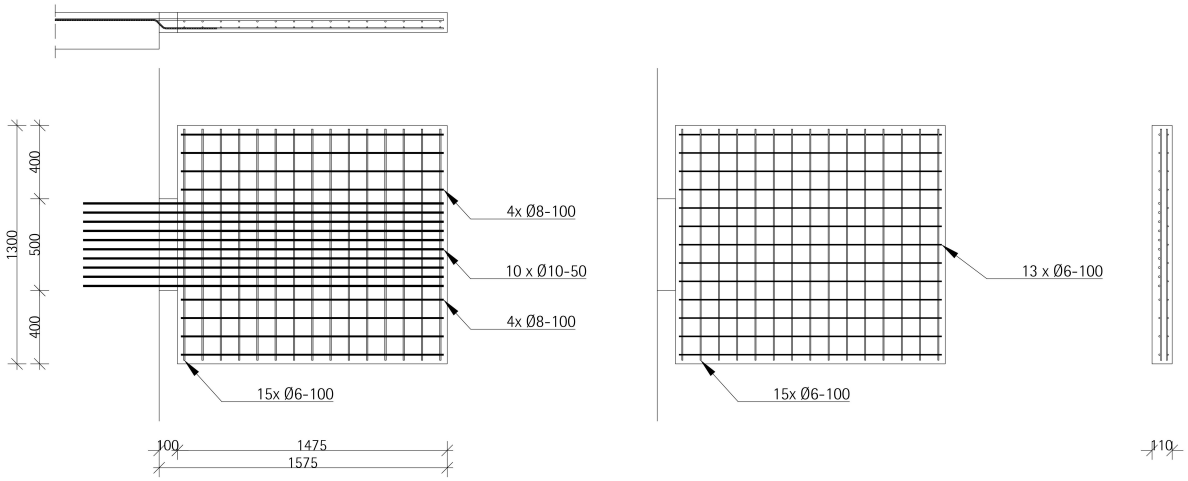

Figure 11.8: Design of balcony with ridge, including reinforcement configuration. Left: Top reinforcement. Right: Bottom reinforcement.

The utter limit of thickness is 80 mm, which is incorporated in the Eurocode definition of a plate (article 9.3(1)(2)a) in the Dutch national annex of Eurocode 2). This thickness appeared to be impossible to apply due to bending moment resistance and reinforcement configuration. An increase of 30 mm resulted in the slab in figure 11.8, with a thickness of 110 mm, a width of 1300 mm and a length of 1575 mm. These dimensions include the ridge with a thickness of 110 mm, a width of 500 mm and a length of 100 mm, this is shown

in the top view in figure 11.8.

Because the length of the disturbed region covers more than 80% of the total length, see figure 11.3, and the top reinforcement from the ridge needs overlap outside of the disturbed region, it has been decided to let the ridge reinforcement continue to the end of the slab and combine it with the ⊘8-100 reinforcement net. For this purpose 5 bars from the net in longitudinal direction have to be replaced by 10 ⊘10 in the middle of the slab.

The bottom reinforcement net (⊘6 – 100) is applied for practical reasons. It is undesirable to have a big difference in reinforcement area's in the top and the bottom of the cross section because of the risk of uneven curvature induced by shrinkage, hence the choice for a 6 mm diameter.

Table 11.2 presents the final design of the balcony with in plane ridge connection. These dimensions and properties correspond to the images in figure 11.8.

Element	Global dimensions	[mm]
Slab	Length	1475
	Width	1300
	Height	110
Ridge	Length	100
	Width	500
	Height	110
Reinforcement	Ridge top	10 x ⊘10-50
	Slab top	10 x ⊘10-50 2 x 4 x ⊘8-100
	Slab top cross	⊘6-100
	Slab bottom net	⊘6-100
	Shear reinforcement	2 x ⊘6

Table 11.2: Main geometric properties of final design of balcony with in-plane ridge connection.

Design check results

Table 11.3 presents how well this balcony design performs on the several checks. The origin of these values can be found in appendix F.

Element	Category	Capacity		Acting		UC [-]
Slab	Bending moment	33.9	kNm	18.2	kNm	0.54
	Shear force	106.7	kN	15.2	kN	0.14
	Crack width	≤ 0.20	mm	0.05	mm	0.25
	Cross bending moment	7.1	kNm	5.57	kNm	0.78
Ridge	Bending moment	21.6	kNm	18.2	kNm	0.85
	Shear Force	49.3	kN	15.2	kN	0.31
	Crack width	0.20	mm	0.09	mm	0.45
General	Eigen Frequency	≥ 5	Hz	8.65	Hz	-
	Deflection	≤ 12.6	mm	4.02	mm	0.32

Table 11.3: Design check results for balcony with in-plane ridge connection.

12

Numerical analysis DIANA FEA

This chapter presents the characteristics of the DIANA FEA model developed for the analysis of the balcony designed in the previous chapter. Appendix D elaborates on the specifics of several characteristics of the model.

12.1. Geometry

Figure 12.1 displays the geometry as it was modelled in DIANA FEA, based on the balcony design described in paragraph 11.11. Because of a more complex geometry it has been decided that modeling this balcony in 3D is worth the investment.

The balcony is modelled as a block solid. All but the bottom reinforcement bars are modelled as lines. The bottom reinforcement net is modelled as a sheet with reinforcement grid properties because it has constant spacing and reinforcement diameter. The top reinforcement is modelled individually because of changing reinforcement diameters and spacing.

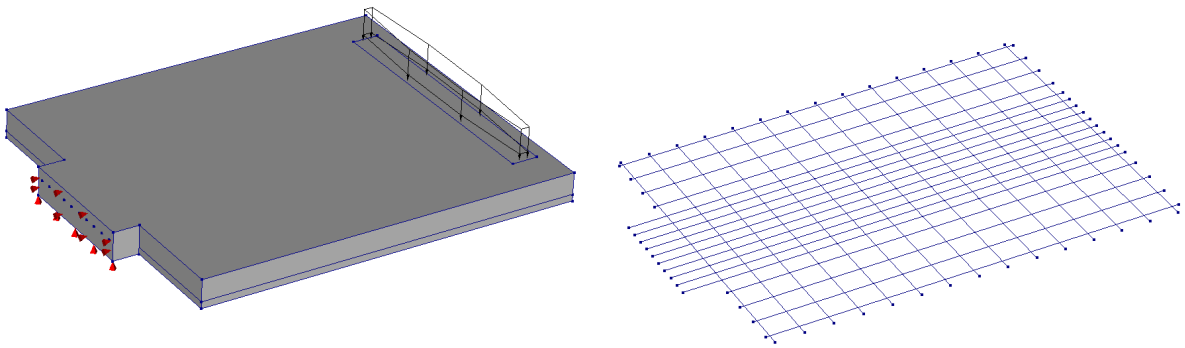

Figure 12.1: Left: Modelled 3D-geometry in DIANA FEA. Rigth: Modelled top reinforcement in DIANA FEA. Bottom reinforcement net is not displayed.

12.2. Meshing

Again a mesh refinement study has been performed. According to [17] the maximum mesh size for a 3D slab structure is $min\left(\frac{l}{50}, \frac{b}{50}, \frac{h}{6}\right) \approx 20mm$. Eventually the applied mesh size is 20 mm. A further decrease of mesh size appeared to be impossible because of a lack of computational power and digital storage space.

The applied elements, further described in appendix D, are all solid isoparametric quadrilateral elements with the following names according to DIANA FEA:

- CHX60
- CPY39

- CTE30
- CTP45

12.3. Boundary conditions

The balcony is clamped at the ridge. To prevent singularity as a result of a too stiff connection the full face of the ridge at the location of the connection is only restrained in horizontal direction. The vertical support is facilitated by the edge of the bottom of the ridge, resulting in similar support conditions as for the variants in part II. For a schematization, see figure 12.2.

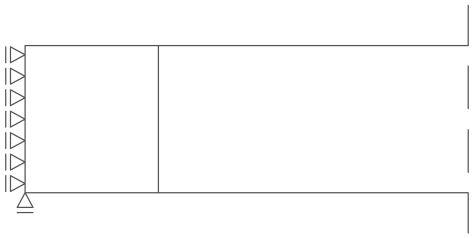

Figure 12.2: Configuration of boundary conditions at the in-plane ridge.

12.4. Loading

The point load Q and the weight of a balustrade are both modelled as a distributed force with a length of 1 m and a width of 0.1 m, see figure 12.1. This choice has been made to prevent concentrated loading which increases the risk for singularities. The fact that the area of interest is far away from the loading point justifies this choice. The magnitude of the distributed loads is $Q = \frac{5000}{1000x100} = 0.05N/mm^2$ and $g = 0.01N/mm^2$.

12.5. Material models

The concrete material models are similar to the model applied in part II of this report. The material characteristics applied in DIANA FEA are presented in table 8.1 and 8.2.

12.6. Numerical models

For the analysis the same approach as in part II of this report has been applied. An overview is given in table 8.3. The analysis is executed following the sequence in the table so again the model is loaded to the characteristic load combination and then partially unloaded to the frequent load combination.

12.7. Results

This paragraph elaborates on several characteristics of the numerical results. More visualizations of the results from the analysis performed with DIANA FEA are attached in appendix I.

Crack pattern

From the results of the numerical nonlinear analysis of the balcony with the in-plane ridge it is observed that in the corners (location of circles in figure 12.3) between the slab and the ridge the biggest crack width occurs, as can be seen in figure 12.4. The right image in figure 12.4 is a slice (taken in the middle of the ridge) of the results presented in the left image. As can be observed, the maximum numerical crack widths in the legends differ because the maximum crack width occurs in the corners and thus is not present in the slice of the results on the right.

Stresses and strains

To clarify the increase in crack width in the corners between the ridge and the slab in addition a linear analysis has been performed on the balcony model. During this analysis the balcony is loaded by the frequent load combination. The results are assessed through the help of two cross sections, A and B, visualized in figure 12.5.

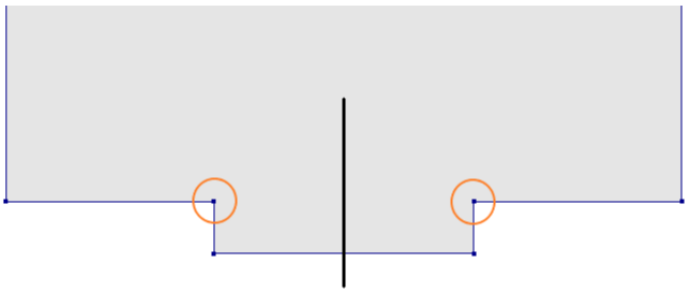

Figure 12.3: Display of locations relevant for crack width considerations. At the location of the circles numerically the biggest crack widths occur.

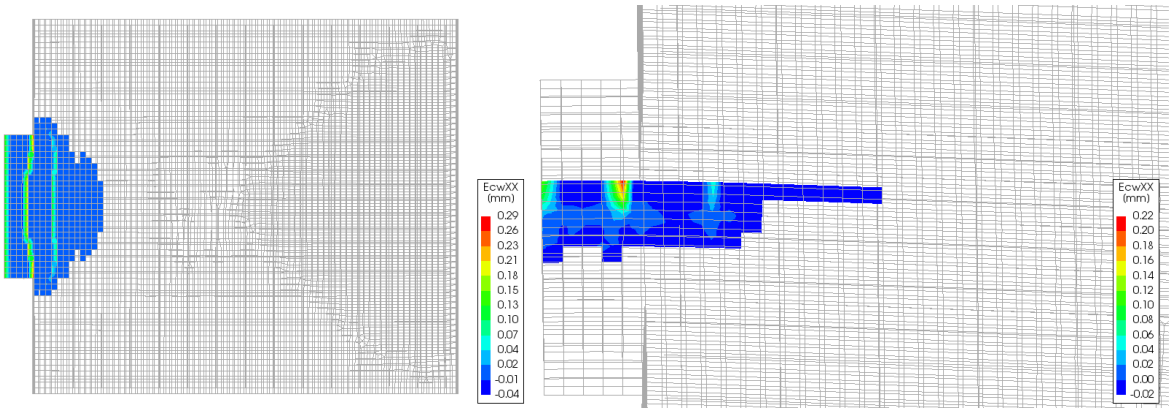

Figure 12.4: Left: DIANA FEA nonlinear output for maximum crack width for frequent load combination in the corner between the slab and the ridge. Right: DIANA FEA nonlinear output for maximum crack width for frequent load combination, slice in the middle of the ridge of the results in the left image.

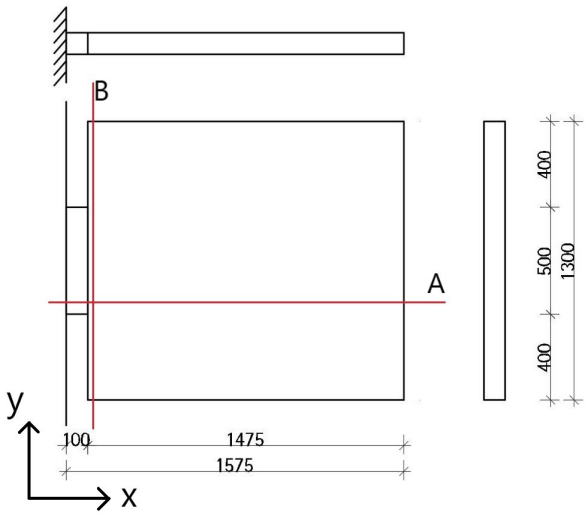

Figure 12.5: Visualization of locations of utilized cross sections for the analysis of the numerical results for the balcony with the in-plane ridge.

From the linear analysis a clarification of the increased crack width in the corners between the slab and ridge is observed. It is found that this specific balcony geometry induces concentrated stresses and strains in the corners. This is displayed in figures 12.6 and 12.7. Obviously this local increase in stresses and strains also results in an increase of the crack width compared to the other regions.

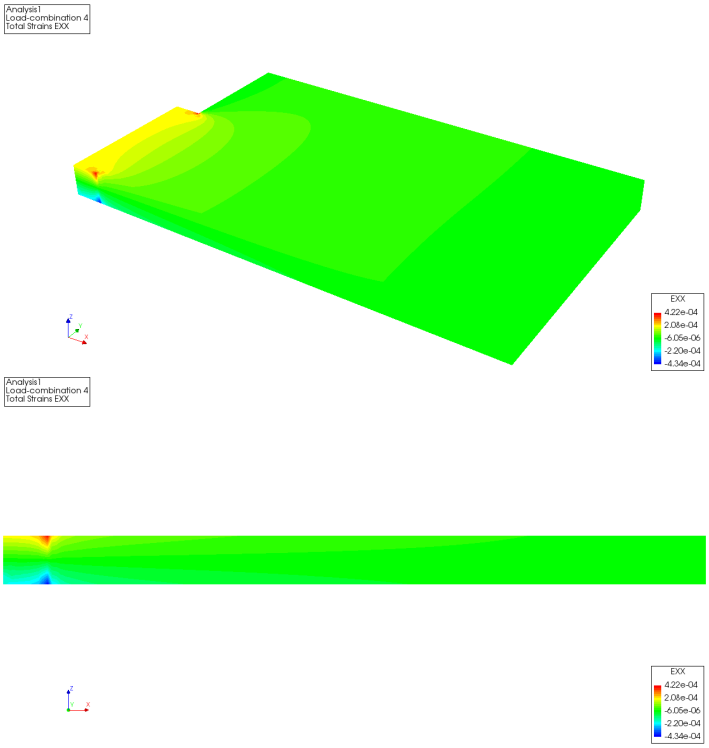

Figure 12.6: Visualization of strains in x-direction in longitudinal cross section (cross section A) following from the linear analysis. The top image presents an overview to visualize where the cross section has been made.

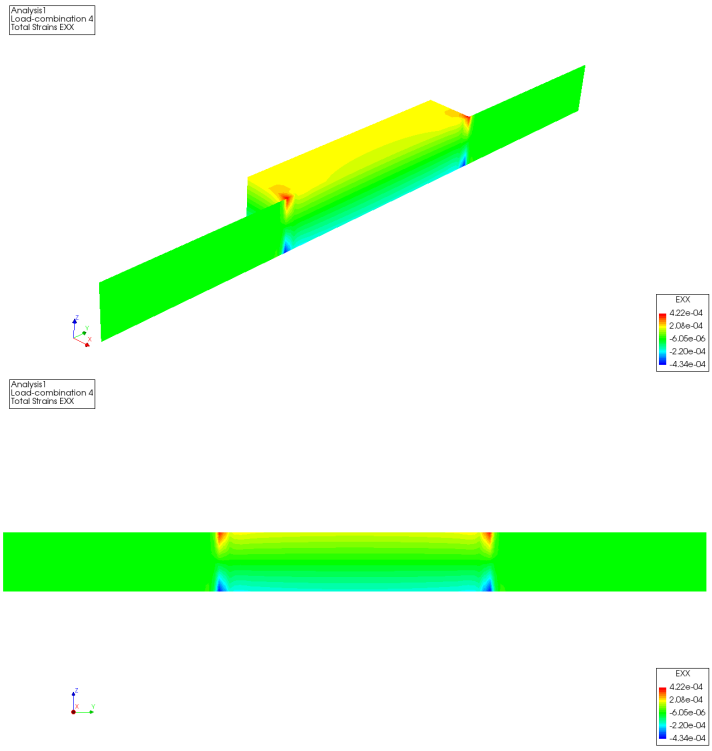

Figure 12.7: Visualization of strains in x-direction at the interface between the slab and the ridge (cross section B) following from the linear analysis. The top image presents an overview to visualize where the cross section has been made.

The effect of the concentrated stresses is clearly visible when plotting the steel stresses on the interface between the slab and the ridge for both the linear and the nonlinear analysis. The graphs are presented in figure 12.8. It is observed that because of the change in geometry the bars at the sides are loaded more heavily. In an undisturbed distribution the bars in the middle would be loaded heaviest (see for example figure 16.8).

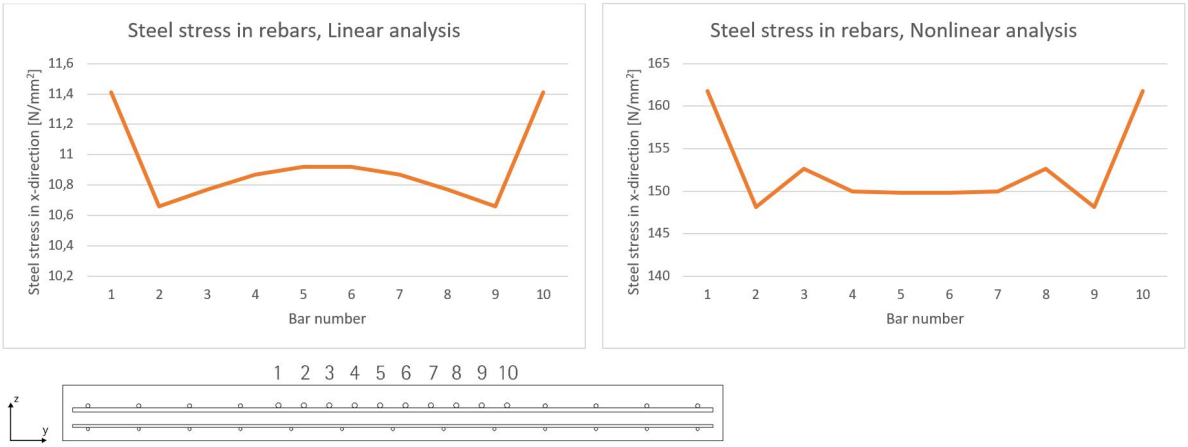

Figure 12.8: Visualization of distribution of reinforcement stresses in reinforcement protruding through the ridge at the interface between the ridge and the slab. Left graph depicts the linear results, right graph the nonlinear results. The bottom image presents the bar numbers against which the stresses are plotted.

The graphs in figure 12.8 display the influence of cracking on the steel stress as well. As soon as the concrete cracks, the contribution of the cracked concrete decreases. For equilibrium the steel stress should then increase. This can be observed when comparing the graph containing the linear results with the graphs containing the nonlinear results, the steel stress in the right graph is higher. Furthermore the peak stresses in the corners obviously influence the cracking behaviour and thus the stress distribution over the reinforcement bars, visualized by the different shapes of the graphs in figure 12.8.

Remarkable is that the steel stresses following from the linear analysis are a lot smaller than the stresses resulting from the nonlinear analysis. This can be contributed to a number of facts, namely, in the linear analysis all of the concrete keeps on contributing since cracking is not possible, reducing the required strain to find equilibrium with the external forces. Furthermore, the reinforcement has a concrete cover of 35 mm. With a cross-sectional height of 110 mm this means that the axis of the reinforcement is located closely to the neutral axis of the entire cross section, resulting in an even smaller steel strain. In the nonlinear analysis cracking is taken into account, resulting in a reduced cross section and a limited concrete tensile capacity. For equilibrium this requires the steel stress to increase.

In the calculation below, for a cross section behaving linearly, the stress in the reinforcement is calculated which results in a stress with a similar order of magnitude as the numerical linear analysis and corresponds to the average stress. The location of the neutral axis in the ridge for full linear behaviour is determined to be 56 mm from the bottom of the cross section, taking into account the location of the reinforcement and its modulus of elasticity.

$$\sigma = \frac{M_{fc}}{W}; M_{fc} = 9.6 * 10^6 N/mm^2; W = 1/6bh^2$$

$$\varepsilon_{ct} = \varepsilon_{cc} = \frac{\sigma_c}{E_c} = 0.0002$$

$$\sigma_s = \frac{\varepsilon_{ct}}{0.5h}(h - 56 - c - 0.5\varnothing) * E_s = 11.0 \quad N/mm^2$$

The increase in loading of the elements located at the sides of the ridge and the change in stress distribution over all reinforcement bars can be contributed to the channelling of forces from the full width of the slab towards the width of the ridge. This phenomenon induces the peak stress concentrations in the corners and is visualized in figure 12.9. The effect is confirmed by the results displayed in figure 12.11, where with the help of the steel strains the flow of forces is visible.

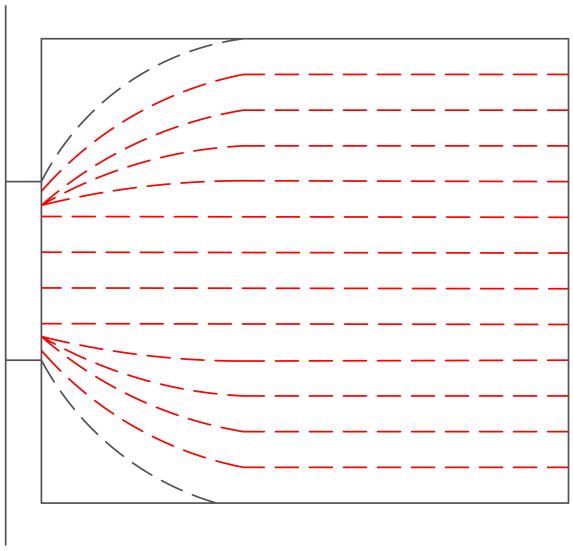

Figure 12.9: Visualization of channelling of forces from the full width of the slab towards the width of the ridge.

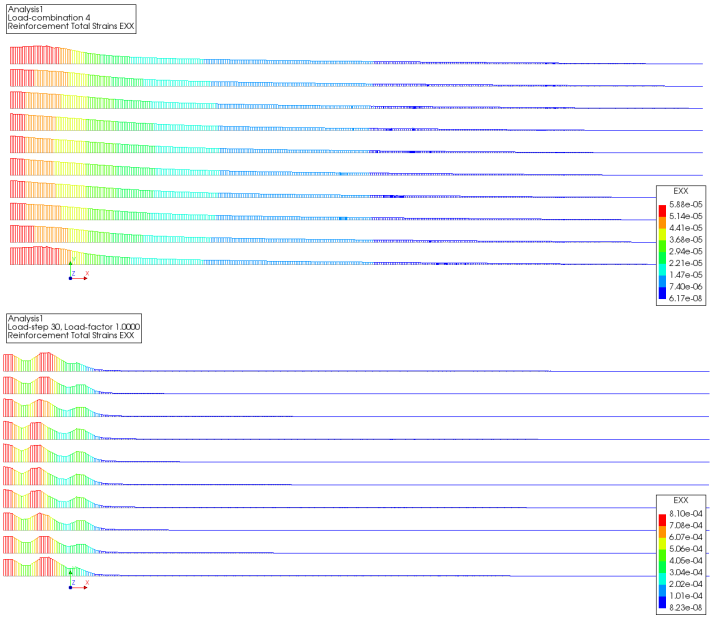

Figure 12.10: Visualization of strain results in longitudinal top reinforcement. Top: results from linear analysis. Bottom: results from nonlinear analysis.

When assessing the strain diagrams of the reinforcement protruding through the ridge in figure 12.10 (the same rebars as in the graphs in figure 12.8), the effect of the geometric disturbance is visible again. In the the results from the linear analysis it can be seen that the maximum strain in the outer bars occurs at the interface between the slab and the ridge and not at the clamped support. The results from the nonlinear analysis furthermore confirm the theory of concrete stress dropping and steel stress increasing within cracks depicted in figure 6.3. The reinforcement strains display that the concrete is cracked over the full width of the interface between the ridge and the slab. This is visible because of the local strain increase in the reinforcement at that interface, lasting the whole width of the ridge.

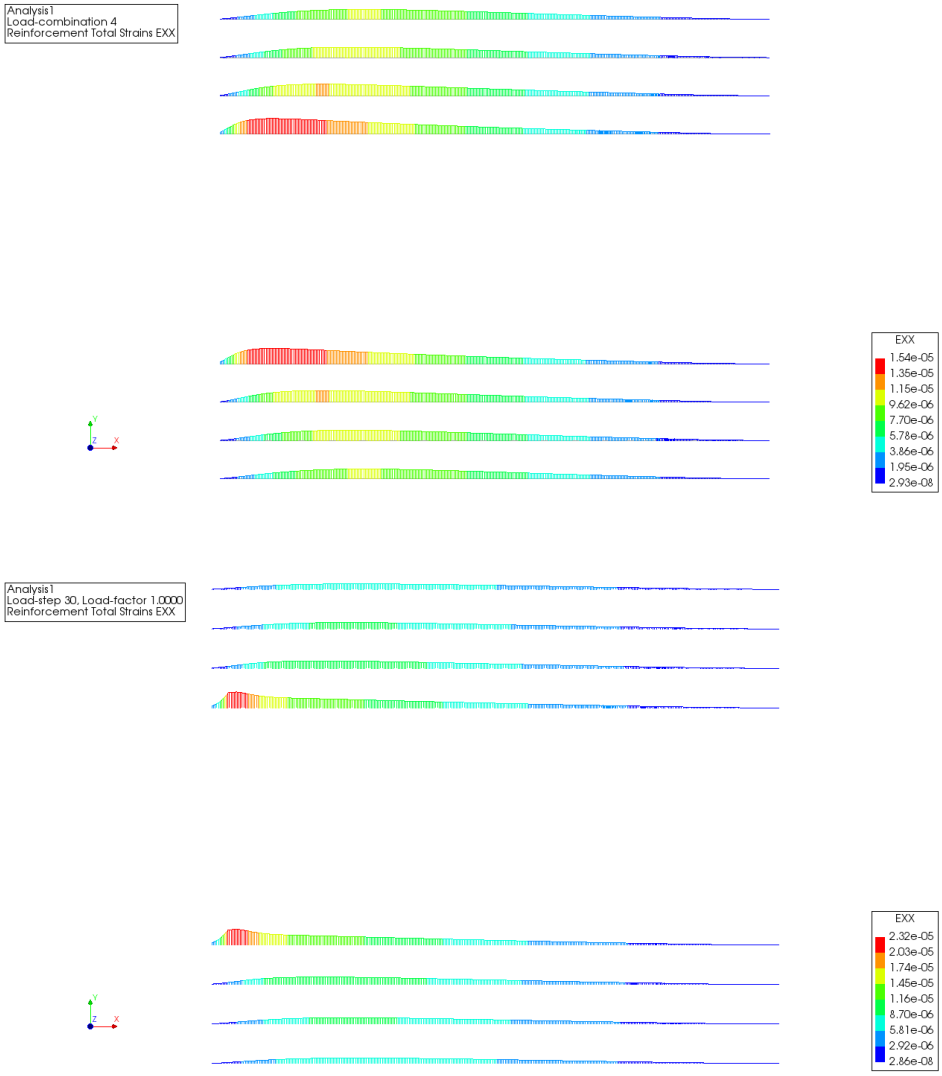

Figure 12.11: Reinforcement strains of rebars outside the ridge visualizing the channelling of forces. The top image follows from the linear analysis, the bottom one from the nonlinear analysis. The rebars from the ridge are intentionally left out since otherwise the results in the other bars are damped out in the visualization because of the differences in magnitude.

13

Comparison of results

This chapter, and specifically table 13.1, presents the results of the numerical analysis and compares them with the analytical results of the design presented in chapter 11.

Element	Category	Numerical	Analytical
Slab	Reinforcement strain	$8.1*10^{-4}$	$5.6*10^{-4}$
	$s_{r,max}$	-	138.3 mm
	Crack width - hybrid	0.11 mm	0.0466 mm
	Crack width - DIANA FEA	0.22 mm	0.0466 mm
	Reinforcement stress	162 N/mm^2	112 N/mm^2
Ridge	Reinforcement strain	$8.1*10^{-4}$	$9.75*10^{-4}$
	$s_{r,max}$	-	149.5 mm
	Crack width - hybrid	0.12 mm	0.094 mm
	DIANA FEA crack width	0.22 mm	0.094 mm
	Reinforcement stress	162 N/mm^2	195 N/mm^2
Corner	DIANA FEA crack width	0.29 mm	0.094 mm
General	Deflection	-6.73 mm	-4.02 mm
	Eigen frequency	6.07 Hz	8.65 Hz

Table 13.1: Comparison of numerical and analytical results for balcony with in-plane ridge.

In table 13.1 the results are subdivided over four 'elements'. For the element 'Slab' the analytical crack width is determined utilizing the width of the slab, whereas for the element 'Ridge' the width of the ridge is used. Since the area around the interface between the slab and the ridge is a geometrically disturbed region this approach should have led to an upper and lower limit crack width prediction for the area around the interface between the ridge and the slab. The crack widths for the category 'Crack width - hybrid' in the numerical columns in the table are produced by multiplying the numerically obtained reinforcement strains in the cracked area with the analytically produced maximum crack spacing $s_{r,max}$, as is explained in paragraph 8.7.

13.1. Crack widths

In the previous chapter it has been observed that the maximum crack width in the numerical analysis occurs in the corner between the ridge and the slab. With the help of an additional linear analysis it was found that this maximum crack width was induced by concentrated peak stresses resulting from the geometric disturbance, being the transition from the full width of the slab towards the width of the ridge.

Comparing the numerically obtained crack widths in table 13.1 with the analytically predicted crack widths, it can be observed that for all elements the numerical crack widths exceed the analytical crack widths. From the background assessment in appendix A on the analytical method proposed by article 7.3.4 in Eurocode 2 and the approach DIANA FEA utilizes, and the differences between those two, it is a logical result that analytically

smaller crack widths are predicted. It becomes clear that the analytical Eurocode 2 method is not able to take into account occurring peak stress concentrations. DIANA FEA is able to take into account these stresses and thus comes up with bigger crack widths.

A remarkable, counter intuitive, characteristic of the results is that the hybrid crack width, which is supposed to compensate for neglecting bond-slip and inhomogeneous behaviour, is smaller than the crack widths predicted by DIANA FEA. After consulting dr. ir. M.A.N. Hendriks from TU Delft, it became clear that the method for the hybrid crack width is mainly developed for structures with a big element size (i.e. an element size bigger than the crack spacing). In part IV the hybrid crack width was again determined and the same phenomenon occurred, confirming that the method is invalid for these small structures. Nonetheless, when interpreting numerical results it should thus still be thought of that bond-slip is not taken into account which could mean that the numerical crack width is an underestimation of reality (see appendix A).

13.2. Crack spacing

An observation worthy of attention is that numerically in the ridge both the crack spacing (extracted from figure 12.4) and the stresses in the reinforcement appear smaller than the results of the analytical prediction but the numerical crack width is bigger. For starters this might be contributed to the fact that the analytical crack width prediction is not suitable for these slender structures with a high concrete cover. As shown in part II of this report, the reinforcement falls out of the effective area resulting in an effective reinforcement ratio equal to zero, which should make the method invalid for this case.

Furthermore, it is observed in the results presented in figure 12.4 that three localized cracks occur. One in the ridge, one on the interface between the slab and the ridge, and one in the slab. However, when analytically predicting crack widths, a maximum crack spacing is determined for a single specific geometry. Because the geometry is disturbed and now is a combination of geometries, the analytical method might not be applicable in this region. Moreover, again in figure 12.4, it can be observed that the crack spacing is not constant over the length of the cracks. This is an effect that cannot be predicted by an analytical method and thus results in an incompatibility.

To finalize, as is already discussed in paragraph 8.7, the analytical prediction of the crack spacing is done with the help of several empirically determined parameters for which it is unknown whether they are valid for HSC and/or slender structures.

13.3. Steel stress

The maximum steel stresses in the category slab appear numerically bigger than analytically predicted. This can be explained by the fact that in the analytical prediction the stress is assumed to be fully spread over the cross section. In the previous chapter however, it is evinced that the load spreads gradually over the width of the slab. Near the ridge in the slab the stresses are thus more concentrated towards the width of the ridge, resulting in a higher numerically obtained steel stress.

For the ridge analytically the steel stress is determined over the width of the ridge. This results in a steel stress bigger than numerically obtained, which is induced by the contribution of the uncracked concrete in the numerical analysis. Despite the cracks a part of the concrete is still contributing to the force equilibrium, resulting in a smaller steel stress than analytically predicted.

13.4. Deflection

Comparing the analytically predicted deflection with the numerically obtained deflection it is observed that the analytical value is smaller than the numerical value. It should furthermore be mentioned that in the analytical prediction creep effects are accounted for, which are not incorporated in the numerical analysis. Taking creep numerically into account would increase the discrepancy even more. The reason for the difference in the results can be brought back to stiffness. The numerically predicted crack widths are bigger than analytically determined. Numerically thus the stiffness is smaller, resulting in a bigger deflection.

13.5. Dynamic behaviour

The reduced stiffness treated in the previous paragraph influences the dynamic behaviour of the balcony too. For the numerical model the spring stiffness is determined by dividing the equivalent force determined in paragraph 11.6 by the deflection that followed numerically from the nonlinear assessment of the characteristic bending moment. Obviously, because of a smaller stiffness, the deflection is bigger, the spring stiffness for the single-mass-spring-system is smaller and thus the eigen frequency turns out smaller. However, the eigen frequency remains in the required range (≥5 Hz) according to Eurocode 2.

IV

Cantilever slab with out-of-plane ridge connection

14

Method

Now that the step towards the balcony with an in-plane ridge has been concluded, the final step towards the remake of a Hi-Con balcony design will be made. This balcony was originally designed in UHPFRC, but will now be designed in HSC, concrete grade C90/105. The balcony slab again will have a constant height and width over the length but this time the ridge will be an out-of-plane one. Applying an out-of-plane ridge is beneficial for the connection to the bearing structure. A schematization of the pursued geometry is displayed in figure 14.1.

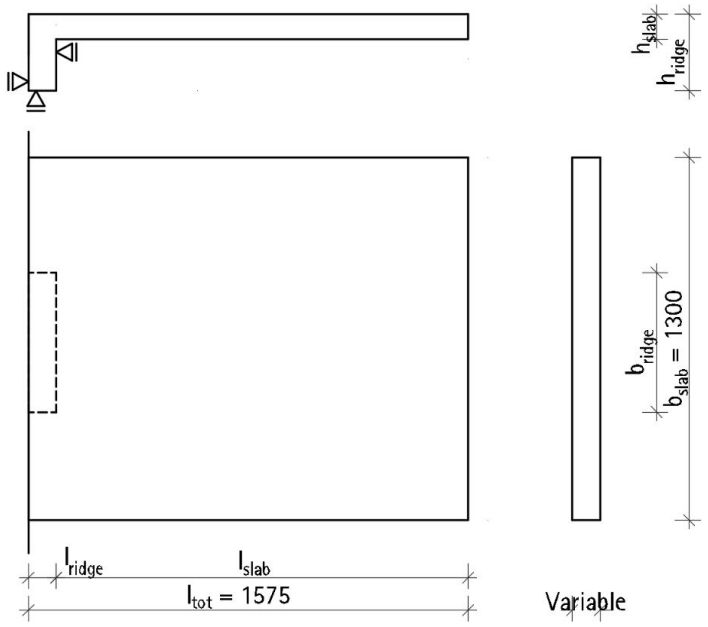

Figure 14.1: Schematic drawing of Hi-Con designed cantilever balcony.

For the design of this balcony the script used for the previous two balcony designs again is modified. The goal of the design of this balcony is to verify or reject the hypothesis that it is not possible/safe to recreate the Hi-Con UHPFRC balcony in C90/105. Possibility will depend mostly on fulfilling detailing demands whereas when speaking about safety durability is meant.

To finalize this research the analytical results will again be compared with structural non-linear finite element analysis results from DIANA FEA.

15

Design

This chapter specifically elaborates on the additions and developments of the script from part III of this report to become able to design and check the HSC Hi-Con shaped balcony depicted in figure 14.1. Since the script of part III has been used as a basis, treating the complete new script will result in a lot of duplicate information on characteristics and methods. The full script can be found in appendix J. It is advised to read this chapter accompanied by the script. Additionally a strut-and-tie model has been developed for designing the ridge and the onset of the slab since those are disturbed regions.

15.1. Supports

In practice the engineers from Pieters Bouwtechniek have developed a connection for this balcony in co-operation with Schöck. It has been assumed that this connection is suitable for this balcony design as well, resulting in the support reactions presented in figure 15.1 and 15.4. It has been assumed that each supporting force is spread over an area of 50 x 250 mm, which in practice can be realized with the application of small steel plates and/or profiles. More about the spreading of the support forces can be found in paragraph 15.7. The reasoning behind the locations of the supports is that it is desirable to only have supports resulting in compressive supporting forces.

15.2. Loading

The balcony is loaded in a similar manner as the balcony in part III of this report. During the design and check process a distinction between the loading in the slab and in the ridge is being made. The maximum loading on the ridge is determined at location 1 in figure 15.1, whereas the maximum loading on the slab is determined at location 2.

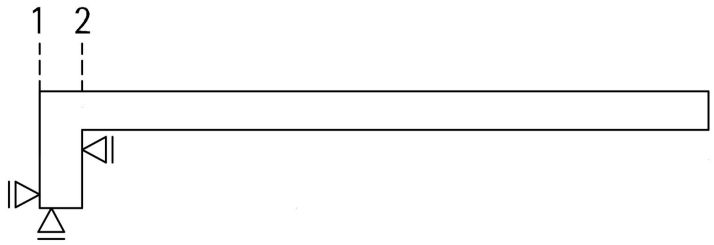

Figure 15.1: Locations where cross sectional loads are determined.

15.3. Bending moment resistance

The balcony's bending moment resistance is determined at locations A, B and C, depicted in the bending moment diagram in figure 15.2, in a similar manner as for part II and III of this report. At location A the horizontal cross section of the ridge is checked for the moment at that location. Locations B and C are chosen to establish an upper and lower limit of the bending moment resistance of the slab near the ridge. In B the

bending moment resistance of the slab with just the width of the ridge has been calculated and compared to the maximum occurring moment (at the corner), resulting in a lower limit of the bending moment resistance. In C the full cross section of the slab has been accounted for, which results in an upper limit. This approach has been chosen since the region near the ridge is a transition zone where the active width lies somewhere between the width of the slab and the width of the ridge. The main reinforcement in this area is determined through the application of a strut-and-tie model, described in 15.5.

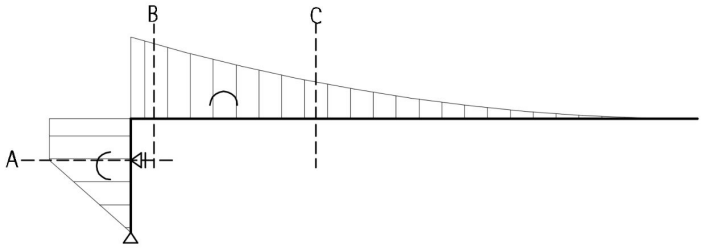

Figure 15.2: Bending moment diagram with indication of sections.

15.4. Shear force resistance

The shear force resistance is determined and checked with a comparable tactic as the bending moment resistance. In the slab no shear reinforcement is allowed because of the height being smaller than 200 mm. Once more the resistance is calculated at B with the width of the ridge and at C with the full width of the slab. In B and C the vertical shear resistance is calculated with the height of the slab.

Determining the shear resistance and designing shear reinforcement at location A is more difficult. For starters the ridge does not fulfil the requirement of slab geometry and thus shear reinforcement may be applied for smaller dimensions. This shear force is calculated with the strut-and-tie model from figure 15.4. The process of creating and checking a strut-and-tie model is further elaborated in paragraph 15.5.

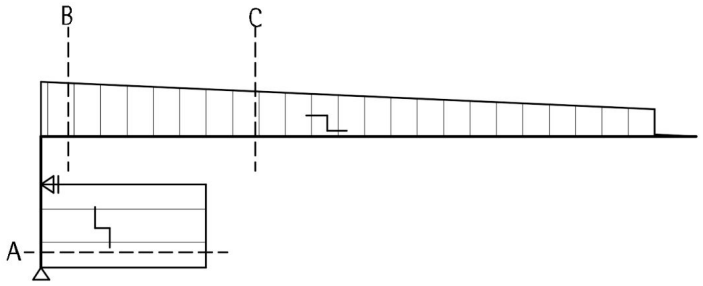

Figure 15.3: Shear force diagram with indication of sections.

The first step in determining the shear force resistance is looking at it without reinforcement. The shear force may be reduced in case the demands in the second case in equation 15.1 are met, following from chapter 6.2 in Eurocode 2 and [7]. In this equation $V_{Ed,0}$ represents the actual working shear force and this force may be checked against $V_{Rd,c}$.

$$V_{Ed} = \begin{cases} V_{Ed,0} \\ \frac{a_v}{2*d} * V_{Ed,0} \quad for \quad V_{Ed} \leq 0.5 * b * d * \left(0.6 * \left(1 - \frac{f_{ck}}{250}\right)\right) \quad and \quad 0.5 \leq \frac{a_v}{d} \leq 2 \end{cases} \tag{15.1}$$

In case V_{Ed} is bigger than $V_{Rd,c}$ shear reinforcement is applied for the non-reduced shear force and the shear force resistance is checked according to the moethod proposed by paragraph 6.2.3 in Eurocode 2.

15.5. Strut-and-tie model

The complete ridge and the first part of the slab are so called disturbed regions (introduction of disturbed regions in paragraph 11.4) because of the geometric irregularities and concentrated support loads. The ridge

can be regarded as a console (rotated) and may be designed with the help of a strut-and-tie model.

Utilizing the information in the Cement articles [7], [3], [4], and [5] written by dr. ir. C.R. Braam a strut-and-tie model in the shape depicted in the right image in figure 15.4 emerged as a representation of the ridge-slab-connection interaction.

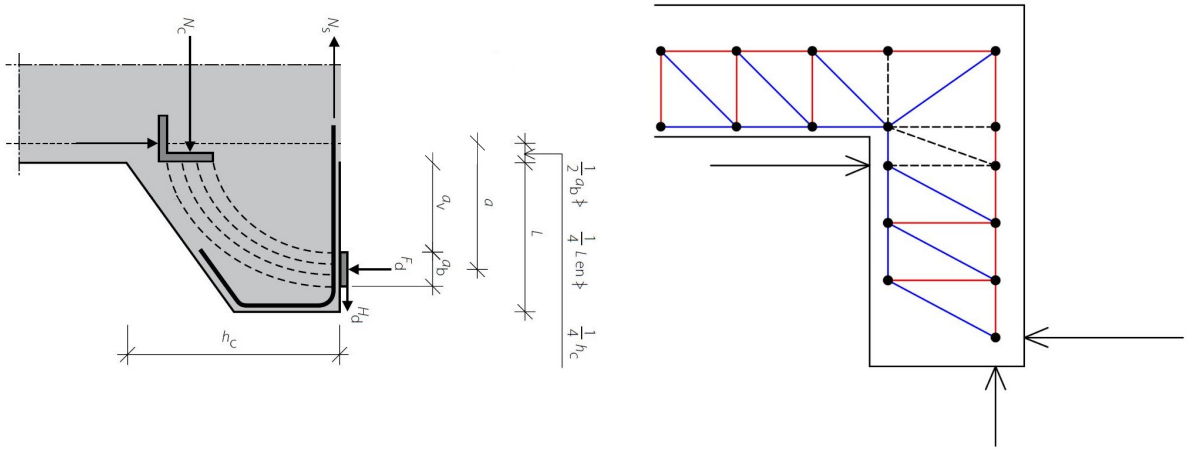

Figure 15.4: Left: modified image of a console, source original image: [7]. Right: Strut-and-tie model of ridge with reaction forces. The red lines indicate tensile ties whereas the blue lines represent the compressive struts. The black dotted lines indicate bars without normal forces. The arrows represent support reactions.

According to [7], the console may be considered as a deep beam in case $2a \leq 3h_c$. For that instance the internal lever arm is determined with equation 15.2.

$$z \begin{cases} = 0.2 * l + 0.4 * h \\ \leq 0.8 * l \end{cases} \tag{15.2}$$

The general lay-out of the strut-and-tie model then emerges in an iterative way from the main geometry, the location of the tensile reinforcement, the internal lever arm, the boundaries for the angle between a compressive diagonal and a tensile tie, and a practical configuration of the reinforcement. According to article 6.2.3(2) in Eurocode 2 the angle θ, the angle between the compressive strut and the tensile tie, should fulfill the demand expressed in equation 15.3.

$$1 \leq cot\theta \leq 2.5 \rightarrow 45^o \leq \theta \leq 62.8^o \tag{15.3}$$

Loading the strut-and-tie model with the supporting forces and assuming supports at the tensile tie and compressive strut in the slab, the normal forces can be found.

Following the advice of several engineers at Pieters Bouwtechniek it has been decided to not perform checks on the capacity of the knots and the compressive struts.

15.6. Stiffness, deflection and the first eigen frequency

Because of the fact that the ridge is well supported for the determination of the stiffness, deflection, and the first eigen frequency it is assumed that deformation takes place in a similar manner as for the balcony in part III of this report. More explicit: it is assumed that the ridge has the same height as the slab and is clamped at the end. Figure 15.5 schematizes the effect on which this decision is based.

Corresponding to the balcony with the in-plane ridge the influence of the bearing structure and the connection system is neglected. This results in an underestimation of the total deformation and should be taken into account when interpreting the results.

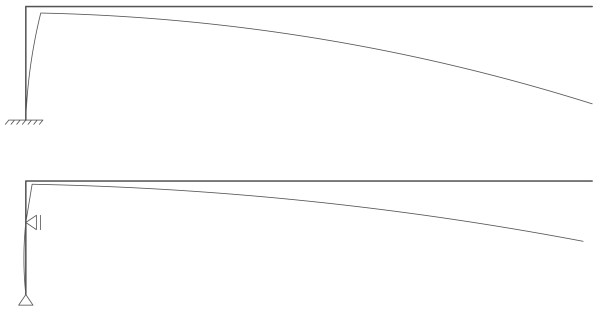

Figure 15.5: Schematization of difference in deformation behaviour due to support.

15.7. Splitting forces

In paragraph 11.4 the influence of disturbed regions has been discussed with the help of the splitting force in the bottom of the slab displayed in figure 11.3. The same mechanism might occur for the balcony with the out-of-plane ridge. However, results from the non linear finite element analysis showed that the effect of the splitting force was not noticeable. This has to do with the bending moment in cross direction of the slab. This cross bending moment, mostly due to the dead weight of the balcony, induces an analytically determined compressive stress in the bottom of the slab of around 2 N/mm^2, determined with the schematization presented in figure 11.7. When the splitting force is evenly spread over the concrete, the induced tensile stress is around 0.2 N/mm^2 resulting in a residual compressive stress of 1.8 N/mm^2.

To prevent the support forces from inducing splitting forces as depicted in figure 15.6, the support loads are spread over an area of 50 x 250 mm. In practice this can be achieved by applying small steel profiles/plates to evenly spread the load. The minor splitting force that will remain can be taken up by the concrete and/or reinforcement in that area.

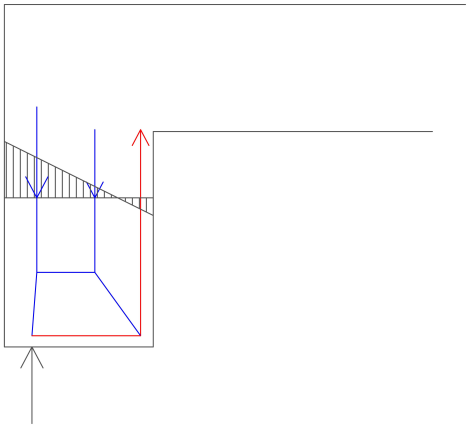

Figure 15.6: Visualization of splitting force induced by vertical compressive supporting force.

15.8. Detailing

The biggest challenge designing this balcony is fitting in all reinforcement according to the detailing rules in chapter 8 and 9 of Eurocode 2. Eventually this is what governed the slab height and ridge thickness. For the slab, to fit in all longitudinal and cross reinforcement and maintaining a free space of at least 21 mm between the top and bottom cross layer, a certain height will be required. The required free space follows from article 8.2(2) in Eurocode 2 and is a result of the maximum grain size, equal to 16 mm, increased by 5 mm. For the thickness of the ridge the maximum distance between the legs of the shear reinforcement appeared to be governing (≤0.75*d according to article 9.2.2(8) in Eurocode 2). To fulfil the requirement the reinforcement height d had to be increased, which lead to an increase in ridge thickness.

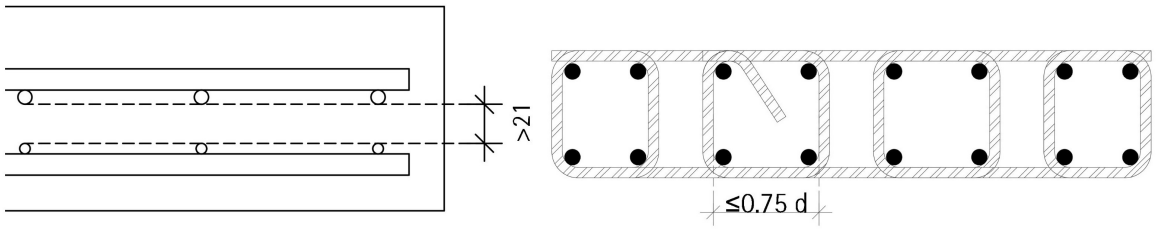

Figure 15.7: Governing detailing aspects for slab height and ridge thickness.

The detailing of areas far away from the ridge has been neglected under the assumption that it will not contribute to the relevance and accuracy of this research. Aspects that are left out are for example detailing of reinforcement at the edges, anchoring of the bars at the edges of the slab, etc. In the areas of interest it has been pursued to fulfil all Eurocode 2 detailing demands. The anchorage of the main reinforcement is facilitated by bending the main reinforcement into the ridge.

15.9. Design results

In table 15.1 and figure 15.8 the final design of the balcony with an out-of-plane ridge is presented. In appendix L the images are presented in a larger size. The balcony possesses a lot of similar characteristics compared to the one in part III of this report. The biggest differences are mainly found in and near the area of the ridge.

Geometry

The lower limit height of the slab again is dependent of the free vertical space between the reinforcement bars demand, as is depicted in figure 15.7. The reason behind an increase of 5 mm compared to the balcony in part III is an increase of reinforcement diameters. The diameters are increased for the ridge to be able to withstand the bending moment in between the supports. The tapered shape of the Hi-Con balcony with a minimum height of 65 mm and a maximum height of 110 mm thus cannot be copied.

The length of the ridge is iteratively established taking into account bending moment and shear resistance and detailing rules like reinforcement ratio and reinforcement spacings and distances. The ridge is densely packed with shear reinforcement because of the high shear force induced by the horizontal load bearings. The exact configuration of the shear reinforcement is depicted in figure 15.9. The configuration emerged from a trial and error process. Again it appeared that the thickness of the ridge in the Hi-Con balcony (100 mm) could not be reproduced in HSC because of detailing rules.

In correspondence with the balcony from part III the reinforcement from the ridge protrudes through the total length of the balcony because of the extensive dimension of the disturbed region. The diameter of the reinforcement in the compressed part of the ridge is determined according to the fact that a big differentiation in reinforcement diameters is undesirable regarding shrinkage after casting of the element.

Design check results

Table 15.2 presents the results of the design checks on the design presented in figure 15.8. The first element in the location column states *Transition zone slab to ridge*, this zone is marked in red in figure 15.10. Since this area is a disturbed region, besides the check with the strut-and-tie model, it is checked with a fictitious lower limit cross sections. This fictitious cross section has the height of the slab and the width of the ridge and only the reinforcement of the ridge is taken into account. This results in a lower limit of the capacity of this part and thus is a conservative check.

In appendix K the results following from the strut-and-tie model are more explicitly presented.

Element	Global dimensions	[mm]
Slab	Length	1575
	Width	1300
	Height	115
Ridge	Length	135
	Width	500
	Height	315
Reinforcement	Ridge top	8 x ⌀12
	Slab top	8 x ⌀12 2 x 4 x ⌀8-100
	Slab top cross	⌀8-100
	Slab bottom grid	3 x 8 sections of ⌀6-100
	Shear stirrups	⌀6

Table 15.1: Main geometric properties of final design of balcony with out-of-plane ridge connection.

Location	Category	Capacity		Acting		UC [-]
Transition zone slab to ridge	Bending moment	26.0	kNm	11.7	kNm	0.45
	Shear force	53.3	kN	11.4	kN	0.21
	Crack width	≤ 0.20	mm	0.08	mm	0.40
	Cross bending moment	13.5	kNm	5.6	kNm	0.41
Ridge	Bending moment	36.6	kNm	19.2	kNm	0.74
	Shear force vertical	119	kN	12.0	kN	0.10
	Shear force horizontal	155.7	kN	128	kN	0.82
	Crack width	0.30	mm	0.04	mm	0.13
Strut-and-tie model	Vertical tensile force ridge	394	kN	273	kN	0.7
	Vertical shear force slab	12	kN	53.6	kN	0.22
	Horizontal shear force ridge	155.7	kN	128	kN	0.82
General	Eigen Frequency	≥ 5	Hz	8.8	Hz	-
	Deflection	≤ 12.6	mm	3.83	mm	0.30

Table 15.2: Design check results for balcony with out-of-plane ridge connection. In the transition zone a fictitious cross section with the height of the slab and the width of the ridge is considered.

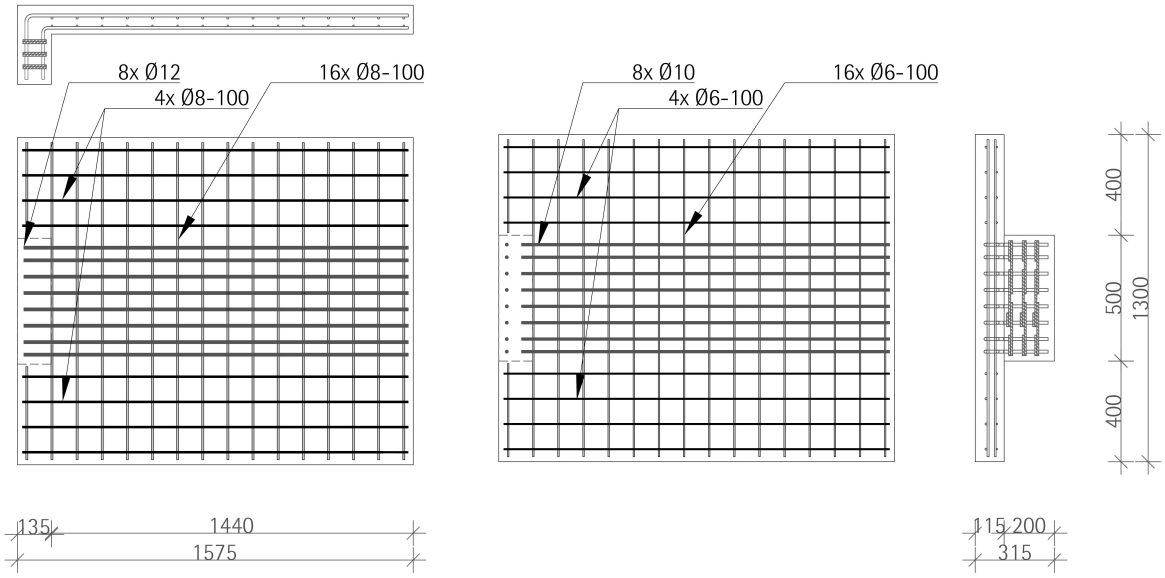

Figure 15.8: Final design remake of Hi-Con balcony. Left: Top reinforcement. Right: Bottom reinforcement. A bigger version of the design images are attached in appendix L.

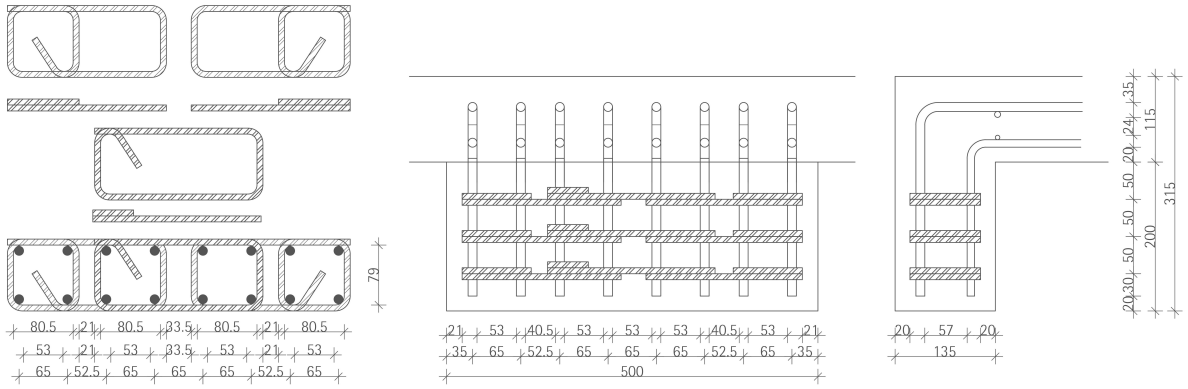

Figure 15.9: Lay-out shear reinforcement. A bigger version of the image is attached in appendix L.

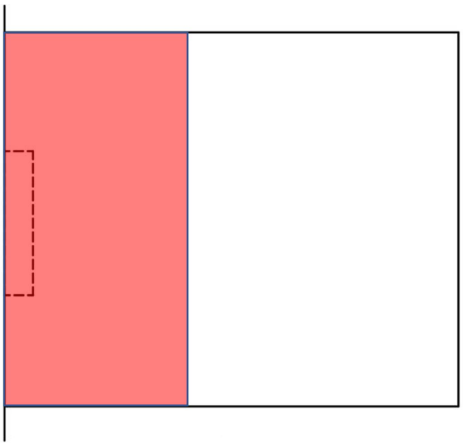

Figure 15.10: Visualization of transition zone where a fictitious cross section is used to determine shear force and bending moment resistance.

16

Numerical analysis DIANA FEA

The similarities between the DIANA FEA models of part III and IV of this report are big. To prevent excess duplicate information it has been decided to only treat some characteristics on short notice. A further elaboration can be found in chapter 12 and appendix D.

16.1. Geometry

The geometry of both the concrete and reinforcement design which emerged from the previous chapter has been modelled in DIANA FEA, resulting in the model displayed in figures 16.1 and 16.2.

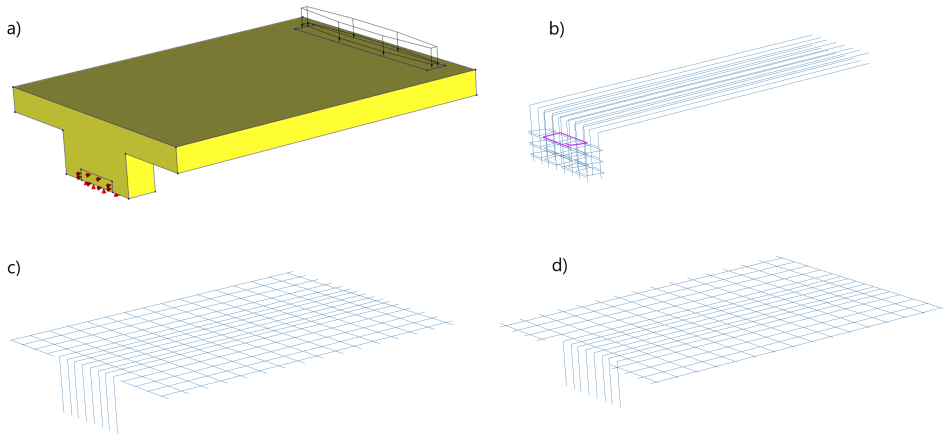

Figure 16.1: a) Overview of main geometry of balcony slab with out-of-plane ridge. b) Display of main reinforcement in ridge, protruding completely through the slab in combination with shear reinforcement in ridge. c) Reinforcement in top of slab and backside of ridge. d) Reinforcement in bottom of slab and frontside of ridge.

16.2. Meshing

The results from the mesh refinement study of chapter 12 have been used since a large part of the geometry is similar. The conclusion on the mesh refinement study was that a mesh smaller than 20 mm appeared not feasible in terms of insufficient resources like computational power and digital storage space. Thus again a mesh of 20 mm is applied. DIANA FEA also applies similar isoparametric quadrilateral solid elements, listed below.

- CHX60
- CPY39
- CTE30
- CTP45

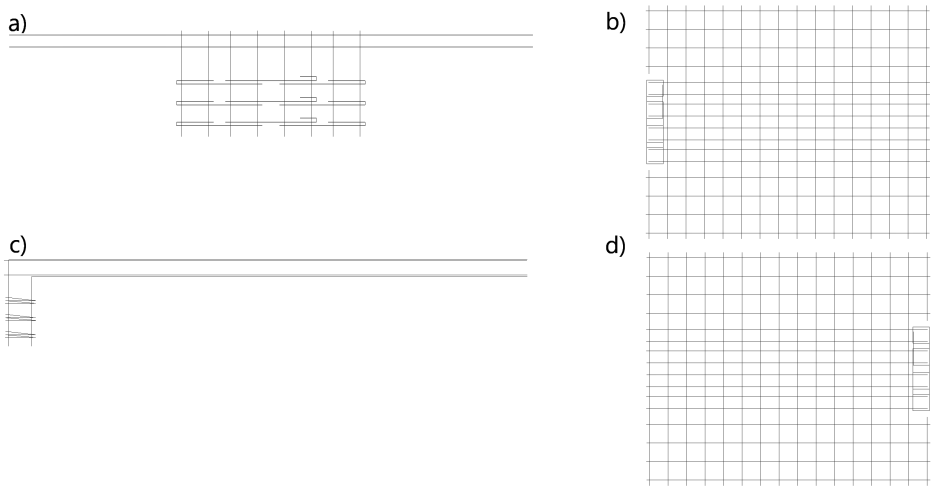

Figure 16.2: a) Backside view of reinforcement in ridge and slab. b) Top view of reinforcement in ridge and slab. c) Side view of reinforcement in slab and ridge. Difference in vertical location of longitudinal reinforcement occurs because of different reinforcement diameters. d) Bottom view of reinforcement in slab and ridge.

16.3. Boundary conditions

The restraints for the supports are in accordance with figure 15.1. This means that the bottom of the ridge is supported only in vertical direction and that the ridge is supported on two locations in horizontal direction.

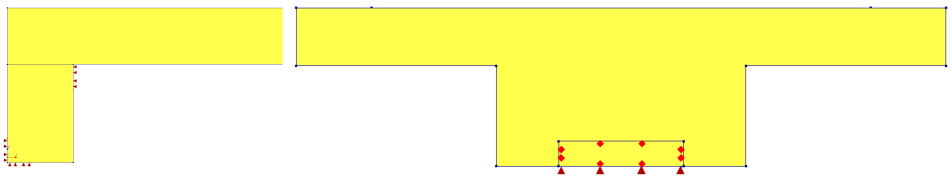

Figure 16.3: Display of boundary conditions modelled in DIANA FEA from the side and the back.

16.4. Loading, material models and the numerical analysis

The loading, the material models and the characteristics of the numerical analysis fully correspond to those presented in chapter 12.

16.5. Results

This pararaph elaborates on several characteristics of the results from the numerical analysis. More visualizations of the results from the analysis performed with DIANA FEA are attached in appendix M. Again, to find a clarification for some characteristics of the nonlinear results a linear analysis for the frequent load combination is executed.

Crack pattern

In a similar way as in paragraph 12.7 the numerical results, both linear and nonlinear, are assessed. For this chapter three cross sections have been used (1, 2, and 3), depicted with the red lines in figure 16.4, because now stresses and strains in both x (longitudinal) and z (vertical) direction are of importance.

In the corner between the ridge and the slab, at the location where the backside of the ridge and the backside of the slab are connected (figure 16.6), the maximum crack width is found. Here, in a similar way as in part III, the width over which the bending moment is transferred, is suddenly decreased. The crack patterns of the slab and the ridge are visualized in figures 16.5 and 16.6.

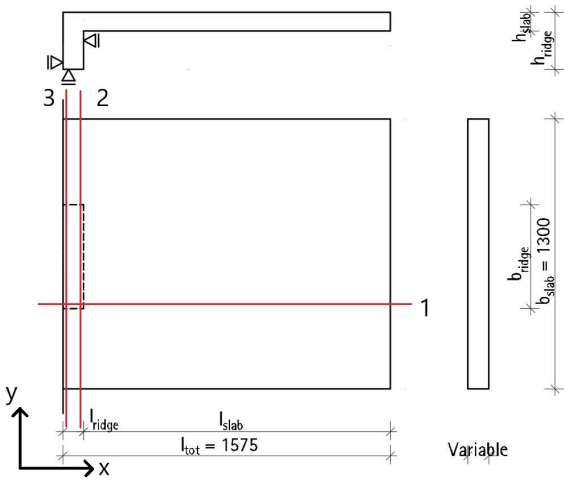

Figure 16.4: Visualization of locations of utilized cross sections for the analysis of the numerical results for the balcony with the out-of-plane ridge.

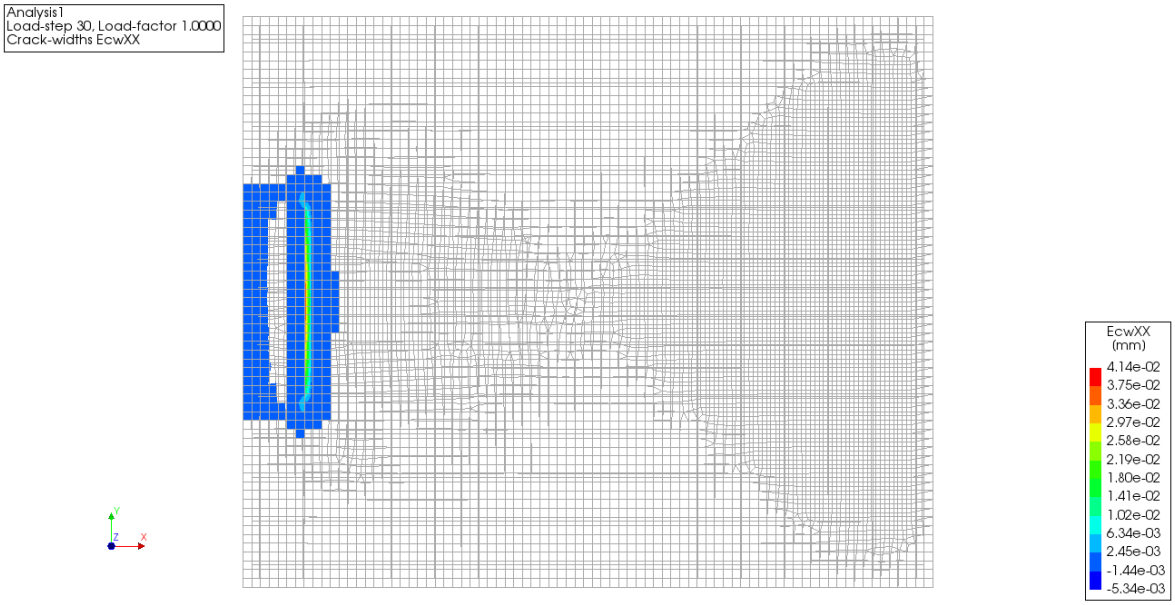

Figure 16.5: Crack width in x-direction from frequent load combination after characteristic load combination has occurred.

Stresses and strains in x-direction (slab)

It is observed in figures 16.9 and 16.10 that no concentrated peak stresses occur despite the fact that the slab is only locally connected to the ridge. It appears that the strain distribution behaves undisturbed. This is endorsed by the reinforcement stresses presented in figure 16.7, and a zoom into the bars protruding the ridge in figure 16.8. To the contrary of the reinforcement stresses in the balcony with the in-plane ridge it can now be observed that the maximum stress occurs in the middle at the bars with the biggest diameter. In figure 16.5 it is shown that at this location indeed the biggest cracks occur. The maximum tensile stresses occur directly above the edge of the ridge, as is visible in figures 16.9 and 16.10, because that edge of the ridge functions as an 'intermediate support' (visualized in figure N.2).

In appendix N a clarification for the absence of concentrated peak stresses has been sought for. From this research it appears that no peak stress concentrations occur because the top of the slab is undisturbed in the area loaded in tension, contrary to the balcony with the in-plane ridge. It appears that tensile peak stress concentrations are induced by a geometric disturbance of an area loaded in tension. It is also found that the

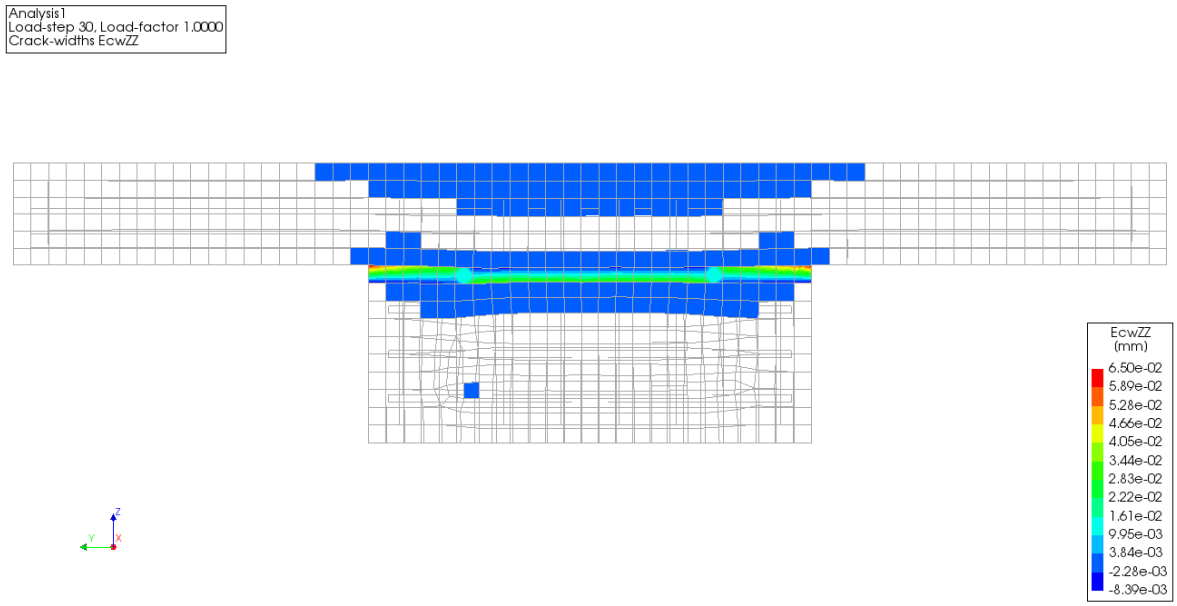

Figure 16.6: Crack width in z-direction from frequent load combination after characteristic load combination has occurred.

more slender the cross section, the more pronounced the effect is.

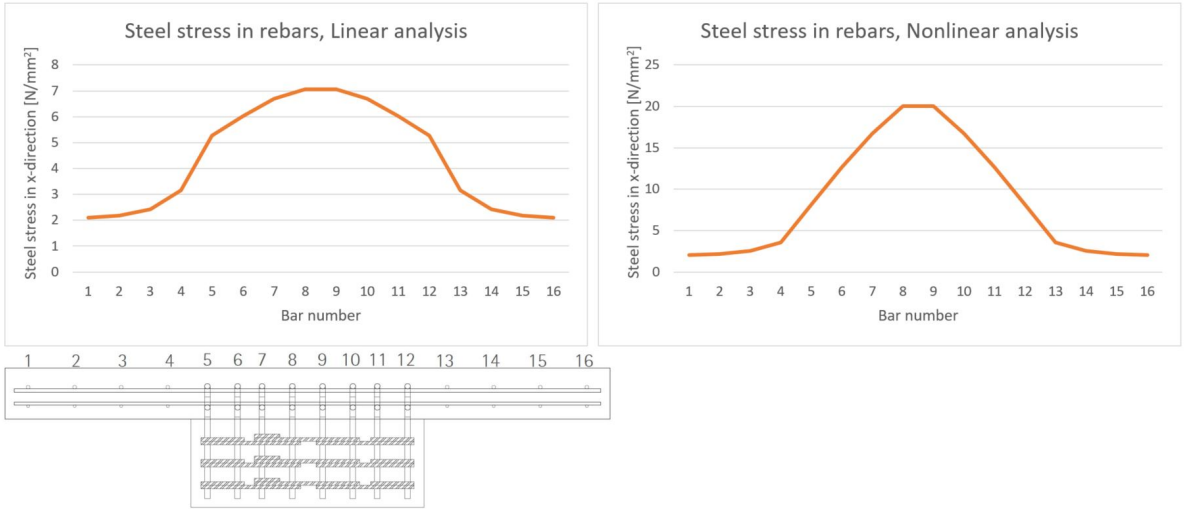

Figure 16.7: Visualization of distribution of reinforcement stresses in reinforcement bars over the full width of the slab at the location with the out-of-plane ridge. The left graph depicts the stresses obtained through the linear analysis, the results in the right graph originate from the nonlinear analysis. The bottom image presents the bar numbers against which the stresses are plotted.

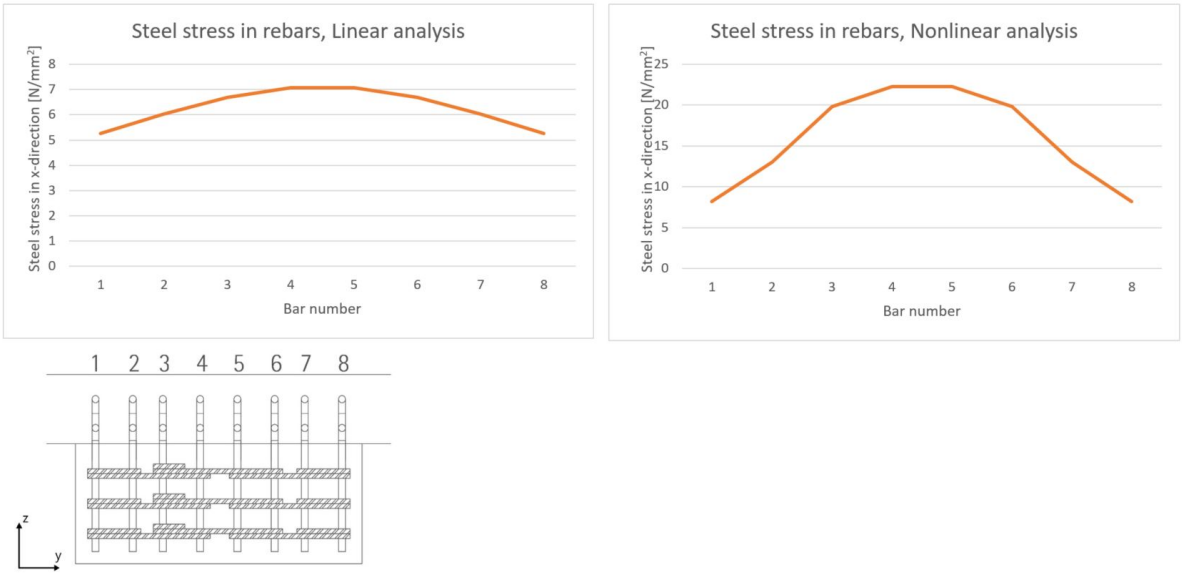

Figure 16.8: Reinforcement stresses in x-direction of bars protruding through the ridge. The results are a zoom in on the bars in the middle of the graphs in figure 16.7 The bottom image depicts the reinforcement numbering.

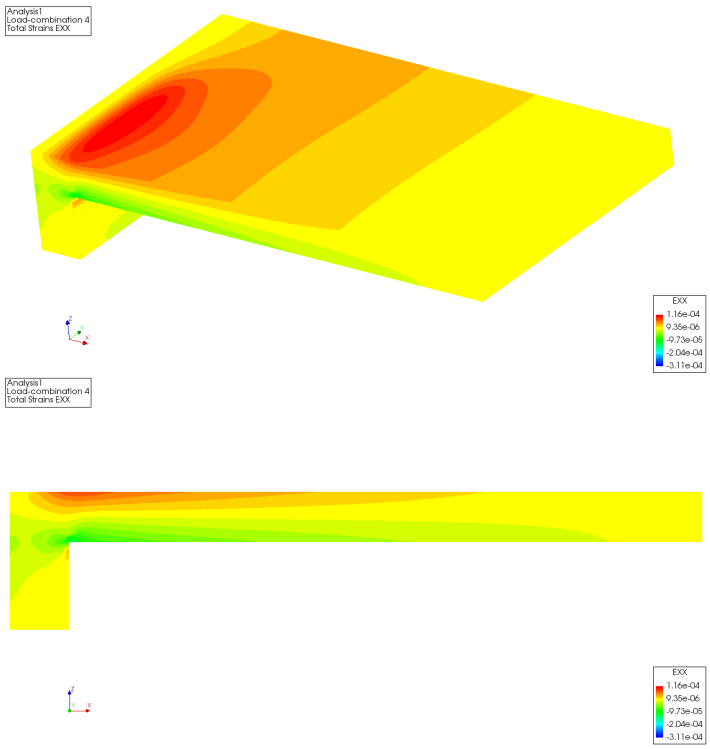

Figure 16.9: Visualization of strains in x-direction in longitudinal cross section (cross section 1) following from the linear analysis. The top image presents an overview to visualize where the cross section has been made.

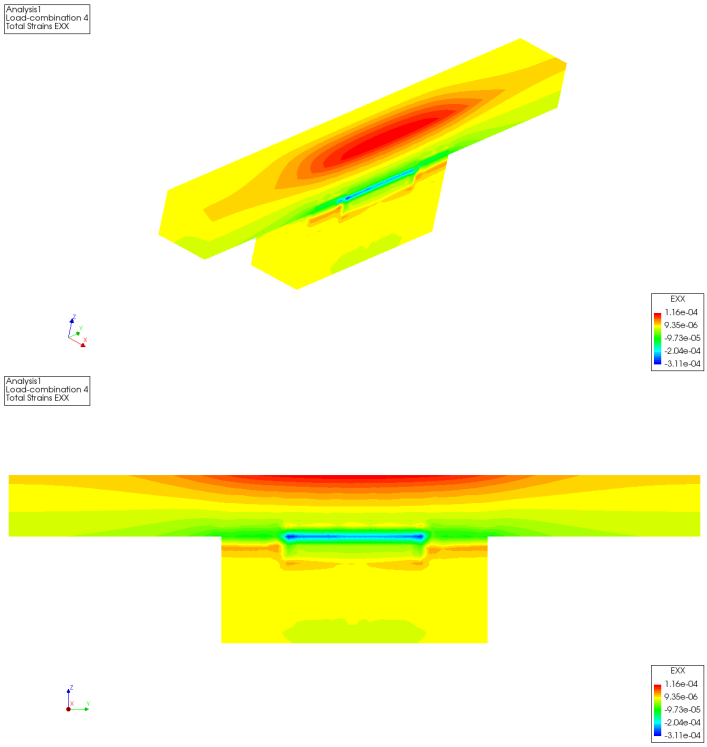

Figure 16.10: Visualization of strains in x-direction at the interface between the slab and the ridge (cross section 2) following from the linear analysis. The top image presents an overview to visualize where the cross section has been made.

Stresses and strains in z-direction (ridge)

In a similar manner as for the stresses and strains in x-direction, the stresses and strains in z-direction at the backside of the ridge and slab following from the linear analysis are assessed. They are presented in figure 16.12 and 16.13. It can be observed that a similar phenomenon as in part III appears. The stress and strain distributions again are disturbed by the transition from the width of the slab towards the width of the ridge. This results in bigger strains and stresses, and thus crack widths, at the edges of the ridge, see figure 16.11. Where initially the maximum steel stress would occur in the middle, because of the peak stress concentrations induced by the geometric disturbance the stress distribution shifts and the bars at the edge are loaded heaviest.

It can be observed however that the effect is less pronounced compared to the results of the balcony with the in-plane ridge resulting in numerical cracks with a smaller width. In appendix N a clarification for this effect is sought for and found in a combination of three aspects.

1. The eccentric normal compressive supporting force following from the shear force reduces, although marginally (substantiated in appendix N), the tensional stresses in the outer fibre of the ridge in part IV.
2. The height of the ridge in part IV to take up the bending moment (135 mm) is bigger than the height of the ridge in part III (110 mm), resulting in a bigger internal lever arm (substantiated in appendix N).
3. The concrete cover in the ridge in part IV equals 20 mm and the ridge in part III possesses a concrete cover of 35 mm, resulting in an increase of the internal lever arm (substantiated in appendix N).

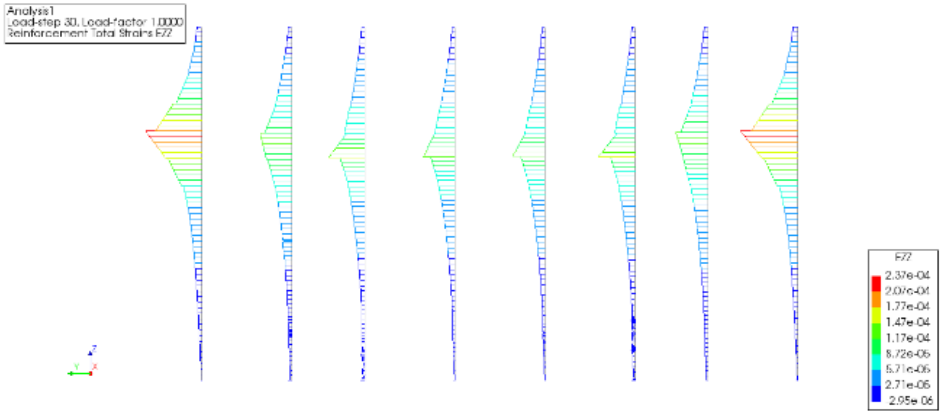

Figure 16.11: Strains in z-direction in reinforcement at the back side of the ridge following from the nonlinear analysis.

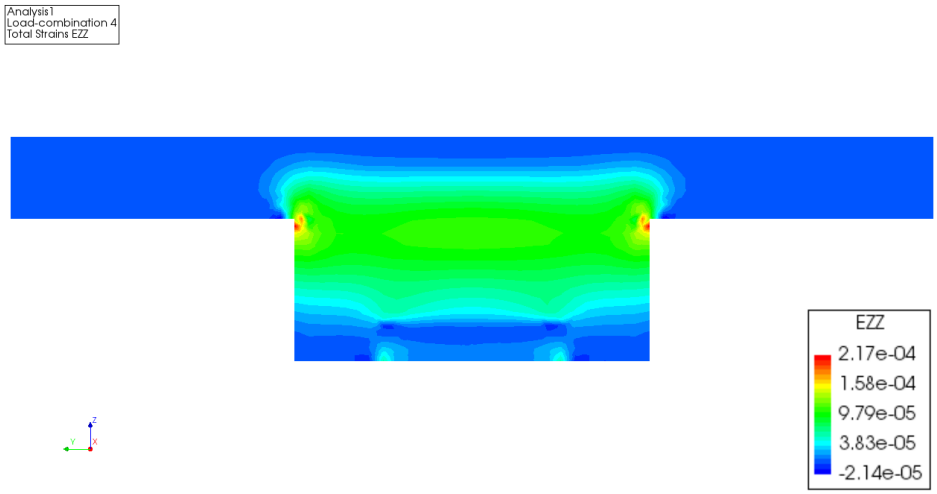

Figure 16.12: Strains in z-direction at the back side of the ridge (cross section 3) following from the nonlinear analysis.

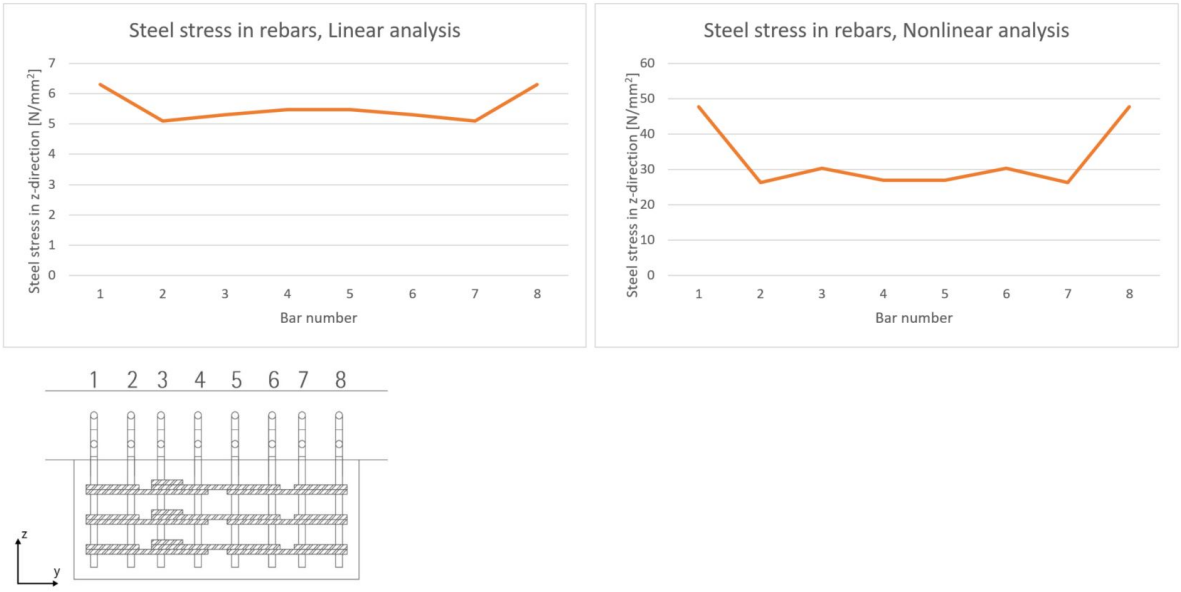

Figure 16.13: Steel stresses in z-direction in reinforcement at backside of slab. The image on the bottom depicts the reinforcement numbering against which the stresses are plotted.

Steel stresses

The difference between the linearly and nonlinearly obtained steel stresses depicted in figures 16.7, 16.8 and 16.13 can, similar to part III, be contributed to the contribution of the concrete in the linear analysis. In the linear analysis the concrete does not crack and has no tensile strength limits, strains thus are smaller resulting in smaller steel stresses.

It is observed that the steel stresses in the ridge are significantly smaller compared to part III. Firstly, as discussed in appendix N, this can be contributed to a bigger internal lever arm induced by a higher cross section and a smaller concrete cover. Furthermore, the steel stresses are smaller because cracking is less severe. The smaller cracks result in a bigger contribution of the concrete around the cracks and thus smaller steel stresses.

17

Comparison of results

This chapter elaborates on the difference in results between the analytical and numerical analysis from the past two chapters. Table 17.1 contains the results from both analysis for comparison.

Element	Category	Numerical	Analytical
Slab	Reinforcement strain	$1.11*10^{-4}$	$8.45*10^{-4}$
	$s_{r,max}$	-	151.8 mm
	Crack width - DIANA FEA	0.041 mm	0.081 mm
	Crack width - Hybrid	0.017 mm	0.081 mm
	Reinforcement stress	22.3 N/mm^2	169 N/mm^2
Ridge	Reinforcement strain	$2.37*10^{-4}$	$6*10^{-4}$
	$s_{r,max}$	-	106.1 mm
	Crack width - DIANA FEA	0.032 mm	0.040 mm
	Crack width - Hybrid	0.025 mm	0.040 mm
	Reinforcement stress	47.5 N/mm^2	124 N/mm^2
Corner	Crack width - DIANA FEA	0.065 mm	0.040 - 0.081 mm
General	Deflection	-2.39 mm	-3.83 mm
	Eigen frequency	10.2 Hz	8.8 Hz

Table 17.1: Comparison of numerical and analytical results for balcony with out-of-plane ridge.

The crack width results in table 17.1 are composed in a similar manner as the results in chapter 13. The crack widths in the rows belonging to 'Slab' in the table are crack widths for the coloured area on the top of the balcony in figure 17.1, where the crack widths belonging to 'Ridge' are located at the coloured area on the ridge. The location of the circle again represents the element Corner. The hybrid crack widths again appear smaller than numerically obtained crack widths, confirming the hypothesis described in paragraph 13.1. For this reason they are not further addressed.

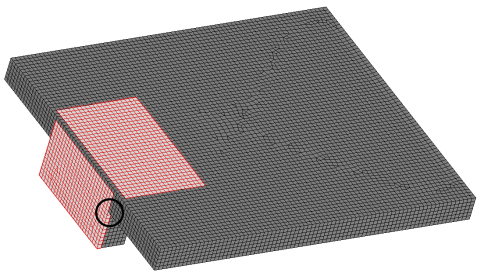

Figure 17.1: Area's of interest for the analysis of crack widths and reinforcement strains and stresses. The location of the circle belongs to element Corner in table 17.1.

17.1. Crack width in slab

From the results in table 17.1 it is observed that the analytically predicted crack widths for the slab are bigger than the numerically obtained values. For starters, as has been assessed in paragraph 16.5, the slab is not prone to concentrated peak stresses. The absence of these peak stresses limit the numerically obtained crack widths. It turns out that the conservative characteristics of the analytical method (described in appendix A) result in bigger crack width predictions compared to the numerically obtained results. It should however be kept in mind that numerically bond-slip is not accounted for which reduces the numerically predicted crack width.

It should be mentioned that the crack width in the slab near the ridge is analytically determined in a conservative way with a reduced cross section possessing the width of the ridge (500 mm) in stead of the width of the slab (1300 mm). This conservative choice is made because the slab is connected over this width of 500 mm after which the effective cross section gradually increases towards the width of the slab. However, cracking occurs before the force distribution is spread over the full width of the slab, predicting crack widths with the full width thus would be too optimistic. This effect is assessed and visualized in figure 12.11 attached in paragraph 12.7. When considering the full width of the slab the analytical crack width prediction results in 0.046 mm, which is close to the numerical value. From this fact it can be concluded that the conservative characteristics even outweigh the effect of the analytical analysis of an unrealistically wide cross section.

17.2. Crack width in ridge and corner

The results of the crack width predictions in table 17.1 show that all analytical predictions result in bigger crack widths than numerically obtained. This result is remarkable since, as discussed in paragraph 16.5, in the transition zone from the backside of the ridge towards the backside of the slab concentrated peak stresses occur. However, it has also been observed in paragraph 16.5 and appendix N that the effect of the geometric disturbance for the balcony with the out-of-plane ridge is less pronounced compared to the balcony with the in-plane ridge. In appendix N it appeared that elements with a smaller slenderness and concrete cover are less prone to the effect of the peak stress concentrations, resulting in less severe numerical crack widths.

17.3. Crack spacing

When analytically predicting the maximum crack spacing, this is done for a single geometry. In this case thus separately for the ridge and the slab. From the numerical analysis it appears that in both geometries only one crack occurs, see figures 16.5 and 16.6. It is thus not possible to compare the numerical crack spacing with the analytically predicted maximum crack spacing. I case more than one localized crack in both geometries occurred, the comparison would have been possible.

17.4. Steel stress

The steel stresses determined by the numerical analysis are smaller than the analytically predicted stresses. This can be contributed to the fact that because of smaller cracks the concrete contributes more to the force equilibrium and thus a smaller steel strain (and stress) is required. The cracks in the slab are smaller because no peak stress concentrations occur. In the ridge they are smaller because of a higher cross section and a reduced concrete cover compared to the balcony with the in-plane ridge, reducing the effect of the geometric disturbance.

17.5. Deformation

Contrary to the balcony in part III of this report the analytically predicted deformation is bigger than the numerically obtained value. Taking into account the bigger crack widths in the analytical assessment this result might be contributed to a less decreased stiffness in the numerical analysis and thus leading to a smaller deflection. It should be mentioned though that in the analytical assessment creep is taken into account, which is not in the numerical analysis. Taking into account the creep should decrease the difference in deformation results between the two methods.

17.6. Dynamic behaviour

In a similar manner as in paragraph 13.5 the dynamic behaviour is determined. In accordance with the observation described in the previous paragraph it appears that the numerical stiffness is bigger than analytically determined, resulting in a higher first eigenfrequency.

V

Conclusions & Recommendations

18

Conclusions

This chapter elaborates on the conclusions that can be drawn based on the results obtained in parts II, III and IV. The conclusions will be handled per part of this report (II, III, and IV). In the end the conclusions are summarized by answering the sub-questions and the main research question presented in chapter 3.

18.1. Part II

In this part the influence of slab height, reinforcement diameter, and reinforcement spacing on the reliability of analytical crack width predictions is investigated. By varying these three parameters a dataset of 105 alternatives was developed. The common denominator in this dataset was found in loading each of them until the bending moment from the characteristic load combination exceeded the analytical cracking moment by 10%.

From the analytical analysis of these variants, of which all results can be found in appendix E, it can be concluded that there is an unreliability in analytical crack width predictions. This conclusion is based on the observed discrepancy between the different analytical models. The difference occurs because all assessed analytical crack width prediction methods utilize different approaches containing different empirical parameters. For future research it is interesting to find out which method predicts crack widths most accurately for which case.

It furthermore is observed that the method described in article 7.3.4 in Eurocode 2 looses its compatibility when the balcony cross sections have a height equal to or less than 120 mm. At this moment the reinforcement is not located in the effective area, which should result in an effective reinforcement ratio equal to zero and thus making a crack width prediction impossible. This problem does not only occur in slender HSC balconies but can occur in every slender structure. When utilizing this method for slender cross sections both manually or through computer software specific care should be taken to critically judge obtained results.

The numerical analysis should have given an insight in the influence of the several parameters on crack width prediction reliability. However, as discussed in the section Remark in chapter 9, it did not deliver the desired results. To limit calculation time for the big dataset a too homogeneous 2D model emerged, which appeared unable to let cracks localize before failure. This resulted in unrealistically small cracks in a fine pattern until a small amount of cracks propagated and induced failure. It thus was not possible to come to a conclusion on the influence of the three parameters on the analytical crack width prediction.

18.2. Part III

In the numerical analysis results of the balcony with the in-plane ridge presented in chapters 12 and 13 it has been observed that the transition from the width of the slab to the width of the ridge, being a geometric disturbance, induces tensile peak stress concentrations in the corners between the ridge and the slab. The peak stress concentrations influence the cracking behaviour resulting in bigger numerically predicted crack widths compared to the analytically obtained values.

The difference between the numerical and analytical predictions can be contributed to the fact that the analytical crack width prediction method proposed by article 7.3.4 in Eurocode 2 is not able to take peak stress concentrations and their effect on the cracking behaviour into account, as is assessed in appendix A. This means that the geometric disturbance has a negative influence on the reliability of the analytical crack width prediction method.

As a last remark it was observed that for both the deflection and the dynamic behaviour the analytical results were more optimistic compared to the numerically obtained results. Because numerically the peak stress concentrations are taken into account, the stiffness of the balcony is more reduced because of the increased crack widths. This decreased stiffness induced numerically bigger deflections and a lower first eigenfrequency compared to the analytical analysis results.

18.3. Part IV

The pursue of reproducing a Hi-Con shaped balcony in HSC in part IV showed several difficulties during the process. At first it appeared to be impossible to create a slab with tapering height with a minimum height of 65 mm at the end of the cantilever. Because of vertical spacing between reinforcement bars the limit height in terms of detailing for this balcony is a constant height of 115 mm whereas for the Hi-Con balcony the maximum height is 110 mm. Furthermore, it appeared that the minimum dimension of the ridge in longitudinal direction is 135 mm. Decreasing this size results in detailing issues for the shear reinforcement present in the ridge. It can thus be concluded that an exact reproduction in HSC is not possible in case the design obeys to detailing rules from Eurocode 2.

The numerical analysis of the balcony with the out-of-plane ridge showed no concentrated peak stresses in the slab, despite the fact that the slab is only locally supported. A further analysis of the absence of the peak stresses, presented in appendix N, proved that they do not occur because the width of the top of the slab is kept constant. The absence of concentrated peak stresses results in the fact that analytically predicted crack widths are bigger than the numerical predictions.

Regarding the ridge the geometric disturbance is present and induces peak stress concentrations. However, the stress concentrations are from a different magnitude compared to the balcony with the in-plane ridge. Because of a higher cross section and a smaller concrete cover, both resulting in a bigger internal lever arm, the stresses are limited. This results in that the conservative characteristics of the analytical method outweigh the increase of numerical crack widths because of the geometrical disturbance.

Combining the findings from part III and IV it appears that there are two important factors determining whether a geometric disturbance influences the analytical crack width predictions. Firstly, it depends on whether the geometric disturbance is present in an area loaded in tension, and secondly, the slenderness of the element influences the severity of the increase of crack widths because of the geometric disturbance.

18.4. Research questions

The conclusions drawn in the previous paragraph can be extrapolated towards answers on the sub-questions and the main research question subsequently.

What is the influence of slab height, reinforcement diameter and reinforcement spacing on the reliability of analytical crack width predictions in slender high strength concrete cantilevering balconies?

To be able to answer this sub-question a big dataset was required in which the three parameters were varied. To limit calculation time for this dataset it has been decided to perform numerical analysis on 2D models. This has resulted in too homogeneous models in terms of geometry, boundary conditions and material characteristics, inducing the fact that cracks would not localize until just before failure. This means that no solid conclusion based on the comparison of analytical and numerical results can be drawn on the influence of cross sectional height, reinforcement diameter and reinforcement spacing on the reliability of analytical crack width predictions according to article 7.3.4 in Eurocode 2.

It has been discovered though, that for small cross sectional heights (≤ 120 mm) restrictions on the applicability of the analytical Eurocode 2 method occur because the reinforcement is not located in the effective area denoted by the width of the cross sections and the effective height $h_{c,eff}$. The reinforcement being absent in the effective area means the fictitious hidden tensile member does not contain any reinforcement and the crack width prediction thus should not be possible.

What is the influence of geometrical disturbances on the reliability of analytical crack width predictions in slender high strength concrete cantilevering balconies?

From the results presented in part III and IV of this report it can be concluded that geometrical disturbances influence the stress and strain distribution on and around the disturbance. More specific, the geometric disturbance induces peak stress concentrations as is visible in both parts. In general, these peak stress concentrations numerically result in an increased crack width compared to undisturbed regions. Moreover, as is explained in appendix A, the analytical Eurocode 2 method is not able to take into account these concentrated peak stresses.

In part III the peak stresses resulted in numerical crack widths being bigger than analytically determined whereas in part IV the numerical crack widths were smaller than analytically predicted. It turned out that the severity of the effect of the geometric disturbance on the stress distribution and magnitude is related to how heavy the element is loaded compared to its capacity. The ridge in part IV has a higher cross section to resist a bending moment of similar magnitude as the ridge in part III (135 mm instead of 110 mm) and a smaller concrete cover (20 mm instead of 35 mm), resulting in a bigger internal lever arm and thus smaller overall strains. The overall smaller strains result in smaller peak stresses and crack widths induced by the geometric disturbance which do not outweigh the conservative characteristics of the analytical prediction.

The fact that in part III the analytically predicted crack widths were smaller than numerically occurring can be contributed to the slenderness of the ridge in part III. The higher slenderness induces bigger peak stress concentrations, resulting in the fact that the conservative characteristics of the analytical approach do not outweigh the influence of these peak stresses in the numerical analysis.

Is it analytically possible to recreate a durable Hi-Con balcony in high strength concrete when applying currently prescribed methods, taking into account all rules and legislations from Eurocode 2?

The design process in chapter 15 of this report showed that it is not possible to completely reproduce the Hi-Con shaped balconies in HSC, mainly in terms of detailing rules. Nonetheless, the final result does have a lot in common with the Hi-Con shaped balconies, so the concept can be reproduced. Moreover, the analytical checks of crack width, dynamics, deflection and all ULS-checks were positive.

Is it possible to recreate a durable Hi-Con balcony in high strength concrete while obeying all rules and legislations from Eurocode 2?

The same balcony design as for the previous sub-question is assessed, thus it is again not possible to create an identical reproduction of the Hi-Con design. For the less slender design, in terms of durability (crack widths) and deflection, based on the results of the numerical analysis it appears possible to make a reproduction of the concept in HSC. The numerical crack widths and deflections do not exceed the limits demanded by Eurocode 2 because of a more beneficial geometry compared to the balcony with the in-plane ridge. Furthermore, it appeared that the analytical procedures of predicting crack widths and deflections result in bigger crack widths compared to the numerical analysis as long as the effect of geometrical disturbances remains limited. The effects can be contained by designing more robust and less slender. Obviously this conclusion depends on the accuracy of the numerical model. It is thus advised to perform a laboratory test to verify the numerical model.

For determining whether it is safe in terms of ULS-checks further research is required. Especially in terms of ultimate strength and the ductility this should be further investigated since high strength concrete is known to behave brittle.

To which extent gives the analytical Eurocode 2 crack width prediction method an insight in the cracking behaviour of slender high strength concrete cantilevering balconies?

In general, it can be concluded from the background analysis of the method proposed by article 7.3.4 in Eurocode 2 that this method possesses some conservative characteristics, namely:

- The increase in steel strain after cracking is assumed to be fully concentrated within a crack;
- The crack width is predicted with a prediction of the maximum crack spacing.

In the topside of the slab in part IV of this report it has been shown that these conservative characteristics result in a bigger crack width prediction than numerically obtained for undisturbed regions.

However, on several occasions one should take specific care when this crack width prediction method is utilized. In part II of this report it is observed that when slender cross sections are assessed, the effective height $h_{c,eff}$ is that low that the reinforcement is located outside this effective area. This should result in an effective reinforcement ratio equal to zero. Nonetheless, when not specifically noticed, the method can still produce a crack width prediction, especially when software based on Eurocode 2 is utilized. The actual effect of this flaw is not specifically known, but it might influence the reliability of the analytical crack width prediction.

From the results obtained in part III and IV it can be concluded that in case a geometric disturbance in an area loaded in tension is present, specific care should be taken. The geometric disturbance causes concentrated peak stresses which can induce an increase in crack width. The analytical crack width prediction method is not able to take into account these locally increased stresses. The severity of the effects induced by the geometric disturbance depends on the geometry of the element and to which extent the element is loaded compared to its capacity. A less slender and less heavily loaded element is less prone to these concentrated peak stresses compared to a more slender cross section.

In the introduction of this report the differences between NSC, HSC and UHPFRC were given as an initiation of this research. The differences were found in material characteristics, fracture mechanics, stress-strain behaviour and durability and were assumed to lead to an unreliability in analytical crack width predictions and unacceptable big crack widths for slender high strength concrete cantilevering balconies. It appears that for undisturbed regions these differences do not negatively affect the numerically observed cracking behaviour of the HSC balcony enough to overcome the conservative characteristics of the numerical crack width prediction method proposed by article 7.3.4 of Eurocode 2. Positive aspects being accountable for this result could be the tensile capacity of the concrete and the fact that HSC is more homogeneous, less porous and more dense compared to conventional concrete, resulting in a finer crack pattern.

19

Recommendations

During this research assumptions have been made, simplifications have been applied and issues have been discovered which need further research or clarification to determine their influence. This chapter presents propositions for further research.

Investigate the influence of reinforcement being outside of effective area during analytical prediction of crack widths.
In part II of this research it has been discovered that for cross sections with a limited height the reinforcement can be located outside the effective area of the hidden tensile member, as depicted in figure 9.1. The method in article 7.3.4 in Eurocode 2 however, utilizes this hidden tensile member to predict the crack width and does not state any limits to the applicability of this method. It is questioned to which extent and in which way the reinforcement being located outside the effective area/hidden tensile member influences the (reliability of the) crack width prediction.

Investigate what initiates the big discrepancy between all analytical models.
The analytical results in chapter 9 and appendix E show a big difference in the magnitude of analytically predicted crack widths. For the sake of the reliability of the crack width predictions it is desirable to know under which conditions and for which cases the different methods utilized in this report (and other available methods) predict the crack widths most accurately.

Investigate to which extent the analytical crack spacing $s_{r,max}$ is accurate for slender and/or HSC cross sections.
It appeared difficult to compare the analytically predicted crack spacing with the numerically obtained crack spacing. In part III numerically one localized crack occurred in the ridge, one in the interface between the slab and the ridge and one in the ridge. Analytically for the ridge and the slab separately a maximum crack spacing has been determined. Since in both elements numerically only one crack occurred, a comparison could not be made.

Furthermore, since the determination of $s_{r,max}$ includes some parameters possessing an empirical/experimental character, it is not known whether this crack spacing prediction method is suitable for slender and/or high strength concrete sections.

Find a way to model bond-slip in non-linear structural finite element analysis in DIANA FEA.
For all numerical models developed in this research bond-slip is not modelled, which might result in an underestimation of crack widths. Initially it has been pursued to apply a bond-slip model (see appendix D) but an unambiguous method has not been found, especially around the determination of the normal stiffness (DSNY) and the shear stiffness (DSXX). Nonetheless, it is known that bond-slip influences crack widths (appendix A) and thus should be taken into account to come to a more reliable conclusion on the matter.

Investigate the influence of concrete being modelled as homogeneous material on the numerical analysis.

in DIANA FEA almost all concrete models are by default homogeneous. Since in practice concrete is inhomogeneous for this research it is interesting to learn what the influence of modelling the concrete homogeneously is on the numerical crack width prediction and how that relates to the analytical prediction and the crack widths occurring in practice.

Investigate ULS-capacity of balcony from part IV.

To be able to fully state that it is possible and safe to create and apply the balcony designed and checked in part IV of this report in practice, a ULS check with DIANA FEA should be executed. For example brittle behaviour is a known issue for the application of HSC and is undesirable. It should thus be excluded that this balcony possesses this behaviour.

Perform laboratory testing.

From the conclusions and the previous recommendations it appears that there still is a significant uncertainty in the produced results. Properties of the materials and material behaviour in the finite element models, the applied numerical analysis, the way of loading and utilizing the analytical crack spacing for numerical results for example all have uncertainties which might influence the validity of the finite element results. To validate the numerical model and assess the analytical crack width prediction reliability the balcony from part IV should be tested in a laboratory.

Bibliography

[1] Said M. Allam, Mohie S. Shoukry, Gehad E. Rashad, and Amal S. Hassan. Crack width evaluation for flexural RC members. *Alexandria Engineering Journal*, 51(3):211–220, 2012.

[2] C. R. Braam. Scheurvorming volgens Eurocode 2. *Cement*, 3:78–83, 2009.

[3] C. R. Braam. Rekenvoorbeelden bij Eurocode 2 (6) - Staafwerkmodellen. *Cement*, 5:86–93, 2009.

[4] C. R. Braam. Rekenvoorbeelden bij Eurocode 2 (7) - Staafwerkmodellen (2). *Cement*, 6:90–95, 2009.

[5] C. R. Braam. Rekenvoorbeelden bij Eurocode 2 (8) - Staafwerkmodellen (3). *Cement*, 7:94–101, 2009.

[6] C. R. Braam. Scheurwijdte. *Cement*, 2:93–97, 2010.

[7] C. R. Braam. Rekenvoorbeelden bij Eurocode 2 (13) - Consoles. *Cement*, 4:58–65, 2010.

[8] C. R. Braam. Doorbuiging in de GTB. *Cement*, 7:80–85, 2010.

[9] CAE Nederland. Ultra Hoge Sterkte Beton - Al het laatste nieuws en informatie over (vv)UHSB. URL `www.uhsb.nl`.

[10] P Chana, R.S. Narayanan, and J.C. Walraven. Eurocode 2 Commentary. Technical report, European Concrete Platform ASBL, 2008.

[11] DIANA FEA. Diana Finite Element Analysis User's Manual, 2017. URL `https://dianafea.com`.

[12] Norberto Dominguez, Delphine Brancherie, Luc Davenne, and Adnan Ibrahimbegović. Prediction of crack pattern distribution in reinforced concrete by coupling a strong discontinuity model of concrete cracking and a bond-slip of reinforcement model. *Engineering Computations*, 22(5/6):558–582, 2005. ISSN 0264-4401. doi: 10.1108/02644400510603014. URL `http://www.emeraldinsight.com/doi/10.1108/02644400510603014`.

[13] M. Eriksen and M. Kolstad. Investigation of Cracking Behavior in Reinforced Concrete Panels with Bond-slip Reinforcement. Technical Report June, Norwegian University of Science and Technology, 2016.

[14] Walraven et al. *fib Model Code for Concrete Structures 2010*. Fédération internationale du béton, Lausanne, Switzerland, 2013 edition, 2010. ISBN 9783433030615.

[15] P.H. Feenstra. Computational Aspects of Biaxial Stress in Plan and Reinforced Concrete. Technical report, Delft University of Technology, Delft, 1993. URL `https://repository.tudelft.nl/islandora/object/uuid:faf2fd16-1c43-4711-b783-9e8e00d10c21?collection=research`.

[16] E.A. Hansen, M. Leive, J. Rodriguez, and R. Cather. *Mechanical properties of high strength concrete - influence of test conditions, specimens and constituents*. Paris, 2 edition, 1996.

[17] M.A.N. Hendriks, A. De Boer, B. Beletti, J.A. Den Uijl, P.H. Feenstra, and C. Damoni. Guidelines for Nonlinear Finite Element Analysis of Concrete Structures V 2.0. Technical report, Rijkswaterstaat, 2016.

[18] Harald Müller, Arnon Bentur, Mario Alberto Chiorino, Jean-Luc Clement, Manfred Curbach, Torsten Faust, Tor Arne Hammer, Jean-Paul Jaccoud, Christoph Kessler-Kramer, Gert König, Jacques Marchand, Viktor Mechtcherine, Bertil Persson, S.A. Reddi, H.W. Reinhardt, Tassilo Rinder, Keitetsu Rokugo, Luc Taerwe, Tamon Ueda, and Joost Walraven. *Constitutive Modelling of High Strength/High Performance Concrete*. FIB, Lausanne. ISBN 9782883940826.

[19] Hikaru Nakamura and Takeshi Higai. Compressive Fracture Energy And Fracture Zone Length of Concrete. *Modelling of Inelastic Behaviour of RC Structures under Seismic Loads*, (November):471–487, 2001.

[20] NEN-EN 1990+A1+A1/C2. Grondslagen van het constructief ontwerp, 2011.

[21] NEN-EN 1990+A1+A1/C2 NB. Grondslagen van het construtief ontwerp; nationale bijlage, 2011.

[22] NEN-EN 1991-1-1+C1. Algemene belastingen op constructies, 2011.

[23] NEN-EN 1991-1-1+C1 NB. Algemene belastingen op constructies; nationale bijlage, 2011.

[24] NEN-EN 1992-1-1+C2. Ontwerp en berekening van betonconstructies - Deel 1-1: Algemene regels en regels voor gebouwen, 2011.

[25] NEN-EN 1992-1-1+C2 NB. Ontwerp en berekening van betonconstructies - Deel 1-1: Algemene regels en regels voor gebouwen; Nationale Bijlage, 2016.

[26] J.P. Ollivier, J.C. Maso, and B. Bourdette. Interfacial Transition Zone in Concrete. *Advanced cement based materials, Elsevier*, 2:30–38, 1995.

[27] G. Remmel. On the tensile and Shear Behaviour of High Strength Concrete Members. *Deutscher Ausschuss für Stahlbeton*, 444, 1994.

[28] J. G. Rots, P. Nauta, G. M A Kusters, and J. Blaauwendraad. Smeared Crack Approach and Fracture Localization in Concrete. *Heron*, 30(1), 1985. ISSN 00467316.

[29] R. Sagel, P. Lagendijk, and C. R. Braam. *Grafieken en Tabellen voor Beton*. Betonvereniging, Gouda, 2013 edition.

[30] G.J. Schreppers. Bond-slip Reinforcements and Pile Foundations. *TNO Diana*, (January), 2015.

[31] G.J. Schreppers, C. Frissen, and H.J. Kang. Prediction of crack-width and crack-pattern. *TNO Diana*, (November), 2011.

[32] Jacek Tejchmann and Jerzy Bobinski. *Continuous and Discontinuos Modelling of Fracture in Concrete Using FEM*, volume 1. Springer, Berlin, 2013. ISBN 978-3-642-28462-5.

[33] K. van Breugel, C. R. Braam, C. Van der Veen, and J. Walraven. *Concrete Structures under Imposed Thermal and Shrinkage Deformations - Theory and Practice*. TU Delft, Delft, 2016.

[34] F.J. Vecchio and M.P. Collins. Compression response of cracked reinforced concrete. *Journal of Structural Engineering*, 119(12):3590–3610, 1993.

Appendices

A

Background of analytical and numerical crack width prediction method

Background of analytical Eurocode 2 crack width prediction method

Article 7.3.4 of Eurocode 2 proposes to predict crack width through equation A.1.

$$w_k = (\varepsilon_{sm} - \varepsilon_{cm}) * s_{r,max} \tag{A.1}$$

The expression utilizes the difference ins teel strain and concrete strain and multiplies this strain difference with a prediction of the maximum crack spacing. This approach leads to an upper limit of the crack width prediction because of two reasons. First, the prediction is determined with the maximum crack spacing. In case the crack spacing appears smaller, the crack widths in practice will be smaller. Furthermore, it is assumed that the increase in steel strain after cracking is localized completely within the cracks. In practice the uncracked concrete parts still contribute as well and will undergo a certain elongation.

The strain difference $(\varepsilon_{sm} - \varepsilon_{cm})$ is determined through equation A.2.

$$(\varepsilon_{sm} - \varepsilon_{cm}) = \frac{\sigma_s - k_t * \frac{f_{ct,eff}}{\rho_{p,eff}} * \left(1 + \alpha_e * \rho_{p,eff}\right)}{E_s} \tag{A.2}$$

The parameters containing the subscript eff represent the geometry of the hidden tensile member. When cracking is analytically assessed by using the hidden tensile member method, it is assumed that the tensile stresses in a cross section are accounted for by a specific part of the cross section called the hidden tensile member. For this member then the crack width is determined as if it were a centrically loaded prismatic beam. To come to the background, first $\frac{f_{ct,eff}}{\rho_{p,eff}} * \left(1 + \alpha_e * \rho_{p,eff}\right)$ from the numerator in equation A.2 will be assessed.

This part of the equation specifically originates form the hidden tensile member, loaded centrically by a tensional normal force. The total normal force in this member is divided over both the steel and the concrete equally. The force in the steel of this member is denoted by equation A.3.

$$N_s = \varepsilon_s * E_s * A_s \tag{A.3}$$

The normal force in the concrete is described in a similar way, presented in equation A.4

$$N_c = \varepsilon_c * E_c * A_c \tag{A.4}$$

As long as the member is uncracked, it may be assumed that the strain in the steel and the concrete are equal, resulting in a fully cooperative composite cross section. The total normal force then equals:

$$N_{total} = N_c + N_s = \varepsilon * E_c * A_c + \varepsilon * E_s * A_s \tag{A.5}$$

Equation A.5 can be rewritten by using the relations $\alpha_e = \frac{E_s}{E_c}$ and $\rho = \frac{A_s}{A_c}$, resulting in the following relation:

$$N_{total} = E_c A_c (1 + \alpha_e \rho \tag{A.6}$$

Since the increase in steel strain after cracking is desired to know, the steel strain at the onset of cracking is required. The onset of cracking happens when the concrete reaches its tensile capacity, f_{ctm}. Then $\varepsilon * E_c = f_{ctm}$, resulting in a normal cracking force described in equation A.7.

$$N_{cr} = f_{ctm} A_c (1 + \alpha_e \rho \tag{A.7}$$

As soon as the concrete is cracked, the stress at the location of the crack in the concrete drops to zero, visualized in figure A.1. The full normal force, N_{cr}, then is transferred by the reinforcement. The steel stress is then described by equation A.8

$$\sigma_{sr} = \frac{N_{cr}}{A_s} = f_{ctm}(1 + \alpha_e \rho) = f_{ctm} \frac{1}{\rho}(1 + \alpha_e \rho) = \frac{f_{ctm}}{\rho}(1 + \alpha_e \rho) \tag{A.8}$$

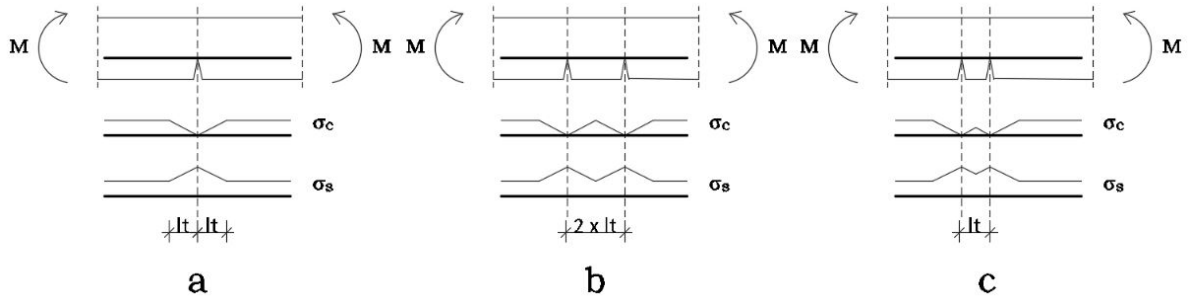

Figure A.1: Stresses in concrete and reinforcement at the location of a crack, visualizing steel stress increase and concrete stress drop at the location of a crack.

So what basically is written in the crack width prediction formula, regarding the hidden tensile member, is:

$$(\varepsilon_{sm} - \varepsilon_{cm}) = \frac{\sigma_s - k_t * \frac{f_{ct,eff}}{\rho_{p,eff}} * \left(1 + \alpha_e * \rho_{p,eff}\right)}{E_s} = \frac{\sigma_s}{E_s} - k_t * \frac{\sigma_{sr}}{E_s} = \varepsilon_s - k_t * \varepsilon_{sr} \tag{A.9}$$

Resulting in a total crack width prediction formula:

$$w_k = (\varepsilon_s - k_t * \varepsilon_{sr}) * s_{r,max} \tag{A.10}$$

Background of numerical crack width prediction method applied by DIANA FEA

In the numerical model the structure, in this case a balcony, is subdivided in a finite number of elements. Each element contains a number of integration points, the amount of integration points depends on the type of element. In those integration points the strains following from the loading are determined and through the predefined constitutive relations of the material these strains can be converted into stresses.

To be able to model cracking in a finite element model the constitutive relationship between stress and strain should contain a non-linearity. For the elements in this research loaded in tension the Hordijk tension softening curve, figure A.2, has been used. It can be seen that the elements are linear elastic in tension until their capacity ft is reached. In other words, when the principal stress exceeds the tensile capacity, the element cracks and then keeps following the tension softening curve.

When cracking occurs, the constitutive relationship changes [32]. By using a smeared crack approach, the strain is spread over a finite area/volume. However, in between the cracks the concrete still contributes. This means that the total strain is a combination of crack strain and concrete strain. The model is thus able treat the material in and around the crack differently than the constitutive behaviour of the remaining concrete.

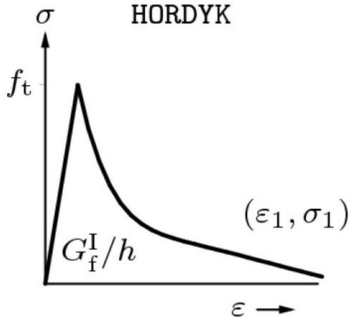

Figure A.2: Hordijk nonlinear stress-strain relationship for concrete loaded in tension, source: [11].

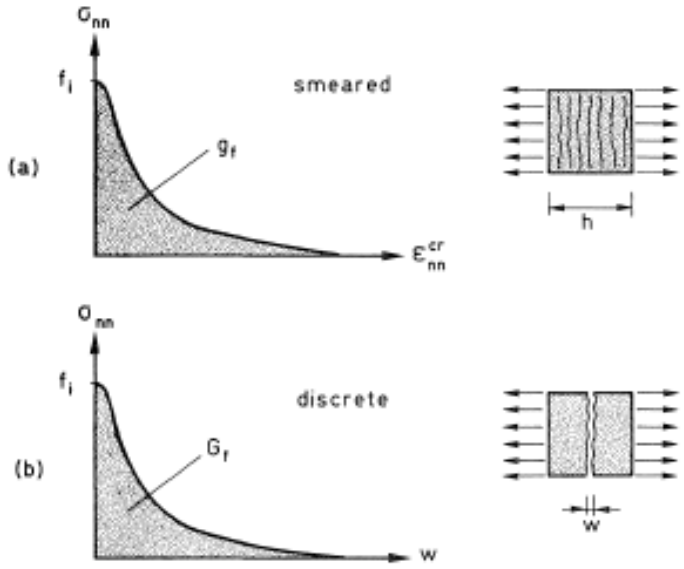

Figure A.3: Visualization of the transition of a smeared crack towards a localized crack, source: [28].

$$\varepsilon = \varepsilon_c + \varepsilon_{cr} \tag{A.11}$$

In the smeared cracking approach, the crack strain is smeared over an area within the finite element [28]. Within this approach, the crack width w is determined through the smeared crack strain in the element. The crack strain is smeared over a certain area called the crack bandwidth h, see figure A.3. With the help of this bandwidth the strain can be converted towards a crack width in a localized crack through the following relation:

$$w = \int_h \varepsilon_{cr}\, dn \tag{A.12}$$

Comparison of analytical Eurocode 2 method and the DIANA FEA numerical method

In the analytical determination two conservative choices are made. Firstly, the crack width is predicted with the maximum crack spacing where in practice this spacing can be smaller. This would result in smaller cracks. Secondly, the increase in strain after cracking is assumed to be fully taken up by the steel stress whereas the concrete in between the cracks keeps on contributing as well.

In the numerical analysis for all integration points the strains are determined, converted to stresses, which then are converted to internal forces. All internal and external forces together should result in an equilibrium

everywhere in the structure as long as the structural capacity is not exceeded.

Since everywhere a force equilibrium should be present, the numerical method is able to determine for example peak stress concentrations at for example local disturbances. Analytically this is not possible, which can result in an underestimation of the actual crack width in case disturbed regions are assessed.

Influence of bond-slip and homogeneity of concrete in numerical analysis

It is known that in reality the bond between the concrete and reinforcement is not perfect for a variety of aspects. For example the bond is not infinitely strong and stiff. This means that when a reinforced concrete member is loaded a certain relative displacement between the reinforcement and the concrete can occur, denoted as bond-slip. The complexity of this mechanism, according to [12], depends on material characteristics, specific geometry, loading type, and structural configuration. According to the same research the broad perspective of influential parameters makes developing an unambiguous method for modelling bond-slip difficult.

From *Continuous and discontinuous modelling of fracture in concrete using FEM* [32] it can be concluded that the ultimate load of a structure is only marginally affected by whether bond-slip is accounted for during the analysis or not. What is observed is that the crack spacing increases when bond-slip is taken into account, which then results to an increase of predicted crack widths.

Regarding modelling concrete homogeneously and the effect it has on the crack width prediction, according to [12] variations within a material will influence the cracking behaviour. In [32] it is stated that for localization of cracks a discrete crack model should be applied. Combining these two statements it can thus be concluded that in case no disturbance is present and the concrete is modelled homogeneously, localization of cracking might not occur in case the smeared cracking approach is applied. In case the model does contain disturbances in for example the geometry, localization can occur.

B

Script fully clamped cantilever

This appendix presents the script and specifically highlights the process for determining the bending moment resistance.

Bending moment resistance

$$d = h - c_{top} - 0.5 * \phi \tag{B.1}$$

$$A_s = \frac{b}{s_{reb}} * \pi * \left(\frac{\phi}{2}\right)^2 \tag{B.2}$$

$$\rho_l = \frac{A_s}{b * d} \tag{B.3}$$

$$x_u = \frac{A_s * f_{yd}}{\left(\frac{1}{2}\frac{\varepsilon_{c3}}{\varepsilon_{cu3}} + \left(1 - \frac{\varepsilon_{c3}}{\varepsilon_{cu3}}\right)\right) * b * f_{cd}} \tag{B.4}$$

$$\rho_{l,max} = \frac{\left(\frac{1}{2}\frac{\varepsilon_{c3}}{\varepsilon_{cu3}} + \left(1 - \frac{\varepsilon_{c3}}{\varepsilon_{cu3}}\right)\right) * b * f_{cd} * x_u}{b * d} \leq 0.04 \tag{B.5}$$

$$\beta x_u = \frac{\left(1 - \frac{\varepsilon_{c3}}{\varepsilon_{cu3}}\right) * x_u * f_{cd} * 0.5 * \left(1 - \frac{\varepsilon_{c3}}{\varepsilon_{cu3}}\right) * x_u + 0.5 * \left(\frac{\varepsilon_{c3}}{\varepsilon_{cu3}}\right) * x_u * f_{cd} \left(\left(1 - \frac{\varepsilon_{c3}}{\varepsilon_{cu3}}\right) * x_u + \frac{\frac{\varepsilon_{c3}}{\varepsilon_{cu3}} * x_u}{3}\right)}{f_{cd} * \left(1 - \frac{\varepsilon_{c3}}{\varepsilon_{cu3}}\right) * x_u + 0.5 * f_{cd} * \left(\frac{\varepsilon_{c3}}{\varepsilon_{cu3}}\right) * x_u} \tag{B.6}$$

$$z = d - \beta x_u \tag{B.7}$$

$$\varepsilon_s = \frac{\varepsilon_{cu3}}{x_u} * (d - x_u) \tag{B.8}$$

$$N_s = \begin{cases} f_{yd} * A_s & \text{for } \frac{f_{yd}}{E_s} \leq \varepsilon_s < 0.045 \\ E_s * \varepsilon_s * As & \text{else} \end{cases} \tag{B.9}$$

$$M_{Rd} = N_s * z \tag{B.10}$$

$$UC = \frac{M_{Ed}}{M_{Rd}} \tag{B.11}$$

```
> restart;
```

Dimensioning and checking of a cantilevering slab, fully clamped over width of slab.

All units in N and mm

Geometric Characteristics

```
> l := 1575 : b := 1300 : h := X :
```

Material Properties Concrete: C90/105

```
> γc := 1.5 : Ecm := 43600 : fck := 90 : fcd := fck/γc : fctm := 5.05 : fctk := 3.54 : fctd :=
      fck/γc : fctmfl := max((1.6 − h/1000) fctm, fctm) : εc3 := 2.3·10^−3 : εcu3 := 2.6·10^−3 :
      fcmcube := 105 + 8 :
```

Material Properties Reinforcement: B500b

```
> γs := 1.15 : fyk := 500 : fyd := fyk/γs : Es := 200000 :
```

Loads

A point load is calculated to make sure that Mk=1.1*Mcr so the member will always be in the fully developed crack pattern.

```
> G := 2.5·10^−5 : Wc := 1/6·b·h^2; Q := (1.1·fctm·Wc − 0.5·l^2·b·h·G)/(l − 100);
```

Reinforcement configuration

```
> ϕmain := X; αe := Es/Ecm : sreb := X; n := ceil(b/sreb)
```

Concrete Cover

```
> ctop := 30 : cother := 20 mm :
```

Check rebar spacing

dg+5=16+5= 21 mm

```
> if 21 < sreb − ϕmain < min(3·h, 400) then print(Rebar spacing main reinforcement is OK)
      else print(Rebar spacing main reinforcement doesnot fulfill requirements) end if;
```

Cross Sectional Properties

```
> Ic := 1/12·b·h^3;
```

> $EI0 := Ecm \cdot Ic;$

> $Wc := \frac{1}{6} \cdot b \cdot h^2;$

Bending moments and shear forces.

> $Mk := l \cdot b \cdot h \cdot 0.5 \cdot l \cdot G + Q \cdot (l - 100);$

> $Vk := l \cdot b \cdot h \cdot G + Q;$

> $Mfc := l \cdot b \cdot h \cdot 0.5 \cdot l \cdot G + Q \cdot (l - 100) \cdot 0.5;$

> $Vfc := l \cdot b \cdot h \cdot G + Q \cdot 0.5;$

> $Mqb := l \cdot b \cdot h \cdot 0.5 \cdot l \cdot G + Q \cdot (l - 100) \cdot 0.3;$

> $Vqb := l \cdot b \cdot h \cdot G + Q \cdot 0.3;$

> $Mg := l \cdot b \cdot h \cdot 0.5 \cdot l \cdot G;$

> $Vg := l \cdot b \cdot h \cdot G;$

> $Med := 1.2 \cdot l \cdot b \cdot h \cdot 0.5 \cdot l \cdot G + 1.5 \cdot Q \cdot (l - 100);$

> $Ved := 1.2 \cdot l \cdot b \cdot h \cdot G + 1.5 \cdot Q;$

Cracking moment

For the calculation of crack widths under pure bending, fctm instead of fctmfl should be applied.

> $Mcr := fctm \cdot Wc;$

> **if** $Mk > Mcr$ **then** $print(Cross\ section\ is\ considered\ cracked)$
> **else** $print(Cross\ section\ is\ considered\ uncracked)$ **end if**

Check main bending moment resistance

> $d := h - ctop - 0.5 \cdot \phi main;$

> $Asmain := evalf\left(\mathrm{ceil}\left(\frac{b}{sreb}\right) \cdot \pi \cdot \left(\frac{\phi main}{2}\right)^2\right);\ n := \mathrm{ceil}\left(\frac{b}{sreb}\right)$

> $\rho l := \frac{Asmain}{b \cdot d};$

> $xu := \frac{Asmain \cdot fyd}{\left(\frac{1}{2} \cdot \frac{\varepsilon c3}{\varepsilon cu3} + \left(1 - \frac{\varepsilon c3}{\varepsilon cu3}\right)\right) \cdot fcd \cdot b};$

Determine a maximum reinforcement ratio for which yielding of steel occurs before crushing of concrete and fulfill maximum reinforcement ratio criterium from national annex EC2 art. 9.2.1.1.

> $eq1 := (\rho lmax \cdot b \cdot d) \cdot fyk = \left(\frac{1}{2} \cdot \frac{\varepsilon c3}{\varepsilon cu3} + \left(1 - \frac{\varepsilon c3}{\varepsilon cu3}\right)\right) \cdot fck \cdot b \cdot xu :$
> $\rho lmax := solve(eq1, \rho lmax);$

> $\rho lmax := \min(0.04, \rho lmax);$

> **if** $\rho l > \rho lmax$ **then** $print(Reinforcement\ ratio\ is\ too\ high)$ **end if**

center of gravity compression zone on maximum capacity, β≠0.39 because of HSC:

$$> \beta xu := \frac{1}{fcd\cdot\left(1-\frac{\varepsilon c3}{\varepsilon cu3}\right)xu+0.5\cdot fcd\cdot\left(\frac{\varepsilon c3}{\varepsilon cu3}\right)xu}\left(\left(1-\frac{\varepsilon c3}{\varepsilon cu3}\right)\cdot xu\cdot fcd\cdot 0.5\left(1-\frac{\varepsilon c3}{\varepsilon cu3}\right)xu+0.5\cdot\left(\frac{\varepsilon c3}{\varepsilon cu3}\right)\cdot xu\cdot fcd\cdot\left(\left(1-\frac{\varepsilon c3}{\varepsilon cu3}\right)xu+\frac{\left(\frac{\varepsilon c3}{\varepsilon cu3}\right)xu}{3}\right)\right);$$

$$> \beta := \frac{\beta xu}{xu}; z := d-\beta xu;$$

$$> Ns := fyd\cdot Asmain : Mrd := Ns\cdot z;$$

$$> UCM := \frac{Med}{Mrd};$$

Check main shear resistance

> **if** $h < 200$ **then** *print*(*No shear reinforcement allowed*) **end if**

$$> k := 1+\sqrt{\frac{200}{d}};$$

> **if** $k \le 2$ **then** $k := k$ **else** $k := 2$ **end if**

$$> Crdc := \frac{0.18}{\gamma c};$$

$$> vmin := evalf\left(0.035\cdot k^{\frac{3}{2}}\cdot fck^{\frac{1}{2}}\right);$$

$$> Vrdcmin := vmin\cdot b\cdot d;$$

$$> Vrdc := evalf\left(\left(Crdc\cdot k\cdot(100\cdot\rho l\cdot fck)^{\frac{1}{3}}\right)\cdot b\cdot d\right);$$

$$> Vrdc := \max(Vrdcmin, Vrdc);$$

$$> UCV := \frac{Ved}{Vrdc};$$

Check detailing and element specific rules

> **if** $l \ge 5\cdot h$ **and** $b \ge 5\cdot h$ **then** *print*(*Balcony may be considered as plate element*) **end if**

> **if** $h \ge 80$ **then** *print*(*Height of balcony is sufficient as plate element*)
else *print*(*Height of balcony plate is insufficient*) **end if**

> **if** $\min\left(\frac{fctm\cdot Wc}{fyd\cdot z}, 0.26\cdot\frac{fctm}{fyk}\cdot b\cdot d\right) < Asmain$ **then** *print*(*Area of reinforcement is sufficient*)
else *print*(*Area of main reinforcement should be increased*) **end if**;

>

Crack width EC2

Uses effective height. For long term kt=0.4 this method is verified with technosoft results.

$$> xe := d\cdot\left(-\alpha e\cdot\rho l+\sqrt{(\alpha e\cdot\rho l)^2+2\,\alpha e\cdot\rho l}\right);$$

> $wmax := 0.2;$

> $Mlin := fyd \cdot Asmain \cdot \left(d - \frac{1}{3} xe \right);$

> **if** $Mfc \le Mlin$ **then** $z := d - \frac{1}{3} xe$ **else** $z := d - \beta xe$ **end if**;

> $hceff := \min\left((h - d) \cdot 2.5, \frac{(h - xe)}{3} \right);$

> **if** $hceff < ctop + 0.5 \cdot \phi main$
then *print*(*Reinforcement isnt located wihtin hidden tensile member*) **end if**;

> $\rho peff := \frac{Asmain}{hceff \cdot b};$

k1=0.8 for good bonding, k2=0.5 for pure bending, k3 en k4 follow from national annex. kt=0.6 because of short term loading.;

> $k1 := 0.8 : k2 := 0.5 : k3 := 3.4 : k4 := 0.425 : kt := 0.6 :$

> $fcteff := fctm :$

> **if** $sreb \le \left(5 \cdot \left(ctop + \frac{\phi main}{2} \right) \right)$ **then** $srmax := k3 \cdot ctop + \frac{k1 \cdot k2 \cdot k4 \cdot \phi main}{\rho peff}$ **else** $srmax := 1.3(h - xe)$ **end if**:

> **if** $srmax > \max\left((50 - 0.8\, fck) \cdot \phi main, 15 \cdot \phi main \right)$ **then** $srmax := \max\left((50 - 0.8\, fck) \cdot \phi main, 15 \cdot \phi main \right)$ **end if**;

> $\sigma sr := \frac{fcteff}{\rho peff} \cdot (1 + \alpha e \cdot \rho peff);\ \sigma s := \frac{Mfc}{Asmain \cdot z};$

> $straindifference := \frac{(\sigma s - kt \cdot \sigma sr)}{Es};\ minstraindifference := \left(0.6 \cdot \frac{\sigma s}{Es} \right);$

> **if** $straindifference \le minstraindifference$ **then** $straindifference := minstraindifference$ **end if**;

> $wkEC := straindifference \cdot srmax;$

> **if** $wkEC \le wmax$ **then** *print*(*Crack width is small enough*) **else** *print*(*Crack width is too big*) **end if**;

Crack Width Van Breugel et al.

Short term instantaneous loading thus σcr = fctm.

> **if** $Mcr > Mk$ **then** *print*(*No fully developed crack pattern*) **end if**

>

> $\sigma cr := fctm;\ \sigma scr := \frac{Mcr}{z \cdot Asmain};\ \sigma s := \frac{Mfc}{Asmain \cdot z};$

> $wm0 := 2 \cdot \left(\frac{(0.4 \cdot \phi main)}{fcmcube \cdot Es} \cdot \left(\frac{\sigma cr}{\rho l} \right)^2 \cdot (1 + \alpha e \cdot \rho l) \right)^{0.85};$

> $lm := 1.8 \cdot wm0 \cdot \frac{Es}{\sigma scr};$

> **if** $Mk \ge Mcr$ **then** $wmv := \frac{lm}{Es} \cdot (\sigma s - 0.5 \cdot \sigma scr)$ **end if**

> **if** $Mk > Mcr$ **then** $wmaxVB := wmv \cdot 1.7$ **else** $wmaxVB := wmv \cdot 1.3$ **end if**

Egyption Code

Egyptian code - Uses effective height
β1=0.8 for bars with profile, β2=1 for single short time loading. β=1.7 for determination of crack width induced by loading (not imposed deformation!)

> **if** $hceff < ctop + 0.5 \cdot \phi main$
> **then** $print(Reinforcement\ isnt\ located\ wihtin\ hidden\ tensile\ member)$ **end if**;

> $epsmeansteel := \frac{\sigma s}{Es} \cdot \left(1 - 0.8 \cdot 0.1 \left(\frac{\sigma scr}{\sigma s}\right)^2\right)$;

> $Srm := 50 + \frac{0.25 \cdot k1 \cdot k2 \cdot \phi main}{\rho peff}$;

> $wkEG := 1.7 \cdot epsmeansteel \cdot Srm$;

Crack Width American Standards ACI 318

American building code - based on z-factor method. Uses some kind of effective area but takes location of reinforcement into account.

> $\beta := \frac{(h - xu)}{(d - xu)} : dc := h - d : Ae := 2 \cdot dc \cdot b : nb := \text{ceil}\left(\frac{b}{sreb}\right) : A0 := \frac{Ae}{nb}$:

> $wmaxACI := 0.011 \cdot \beta \cdot \sigma s \cdot (dc \cdot A0)^{\frac{1}{3}} \cdot 10^{-3}$;

C

Verification of script

This appendix contains both the script used for the dimensioning and checking of a slab and the Technosoft Liggers output for the same slab.

As mentioned in chapter 7 the results from the script and the Technosoft output are about a fully clamped cantilevering slab with a height of 160 mm and reinforcement ⌀12-80. This configuration has been randomly picked from the data set. For either the script as the Technosoft output the upper limit value of the predicted crack width based on the Eurocode method is 0.041 mm.

```
> restart;
```

Dimensioning and checking of a cantilevering slab, fully clamped over width of slab.

All units in N and mm

Geometric Characteristics

```
> l := 1575 : b := 1300 : h := 160 :
```

Material Properties Concrete: C90/105

```
> γc := 1.5 : Ecm := 43600 : fck := 90 : fcd := fck/γc : fctm := 5.05 : fctk := 3.54 : fctd :=
      fck/γc : fctmfl := max((1.6 − h/1000) fctm, fctm) : εc3 := 2.3·10^−3 : εcu3 := 2.6·10^−3 :
      fcmcube := 105 + 8 :
```

Material Properties Reinforcement: B500b

```
> γs := 1.15 : fyk := 500 : fyd := fyk/γs : Es := 200000 :
```

Loads

A point load is calculated to make sure that Mk=1.1*Mcr so the member will always be in the fully developed crack pattern.

```
> G := 2.5·10^−5 : Wc := 1/6·b·h^2; Q := (1.1·fctm·Wc − 0.5·l^2·b·h·G)/(l − 100);
```

$$Wc := \frac{16640000}{3}$$

$$Q := 16516.68362 \tag{4.1}$$

Reinforcement configuration

```
> ϕmain := 12; αe := Es/Ecm : sreb := 80; n := ceil(b/sreb)
```

$$\phi main := 12$$

$$sreb := 80$$

$$n := 17 \tag{5.1}$$

Concrete Cover

```
> ctop := 30 : cother := 20 mm :
```

Check rebar spacing

dg+5=16+5= 21 mm

> **if** $21 < sreb - \phi main < \min(3 \cdot h, 400)$ **then** *print*(*Rebar spacing main reinforcement is OK*)
> **else** *print*(*Rebar spacing main reinforcement doesnot fulfill requirements*) **end if**;

Rebar spacing main reinforcement is OK **(7.1)**

Cross Sectional Properties

> $Ic := \frac{1}{12} \cdot b \cdot h^3$;

$$Ic := \frac{1331200000}{3} \quad \textbf{(8.1)}$$

> $EI0 := Ecm \cdot Ic$;

$$EI0 := \frac{58040320000000}{3} \quad \textbf{(8.2)}$$

> $Wc := \frac{1}{6} \cdot b \cdot h^2$;

$$Wc := \frac{16640000}{3} \quad \textbf{(8.3)}$$

Bending moments and shear forces.

> $Mk := l \cdot b \cdot h \cdot 0.5 \cdot l \cdot G + Q \cdot (l - 100)$;

$$Mk := 3.081173334\ 10^7 \quad \textbf{(9.1)}$$

> $Vk := l \cdot b \cdot h \cdot G + Q$;

$$Vk := 24706.68362 \quad \textbf{(9.2)}$$

> $Mfc := l \cdot b \cdot h \cdot 0.5 \cdot l \cdot G + Q \cdot (l - 100) \cdot 0.5$;

$$Mfc := 1.863067917\ 10^7 \quad \textbf{(9.3)}$$

> $Vfc := l \cdot b \cdot h \cdot G + Q \cdot 0.5$;

$$Vfc := 16448.34181 \quad \textbf{(9.4)}$$

> $Mqb := l \cdot b \cdot h \cdot 0.5 \cdot l \cdot G + Q \cdot (l - 100) \cdot 0.3$;

$$Mqb := 1.375825750\ 10^7 \quad \textbf{(9.5)}$$

> $Vqb := l \cdot b \cdot h \cdot G + Q \cdot 0.3$;

$$Vqb := 13145.00509 \quad \textbf{(9.6)}$$

> $Mg := l \cdot b \cdot h \cdot 0.5 \cdot l \cdot G$;

$$Mg := 6.449625000\ 10^6 \quad \textbf{(9.7)}$$

> $Vg := l \cdot b \cdot h \cdot G$;

$$Vg := 8190.000000 \quad \textbf{(9.8)}$$

> $Med := 1.2 \cdot l \cdot b \cdot h \cdot 0.5 \cdot l \cdot G + 1.5 \cdot Q \cdot (l - 100)$;

$$Med := 4.428271251\ 10^7 \quad \textbf{(9.9)}$$

> $Ved := 1.2 \cdot l \cdot b \cdot h \cdot G + 1.5 \cdot Q$;

$$Ved := 34603.02543 \quad \textbf{(9.10)}$$

Cracking moment

For the calculation of crack widths under pure bending, fctm instead of fctmfl should be applied.

> $Mcr := fctm \cdot Wc$;

$$Mcr := 2.801066667\ 10^{7} \quad (10.1)$$

> **if** $Mk > Mcr$ **then** *print*(*Cross section is considered cracked*)
> **else** *print*(*Cross section is considered uncracked*) **end if**

Cross section is considered cracked (10.2)

Check main bending moment resistance

> $d := h - ctop - 0.5 \cdot \phi main;$

$$d := 124.0 \quad (11.1)$$

> $Asmain := evalf\left(\text{ceil}\left(\frac{b}{sreb}\right) \cdot \pi \cdot \left(\frac{\phi main}{2}\right)^2\right);\ n := \text{ceil}\left(\frac{b}{sreb}\right)$

$$Asmain := 1922.654704$$
$$n := 17 \quad (11.2)$$

> $\rho l := \frac{Asmain}{b \cdot d};$

$$\rho l := 0.01192713836 \quad (11.3)$$

> $xu := \frac{Asmain \cdot fyd}{\left(\frac{1}{2} \cdot \frac{\varepsilon c3}{\varepsilon cu3} + \left(1 - \frac{\varepsilon c3}{\varepsilon cu3}\right)\right) \cdot fcd \cdot b};$

$$xu := 19.21693856 \quad (11.4)$$

Determine a maximum reinforcement ratio for which yielding of steel occurs before crushing of concrete and fulfill maximum reinforcement ratio criterium from national annex EC2 art. 9.2.1.1.

> $eq1 := (\rho lmax \cdot b \cdot d) \cdot fyk = \left(\frac{1}{2} \cdot \frac{\varepsilon c3}{\varepsilon cu3} + \left(1 - \frac{\varepsilon c3}{\varepsilon cu3}\right)\right) \cdot fck \cdot b \cdot xu:$
> $\rho lmax := solve(eq1, \rho lmax);$

$$\rho lmax := 0.01555713699 \quad (11.5)$$

> $\rho lmax := \min(0.04, \rho lmax);$

$$\rho lmax := 0.01555713699 \quad (11.6)$$

> **if** $\rho l > \rho lmax$ **then** *print*(*Reinforcement ratio is too high*) **end if**

center of gravity compression zone on maximum capacity, β≠0.39 because of HSC:

> $$\beta xu := \frac{1}{fcd \cdot \left(1 - \frac{\varepsilon c3}{\varepsilon cu3}\right) xu + 0.5 \cdot fcd \cdot \left(\frac{\varepsilon c3}{\varepsilon cu3}\right) xu} \left(\left(1 - \frac{\varepsilon c3}{\varepsilon cu3}\right) \cdot xu \cdot fcd \cdot 0.5 \left(1 - \frac{\varepsilon c3}{\varepsilon cu3}\right) xu + 0.5 \cdot \left(\frac{\varepsilon c3}{\varepsilon cu3}\right) \cdot xu \cdot fcd \cdot \left(\left(1 - \frac{\varepsilon c3}{\varepsilon cu3}\right) xu + \frac{\left(\frac{\varepsilon c3}{\varepsilon cu3}\right) xu}{3}\right)\right);$$

$$\beta xu := 6.482106157 \quad (11.7)$$

> $\beta := \frac{\beta xu}{xu};\ z := d - \beta xu;$

$$\beta := 0.3373121133$$

$$z := 117.5178938 \quad (11.8)$$

> $Ns := fyd \cdot Asmain : Mrd := Ns \cdot z;$

$$Mrd := 9.823753535\ 10^{7} \quad (11.9)$$

> $UCM := \frac{Med}{Mrd};$

$$UCM := 0.4507718191 \quad (11.10)$$

Check main shear resistance

> **if** $h < 200$ **then** *print*(*No shear reinforcement allowed*) **end if**

No shear reinforcement allowed (12.1)

> $k := 1 + \sqrt{\frac{200}{d}};$

$$k := 2.270001270 \quad (12.2)$$

> **if** $k \leq 2$ **then** $k := k$ **else** $k := 2$ **end if**

$$k := 2 \quad (12.3)$$

> $Crdc := \frac{0.18}{\gamma c};$

$$Crdc := 0.1200000000 \quad (12.4)$$

> $vmin := evalf\left(0.035 \cdot k^{\frac{3}{2}} \cdot fck^{\frac{1}{2}}\right);$

$$vmin := 0.9391485502 \quad (12.5)$$

> $Vrdcmin := vmin \cdot b \cdot d;$

$$Vrdcmin := 1.513907463\ 10^{5} \quad (12.6)$$

> $Vrdc := evalf\left(\left(Crdc \cdot k \cdot \left(100 \cdot \rho l \cdot fck\right)^{\frac{1}{3}}\right) \cdot b \cdot d\right);$

$$Vrdc := 1.838664685\ 10^{5} \quad (12.7)$$

> $Vrdc := \max(Vrdcmin, Vrdc);$

$$Vrdc := 1.838664685\ 10^{5} \quad (12.8)$$

> $UCV := \frac{Ved}{Vrdc};$

$$UCV := 0.1881964978 \quad (12.9)$$

Check detailing and element specific rules

> **if** $l \geq 5 \cdot h$ **and** $b \geq 5 \cdot h$ **then** *print*(*Balcony may be considered as plate element*) **end if**

Balcony may be considered as plate element (13.1)

> **if** $h \geq 80$ **then** *print*(*Height of balcony is sufficient as plate element*)
> **else** *print*(*Height of balcony plate is insufficient*) **end if**

Height of balcony is sufficient as plate element (13.2)

> **if** $\min\left(\frac{fctm \cdot Wc}{fyd \cdot z}, 0.26 \cdot \frac{fctm}{fyk} \cdot b \cdot d\right) < Asmain$ **then** *print*(*Area of reinforcement is sufficient*)
> **else** *print*(*Area of main reinforcement should be increased*) **end if**;

Area of reinforcement is sufficient (13.3)

Crack width EC2

Uses effective height.

$$xe := d\cdot\left(-\alpha e\cdot\rho l+\sqrt{(\alpha e\cdot\rho l)^2+2\,\alpha e\cdot\rho l}\right);$$

$$xe := 34.79121089 \tag{14.1}$$

$$wmax := 0.2;$$

$$wmax := 0.2 \tag{14.2}$$

$$Mlin := fyd\cdot Asmain\cdot\left(d-\frac{1}{3}xe\right);$$

$$Mlin := 9.396174849\,10^7 \tag{14.3}$$

$$\textbf{if } Mfc \le Mlin \textbf{ then } z := d-\frac{1}{3}xe \textbf{ else } z := d-\beta xe \textbf{ end if};$$

$$z := 112.4029297 \tag{14.4}$$

$$hceff := \min\left((h-d)\cdot 2.5,\ \frac{(h-xe)}{3}\right);$$

$$hceff := 41.73626303 \tag{14.5}$$

$$\textbf{if } hceff < ctop+0.5\cdot\phi main \textbf{ then } print(Reinforcement\ isnt\ located\ wihtin\ hidden\ tensile\ member) \textbf{ end if};$$

$$\rho peff := \frac{Asmain}{hceff\cdot b};$$

$$\rho peff := 0.03543597461 \tag{14.6}$$

k1=0.8 for good bonding, k2=0.5 for pure bending, k3 en k4 follow from national annex. kt=0.6 because of short term loading. For verification kt=0.4.

$$k1 := 0.8 : k2 := 0.5 : k3 := 3.4 : k4 := 0.425 : kt := 0.4 :$$

$$fcteff := fctm :$$

$$\textbf{if } sreb \le \left(5\cdot\left(ctop+\frac{\phi main}{2}\right)\right) \textbf{ then } srmax := k3\cdot ctop+\frac{k1\cdot k2\cdot k4\cdot\phi main}{\rho peff} \textbf{ else } srmax := 1.3(h-xe) \textbf{ end if};$$

$$srmax := 159.5686156 \tag{14.7}$$

$$\textbf{if } srmax > \max((50-0.8\,fck)\cdot\phi main, 15\cdot\phi main) \textbf{ then } srmax := \max((50-0.8\,fck)\cdot\phi main, 15\cdot\phi main) \textbf{ end if};$$

$$\sigma sr := \frac{fcteff}{\rho peff}\cdot(1+\alpha e\cdot\rho peff);\ \sigma s := \frac{Mfc}{Asmain\cdot z};$$

$$\sigma sr := 165.6756811$$

$$\sigma s := 86.20843505 \tag{14.8}$$

$$straindifference := \frac{(\sigma s-kt\cdot\sigma sr)}{Es};\ minstraindifference := \left(0.6\cdot\frac{\sigma s}{Es}\right);$$

$$straindifference := 0.00009969081305$$

$$minstraindifference := 0.0002586253051 \tag{14.9}$$

$$\textbf{if } straindifference \le minstraindifference \textbf{ then } straindifference := minstraindifference \textbf{ end if};$$

$$straindifference := 0.0002586253051 \tag{14.10}$$

> $wkEC := straindifference \cdot srmax;$

$$wkEC := 0.04126848189 \quad (14.11)$$

> **if** $wkEC \le wmax$ **then** $print(Crack\ width\ is\ small\ enough)$ **else** $print(Crack\ width\ is\ too\ big)$ **end if**;

$$Crack\ width\ is\ small\ enough \quad (14.12)$$

Crack Width Van Breugel et al.

Short term instantaneous loading thus σcr = fctm.

> **if** $Mcr > Mk$ **then** $print(No\ fully\ developed\ crack\ pattern)$ **end if**

>

> $\sigma cr := fctm;\ \sigma scr := \frac{Mcr}{z \cdot Asmain};\ \sigma s := \frac{Mfc}{Asmain \cdot z};$

$$\sigma cr := 5.05$$

$$\sigma scr := 129.6117933$$

$$\sigma s := 86.20843505 \quad (15.1)$$

> $wm0 := 2 \cdot \left(\frac{(0.4 \cdot \phi main)}{fcmcube \cdot Es} \cdot \left(\frac{\sigma cr}{\rho l} \right)^2 \cdot (1 + \alpha e \cdot \rho l) \right)^{0.85};$

$$wm0 := 0.1300889052 \quad (15.2)$$

> $lm := 1.8 \cdot wm0 \cdot \frac{Es}{\sigma scr};$

$$lm := 361.3251902 \quad (15.3)$$

> **if** $Mk \ge Mcr$ **then** $wmv := \frac{lm}{Es} \cdot (\sigma s - 0.5 \cdot \sigma scr)$ **end if**

$$wmv := 0.03866638129 \quad (15.4)$$

> **if** $Mk > Mcr$ **then** $wmaxVB := wmv \cdot 1.7$ **else** $wmaxVB := wmv \cdot 1.3$ **end if**

$$wmaxVB := 0.06573284819 \quad (15.5)$$

Egyption Code

Egyptian code - Uses effective height

β1=0.8 for bars with profile, β2=1 for single short time loading. β=1.7 for determination of crack width induced by loading (not imposed deformation!)

> **if** $hceff < ctop + 0.5 \cdot \phi main$ **then** $print(Reinforcement\ isnt\ located\ wihtin\ hidden\ tensile\ member)$ **end if**;

> $epsmeansteel := \frac{\sigma s}{Es} \cdot \left(1 - 0.8 \cdot 0.1 \left(\frac{\sigma scr}{\sigma s} \right)^2 \right);$

$$epsmeansteel := 0.0003530951996 \quad (16.1)$$

> $Srm := 50 + \frac{0.25 \cdot k1 \cdot k2 \cdot \phi main}{\rho peff};$

$$Srm := 83.86389152 \quad (16.2)$$

> $wkEG := 1.7 \cdot epsmeansteel \cdot Srm;$

$$wkEG := 0.05034029378 \quad (16.3)$$

Crack Width American Standards ACI 318

American building code - based on z-factor method. Uses some kind of effective area but takes location of reinforcement into account.

> $\beta := \frac{(h - xu)}{(d - xu)} : dc := h - d : Ae := 2 \cdot dc \cdot b : nb := \mathrm{ceil}\left(\frac{b}{sreb}\right) : A0 := \frac{Ae}{nb} :$

> $wmaxACI := 0.011 \cdot \beta \cdot \sigma s \cdot (dc \cdot A0)^{\frac{1}{3}} \cdot 10^{-3};$

$$wmaxACI := 0.07428678746 \quad \textbf{(17.1)}$$

TS/Liggers Rel: 6.24d 23 okt 2017
Project.....: THESIS - Cantilever balcony, fully clamped
Onderdeel....:
Constructeur.: Sven Hildering
Opdrachtgever:
Dimensies....: kN/m/rad
Datum.....: 08/08/2017
Bestand.....: c:\users\svehil\documents\thesis\simpele uitkragende plaat\
simpele uitkragende plaat.dlw

Betrouwbaarheidsklasse	: 2	Referentieperiode	: 50
Toevallige inklemmingen begin	: geen	Toevallige inklemming eind	: geen
Herverdelen van momenten	: nee	Maximale deellengte	: 0.000
Ouderdom bij belasten	: 28	Relatieve vochtigheid	: 50%

Doorbuigingen(beton) zijn dmv gecorrigeerde stijfheden berekend.

Fysisch lineair : Er is gerekend met de e-modulus uit de materiaaltabel.
Fys.NLE.kort : Er is gerekend met een gecorrigeerde e-modulus (korte duur).
Deze e-mod. is berekend mbv de krachten uit de fysisch lineair berekening.

Toegepaste normen volgens Eurocode met Nederlandse NB

Belastingen	NEN-EN 1990:2002	C2:2010	NB:2011(nl)
	NEN-EN 1991-1-1:2002	C1:2009	NB:2011(nl)
Beton	NEN-EN 1992-1-1:2011(nl)	C2/A1:2015(nl)	NB:2016(nl)

K82509

GEOMETRIE

Ligger:1

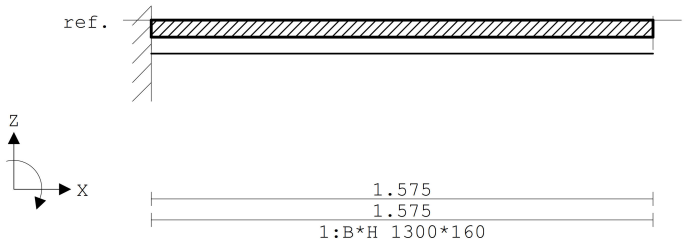

PROFIELVORMEN [mm]

1 B*H 1300*160

VELDBELASTINGEN

Ligger:1 B.G:1 Permanent

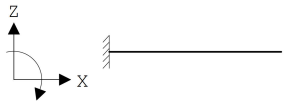

VELDBELASTINGEN

Ligger:1 B.G:2 Veranderlijk

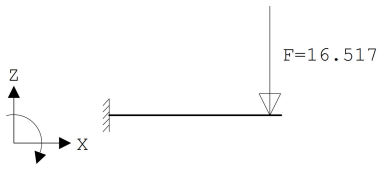

Pieters Bouwtechniek Delft Blad: 52

TS/Liggers Rel: 6.24d 23 okt 2017

Project.....: THESIS - Cantilever balcony, fully clamped
Onderdeel....:

BELASTINGCOMBINATIES

BC	Type	BG	Gen.	Factor	BG	Gen.	Factor	BG	Gen.	Factor	BG	Gen.	Factor
1	Fund.	1	Perm	1.35									
2	Fund.	1	Perm	0.90									
3	Fund.	1	Perm	1.35	2	psi0	1.50						
4	Fund.	1	Perm	1.20	2	Extr	1.50						
5	Fund.	1	Perm	0.90	2	Extr	1.50						
6	Fund.	1	Perm	0.90	2	psi0	1.50						
7	Kar.	1	Perm	1.00	2	Extr	1.00						
8	Quas.	1	Perm	1.00									
9	Quas.	1	Perm	1.00	2	psi2	1.00						
10	Freq.	1	Perm	1.00									
11	Freq.	1	Perm	1.00	2	psi1	1.00						
12	Blij.	1	Perm	1.00									

GUNSTIGE WERKING PERMANENTE BELASTINGEN

BC	Velden met gunstige werking
1	Geen
2	Alle velden de factor:0.90
3	Geen
4	Geen
5	Alle velden de factor:0.90
6	Alle velden de factor:0.90

MOMENTEN Fysisch lineair Ligger:1 B.C:7 Karakteristiek (6.14b)

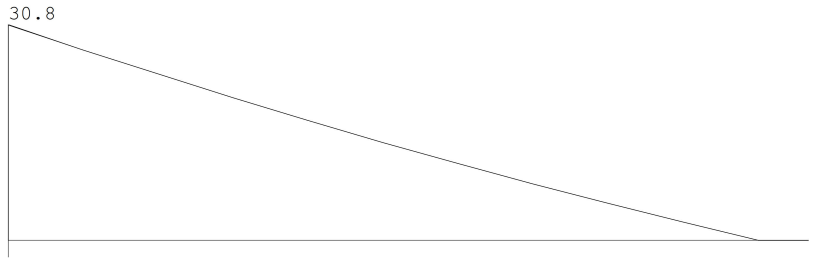

MATERIAALGEGEVENS [N][mm] t.b.v. materiaal:1 C90/105

Spanning-rek diagrammen
T.b.v sterkte
E-modulus: 26087

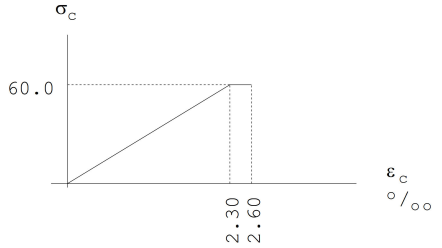

Project.....: THESIS - Cantilever balcony, fully clamped
Onderdeel....:

T.b.v korte-duur
E-modulus: 43631

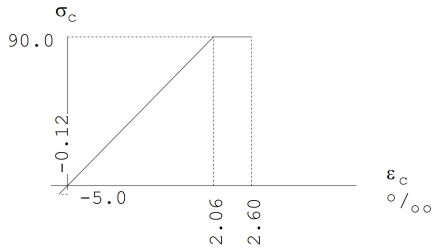

lange-duur
E-modulus: 22036

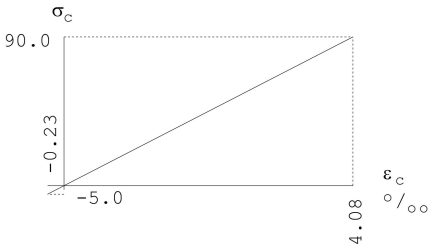

PROFIELGEGEVENS Vloer [N][mm]

t.b.v. profiel:1 B*H 1300*160

Algemeen

Materiaal : C90/105
Oppervlak : 2.080000e+05 Traagheid : 4.4373e+08
Staaftype : 0:normaal Vormfactor : 0.00

Doorsnede

breedte : 1300 hoogte : 160 zwaartepunt tov onderkant : 80
Referentie : Boven

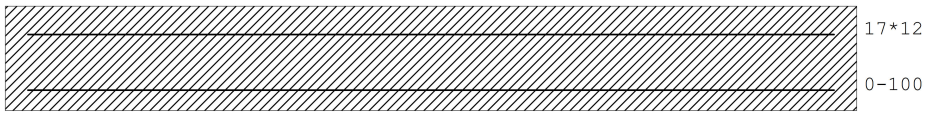

Fictieve dikte : 142.5
Breedte lastvlak a_b 6.1(10) : 0

Betonkwaliteit element : C90/105 Kruipcoëf. : 0.980
Treksterkte $f_{ct,eff}$ art. 7.1(2) : f_{ctm} (5.04 N/mm²)
Soort spanningsrekdiagram : Bi-lineair diagram
Doorbuiging volgens art.7.3.4(3): Ja
Langeduur scheurmoment begrensd : Ja
Staalkwaliteit hoofdwapening : 500 ε_{uk} : 5.00
Soort spanningsrekdiagram : Bi-lineair diagram met horizontale tak
Staalkwaliteit beugels : 500
Bundels toepassen : Nee
Geprefabriceerd element : Nee

Betondekking	Boven	Onder
Milieu	XD3	X0
Gestort tegen bestaand beton	Nee	Nee
Element met plaatgeometrie	Ja	Ja
Specifieke kwaliteitsbeheersing	Ja	Nee
Oneffen beton oppervlak	Nee	Nee
Ondergrond	Glad / N.v.t.	Glad / N.v.t.
Constructieklasse	S1	S2
Grootste korrel	31.5	

Pieters Bouwtechniek Delft Blad: 54

TS/Liggers Rel: 6.24d 23 okt 2017

Project.....: THESIS - Cantilever balcony, fully clamped
Onderdeel....:

Betondekking		Boven			Onder		
Hoofdwapening	:	1ste laag			1ste laag		
Nominale dekking	:	30			17		
Toegepaste dekking	:	30			17		
Gelijkwaardige diameter	:	12			12		
$C_{min,b}$ $C_{min,dur}$ ΔC_{dur}	:	12	25	0	12	10	0
C_{min} ΔC_{dev} C_{nom}	:	25	5	30	12	5	17
Beugel / Verdeelwapening	:	2de laag			2de laag		
Nominale dekking	:	30			15		
Toegepaste dekking	:	42			29		
Gelijkwaardige diameter	:	6			6		
$C_{min,b}$ $C_{min,dur}$ ΔC_{dur}	:	6	25	0	6	10	0
C_{min} ΔC_{dev} C_{nom}	:	25	5	30	10	5	15

Wapening		Boven	Onder
Basiswapening	:	17*12	0-100
Hoofdwapening laag	:	1	1
Automatisch verhogen basiswap.	:	Nee	Nee
Art. 7.3.2 minimum wapening	:	Ja	Ja
Bijlegdiameters	:	8;10;12	8;10;12
Diameter nuttige hoogte	:	12.0	12.0
diameter verdeelwapening	:	6.0	6.0
Min.tussenruimte	:	50	50
Aanhechting	:	Automatisch	Automatisch

Beugels

Voorkeur h.o.h. afstand : 300;150;100;75;60;50
Beugeldiameter : 8
Betonkwaliteit : C90/105
Breedte t.b.v. dwarskracht : 1300 Hoogte t.b.v. dwarskr: 160
Aantal beugelsneden per beugel : 2 Ontwerpen
Min. hoek betondrukdiagonaal θ : 21.8 z berekenen via: MRd

Hoofdwapening Fysisch lineair Ligger:1 Fundamentele combinatie

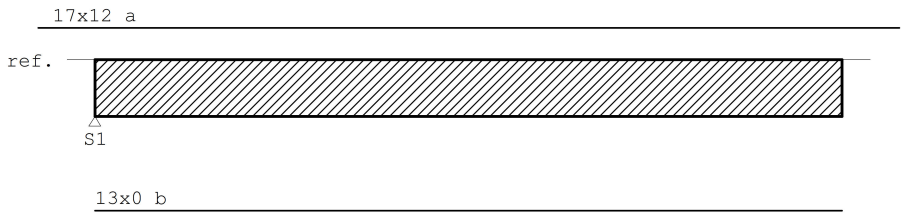

Project.....: THESIS - Cantilever balcony, fully clamped
Onderdeel....:

MEd dekkingslijn Fysisch lineair Ligger:1 Fundamentele combinatie

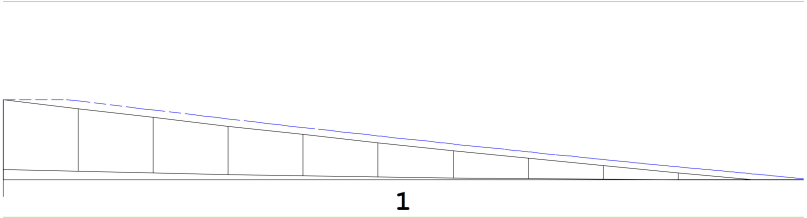

Hoofdwapening Ligger:1

Geb.	Pos. [mm]	M_{Ed} [kNm]	z	B/O	Ab [mm²]	Aa [mm²]	Basiswapening +Bijlegwapening	Opm.
1	S1+0	44.28	117	Bov	841	1924	17x12	

Scheurvorming volgens artikel 7.3.4 Ligger:1

Geb.	Pos. [mm]	Zijde	$M_{E;freq}$ [kNm]	$s_{r,max}$ [mm]	$\varepsilon_{sm}-\varepsilon_{cm}$ [‰]	w_k [mm]	k_x	w_{max} [mm]	U.C.	Opm.
1	S1+0	Bov	18.63	159	0.259	0.041	1.00	0.200	0.21	
1	S1+150	Bov	18.25	159	0.253	0.040	1.00	0.200	0.20	
1	S1+300	Bov	15.86	159	0.220	0.035	1.00	0.200	0.18	
1	S1+439	Bov	13.75	159	0.191	0.030	1.00	0.200	0.15	
1	S1+579	Bov	11.73	159	0.163	0.026	1.00	0.200	0.13	
1	S1+718	Bov	9.82	159	0.136	0.022	1.00	0.200	0.11	
1	S1+857	Bov	8.01	159	0.111	0.018	1.00	0.200	0.09	
1	S1+996	Bov	6.30	159	0.087	0.014	1.00	0.200	0.07	
1	S1+1136	Bov	4.68	159	0.065	0.010	1.00	0.200	0.05	
1	S1+1275	Bov	3.17	159	0.044	0.007	1.00	0.200	0.04	
1	S1+1425	Bov	1.66	159	0.023	0.004	1.00	0.200	0.02	
1	S1+1575	Bov	0.26	159	0.004	0.001	1.00	0.200	0.00	

Scheurvorming volgens artikel 7.3.4 (tussenresultaten)

Ligger:1

Geb.	Pos. [mm]	Zijde	Frm.	σ_s [N/mm²]	k_t	$\rho_{p,eff}$	A_s [mm²]	$A_{c,eff}$ [mm²]	k_1	k_2	α_e
1	S1+0	Bov	7.11	86	0.40	0.03543	1922	54261	0.8	0.5	4.584
1	S1+150	Bov	7.11	84	0.40	0.03543	1922	54261	0.8	0.5	4.584
1	S1+300	Bov	7.11	73	0.40	0.03543	1922	54261	0.8	0.5	4.584
1	S1+439	Bov	7.11	63	0.40	0.03543	1922	54261	0.8	0.5	4.584
1	S1+579	Bov	7.11	54	0.40	0.03543	1922	54261	0.8	0.5	4.584
1	S1+718	Bov	7.11	45	0.40	0.03543	1922	54261	0.8	0.5	4.584
1	S1+857	Bov	7.11	37	0.40	0.03543	1922	54261	0.8	0.5	4.584
1	S1+996	Bov	7.11	29	0.40	0.03543	1922	54261	0.8	0.5	4.584
1	S1+1136	Bov	7.11	21	0.40	0.03543	1922	54261	0.8	0.5	4.584
1	S1+1275	Bov	7.11	14	0.40	0.03543	1922	54261	0.8	0.5	4.584
1	S1+1425	Bov	7.11	7	0.40	0.03543	1922	54261	0.8	0.5	4.584
1	S1+1575	Bov	7.11	1	0.40	0.03543	1922	54261	0.8	0.5	4.584

Pieters Bouwtechniek Delft Blad: 56

TS/Liggers Rel: 6.24d 23 okt 2017

Project.....: THESIS - Cantilever balcony, fully clamped
Onderdeel....:

DWARSKRACHTEN Fysisch lineair Ligger:1 Fundamentele combinatie

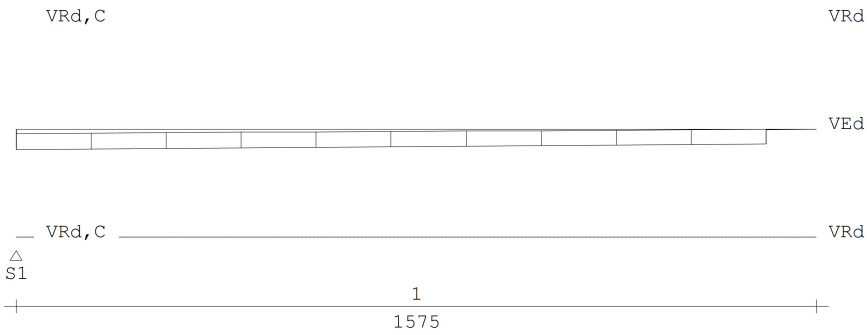

Schuifspanningen

Ligger:1

Geb.	Vanaf [mm]	Tot [mm]	θ [°]	V_{Ed} [kN]	$v_{Ed} < v_{Rd} < v_{Rd,max}$ [N/mm²]	v_{opg} [N/mm²]	Opm.
1	S1+0	S1+1575	21.8	35	0.21 1.14 7.53		71

Opmerkingen
[71] Er wordt voor platen geen minimale dwarskrachtwapening volgens art. 9.3.2 toegepast. Uitgangspunt hiervoor is dat er herverdeling van belastingen in dwarsrichting mogelijk is (zie art. 6.2.1(4)).

Stijfheden (blijvend en quasi-blijvend)

Ligger:1

Veld	Pos [mm]	A_{boven} [mm²]	A_{onder} [mm²]	M_{Eg} [kNm]	E_{Eg}^* [N/mm²]	M_{Qb} [kNm]	$E_{Qb;on}^*$ [N/mm²]	$E_{Qb;\infty}^*$ [N/mm²]
1	0	1923	0	6.4	45240	13.8	45240	23583
1	158	1923	0	5.2	45240	11.8	45240	23583
1	315	1923	0	4.1	45240	9.9	45240	23583
1	473	1923	0	3.2	45240	8.1	45240	23583
1	630	1923	0	2.3	45240	6.5	45240	23583
1	788	1923	0	1.6	45240	5.0	45240	23583
1	945	1923	0	1.0	45240	3.7	45240	23583
1	1103	1923	0	0.6	45240	2.4	45240	23583
1	1260	1923	0	0.3	45240	1.3	45240	23583
1	1418	1923	0	0.1	45239	0.3	45240	23583

Stijfheden (frequent en karakteristiek)

Ligger:1

Veld	Pos [mm]	A_{boven} [mm²]	A_{onder} [mm²]	M_{Ef} [kNm]	$E_{Ef,on}^*$ [N/mm²]	$E_{Ef,\infty}^*$ [N/mm²]	M_{Ek} [kNm]	$E_{Ek;on}^*$ [N/mm²]	$E_{Ek;\infty}^*$ [N/mm²]
1	0	1923	0	18.6	45240	26959	30.8	34689	26391
1	158	1923	0	16.1	45240	27088	27.0	45240	32316
1	315	1923	0	13.7	45240	27227	23.3	45240	32560
1	473	1923	0	11.4	45240	27377	19.7	45240	32818
1	630	1923	0	9.3	45240	27540	16.3	45240	33090
1	788	1923	0	7.3	45240	27717	13.0	45240	33377
1	945	1923	0	5.4	45240	27908	9.8	45240	33679
1	1103	1923	0	3.7	45240	28112	6.7	45240	33992
1	1260	1923	0	2.0	45240	28318	3.8	45240	34298

Project.....: THESIS - Cantilever balcony, fully clamped
Onderdeel....:

Stijfheden (blijvend en quasi-blijvend)

Ligger:1

Veld	Pos [mm]	A_{boven} [mm^2]	A_{onder} [mm^2]	M_{Eg} [kNm]	E_{Eg}^{*} [N/mm^2]	M_{Qb} [kNm]	$E_{Qb;on}^{*}$ [N/mm^2]	$E_{Qb;\infty}^{*}$ [N/mm^2]	
1	1418	1923	0	0.5	45240	28365	1.0	45240	34367

D

Input and analysis properties DIANA FEA

Material properties

This section explains and elaborates on decisions that have been made to come to the material model properties presented in table 8.1 in paragraph 8.5.

Concrete

Cracking model It has been decided to apply a total strain based crack model with a rotating crack orientation and a crack bandwidth specification determined by Rots. According to [17] this concrete model is preferred over the fixed crack orientation since it prevents the stress-locking phenomenon. This phenomenon might result in an overestimation of the failure limit and thus choosing for the rotating crack orientation is a conservative choice. The Rots crack bandwidth model determines crack bandwidth using element dimensions, which is preferable for the prediction of realistic crack widths.

Tensile behaviour Eurocode 2 describes a brittle tensile behaviour of concrete, whereas Model Code 2010 shows a more gentle behaviour. For starters it has been tried to use the Eurocode 2 model, depicted left in figure D.1. This model assumes that at the location of a crack residual strength or stiffness is absent. This results in an unstable numerical model, which obviously has trouble diverging. Alternatives are found in the Model Code 2010 and Hordijk models. Since [17] advises to apply an exponential softening diagram, the Hordijk curve has been used.

For this model the fracture energy has been determined according to the Model Code 2010 method, through the equation below.

$$G_f = 73 * f_{cm}^{0.18} \tag{D.1}$$

The Hordijk-model is advantageous in a numerical sense for two reasons: 1) studying cracking behaviour with this model results in more localized cracks and thus less disseminated cracking [17], and 2) the Hordijk-model allows the user to specify a residual tensile strength. Both reasons facilitate the model to have less trouble finding convergence. Following the advice of ir. C. Frissen from Diana FEA a residual tensile strength of 0.1 N/mm^2 has been applied.

Compressive behaviour Following the advice in the report of Rijkswaterstaat [17] a parabolic stress strain diagram is applied as presented in figure D.2. The value of the compressive fracture energy, denoted as G_c, is described in several ways. The Diana FEA user's manual states that according to Feenstra [15] the fracture energy has a value between 50 to 100 times the tensile fracture energy G_f. However, in the Rijkswaterstaat report, a value of 250 times G_f is advised. This value is based on research results from Nakamura and Higai,[19]. In view of the fact that Feenstra is also incorporated in the development of the Rijkswaterstaat document, it is assumed that the results in his own doctoral thesis are outdated and the method of Nakamura and Higai are used.

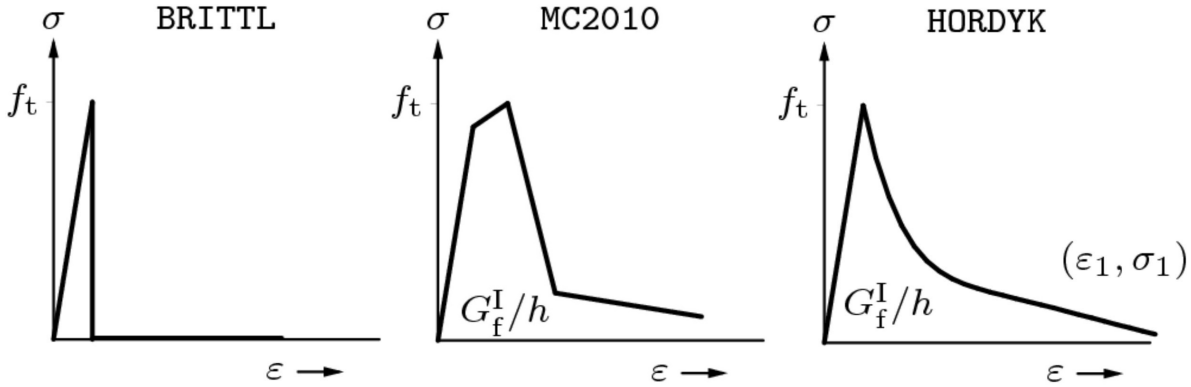

Figure D.1: Tensile behaviour models, source: [11].

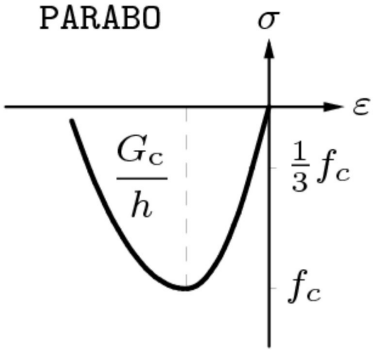

Figure D.2: Compressive stress strain behaviour model, source: [11].

Reduction due to lateral cracking is determined by Vecchio and Collins [34] and described by a factor β_σ, which represents the fraction of compressive strength which resides after lateral cracking. In the Rijkswaterstaat report it is advised to apply $\beta_\sigma^{min} = 0.4$. Diana then automatically determines β_σ through the equation below, taking into account a minimum value of 0.4. In the equation ε_0 represents the maximum compressive strain in a concrete cylinder and ε_1 is the acting average principal tensile strain.

$$\beta_\sigma = \frac{1}{1+K_c} \leq 1 \quad with \quad K_c = 0.027\left(-\frac{\varepsilon_1}{\varepsilon_0} - 0.37\right) \tag{D.2}$$

To finalize the compressive behaviour a residual compressive strength of 0.1 N/mm^2 is applied for numerical stability reasons and the conservative choice of not having a capacity increase when stress confinement occurs is implemented. In other words, the compressive strength of the concrete remains at the initially applied value, even though it is known that the compressive strength increases when a multi-axial compressive force is working.

Reinforcement

The reinforcement has been modelled in the Diana class Reinforcements and Pile Foundations with the Uniaxial nonlinear elasticity material model. The first branch of the graph is linear, followed by an ascending yielding branch. For model stability reasons in the Rijkswaterstaat report it is advised to apply a Young's modulus $E_{s,har}$ equal to 2 % of the initial E_s. The resulting stress strain diagram can be found in figure D.3.

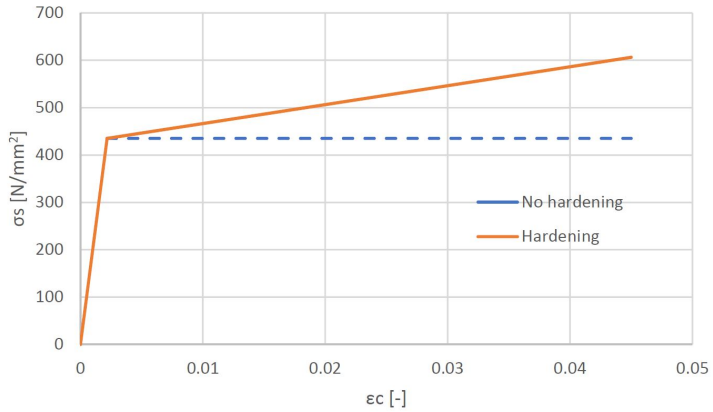

Figure D.3: Stress-strain diagram of reinforcing steel B500 with and without hardening.

Bond-slip The bond between concrete and reinforcement is not infinitely stiff and the properties of the bond influence the interaction between concrete and reinforcement and the overall behaviour of the structure. Assuming a perfect bond would overestimate the capacity of the structure and would underestimate for example crack widths. When modelling reinforcement in most cases a perfect bond is assumed, in which the reinforcement strains in the numerical model are determined in the elements of the concrete the reinforcement is embedded in. In other words, the reinforcement has no own degrees of freedom, and thus bond-slip can not take place. When it is pursued to take bond-slip into account, specific reinforcement elements have to be modelled, as explained in [30]. According to the book *Continuous and Discontinuous modelling of fracture in concrete using FEM* [32], there are different methods of determining bond forces and/or bond-slip. Four methods are presented of which the fib Model Code 1992 method has been chosen to apply. This method has been chosen for its numerical stability because of its residual bond strength. First, using the Model Code 2010, the method has been updated to current standards, and then implemented in Diana using the Friction stress-slip diagram. The diagram has been generated through the following equations:

$$\tau = \begin{cases} \tau_{max} * \left(\frac{u}{u_1}\right)^{0.4} & \text{for } 0 \leq u \leq u_1 \\ \tau_{max} & \text{for } u_1 \leq u \leq u_2 \\ \tau_{max} - \left(\frac{\tau_{max} - \tau_{b,f}}{u_3 - u_2}\right)(u - u_2) & \text{for } u_2 \leq u \leq u_3 \\ \tau_{bf} & \text{for} u > u_3 \end{cases} \tag{D.3}$$

with:

$$\tau_{max} = 2.5 * \sqrt{fcm} \quad \tau_{b,f} = 0.4 * \tau_{max} \quad u_1 = 1 \quad u_2 = 2 \quad u_3 = 6 \tag{D.4}$$

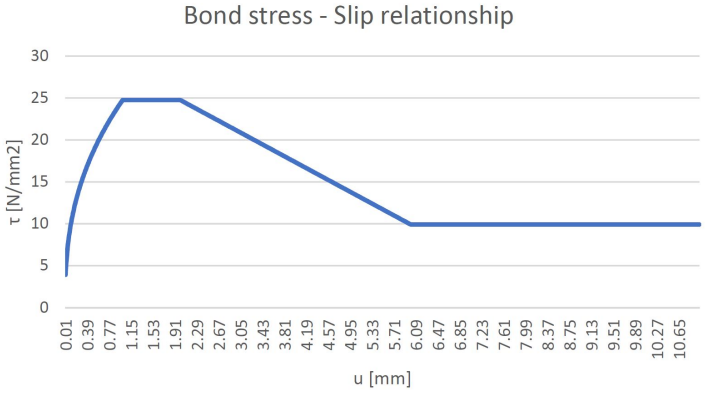

Figure D.4: Bond stress - Slip relationship between concrete and reinforcement.

Values of τ_{max}, u_1, and u_2 follow from the assumption that good bonding conditions will be present. u_3 is the

clear distance between the ribs of the reinforcement and is assumed to be 6 mm.

For taking into account bond-slip, shear stiffness and normal stiffness have to be incorporated. The shear stiffness, DSXX, represents the stiffness along the interface between the reinforcement and the concrete. DSXX is the stiffness modulus of the first part of the graph in figure D.4. The normal stiffness DSNY is the stiffness perpendicular to the interface and is determined through equation D.5. R in the equation represents bar radius. The relations follow from [13]. However, in this research no reliable conclusion on how accurate these stiffness relations are is drawn. Because of the insecurity in determining DSXX and DSNY and the observation of little to no influence it has been decided to take bond slip out of consideration.

$$DSNY = \frac{E_c}{2 * R} \tag{D.5}$$

Meshing and Element types

A mesh refinement study for the balcony in part III of this report has been executed with the results presented in table D.1. Unfortunately because of computation capacity and digital storage space a further decrease in mesh width appeared impossible and a mesh size of 20 mm is applied.

Category	Characteristic load combination	Frequent load combination
50 mm		
Crack width - DIANA FEA	0.32 mm	0.23 mm
$\varepsilon_{s,max}$	$1.45*10^{-3}$	$1.04*10^{-3}$
Displacement	-7.56 mm	-5.39 mm
$\varepsilon_{s,max} * s_{r,max}$	0.20 mm	0.149 mm
25 mm		
Crack width - DIANA FEA	0.45 mm	0.33 mm
$\varepsilon_{s,max}$	$1.21*10^{-3}$	$8.61*10^{-3}$
Displacement	-7.09 mm	-5.04 mm
$\varepsilon_{s,max} * s_{r,max}$	0.18 mm	0.129 mm
20 mm		
Crack width - DIANA FEA	0.40 mm	0.29 mm
$\varepsilon_{s,max}$	$1.13*10^{-3}$	$8.1*10^{-3}$
Displacement	-6.73 mm	-4.79 mm
$\varepsilon_{s,max} * s_{r,max}$	0.17 mm	0.12 mm

Table D.1: Results mesh refinement study

All element types applied in part II, III, and IV of this report are described in table D.2. The specific elements per part are also mentioned in tables D.3 and D.4.

Analysis input

Iterative procedures

Diana approaches/predicts reality by iteratively following an integration scheme as schematized in figure D.5.

In the analysis described in part II, III, and IV of this report two integration schemes have been used: the Secant (Quasi Newton) method and the regular Newton-Raphson method.

Secant (Quasi-Newton) method This integration scheme has been applied for the first two loading blocks for the dead weight and the point load. It has been decided to apply the Secant method, BFGS type, in those stages of the analysis because cracking will occur. Within the iterative process the Secant method uses results from the previous solution vectors to arrive at a better approximation. Furthermore it does not develop a new stiffness matrix for every iteration but only for each increment, reducing calculation time.

Regular Newton-Raphson method The third stage of the analysis, where the point load is partially unloaded, is approached by the Regular Newton-Raphson method, linear type. It has been decided to use this method

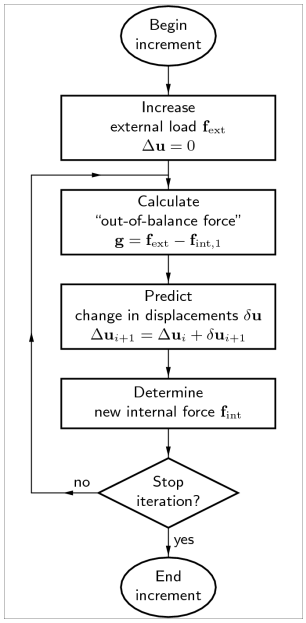

Figure D.5: Schematization of iterative procedure performed by numerical scheme, source: [11].

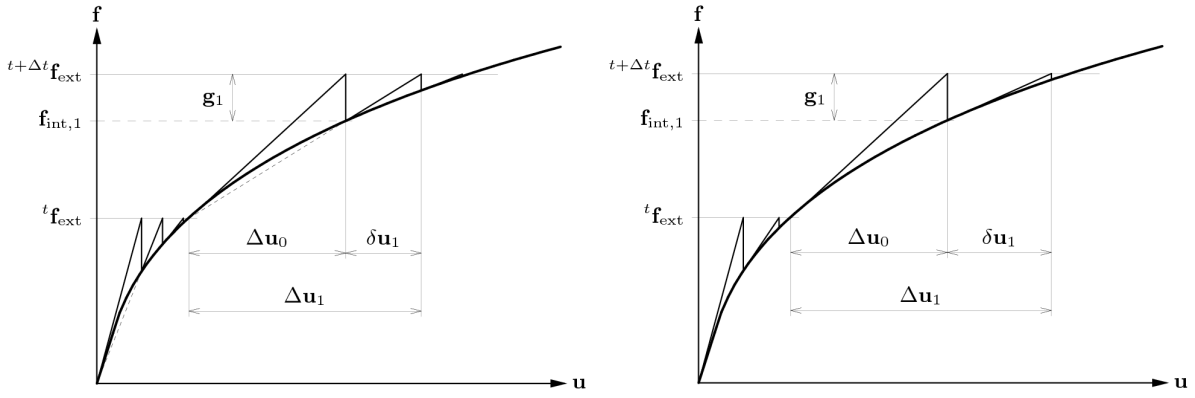

Figure D.6: Visualization of iterative process for the Secant (Quasi-Newton) method respectively for the regular Newton-Raphson method, source: [11].

because due to the unloading cracks will close again, and thus it is preferable to update the stiffness matrix for every iteration. This increases computation time, but also the chance of finding a converged solution.

Convergence criteria For DIANA FEA to be able to judge the accuracy of the result of an iteration in a non linear analysis, convergence criteria should be prescribed. When the results of an iteration are satisfying, the process should be terminated. In this research the iteration results should fulfil both a force norm and a displacement norm at the same time.

For the force norm the relative out of balance force is computed. When this the difference between the relative out of balance force and the external force exceeds a value of 1%, the iteration results are not accepted and a new iteration is started until the maximum amount of iterations has been reached. When the maximum amount of iterations is reached, or when divergence occurs, the process is terminated. In case a satisfying result is found, the analysis continues with the next load step. In case of divergence or an unsatisfying result, the analysis is completely terminated. A similar process is followed to verify the calculated displacements.

Line search Especially with high strength concrete cracks tend to quite suddenly propagate. This highly nonlinear behaviour makes finding convergence more difficult. The cracking can cause the prediction to end up too far from equilibrium, which will result in a diverging analysis. According to DIANA FEA, the line search

algorithm scales incremental displacements automatically which might stabilize the analysis.

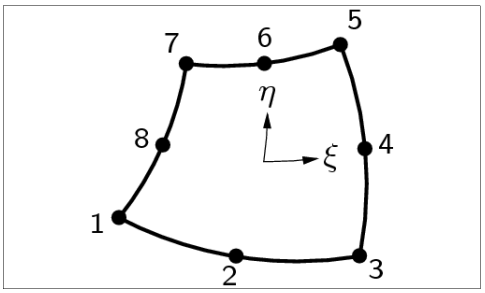

CQ16M is a quadratic isoparametric plane stress element possessing eight nodes. This element is used in the 2D models in part II of this report.

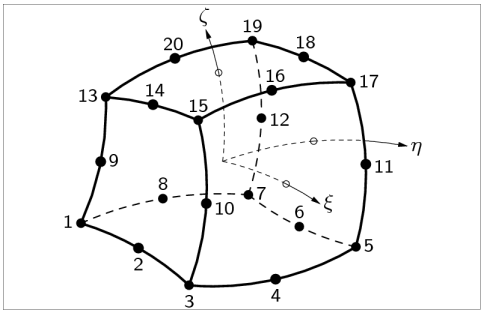

CHX60 is a quadratic isoparametric solid brick element with a cubical shape containing twenty nodes. This element forms the biggest part of the balcony models in part III and IV of this report.

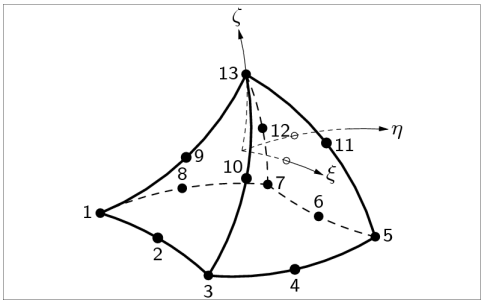

CPY39 is a quadratic isoparametric solid with thirteen nodes in the shape of a pyramid. This shape is, similar to the next two element types, used to fill spaces which cannot be filled with CHX60 elements in the balcony models in part III and IV of this report.

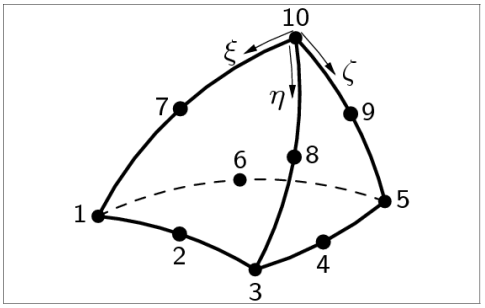

CTE30 is a tetrahedron shaped quadratic and isoparametric ten-noded element. This element type used in part III and IV of this report.

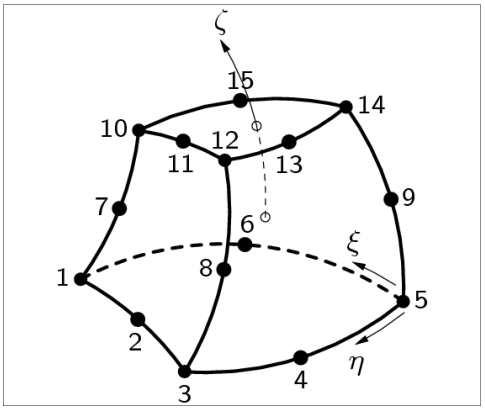

CTP45 is an quadratic isoparametric wedge element with fifteen nodes. This element type used in part III and IV of this report.

Table D.2: Applied elements in DIANA FEA models, source of images: [11].

Category	Comments
Analysis type	Structural Nonlinear
Units	N, mm
Extent of model	10 m
Coordinate system	[x,y]
Major dimensions	1575 x 1300 x XX mm
Material data	§8.5 & §D
Element type Quadratic	CQ16M
Integration scheme	G: Secant (Quasi-Newton) Q: Secant (Quasi Newton) -0.5*Q: Newton-Raphson regular
Mesh density	10 mm
Supports	Left vertical edge Point bottom left See figure 8.2
Constraints	Horizontal [x]: left vertical edge Vertical [y]: Point bottom left
Load cases	Dead weight: G Point load: Q Partial release of point load: -0.5Q

Table D.3: Finite element analysis input parameters with comments for fully clamped cantilevering slab.

Category	Comments
Analysis type	Structural Nonlinear
Units	N, mm
Extent of model	10 m
Coordinate system	[x,y]
Major dimensions	1575 x 1300 x 110 mm
Material data	§12.5 & §D
Element type Quadratic	CQ16M, CPY39, CTE30, CTP45
Integration scheme	G: Secant (Quasi-Newton) Q: Secant (Quasi Newton) -0.5*Q: Newton-Raphson regular
Mesh density	20 mm
Supports	Horizontal support on vertical area Vertical support on horizontal area See figure 12.2 (in-plane ridge) and 16.3 (out-of-plane ridge)
Constraints	Horizontal [x]: vertical edges of ridge Vertical [y]: horizontal edge of ridge
Load cases	Dead weight: G Point load: Q Partial release of point load: -0.5Q

Table D.4: Finite element analysis input parameters with comments for balcony with in-plane ridge and balcony with out-of-plane ridge.

E

Results of fully clamped balcony

The results from the analytical and numerical analysis of the 105 balcony variants is summarized in the tables on the next pages. First a table with a total overview of analytical and numerical results is presented. This followed by graphs showing the influence of reinforcement spacing on crack width prediction for the different variants. This appendix ends with graphs presenting the difference in percentage between the crack width predicted with the Eurocode 2 method and the other methods.

h	Ø	S	n	As	ρ	Q	Mk	Mfc	Med	σc	σrmax	Mcr	Mrd	Mrd/Mk	UC-M	UC-V	wk [mm]				Diana	Remarks
	[mm]	[mm]	[-]	[mm²]	[%]	[kN]	[kNm]	[kNm]	[kNm]	[N/mm²]	[mm]	[kNm]	[kNm]	-	-	-	EC	v. Breugel	Egyptian	ACI	ε_{sy}	wk[mm]	
200	12	150	9	1017.88	0.48	27.17	48.1	28.1	69.7	179.6	180	43.8	71.1	1.48	0.98	0.26	0.097	0.261	0.168	0.181	0.0000442	0.007956	
		120	11	1244.07	0.58	27.17	48.1	28.1	69.7	147.9	180	43.8	86.4	1.80	0.81	0.26	0.08	0.186	0.121	0.14	0.0000438	0.007884	
		100	13	1470.27	0.69	27.17	48.1	28.1	69.7	125.9	180	43.8	101.7	2.11	0.67	0.26	0.068	0.141	0.093	0.113	0.0000434	0.007812	
		80	17	1922.65	0.90	27.17	48.1	28.1	69.7	97.2	175.16	43.8	131.7	2.74	0.53	0.24	0.051	0.09	0.062	0.081	0.0000427	0.007479	
		60	22	2488.14	1.17	27.17	48.1	28.1	69.7	75.9	158.86	43.8	168.3	3.50	0.41	0.22	0.036	0.059	0.043	0.058	0.0000418	0.00684	
	10	150	9	706.86	0.33	27.17	48.1	28.1	69.7	254.5	150	43.8	50	1.04	1.4	0.26	0.115	0.418	0.273	0.248	0.0000454	0.00681	UC-M too high
		120	11	863.94	0.40	27.17	48.1	28.1	69.7	209.3	150	43.8	60.9	1.27	1.15	0.26	0.094	0.298	0.195	0.191	0.0000451	0.006765	UC-M too high
		100	13	1021.02	0.48	27.17	48.1	28.1	69.7	178	150	43.8	71.7	1.49	0.97	0.26	0.08	0.225	0.148	0.155	0.0000448	0.00672	
		80	17	1335.18	0.62	27.17	48.1	28.1	69.7	137.3	150	43.8	93.2	1.94	0.75	0.26	0.062	0.143	0.097	0.11	0.0000443	0.006645	
		60	22	1727.88	0.81	27.17	48.1	28.1	69.7	107	150	43.8	119.6	2.49	0.58	0.25	0.048	0.093	0.066	0.079	0.0000436	0.00654	
	8	150	9	452.39	0.21	27.17	48.1	28.1	69.7	391	120	43.8	32.4	0.67	2.16	0.26	0.14	0.74	0.5	0.369	0.0000467	0.005604	UC-M too high, not enough reinforcement
		120	11	552.92	0.26	27.17	48.1	28.1	69.7	321.4	120	43.8	39.5	0.82	1.77	0.2	0.116	0.528	0.354	0.28	0.0000465	0.00558	UC-M too high, not enough reinforcement
		100	13	653.45	0.30	27.17	48.1	28.1	69.7	273	120	43.8	46.5	0.97	1.5	0.26	0.098	0.399	0.267	0.229	0.0000462	0.005544	UC-M too high
		80	17	854.51	0.40	27.17	48.1	28.1	69.7	210.3	120	43.8	60.6	1.26	1.15	0.26	0.076	0.253	0.172	0.162	0.0000458	0.005496	UC-M too high
		60	22	1105.84	0.51	27.17	48.1	28.1	69.7	163.7	120	43.8	78	1.62	0.89	0.26	0.059	0.164	0.115	0.116	0.0000453	0.005436	
180	12	150	9	1017.88	0.54	21.52	39	23.1	56.3	169	180	35.4	62.2	1.59	0.91	0.25	0.091	0.225	0.148	0.176	0.0000422	0.007596	
		120	11	1244.07	0.66	21.52	39	23.1	56.3	139.2	180	35.4	75.6	1.94	0.74	0.25	0.075	0.161	0.108	0.136	0.0000418	0.007524	
		100	13	1470.27	0.79	21.52	39	23.1	56.3	118.5	180	35.4	88.9	2.28	0.63	0.23	0.063	0.122	0.083	0.11	0.0000414	0.007452	
		80	17	1922.65	1.03	21.52	39	23.1	56.3	91.6	167.32	35.4	115	2.95	0.49	0.21	0.046	0.078	0.056	0.079	0.0000406	0.006793	
		60	22	2488.14	1.33	21.52	39	23.1	56.3	71.5	150.94	35.4	146.7	3.76	0.38	0.2	0.032	0.051	0.039	0.057	0.000038	0.005736	
	10	150	9	706.86	0.37	21.52	39	23.1	56.3	239.1	150	35.4	43.8	1.12	1.28	0.24	0.108	0.36	0.24	0.24	0.0000435	0.006525	UC-M too high
		120	11	863.94	0.46	21.52	39	23.1	56.3	196.7	150	35.4	53.4	1.37	1.06	0.24	0.089	0.257	0.172	0.186	0.0000432	0.00648	UC-M too high
		100	13	1021.02	0.54	21.52	39	23.1	56.3	167.3	150	35.4	62.8	1.61	0.9	0.24	0.075	0.194	0.132	0.15	0.0000429	0.006435	
		80	17	1335.18	0.71	21.52	39	23.1	56.3	129.1	150	35.4	81.6	2.09	0.69	0.24	0.058	0.124	0.087	0.107	0.0000423	0.006345	
		60	22	1727.88	0.92	21.52	39	23.1	56.3	100.7	150	35.4	104.6	2.68	0.54	0.22	0.045	0.08	0.06	0.077	0.0000416	0.00624	
	8	150	9	452.39	0.24	21.52	39	23.1	56.3	366.9	120	35.4	28.4	0.73	1.98	0.24	0.132	0.64	0.437	0.356	0.0000448	0.005376	UC-M too high, not enough reinforcement
		120	11	552.92	0.29	21.52	39	23.1	56.3	301.6	120	35.4	34.7	0.89	1.63	0.24	0.109	0.456	0.31	0.274	0.0000446	0.005352	UC-M too high
		100	13	653.45	0.34	21.52	39	23.1	56.3	256.3	120	35.4	40.9	1.05	1.38	0.24	0.092	0.344	0.235	0.231	0.0000444	0.005328	UC-M too high
		80	17	854.51	0.45	21.52	39	23.1	56.3	197.5	120	35.4	53.2	1.36	1.06	0.24	0.071	0.249	0.153	0.157	0.000044	0.00528	UC-M too high
		60	22	1105.84	0.58	21.52	39	23.1	56.3	153.8	120	35.4	68.4	1.75	0.82	0.24	0.055	0.142	0.103	0.113	0.0000435	0.00522	
160	12	150	9	1017.88	0.63	16.52	30.8	18.6	44.3	158.9	180	28	53.4	1.73	0.83	0.23	0.086	0.19	0.131	0.172	0.0000395	0.00711	
		120	11	1244.07	0.77	16.52	30.8	18.6	44.3	130.9	180	28	64.8	2.10	0.68	0.22	0.071	0.136	0.096	0.134	0.0000391	0.007038	
		100	13	1470.27	0.91	16.52	30.8	18.6	44.3	111.5	179.53	28	76.1	2.47	0.58	0.21	0.06	0.103	0.074	0.108	0.0000387	0.006948	
		80	17	1922.65	1.19	16.52	30.8	18.6	44.3	86.2	156.57	28	98.2	3.19	0.45	0.19	0.041	0.066	0.05	0.078	0.000038	0.00595	
		60	22	2488.14	1.54	16.52	30.8	18.6	44.3	67.4	145.1	28	125.1	4.06	0.35	0.17	0.029	0.043	0.035	0.056	0.0000371	0.005383	
	10	150	9	706.86	0.43	16.52	30.8	18.6	44.3	224.4	150	28	37.7	1.22	1.18	0.23	0.101	0.303	0.21	0.234	0.0000409	0.006135	UC-M too high
		120	11	863.94	0.53	16.52	30.8	18.6	44.3	184.7	150	28	45.9	1.49	0.97	0.23	0.083	0.217	0.152	0.181	0.0000406	0.00609	
		100	13	1021.02	0.63	16.52	30.8	18.6	44.3	157.1	150	28	54	1.75	0.82	0.23	0.071	0.164	0.117	0.147	0.0000403	0.006045	
		80	17	1335.18	0.82	16.52	30.8	18.6	44.3	121.3	150	28	70	2.27	0.63	0.21	0.055	0.105	0.078	0.104	0.0000397	0.005955	
		60	22	1727.88	1.06	16.52	30.8	18.6	44.3	94.7	150	28	89.5	2.91	0.49	0.19	0.043	0.076	0.054	0.076	0.0000391	0.005865	
	8	150	9	452.39	0.28	16.52	30.8	18.6	44.3	343.7	120	28	24.8	0.81	1.8	0.22	0.124	0.541	0.37	0.345	0.0000423	0.005076	UC-M too high
		120	11	552.92	0.34	16.52	30.8	18.6	44.3	282.6	120	28	29.8	0.97	1.48	0.22	0.102	0.386	0.271	0.267	0.0000421	0.005052	UC-M too high
		100	13	653.45	0.40	16.52	30.8	18.6	44.3	240.2	120	28	35.2	1.14	1.26	0.22	0.086	0.291	0.206	0.215	0.0000419	0.005028	UC-M too high
		80	17	854.51	0.52	16.52	30.8	18.6	44.3	185.1	120	28	45.7	1.48	0.97	0.22	0.067	0.185	0.135	0.153	0.0000415	0.00498	
		60	22	1105.84	0.68	16.52	30.8	18.6	44.3	144.3	120	28	58.8	1.91	0.75	0.22	0.052	0.12	0.092	0.11	0.000041	0.00492	
140	12	150	9	1017.88	0.75	12.18	23.6	14.6	33.7	149.6	180	21.4	44.5	1.89	0.76	0.21	0.081	0.155	0.115	0.172	0.0000358	0.006444	
		120	11	1244.07	0.92	12.18	23.6	14.6	33.7	123.3	180	21.4	53.4	2.26	0.62	0.19	0.067	0.111	0.085	0.134	0.0000354	0.006372	
		100	13	1470.27	1.09	12.18	23.6	14.6	33.7	105	169.3	21.4	63.3	2.68	0.53	0.18	0.053	0.084	0.066	0.109	0.0000351	0.005942	
		80	17	1922.65	1.42	12.18	23.6	14.6	33.7	81.3	151.94	21.4	81.5	3.45	0.41	0.16	0.037	0.054	0.045	0.078	0.0000344	0.005227	
		60	22	2488.14	1.84	12.18	23.6	14.6	33.7	63.6	139.36	21.4	103.4	4.38	0.33	0.15	0.027	0.035	0.032	0.057	0.0000337	0.004696	
	10	150	9	706.86	0.52	12.18	23.6	14.6	33.7	210.7	150	21.4	31.5	1.33	1.07	0.21	0.095	0.249	0.183	0.232	0.0000374	0.00561	UC-M too high
		120	11	863.94	0.63	12.18	23.6	14.6	33.7	173.5	150	21.4	38.3	1.62	0.88	0.21	0.078	0.178	0.133	0.18	0.0000371	0.005565	
		100	13	1021.02	0.75	12.18	23.6	14.6	33.7	147.7	150	21.4	45.1	1.91	0.75	0.2	0.066	0.135	0.103	0.146	0.0000368	0.00552	
		80	17	1335.18	0.98	12.18	23.6	14.6	33.7	114.1	150	21.4	58.3	2.47	0.58	0.18	0.051	0.086	0.07	0.104	0.0000363	0.005445	
		60	22	1727.88	1.27	12.18	23.6	14.6	33.7	89.1	148.81	21.4	74.5	3.16	0.45	0.17	0.04	0.056	0.049	0.076	0.0000357	0.005313	
	8	150	9	452.39	0.33	12.18	23.6	14.6	33.7	321.9	120	21.4	20.5	0.97	1.64	0.21	0.116	0.444	0.327	0.339	0.0000389	0.004668	UC-M too high
		120	11	552.92	0.40	12.18	23.6	14.6	33.7	264.8	120	21.4	25	1.06	1.35	0.21	0.095	0.317	0.235	0.262	0.0000387	0.004644	UC-M too high
		100	13	653.45	0.47	12.18	23.6	14.6	33.7	225.1	120	21.4	29.5	1.25	1.14	0.21	0.081	0.239	0.18	0.212	0.0000385	0.00462	UC-M too high
		80	17	854.51	0.62	12.18	23.6	14.6	33.7	173.6	120	21.4	38.3	1.62	0.88	0.21	0.063	0.152	0.119	0.151	0.0000381	0.004572	
		60	22	1105.84	0.80	12.18	23.6	14.6	33.7	135.4	120	21.4	59.2	2.51	0.69	0.19	0.049	0.099	0.082	0.109	0.0000367	0.004404	
	12	150	9	1017.88	0.93	8.47	17.3	11.1	24.5	141.6	180	15.8	35.7	2.06	0.69	0.17	0.076	0.122	0.101	0.177	0.0000306	0.005508	fceff too small

		120	11	1244.07	1.14	8.47	17.3	11.1	24.5	116.8	170.84	15.8	43.2	2.50	0.57	0.16	0.06	0.087	0.075	0.137	0.0000302	0.005159	Hceff too small
		100	13	1470.27	1.35	8.47	17.3	11.1	24.5	99.5	159.25	15.8	50.3	2.91	0.49	0.15	0.047	0.066	0.059	0.11	0.0000299	0.004762	Hceff too small
		80	17	1922.65	1.76	8.47	17.3	11.1	24.5	77.1	144.46	15.8	64.8	3.75	0.38	0.14	0.033	0.043	0.041	0.081	0.0000294	0.004247	Hceff too small
		60	22	2488.14	2.28	8.47	17.3	11.1	24.5	60.4	133.76	15.8	81.8	4.73	0.3	0.13	0.024	0.028	0.03	0.059	0.0000287	0.003839	Hceff too small
	10	150	9	706.86	0.64	8.47	17.3	11.1	24.5	198.7	150	15.8	25.4	1.47	0.97	0.19	0.089	0.196	0.159	0.236	0.0000323	0.004845	Hceff too small
		120	11	863.94	0.78	8.47	17.3	11.1	24.5	163.7	150	15.8	30.8	1.78	0.8	0.18	0.074	0.14	0.117	0.183	0.000032	0.0048	Hceff too small
		100	13	1021.02	0.92	8.47	17.3	11.1	24.5	139.4	150	15.8	36.2	2.09	0.68	0.17	0.063	0.106	0.091	0.149	0.0000318	0.00477	Hceff too small
		80	17	1335.18	1.21	8.47	17.3	11.1	24.5	107.8	150	15.8	46.7	2.70	0.53	0.16	0.049	0.068	0.062	0.107	0.0000313	0.004695	Hceff too small
		60	22	1727.88	1.56	8.47	17.3	11.1	24.5	84.3	141.79	15.8	59.5	3.44	0.41	0.15	0.036	0.044	0.044	0.078	0.0000307	0.004353	Hceff too small
	8	150	9	452.39	0.40	8.47	17.3	11.1	24.5	302.6	120	15.8	16.6	0.96	1.48	0.19	0.109	0.35	0.281	0.342	0.0000339	0.004068	UC-M too high
		120	11	552.92	0.49	8.47	17.3	11.1	24.5	249	120	15.8	20.2	1.17	1.21	0.19	0.09	0.25	0.204	0.265	0.0000338	0.004056	UC-M too high
		100	13	653.45	0.58	8.47	17.3	11.1	24.5	211.8	120	15.8	23.8	1.38	1.03	0.19	0.076	0.189	0.157	0.214	0.0000336	0.004032	UC-M too high
		80	17	854.51	0.76	8.47	17.3	11.1	24.5	163.5	120	15.8	30.1	1.74	0.79	0.18	0.059	0.12	0.106	0.153	0.0000332	0.003984	
		60	22	1105.84	0.99	8.47	17.3	11.1	24.5	127.6	120	15.8	39.6	2.29	0.62	0.17	0.046	0.078	0.073	0.111	0.0000328	0.003936	
100	12	150	9	1017.88	1.22	5.43	12	8	16.8	136.2	173.09	10.9	26.8	2.23	0.63	0.15	0.071	0.089	0.09	0.193	0.0000226	0.003912	Hceff too small
		120	11	1244.07	1.50	5.43	12	8	16.8	112.4	159.05	10.9	32.3	2.69	0.52	0.14	0.054	0.064	0.068	0.152	0.0000224	0.003563	Hceff too small
		100	13	1470.27	1.77	5.43	12	8	16.8	95.9	149.44	10.9	37.7	3.14	0.45	0.13	0.043	0.049	0.054	0.124	0.0000221	0.003303	Hceff too small
		80	17	1922.65	2.31	5.43	12	8	16.8	74.4	137.19	10.9	48.1	4.01	0.35	0.12	0.031	0.032	0.038	0.09	0.0000217	0.002977	Hceff too small
		60	22	2488.14	2.99	5.43	12	8	16.8	58.3	128.34	10.9	60.2	5.02	0.28	0.11	0.022	0.021	0.028	0.067	0.0000212	0.002721	Hceff too small
	10	150	9	706.86	0.84	5.43	12	8	16.8	190.1	150	10.9	19.2	1.60	0.88	0.17	0.096	0.144	0.14	0.253	0.0000245	0.003675	Hceff too small
		120	11	863.94	1.02	5.43	12	8	16.8	156.8	150	10.9	23.3	1.94	0.72	0.16	0.071	0.103	0.104	0.197	0.0000243	0.003645	Hceff too small
		100	13	1021.02	1.21	5.43	12	8	16.8	133.6	150	10.9	27.3	2.28	0.62	0.15	0.06	0.078	0.082	0.161	0.0000241	0.003615	Hceff too small
		80	17	1335.18	1.58	5.43	12	8	16.8	103.4	145.88	10.9	35.1	2.93	0.48	0.14	0.045	0.05	0.057	0.116	0.0000237	0.003457	Hceff too small
		60	22	1727.88	2.04	5.43	12	8	16.8	80.96	134.95	10.9	44.5	3.71	0.38	0.12	0.033	0.033	0.041	0.085	0.0000233	0.003344	Hceff too small
	8	150	9	452.39	0.53	5.43	12	8	16.8	288	120	10.9	12.7	1.06	1.33	0.18	0.103	0.258	0.243	0.361	0.0000264	0.003168	Hceff too small, UC-M too high
		120	11	552.92	0.64	5.43	12	8	16.8	237.2	120	10.9	15.4	1.28	1.09	0.18	0.085	0.184	0.178	0.28	0.0000262	0.003144	Hceff too small, UC-M too high
		100	13	653.45	0.76	5.43	12	8	16.8	201.9	120	10.9	18.1	1.51	0.93	0.17	0.073	0.139	0.139	0.228	0.0000261	0.003132	Hceff too small
		80	17	854.51	1.00	5.43	12	8	16.8	156	120	10.9	23.45	1.95	0.72	0.15	0.056	0.089	0.094	0.163	0.0000258	0.003096	Hceff too small
		60	22	1105.84	1.29	5.43	12	8	16.8	121.8	120	10.9	29.9	2.49	0.56	0.14	0.044	0.058	0.066	0.119	0.0000255	0.00306	Hceff too small
	12	150	9	1017.88	1.78	3.04	7.7	5.5	10.5	137.1	158.85	7	18	2.34	0.59	0.13	0.065	0.058	0.084	0.241	9.09E-06	0.001444	Hceff too small
		120	11	1244.07	2.17	3.04	7.7	5.5	10.5	113.3	147.65	7	21.5	2.79	0.49	0.12	0.05	0.042	0.064	0.191	8.98E-06	0.001326	Hceff too small
		100	13	1470.27	2.57	3.04	7.7	5.5	10.5	96.8	140	7	25	3.25	0.42	0.11	0.041	0.032	0.052	0.158	8.88E-06	0.001243	Hceff too small
		80	17	1922.65	3.36	3.04	7.7	5.5	10.5	75.2	130.24	7	31.4	4.08	0.38	0.1	0.029	0.021	0.04	0.12	8.68E-06	0.00113	Hceff too small
		60	22	2488.14	4.35	3.04	7.7	5.5	10.5	59	123.19	7	38.5	5.00	0.27	0.09	0.022	0.014	0.027	0.088	8.44E-06	0.00104	Hceff too small, too much reinforcement
	10	150	9	706.86	1.21	3.04	7.7	5.5	10.5	189.6	150	7	13.1	1.70	0.81	0.14	0.085	0.093	0.128	0.307	0.0000113	0.001695	Hceff too small
		120	11	863.94	1.48	3.04	7.7	5.5	10.5	156.5	150	7	15.8	2.05	0.67	0.13	0.07	0.067	0.096	0.242	1.12E-05	0.00168	Hceff too small
		100	13	1021.02	1.75	3.04	7.7	5.5	10.5	133.5	149.07	7	18.4	2.39	0.57	0.12	0.06	0.051	0.077	0.198	0.0000111	0.001655	Hceff too small
		80	17	1335.18	2.28	3.04	7.7	5.5	10.5	103.5	137.08	7	23.5	3.05	0.45	0.11	0.043	0.033	0.054	0.145	0.000011	0.001508	Hceff too small
		60	22	1727.88	2.95	3.04	7.7	5.5	10.5	81.2	128.39	7	26.4	3.43	0.36	0.1	0.031	0.022	0.039	0.108	0.0000107	0.001374	Hceff too small
	8	150	9	452.39	0.76	3.04	7.7	5.5	10.5	284.5	120	7	8.75	1.14	1.21	0.16	0.102	0.169	0.217	0.423	0.0000136	0.001632	Hceff too small, UC-M too high
		120	11	552.92	0.92	3.04	7.7	5.5	10.5	234.5	120	7	10.6	1.38	1	0.15	0.084	0.121	0.161	0.333	0.0000135	0.00162	Hceff too small
		100	13	653.45	1.09	3.04	7.7	5.5	10.5	199.8	120	7	12.4	1.61	0.85	0.14	0.072	0.091	0.127	0.272	0.0000134	0.001608	Hceff too small
		80	17	854.51	1.43	3.04	7.7	5.5	10.5	154.6	120	7	16	2.08	0.66	0.13	0.056	0.059	0.088	0.197	0.0000133	0.001596	Hceff too small
		60	22	1105.84	1.85	3.04	7.7	5.5	10.5	120.9	120	7	20.3	2.64	0.52	0.12	0.044	0.038	0.063	0.145	0.0000131	0.001572	Hceff too small

Table E.1: Table presenting analytical and numerical results of the analysis of 105 fully clamped balcony slabs


h=200 Ø8
h=180 Ø8
h=160 Ø8
h=200 Ø10
h=180 Ø10
h=160 Ø10
h=200 Ø12
h=180 Ø12
h=160 Ø12
Crack width [mm]
Rebar spacing [mm]
Eurocode 2
v. Breugel
Egyptian Code
American Code
Diana


h=140 Ø8
h=120 Ø8
h=100 Ø8
h=140 Ø10
h=120 Ø10
h=100 Ø10
h=140 Ø12
h=120 Ø12
h=100 Ø12
Crack width [mm]
Rebar spacing [mm]
Eurocode 2
v. Breugel
Egyptian Code
American Code
Diana

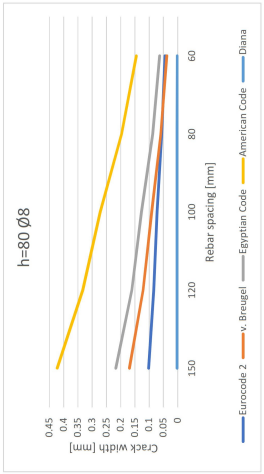
h=80 Ø8
Crack width [mm]
0.45
0.4
0.35
0.3
0.25
0.2
0.15
0.1
0.05
0
0
150
120
100
80
60
Rebar spacing [mm]
Eurocode 2
v. Breugel
Egyptian Code
American Code
Diana

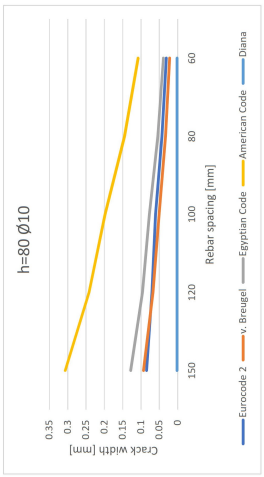
h=80 Ø10
Crack width [mm]
0.35
0.3
0.25
0.2
0.15
0.1
0.05
0
0
150
120
100
80
60
Rebar spacing [mm]
Eurocode 2
v. Breugel
Egyptian Code
American Code
Diana

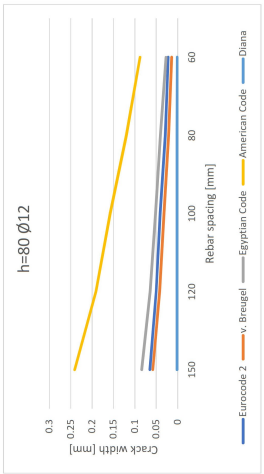
h=80 Ø12
Crack width [mm]
0.3
0.25
0.2
0.15
0.1
0.05
0
0
150
120
100
80
60
Rebar spacing [mm]
Eurocode 2
v. Breugel
Egyptian Code
American Code
Diana

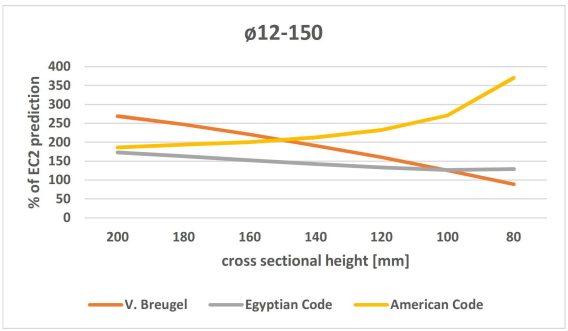
ø12-150
% of EC2 prediction
400
350
300
250
200
150
100
50
0
200 180 160 140 120 100 80
cross sectional height [mm]
V. Breugel
Egyptian Code
American Code

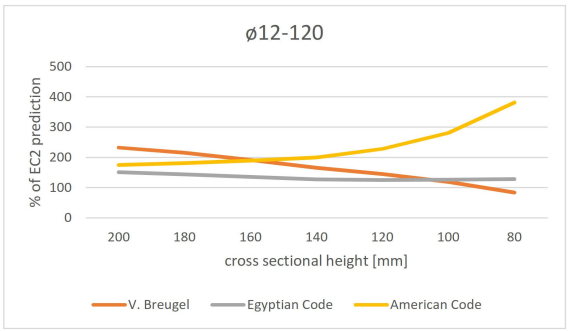
ø12-120
% of EC2 prediction
500
400
300
200
100
0
200 180 160 140 120 100 80
cross sectional height [mm]
V. Breugel
Egyptian Code
American Code

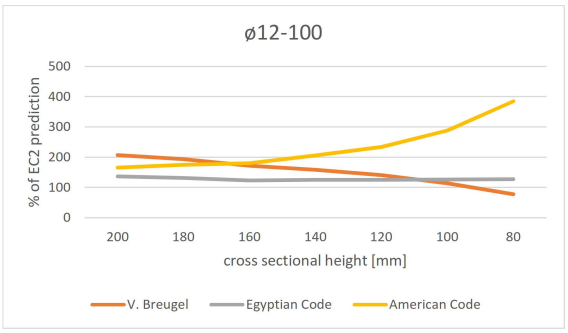
ø12-100
% of EC2 prediction
500
400
300
200
100
0
200 180 160 140 120 100 80
cross sectional height [mm]
V. Breugel
Egyptian Code
American Code

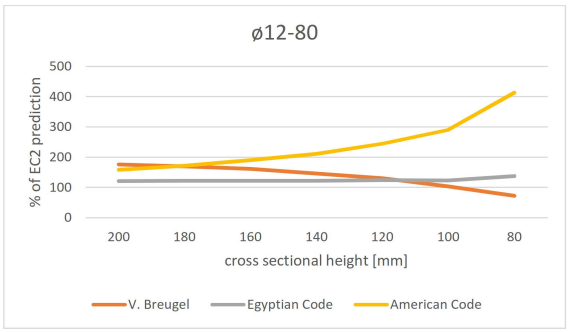
ø12-80
% of EC2 prediction
500
400
300
200
100
0
200 180 160 140 120 100 80
cross sectional height [mm]
V. Breugel
Egyptian Code
American Code

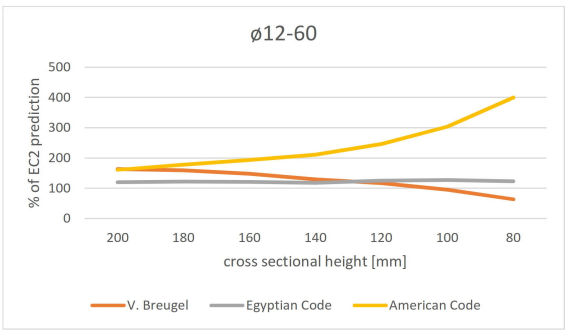
ø12-60
% of EC2 prediction
500
400
300
200
100
0
200 180 160 140 120 100 80
cross sectional height [mm]
V. Breugel
Egyptian Code
American Code

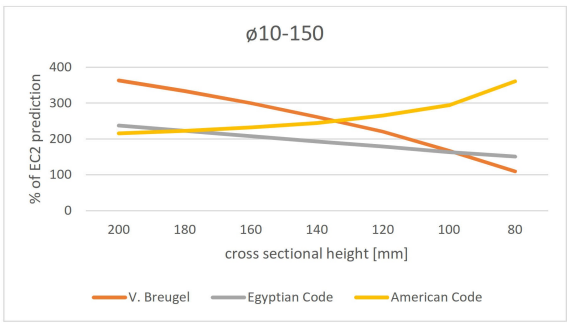
ø10-150
% of EC2 prediction
400
300
200
100
0
200 180 160 140 120 100 80
cross sectional height [mm]
V. Breugel
Egyptian Code
American Code

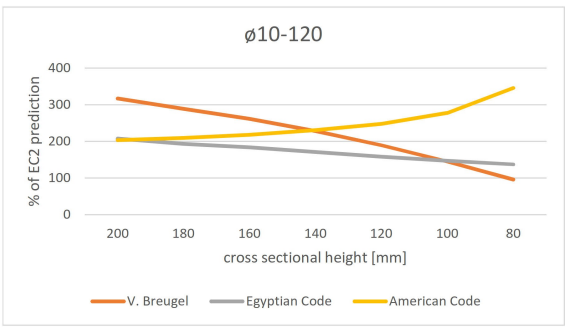
ø10-120
% of EC2 prediction
400
300
200
100
0
200 180 160 140 120 100 80
cross sectional height [mm]
V. Breugel
Egyptian Code
American Code

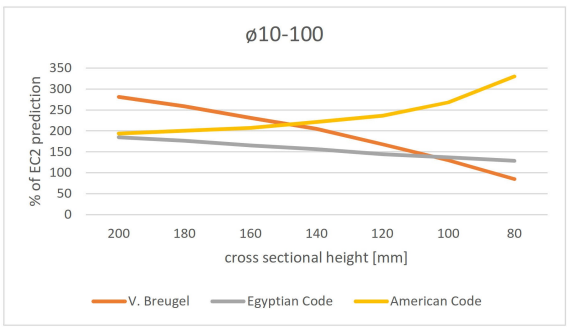
ø10-100
% of EC2 prediction
350
300
250
200
150
100
50
0
200 180 160 140 120 100 80
cross sectional height [mm]
V. Breugel
Egyptian Code
American Code

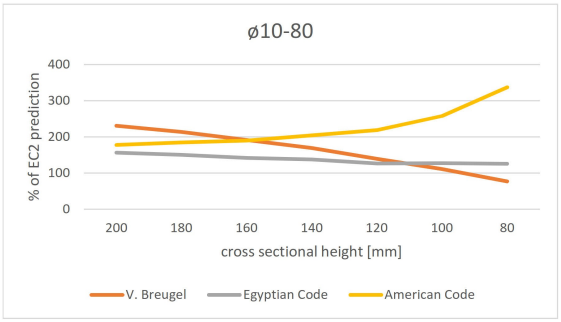
ø10-80
% of EC2 prediction
400
300
200
100
0
200 180 160 140 120 100 80
cross sectional height [mm]
V. Breugel
Egyptian Code
American Code

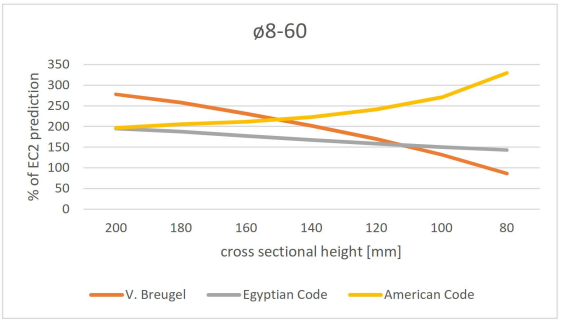
ø8-60
% of EC2 prediction
350
300
250
200
150
100
50
0
200 180 160 140 120 100 80
cross sectional height [mm]
V. Breugel
Egyptian Code
American Code

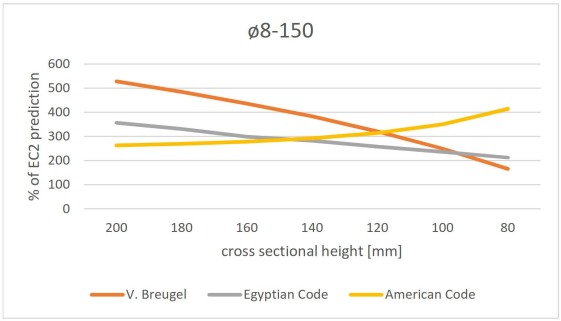
ø8-150
% of EC2 prediction
600
500
400
300
200
100
0
200 180 160 140 120 100 80
cross sectional height [mm]
V. Breugel
Egyptian Code
American Code

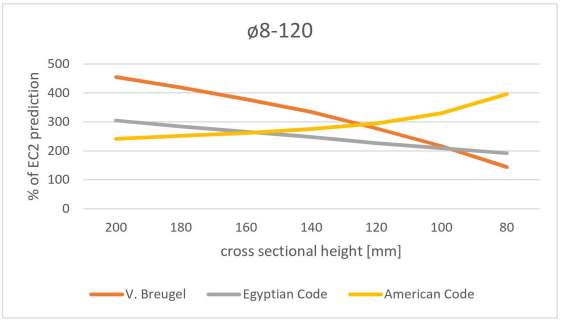
ø8-120
% of EC2 prediction
500
400
300
200
100
0
200 180 160 140 120 100 80
cross sectional height [mm]
V. Breugel
Egyptian Code
American Code

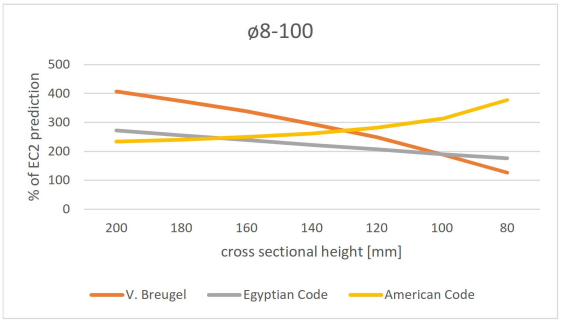
ø8-100
% of EC2 prediction
500
400
300
200
100
0
200 180 160 140 120 100 80
cross sectional height [mm]
V. Breugel
Egyptian Code
American Code

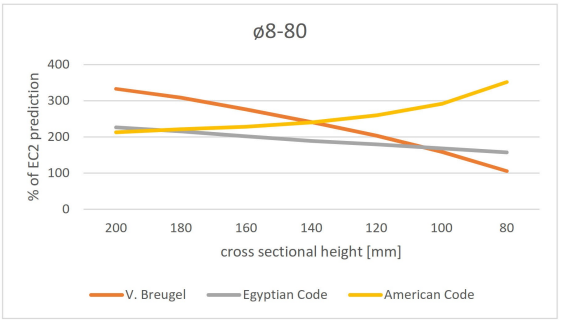
ø8-80
% of EC2 prediction
400
300
200
100
0
200 180 160 140 120 100 80
cross sectional height [mm]
V. Breugel
Egyptian Code
American Code

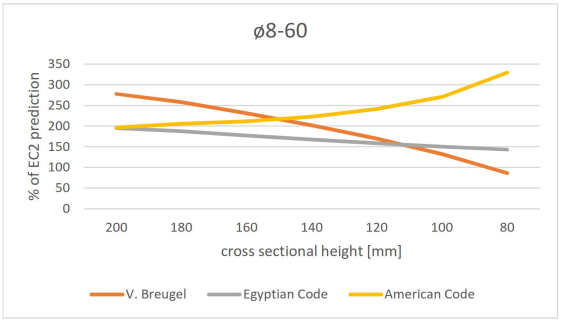
ø8-60
% of EC2 prediction
350
300
250
200
150
100
50
0
200 180 160 140 120 100 80
cross sectional height [mm]
V. Breugel
Egyptian Code
American Code

F

Script balcony with in-plane ridge connection

This appendix contains the script for the design and check process of the balcony with an in-plane ridge.

Dimensioning and checking of a cantilevering slab, supported by an in-plane clamped ridge.

All units in N and mm

```
> restart;
```

Geometry

```
> lridge := 100 : l := 1475 : ltot := lridge + l : b := 1300 : bridge := 500 : h := 110 :
```

Material Properties Concrete: C90/105

```
> γc := 1.5 : Ecm := 43600 : fck := 90 : fcd := fck/γc : fctm := 5.05 : fctk := 3.54 : fctd :=
      fck/γc : fctmfl := max((1.6 − h/1000) fctm, fctm) : εc3 := 2.3·10^−3 : εcu3 := 2.6·10^−3 :
  fcmcube := 105 + 8 :
```

Material Properties Reinforcement: B500b

```
> γs := 1.15 : fyk := 500 : fyd := fyk/γs : Es := 200000 :
```

Loads

```
> G := 25000·10^−9 : g := 0.75·b : Q := 5000 :
```

Reinforcement configuration

```
> ϕtopbig := 10 : αe := Es/Ecm : sreb := 50 : n1 := ceil(bridge/sreb) :
> ϕtopsmall := 8 : srebtopsmall := 100 : n2 := ceil((b − bridge)/srebtopsmall) :
> ϕtopcross := 6 : srebtopcross := 100 :
> ϕbottom := 6 : srebbottom := 100 :
> ϕbottomcross := 6 : srebbottomcross := 100 :
> ϕshear := 6 :
> if ϕtopcross < 0.6·ϕtopbig then print(Top cross reinforcement should be at least '0.6
      ' times diameter main reinforcement) end if;
```

Concrete Cover

```
> cslab := 30 : cridge := 35 :
```

Check rebar spacing

dg+5=16+5= 21 mm

> **if** $21 < sreb - \phi topbig < \min(3 \cdot h, 400)$
> **then** *print*(*Rebar spacing main reinforcement is OK*)
> **else** *print*(*Rebar spacing main reinforcement doesnot fulfill requirements*) **end if**;

Rebar spacing main reinforcement is OK **(7.1)**

Bending moments and shear forces

> $Mk := b \cdot h \cdot l \cdot G \cdot \left(\frac{1}{2} l + lridge \right) + 0.5 \cdot lridge^2 \cdot bridge \cdot h \cdot G + Q \cdot (ltot - 100) + g \cdot ltot;$

$Mk := 1.333374219\ 10^7$ **(8.1)**

> $Vk := b \cdot h \cdot l \cdot G + lridge \cdot bridge \cdot h \cdot G + Q + g;$

$Vk := 11385.62500$ **(8.2)**

> $Mfc := b \cdot h \cdot l \cdot G \cdot \left(\frac{1}{2} l + lridge \right) + 0.5 \cdot lridge^2 \cdot bridge \cdot h \cdot G + 0.5 \cdot Q \cdot (ltot - 100) + g \cdot ltot;$

$Mfc := 9.646242188\ 10^6$ **(8.3)**

> $Vfc := b \cdot h \cdot l \cdot G + lridge \cdot bridge \cdot h \cdot G + 0.5 \cdot Q + g;$

$Vfc := 8885.625000$ **(8.4)**

> $Mqb := b \cdot h \cdot l \cdot G \cdot \left(\frac{1}{2} l + lridge \right) + 0.5 \cdot lridge^2 \cdot bridge \cdot h \cdot G + 0.3 \cdot Q \cdot (ltot - 100) + g \cdot ltot;$

$Mqb := 8.171242188\ 10^6$ **(8.5)**

> $Vqb := b \cdot h \cdot l \cdot G + lridge \cdot bridge \cdot h \cdot G + 0.3 \cdot Q + g;$

$Vqb := 7885.625000$ **(8.6)**

> $Mg := b \cdot h \cdot l \cdot G \cdot \left(\frac{1}{2} l + lridge \right) + 0.5 \cdot lridge^2 \cdot bridge \cdot h \cdot G + g \cdot l;$

$Mg := 5.861242188\ 10^6$ **(8.7)**

> $Vg := b \cdot h \cdot l \cdot G + lridge \cdot bridge \cdot h \cdot G + g;$

$Vg := 6385.625000$ **(8.8)**

> $Med := 1.2 \cdot b \cdot h \cdot l \cdot G \cdot \left(\frac{1}{2} l + lridge \right) + 1.2 \cdot 0.5 \cdot lridge^2 \cdot bridge \cdot h \cdot G + 1.5 \cdot Q \cdot (ltot - 100) + 1.2 \cdot g \cdot ltot;$

$Med := 1.821299062\ 10^7$ **(8.9)**

> $Ved := 1.2 \cdot b \cdot h \cdot l \cdot G + 1.2 \cdot lridge \cdot bridge \cdot h \cdot G + 1.5 \cdot Q + 1.2\ g;$

$Ved := 15162.75000$ **(8.10)**

Cross sectional properties

> $Wcridge := \frac{1}{6} \cdot bridge \cdot h^2 : Wc := \frac{1}{6} \cdot b \cdot h^2 :$

> $Mcrridge := Wcridge \cdot fctm : Mcrslab := Wc \cdot fctm :$

>

Check bending moment resistance ridge

> $dridge := h - cridge - 0.5 \cdot \phi topbig;$

$dridge := 70.0$ **(10.1)**

$$> Asridge := evalf\left(\text{ceil}\left(\frac{bridge}{sreb}\right)\cdot\pi\cdot\left(\frac{\phi topbig}{2}\right)^2\right); n := \text{ceil}\left(\frac{bridge}{sreb}\right)$$

$$Asridge := 785.3981635$$

$$n := 10 \quad \textbf{(10.2)}$$

$$> \rho lridge := \frac{Asridge}{bridge\cdot dridge};$$

$$\rho lridge := 0.02243994753 \quad \textbf{(10.3)}$$

$$> xuridge := \frac{Asridge\cdot fyd}{\left(\frac{1}{2}\cdot\frac{\varepsilon c3}{\varepsilon cu3}+\left(1-\frac{\varepsilon c3}{\varepsilon cu3}\right)\right)\cdot fcd\cdot bridge};$$

$$xuridge := 20.41014718 \quad \textbf{(10.4)}$$

Determine a maximum reinforcement ratio for which yielding of steel occurs before crushing of concrete

$$> eq1 := (\rho lmax\cdot bridge\cdot dridge)\cdot fyk = \left(\frac{1}{2}\cdot\frac{\varepsilon c3}{\varepsilon cu3}+\left(1-\frac{\varepsilon c3}{\varepsilon cu3}\right)\right)\cdot fck\cdot bridge\cdot xuridge:$$

$$\rho lmax := solve(eq1, \rho lmax);$$

$$\rho lmax := 0.02926949677 \quad \textbf{(10.5)}$$

$$> \rho lmax := \min(0.04, \rho lmax);$$

$$\rho lmax := 0.02926949677 \quad \textbf{(10.6)}$$

> **if** $\rho lridge > \rho lmax$ **then** $print(Reinforcement\ ratio\ is\ too\ high)$ **end if**

center of gravity compression zone on maximum capacity

$$> \beta xuridge := \left(\left(1-\frac{\varepsilon c3}{\varepsilon cu3}\right)\cdot xuridge\cdot fcd\cdot 0.5\left(1-\frac{\varepsilon c3}{\varepsilon cu3}\right)xuridge+0.5\cdot\left(\frac{\varepsilon c3}{\varepsilon cu3}\right)\cdot xuridge\cdot fcd\cdot\left(\left(1-\frac{\varepsilon c3}{\varepsilon cu3}\right)xuridge+\frac{\left(\frac{\varepsilon c3}{\varepsilon cu3}\right)xuridge}{3}\right)\right)\Big/\left(fcd\cdot\left(1-\frac{\varepsilon c3}{\varepsilon cu3}\right)xuridge+0.5\cdot fcd\cdot\left(\frac{\varepsilon c3}{\varepsilon cu3}\right)xuridge\right);$$

$$\beta xuridge := 6.884589875 \quad \textbf{(10.7)}$$

$$> \beta := \frac{\beta xuridge}{xuridge}; zridge := dridge - \beta xuridge;$$

$$\beta := 0.3373121132$$

$$zridge := 63.11541012 \quad \textbf{(10.8)}$$

$$> Ns := fyd\cdot Asridge : Mrdridge := Ns\cdot zridge;$$

$$Mrdridge := 2.155249009\ 10^7 \quad \textbf{(10.9)}$$

$$> UC := \frac{Med}{Mrdridge};$$

$$UC := 0.8450527314 \quad \textbf{(10.10)}$$

Check bending moment resistance slab

$$> dslab := \frac{1}{n1\cdot\left(\frac{\phi topbig}{2}\right)^2\cdot\pi + n2\cdot\left(\frac{\phi topsmall}{2}\right)^2\cdot\pi}\left(n1\cdot\left(\frac{\phi topbig}{2}\right)^2\cdot\pi\cdot\left(h - cridge - \frac{\phi topbig}{2}\right) + n2\cdot\left(\frac{\phi topsmall}{2}\right)^2\cdot\pi\cdot\left(h - cridge - \phi topbig + 0.5\cdot\phi topsmall\right)\right);$$

$$dslab := 69.66137565 \quad (11.1)$$

$$> As := evalf\left(\text{ceil}\left(\frac{bridge}{sreb}\right)\cdot\pi\cdot\left(\frac{\phi topbig}{2}\right)^2 + \text{ceil}\left(\frac{b - bridge}{srebtopsmall}\right)\cdot\pi\cdot\left(\frac{\phi topsmall}{2}\right)^2\right);$$

$$As := 1187.522023 \quad (11.2)$$

$$> \rho l := \frac{As}{b\cdot dslab};$$

$$\rho l := 0.01311312719 \quad (11.3)$$

$$> xu := \frac{As\cdot fyd}{\left(\frac{1}{2}\cdot\frac{\varepsilon c3}{\varepsilon cu3} + \left(1 - \frac{\varepsilon c3}{\varepsilon cu3}\right)\right)\cdot fcd\cdot b};$$

$$xu := 11.86928558 \quad (11.4)$$

Determine a maximum reinforcement ratio for which yielding of steel occurs before crushing of concrete

$$> eq2 := (\rho lmax2\cdot b\cdot dslab)\cdot fyk = \left(\frac{1}{2}\cdot\frac{\varepsilon c3}{\varepsilon cu3} + \left(1 - \frac{\varepsilon c3}{\varepsilon cu3}\right)\right)\cdot fck\cdot b\cdot xu :$$

$$\rho lmax := solve(eq2, \rho lmax2);$$

$$\rho lmax := 0.01710407894 \quad (11.5)$$

$$> \rho lmax := \min(0.04, \rho lmax);$$

$$\rho lmax := 0.01710407894 \quad (11.6)$$

$$> \textbf{if } \rho l > \rho lmax \textbf{ then } print(Reinforcement\ ratio\ is\ too\ high) \textbf{ end if}$$

$$> zslab := dslab - \beta\cdot xu;$$

$$zslab := 65.65772185 \quad (11.7)$$

$$> Ns := fyd\cdot As : Mrd := Ns\cdot zslab;$$

$$Mrd := 3.389999594\ 10^7 \quad (11.8)$$

$$> UC := \frac{Med}{Mrd};$$

$$UC := 0.5372564248 \quad (11.9)$$

Check main shear resistance ridge

Apply curved bars through connection since it is assumed that, in computational terms, the connection has no shear resistance.

> $Asshearreq := evalf\left(\frac{Ved\cdot\sqrt{2}}{(0.9*fyd)}\right);$

$$Asshearreq := 54.79971487 \quad (12.1)$$

> $nreq := \mathrm{ceil}\left(\frac{Asshearreq}{\pi\cdot\left(\frac{\phi shear}{2}\right)^2}\right); Asshear := evalf\left(nreq\cdot\pi\cdot\left(\frac{\phi shear}{2}\right)^2\right);$

$$nreq := 2$$

$$Asshear := 56.54866777 \quad (12.2)$$

> $\sigma sshear := \frac{Ved\cdot\sqrt{2}}{Asshear} : fbd := 2.25\cdot1\cdot1\cdot2.07 : lbreq := evalf\left(\left(\frac{\phi shear}{4}\right)\cdot\left(\frac{\sigma sshear}{fbd}\right)\right);$

$$lbreq := 122.1262410 \quad (12.3)$$

Check shear resistance of concrete in ridge.

> **if** $h < 200$ **then** $print(No\ shear\ reinforcement\ allowed)$ **end if**

$$No\ shear\ reinforcement\ allowed \quad (12.4)$$

> $k := 1 + \sqrt{\frac{200}{dridge}};$

$$k := 2.690308510 \quad (12.5)$$

> **if** $k \le 2$ **then** $k := k$ **else** $k := 2$ **end if**

$$k := 2 \quad (12.6)$$

> $Crdc := \frac{0.18}{\gamma c};$

$$Crdc := 0.1200000000 \quad (12.7)$$

> $vmin := evalf\left(0.035\cdot k^{\frac{3}{2}}\cdot fck^{\frac{1}{2}}\right);$

$$vmin := 0.9391485502 \quad (12.8)$$

> $Vrdcmin := vmin\cdot bridge\cdot dridge;$

$$Vrdcmin := 32870.19926 \quad (12.9)$$

> $Vrdc := evalf\left(\left(Crdc\cdot k\cdot\left(100\cdot\rho lridge\cdot fck\right)^{\frac{1}{3}}\right)\cdot bridge\cdot dridge\right);$

$$Vrdc := 49283.40831 \quad (12.10)$$

> $Vrdcridge := \max(Vrdcmin, Vrdc);$

$$Vrdcridge := 49283.40831 \quad (12.11)$$

> $UC := \frac{Ved}{Vrdcridge};$

$$UC := 0.3076643950 \quad (12.12)$$

Check main shear resistance slab

> **if** $h < 200$ **then** $print(No\ shear\ reinforcement\ allowed)$ **end if**

$$No\ shear\ reinforcement\ allowed \quad (13.1)$$

> $k := 1 + \sqrt{\frac{200}{dslab}};$

$$k := 2.694411829 \quad (13.2)$$

> **if** $k \le 2$ **then** $k := k$ **else** $k := 2$ **end if**

$$k := 2 \tag{13.3}$$

> $Crdc := \frac{0.18}{\gamma c}$;

$$Crdc := 0.1200000000 \tag{13.4}$$

> $vmin := evalf\left(0.035 \cdot k^{\frac{3}{2}} \cdot fck^{\frac{1}{2}}\right)$;

$$vmin := 0.9391485502 \tag{13.5}$$

> $Vrdcmin := vmin \cdot b \cdot dslab$;

$$Vrdcmin := 85049.09391 \tag{13.6}$$

> $Vrdc := evalf\left(\left(Crdc \cdot k \cdot (100 \cdot \rho l \cdot fck)^{\frac{1}{3}}\right) \cdot b \cdot dslab\right)$;

$$Vrdc := 1.066095806\ 10^{5} \tag{13.7}$$

> $Vrdc := \max(Vrdcmin, Vrdc)$;

$$Vrdc := 1.066095806\ 10^{5} \tag{13.8}$$

> $UC := \frac{Ved}{Vrdc}$;

$$UC := 0.1422268985 \tag{13.9}$$

Check detailing and element specific rules

> **if** $l \ge 5 \cdot h$ **and** $b \ge 5 \cdot h$ **then** $print(Balcony\ may\ be\ considered\ as\ plate\ element)$ **end if**

Balcony may be considered as plate element (14.1)

> **if** $h \ge 80$ **then** $print(Height\ of\ balcony\ is\ sufficient\ as\ plate\ element)$
> **else** $print(Height\ of\ balcony\ plate\ is\ insufficient)$ **end if**

Height of balcony is sufficient as plate element (14.2)

> **if** $\min\left(\frac{fctm \cdot Wcridge}{fyd \cdot zridge}, 0.26 \cdot \frac{fctm}{fyk} \cdot bridge \cdot dridge\right) < As$
> **then** $print(Area\ of\ ridge\ reinforcement\ sufficient)$
> **else** $print(Area\ of\ ridge\ reinforcement\ should\ be\ increased)$ **end if**;

Area of ridge reinforcement sufficient (14.3)

> **if** $\min\left(\frac{fctm \cdot Wc}{fyd \cdot zslab}, 0.26 \cdot \frac{fctm}{fyk} \cdot b \cdot dslab\right) < As$
> **then** $print(Area\ of\ slab\ reinforcement\ sufficient)$
> **else** $print(Area\ of\ slab\ reinforcement\ should\ be\ increased)$ **end if**;

Area of slab reinforcement sufficient (14.4)

> $Astop := evalf\left(\frac{bridge}{sreb} \cdot \pi \cdot \left(\frac{\phi topbig}{2}\right)^2 + \frac{b - bridge}{srebtopsmall} \cdot \pi \cdot \left(\frac{\phi topsmall}{2}\right)^2\right)$:

$$Astopcross := evalf\left(\mathrm{ceil}\left(\frac{l}{srebtopcross}\right) \cdot \pi \cdot \left(\frac{\phi topcross}{2}\right)^2\right):$$

> **if** $Astopcross < 0.2 \cdot Astop$ **then** $print(top\ cross\ reinforcement\ insufficient)$
> **else** $print(Top\ cross\ reinforcement\ sufficient)$ **end if**

Top cross reinforcement sufficient (14.5)

Bottom splitting force

Conservative assumption that full compressive supporting force is modelled like one point load.
Optimistic assumption that the splitting force is transfered over 1 m.

> $F := \frac{Med}{zridge}$;

$$F := 2.885664624\ 10^{5} \tag{15.1}$$

> $Fspl := 0.25 \cdot F$;

$$Fspl := 72141.61560 \tag{15.2}$$

> $Assplitreq := \frac{Fspl}{0.9 \cdot fyd}$;

$$Assplitreq := 184.3619065 \tag{15.3}$$

> $Assplit := evalf\left(\pi \cdot \left(\frac{\phi bottomcross}{2}\right)^2 \cdot \left(\frac{1000}{srebbottomcross}\right)\right)$

$$Assplit := 282.7433389 \tag{15.4}$$

> **if** $Assplit < Assplitreq$ **then** $print(Splitting\ reinforcement\ should\ be\ increased)$ **else** $print(\ Splitting\ reinforcement\ is\ sufficient)$ **end if**

$$Splitting\ reinforcement\ is\ sufficient \tag{15.5}$$

Stiffness determination ridge

> $\varphi := 0.9 : Einf := \frac{Ecm}{1+\varphi}$; $\alpha einf := \frac{Es}{Einf}$;

$$Einf := 22947.36842$$

$$\alpha einf := 8.715596331 \tag{16.1}$$

> $xeinfridge := d \cdot \left(-\alpha einf \cdot \rho lridge + \sqrt{(\alpha einf \cdot \rho lridge)^2 + 2\,\alpha einf \cdot \rho lridge}\right)$:

> $Icridge := \frac{1}{12} \cdot bridge \cdot h^3$;

$$Icridge := \frac{166375000}{3} \tag{16.2}$$

> $EI0ridge := evalf(Icridge \cdot Ecm)$;

$$EI0ridge := 2.417983333\ 10^{12} \tag{16.3}$$

> $\delta i0ridge := \frac{1+3\cdot\alpha e\cdot\rho l}{1+\alpha e\cdot\rho l} : \delta iinfridge := \frac{1}{1+\varphi} \cdot \frac{1+3\cdot\alpha e\cdot\rho l}{1+\alpha e\cdot\rho l}$:

> $\delta i0ridge := \left(6 \cdot \left(\frac{dridge}{h}\right)^3 \left(\frac{xeridge}{dridge}\right)^2 \left(1 - \frac{1}{3}\frac{xeridge}{dridge}\right)\right) : \delta iinfridge := \frac{1}{1+\varphi} \cdot \left(6 \cdot \left(\frac{dridge}{h}\right)^3 \left(\frac{xeinfridge}{dridge}\right)^2 \left(1 - \frac{1}{3}\frac{xeinfridge}{dridge}\right)\right)$:

Determine loading ratios:

> $\lambda := \frac{Mqb}{Mfc}$; $\mu 2 := \frac{Mcrridge}{Mqb}$; $\mu 3 := \frac{Mcrridge}{Mfc}$;

$$\lambda := 0.8470907146$$

$$\mu 2 := 0.6231712653$$

$$\mu 3 := 0.5278825924 \tag{16.4}$$

> **if** $\mu 2 > 1$ **and** $\mu 3 > 1$ **then** *print*(*Cross section isnt always cracked*) **end if**;

> **if** $\mu 2 < 1$ **and** $\mu 3 > 1$
then *print*(*Cross section isnt always cracked with quasi static load combination*) **end if**;

> **if** $\mu 2 < 1$ **and** $\mu 3 < 1$ **then** *print*(*Cross section is always cracked*) **end if**;

Cross section is always cracked (16.5)

> $\delta csstarridge := \dfrac{\delta i0ridge \cdot \delta i0ridge}{\mu 3^2 \cdot \delta i0ridge + \left(1 - \mu 3^2\right) \cdot \delta 0ridge}$: $\delta csstarstarridge := \dfrac{\delta infridge \cdot \delta iinfridge}{\mu 2^2 \cdot \delta iinfridge + \left(1 - \dfrac{1}{2}\,\mu 2^2\right) \cdot \delta infridge}$:

> $\delta csridge := \dfrac{\delta csstarridge \cdot \delta csstarstarridge}{\lambda \cdot \delta csstarridge + (1 - \lambda) \cdot \delta csstarstarridge}$: $EIfridge := \delta csridge \cdot EI0ridge$;

$$EIfridge := 5.852767655\ 10^{11} \tag{16.6}$$

Stiffness determination slab

> $xeinfslab := d \cdot \left(-\alpha einf \cdot \rho l + \sqrt{(\alpha einf \cdot \rho l)^2 + 2\,\alpha einf \cdot \rho l} \right)$:

> $Ic := \dfrac{1}{12} \cdot b \cdot h^3$;

$$Ic := \frac{432575000}{3} \tag{17.1}$$

> $EI0 := evalf(Ic \cdot Ecm)$;

$$EI0 := 6.286756667\ 10^{12} \tag{17.2}$$

> $\delta i0 := \dfrac{1 + 3 \cdot \alpha e \cdot \rho l}{1 + \alpha e \cdot \rho l}$: $\delta iinf := \dfrac{1}{1 + \varphi} \cdot \dfrac{1 + 3 \cdot \alpha e \cdot \rho l}{1 + \alpha e \cdot \rho l}$:

> $\delta i0 := \left(6 \cdot \left(\dfrac{dslab}{h}\right)^3 \left(\dfrac{xeslab}{dslab}\right)^2 \left(1 - \dfrac{1}{3}\,\dfrac{xeslab}{dslab}\right)\right)$: $\delta iinf := \dfrac{1}{1 + \varphi} \cdot \left(6 \cdot \left(\dfrac{dslab}{h}\right)^3 \left(\dfrac{xeinfslab}{dslab}\right)^2 \left(1 - \dfrac{1}{3}\,\dfrac{xeinfslab}{dslab}\right)\right)$:

Determine loading ratios:

> $Mqbs := \dfrac{1}{2} \cdot b \cdot h \cdot l^2 \cdot G + 0.3 \cdot Q \cdot (l - 100) + g \cdot l$; $Mfcs := \dfrac{1}{2} \cdot b \cdot h \cdot l^2 \cdot G + 0.5 \cdot Q \cdot (l - 100) + g \cdot l$; $Mks := \dfrac{1}{2} \cdot b \cdot h \cdot l^2 \cdot G + Q \cdot (l - 100) + g \cdot l$;

$$Mqbs := 7.389554688\ 10^6$$
$$Mfcs := 8.764554688\ 10^6$$
$$Mks := 1.220205469\ 10^7 \tag{17.3}$$

> $\lambda := \dfrac{Mqbs}{Mfcs}$; $\mu 2 := \dfrac{Mcrslab}{Mqbs}$; $\mu 3 := \dfrac{Mcrslab}{Mfcs}$;

$$\lambda := 0.8431180991$$

$$\mu 2 := 1.791639311$$
$$\mu 3 := 1.510563530 \quad (17.4)$$

> $\delta cs := \frac{\delta 0 \cdot \delta inf}{\lambda \cdot \delta 0 + (1-\lambda)\,\delta inf} : EIfslab := \delta cs \cdot EI0;$

$$EIfslab := 3.980066057\ 10^{12} \quad (17.5)$$

Eigen frequency

For the determination of the eigen frequency the characteristic load combination is applied since this load combination determines to which extend the member is cracked.

> $Feq := evalf\left(\frac{1}{4}\cdot G\cdot l + \left(\frac{ltot-100}{ltot}\right)^3 \cdot Q + g\right);$

$$Feq := 5081.817139 \quad (18.1)$$

> $wr := \frac{Feq\cdot lridge^3}{3\cdot EIfridge} + \frac{Feq\cdot l\cdot lridge^2}{2\cdot EIfridge};\ \varphi r := \frac{Feq\cdot lridge^2}{2\cdot EIfridge} + \frac{Feq\cdot l\cdot lridge}{EIfridge};$

$$wr := 0.06692960112$$
$$\varphi r := 0.001324120757 \quad (18.2)$$

> $ws := wr + \varphi r\cdot l + \frac{Feq\cdot l^3}{3\cdot EIfslab};$

$$ws := 3.385796558 \quad (18.3)$$

> $k := \frac{Feq}{ws};\ m := \frac{Feq}{10};$

$$k := 1500.922176$$
$$m := 508.1817139 \quad (18.4)$$

> $\omega n := \sqrt{\frac{k\cdot 10^3}{m}};$

$$\omega n := 54.34624851 \quad (18.5)$$

> $f := \frac{\omega n}{2\,\pi};$

$$f := 8.649474090 \quad (18.6)$$

> **if** $f \geq 5$ **then** $print(Eigen\,frequency\,is\,OK)$ **else** $print(Eigen\,frequency\,is\,too\,low)$ **end if**;

Eigen frequency is OK (18.7)

Deflection

Deflection at t=∞, creep coefficient equals about 0.9. For this calculation the deflection and rotation of the structure behind the ridge is neglected. In reality this contributes significantly to the total deflection.

> **if** $\frac{Mqb}{Mcrridge} > 1$ **and** $\frac{Mk}{Mcrridge} > 1$ **then** $print(Always\,cracked)$ **end if**;

Always cracked (19.1)

> $qr := bridge\cdot h\cdot G : qs := b\cdot h\cdot G : Fs := 0.3\cdot Q + g + qs\cdot l : Ms := 0.5\cdot qs\cdot l^2 + 0.3\cdot Q\cdot (l$

$-100) + g \cdot l$:

> $wr := \frac{qr \cdot lridge^4}{8 \cdot EIfridge} + \frac{Fs \cdot lridge^3}{3 \cdot EIfridge} + \frac{Ms \cdot lridge^2}{2 \cdot EIfridge}$; $\varphi r := \frac{qr \cdot lridge^3}{6 \cdot EIfridge} + \frac{Fs \cdot lridge^2}{2 \cdot EIfridge} + \frac{Ms \cdot lridge}{EIfridge}$;

$$wr := 0.06757088543$$
$$\varphi r := 0.001329157941 \quad \textbf{(19.2)}$$

> $ws := wr + \varphi r \cdot l + \frac{qs \cdot l^4}{8 \cdot EIfslab} + \frac{g \cdot l^3}{3 \cdot EIfslab} + \frac{Q \cdot l^3}{3 \cdot EIfslab} - \frac{(Q \cdot 100) \cdot l^2}{2 \cdot EIfslab}$;

$$ws := 4.028713635 \quad \textbf{(19.3)}$$

> $lrep := 2\ ltot$;

$$lrep := 3150 \quad \textbf{(19.4)}$$

> $UC := \frac{ws}{0.004 \cdot lrep}$;

$$UC := 0.3197391775 \quad \textbf{(19.5)}$$

Bending moment resistance cross direction

Take into account the possibility of point load Q at the side. Conservative approach by using a clamped beam, cantilevering 1300/2=650 mm.

> $Mkcross := 0.5 \cdot G \cdot h \cdot 1000 \cdot \left(\frac{b}{2}\right)^2 + Q \cdot \left(\frac{b}{2}\right)$; $Medcross := 1.2 \cdot 0.5 \cdot G \cdot h \cdot 1000 \cdot \left(\frac{b}{2}\right)^2 + 1.5 \cdot Q \cdot \left(\frac{b}{2}\right)$

$$Mkcross := 3.830937500\ 10^6$$
$$Medcross := 5.572125000\ 10^6 \quad \textbf{(20.1)}$$

> $dcross := h - cridge - \phi topbig - \phi topcross$;

$$dcross := 59 \quad \textbf{(20.2)}$$

> $Ascross := evalf\left(\text{ceil}\left(\frac{1000}{srebtopcross}\right) \cdot \pi \cdot \left(\frac{\phi topcross}{2}\right)^2\right)$; $n := \text{ceil}\left(\frac{1000}{srebtopcross}\right)$

$$Ascross := 282.7433389$$
$$n := 10 \quad \textbf{(20.3)}$$

> $\rho lcross := \frac{Ascross}{1000 \cdot dcross}$;

$$\rho lcross := 0.004792259981 \quad \textbf{(20.4)}$$

> $xucross := \frac{Ascross \cdot fyd}{\left(\frac{1}{2} \cdot \frac{\varepsilon c3}{\varepsilon cu3} + \left(1 - \frac{\varepsilon c3}{\varepsilon cu3}\right)\right) \cdot fcd \cdot 1000}$;

$$xucross := 3.673826493 \quad \textbf{(20.5)}$$

Determine a maximum reinforcement ratio for which yielding of steel occurs before crushing of concrete

> $eq1 := (\rho lmax3 \cdot 1000 \cdot dcross) \cdot fyk = \left(\frac{1}{2} \cdot \frac{\varepsilon c3}{\varepsilon cu3} + \left(1 - \frac{\varepsilon c3}{\varepsilon cu3}\right)\right) \cdot fck \cdot 1000 \cdot xucross$:

$\rho lmax := solve(eq1, \rho lmax3);$

$$\rho lmax := 0.006250773888 \quad (20.6)$$

> $\rho lmax := \min(0.04, \rho lmax);$

$$\rho lmax := 0.006250773888 \quad (20.7)$$

> **if** $\rho lcross > \rho lmax$ **then** $print(Reinforcement\ ratio\ is\ too\ high)$ **end if**

> $\beta xucross := \beta \cdot xucross;\ zcross := dcross - \beta xucross;$

$$\beta xucross := 1.239226178$$

$$zcross := 57.76077382 \quad (20.8)$$

> $Ns := fyd \cdot Ascross : Mrdcross := Ns \cdot zcross;$

$$Mrdcross := 7.100640891\ 10^{6} \quad (20.9)$$

> $UC := \frac{Medcross}{Mrdcross};$

$$UC := 0.7847355028 \quad (20.10)$$

>

Crack width EC2 ridge

Uses effective height. For long term kt=0.4 this method is verified with technosoft results.

> $xeridge := dridge \cdot \left(-\alpha e \cdot \rho lridge + \sqrt{(\alpha e \cdot \rho lridge)^2 + 2\ \alpha e \cdot \rho lridge} \right);$

$$xeridge := 25.36270744 \quad (21.1)$$

> $wmax := 0.2;$

$$wmax := 0.2 \quad (21.2)$$

> $Mlin := fyd \cdot Asridge \cdot \left(dridge - \frac{1}{3} xeridge \right);$

$$Mlin := 2.101649138\ 10^{7} \quad (21.3)$$

> **if** $Mfc \le Mlin$ **then** $z := dridge - \frac{1}{3} xeridge$ **else** $z := dridge - \beta xeridge$ **end if**;

$$z := 61.54576419 \quad (21.4)$$

> $hceff := \min\left((h - dridge) \cdot 2.5,\ \frac{(h - xeridge)}{3} \right);$

$$hceff := 28.21243086 \quad (21.5)$$

> **if** $hceff < cridge + 0.5 \cdot \phi topbig$
> **then** $print(Reinforcement\ isnt\ located\ wihtin\ hidden\ tensile\ member)$ **end if**;

Reinforcement isnt located wihtin hidden tensile member (21.6)

> $\rho peff := \frac{Asridge}{hceff \cdot bridge};$

$$\rho peff := 0.05567745420 \quad (21.7)$$

k1=0.8 for good bonding, k2=0.5 for pure bending, k3 en k4 follow from national annex. kt=0.6 because of short term loading.

> $k1 := 0.8 : k2 := 0.5 : k3 := 3.4 : k4 := 0.425 : kt := 0.6 :$

> $fcteff := fctm :$

> **if** $sreb \le \left(5\cdot\left(cridge + \frac{\phi topbig}{2}\right)\right)$ **then** $srmax := k3\cdot cridge + \frac{k1\cdot k2\cdot k4\cdot\phi topbig}{\rho peff}$ **else** $srmax := 1.3\,(h - xeridge)$ **end if**;

$$srmax := 149.5330052 \quad (21.8)$$

> **if** $srmax > \max\left((50 - 0.8\,fck)\cdot\phi topbig,\ 15\cdot\phi topbig\right)$ **then** $srmax := \max\left((50 - 0.8\,fck)\cdot\phi topbig,\ 15\cdot\phi topbig\right)$ **end if**;

> $\sigma sr := \frac{fcteff}{\rho peff}\cdot(1 + \alpha e\cdot\rho peff) : \sigma s := \frac{Mfc}{Asridge\cdot zridge}$;

$$\sigma s := 194.5955352 \quad (21.9)$$

> $straindifference := \frac{(\sigma s - kt\cdot\sigma sr)}{Es}$; $minstraindifference := \left(0.6\cdot\frac{\sigma s}{Es}\right)$;

$$straindifference := 0.0006313793050$$
$$minstraindifference := 0.0005837866056 \quad (21.10)$$

> **if** $straindifference \le minstraindifference$ **then** $straindifference := minstraindifference$ **end if**;

> $wk := straindifference\cdot srmax$;

$$wk := 0.09441204490 \quad (21.11)$$

> **if** $wk \le wmax$ **then** $print(Crack\ width\ is\ small\ enough)$ **else** $print(Crack\ width\ is\ too\ big)$ **end if**;

$$Crack\ width\ is\ small\ enough \quad (21.12)$$

Crack width EC2 slab

Uses effective height. For long term kt=0.4 this method is verified with technosoft results.

> $xe := dslab\cdot\left(-\alpha e\cdot\rho l + \sqrt{(\alpha e\cdot\rho l)^2 + 2\,\alpha e\cdot\rho l}\right)$;

$$xe := 20.33233458 \quad (22.1)$$

> $xecross := dcross\cdot\left(-\alpha e\cdot\rho lcross + \sqrt{(\alpha e\cdot\rho lcross)^2 + 2\,\alpha e\cdot\rho lcross}\right)$;

$$xecross := 11.14193246 \quad (22.2)$$

> $Mfc := 0.5\cdot b\cdot h\cdot l^2\cdot G + 0.5\cdot Q\cdot(l - 100) + g\cdot l$;

$$Mfc := 8.764554688\ 10^6 \quad (22.3)$$

> $wmax := 0.2$;

$$wmax := 0.2 \quad (22.4)$$

> $Mlin := fyd\cdot As\cdot\left(dslab - \frac{1}{3}xe\right)$;

$$Mlin := 3.246784900\ 10^7 \quad (22.5)$$

> **if** $Mfc \le Mlin$ **then** $z := dslab - \frac{1}{3}xe$ **else** $z := dslab - \beta xe$ **end if**;

$$z := 62.88393079 \quad (22.6)$$

> $hceff := \min\left((h - dslab)\cdot 2.5,\ \frac{(h - xe)}{3}\right)$;

$$hceff := 29.88922181 \quad (22.7)$$

> $hceffcross := \min\left((h - dcross)\cdot 2.5,\ \frac{(h - xecross)}{3}\right)$;

(22.8)

$$hceffcross := 32.95268918 \quad (22.8)$$

```
> if hceff < cridge + 0.5·φtopbig
    then print(Reinforcement isnt located wihtin hidden tensile member) end if;
```

Reinforcement isnt located wihtin hidden tensile member (22.9)

```
> ρpeff := As/(hceff·b);
```

$$ρpeff := 0.03056213658 \quad (22.10)$$

```
> ρpeffcross := Ascross/(hceffcross·1000);
```

$$ρpeffcross := 0.008580281183 \quad (22.11)$$

k1=0.8 for good bonding, k2=0.5 for pure bending, k3 en k4 follow from national annex. kt=0.6 because of short term loading.

```
> k1 := 0.8 : k2 := 0.5 : k3 := 3.4 : k4 := 0.425 : kt := 0.6 : φeq :=
    evalf((n1·φtopbig^2 + n2·φtopsmall^2)/(n1·φtopbig + n2·φtopsmall)) :
> fcteff := fctm :
> if sreb ≤ (5·(h − dslab)) then srmaxx := k3·cridge + k1·k2·k4·φeq/ρpeff else srmaxx := 1.3(h
    − xe) end if:
> if srmaxx > max((50 − 0.8 fck)·φeq, 15·φeq) then srmaxx := max((50 − 0.8 fck)·φeq, 15
    ·φeq) end if;
```

$$srmaxx := 138.2926829 \quad (22.12)$$

```
> if srebtopcross ≤ (5·(h − dcross)) then srmaxy := k3·cridge + + k1·k2·k4·φtopcross/ρpeffcross
    else srmaxy := 1.3(h − xecross) end if;
```

$$srmaxy := 237.8772230 \quad (22.13)$$

```
> if srmaxy > max((50 − 0.8 fck)·φtopcross, 15·φtopcross) then srmaxy := max((50
    − 0.8 fck)·φtopcross, 15·φtopcross) end if;
```

$$srmaxy := 90 \quad (22.14)$$

```
> srmax := 1/(cos(0.5 π)/srmaxy + sin(0.5 π)/srmaxx);
```

$$srmax := 138.2926829 \quad (22.15)$$

```
> σsr := fcteff/ρpeff·(1 + αe·ρpeff) : σs := Mfc/(As·zslab);
```

$$σs := 112.4093335 \quad (22.16)$$

```
> straindifference := (σs − kt·σsr)/Es; minstraindifference := (0.6·σs/Es);
```

$$straindifference := -0.000003160161500$$

$$minstraindifference := 0.0003372280005 \quad (22.17)$$

```
> if straindifference ≤ minstraindifference then straindifference := minstraindifference end if;
```

(22.18)

$$straindifference := 0.0003372280005 \quad \textbf{(22.18)}$$

> $wk := straindifference \cdot srmax;$

$$wk := 0.04663616494 \quad \textbf{(22.19)}$$

> **if** $wk \leq wmax$ **then** $print(Crack\ width\ is\ small\ enough)$ **else** $print(Crack\ width\ is\ too\ big)$ **end if**;

$$Crack\ width\ is\ small\ enough \quad \textbf{(22.20)}$$

G

Sensitivity analysis of load spreading in disturbed regions

In this appendix the tensile splitting force resulting from a compressive support load is determined in three ways.

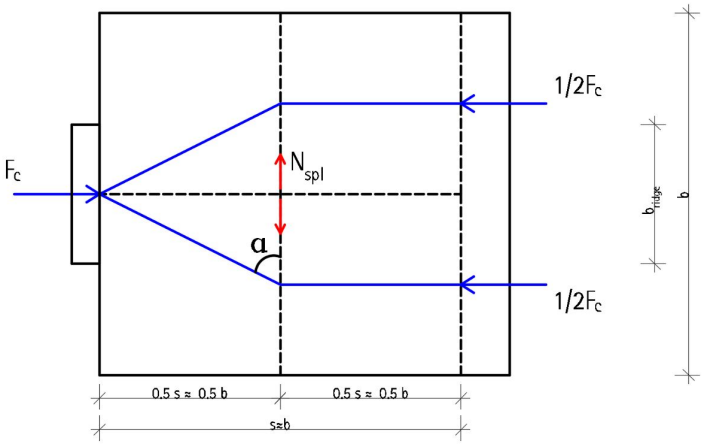

Figure G.1: Visualization of disturbed region and the accompanying tensile splitting force in bottom side of slab due to compressive force from support.

Lettuce structure analogy, one point load

$$tan(\alpha) = \frac{\frac{1}{2}b}{\frac{1}{4}b} = 2 \tag{G.1}$$

$$tan(\alpha) = \frac{\frac{1}{2}F_c}{\frac{1}{4}N_{spl}} = 2 \tag{G.2}$$

$$N_{spl} = \frac{1}{4}F_c \tag{G.3}$$

Moment equilibrium, Console analogy, one point load

From [7] it follows that the internal lever arm z is:

$$z \begin{cases} = 0.2 * l + 0.4 * h = 0.2 * b + 0.4 * b = 0.6 * b \\ \leq 0.8 * l = 0.8 * b \end{cases} \tag{G.4}$$

$$q = \frac{F_c}{b} \tag{G.5}$$

$$M = \frac{1}{2} * q * (\frac{1}{2} * b)^2 = \frac{1}{8} * F_c * b \tag{G.6}$$

$$N_{spl} = \frac{M}{z} = \frac{\frac{1}{8} * F_c * b}{0.6 * b} = 0.21 * F_c \tag{G.7}$$

Two point loads

To determine the splitting force the bending moment in point A is determined for half of the balcony slab.

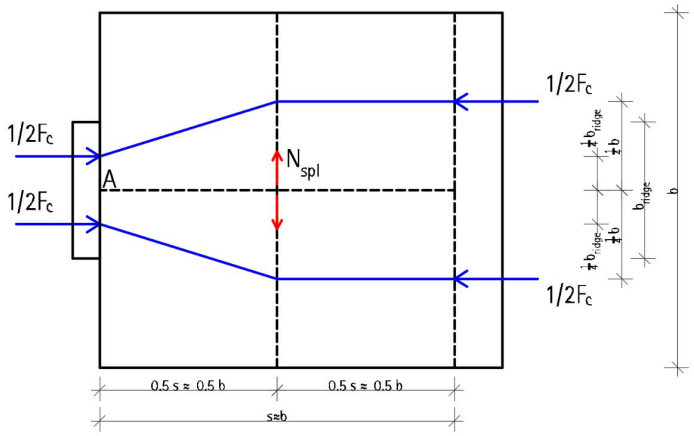

Figure G.2: Visualization of disturbed region and the accompanying tensile splitting force in bottom side of slab due to two compressive forces from support.

$$\frac{F_c}{2} * \left(\frac{1}{4}b - \frac{1}{4} * b_{ridge}\right) = N_{spl} * \frac{1}{2} * b \tag{G.8}$$

$$N_{spl} = \frac{1}{4} * F_c * \left(\frac{b - b_{ridge}}{b}\right) \tag{G.9}$$

for b=1300 mm and b_{ridge}=500 mm:

$$N_{spl} = 0.15 * F_c \tag{G.10}$$

Wrap up

It can be observed that increasing the amount of point loads representing the compressive force in the bottom of the slab reduces the magnitude of the splitting force. This means that working with one point load is a conservative choice.

H

Final design balcony with in-plane ridge

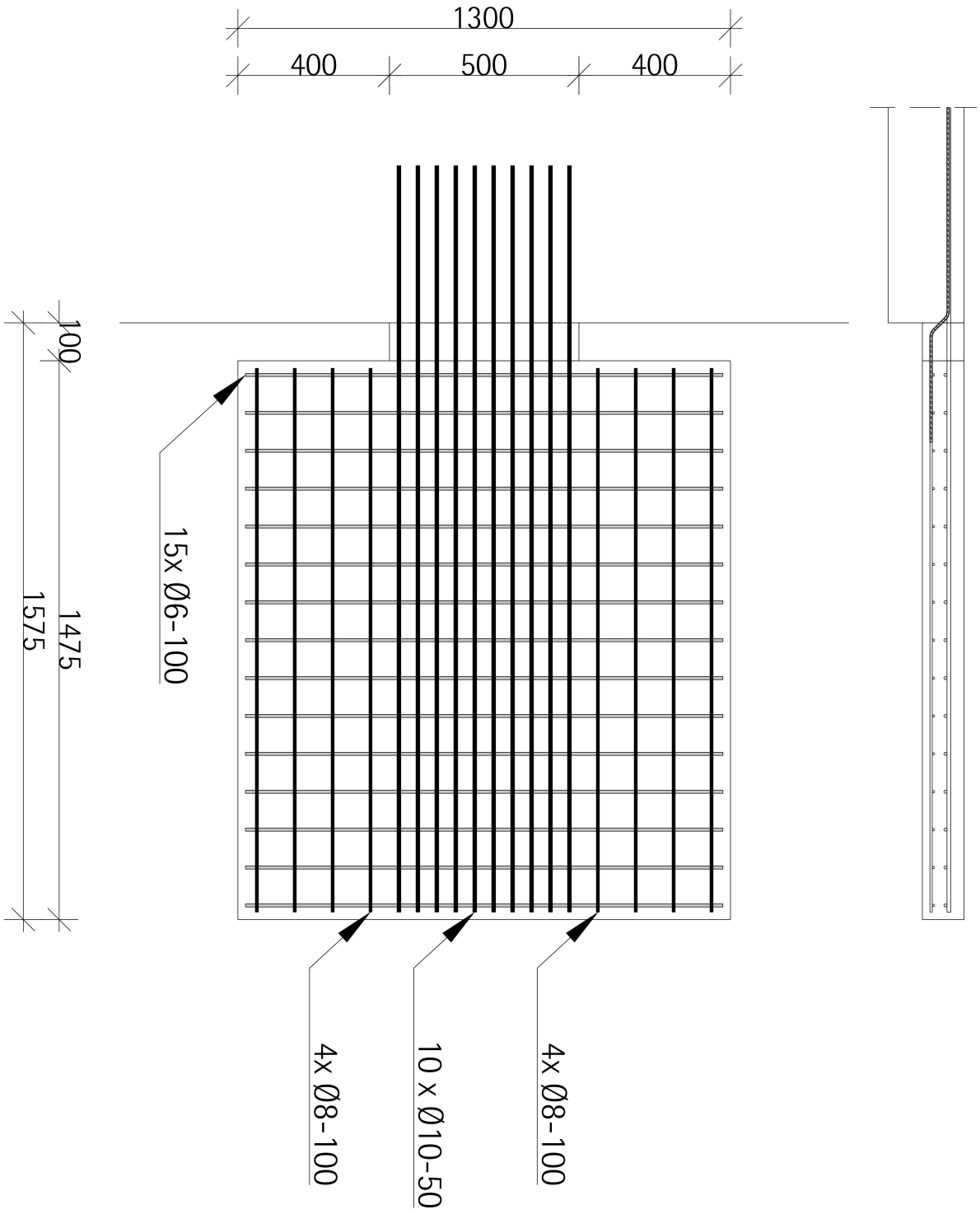

Figure H.1: Design of balcony with ridge, including top reinforcement configuration.

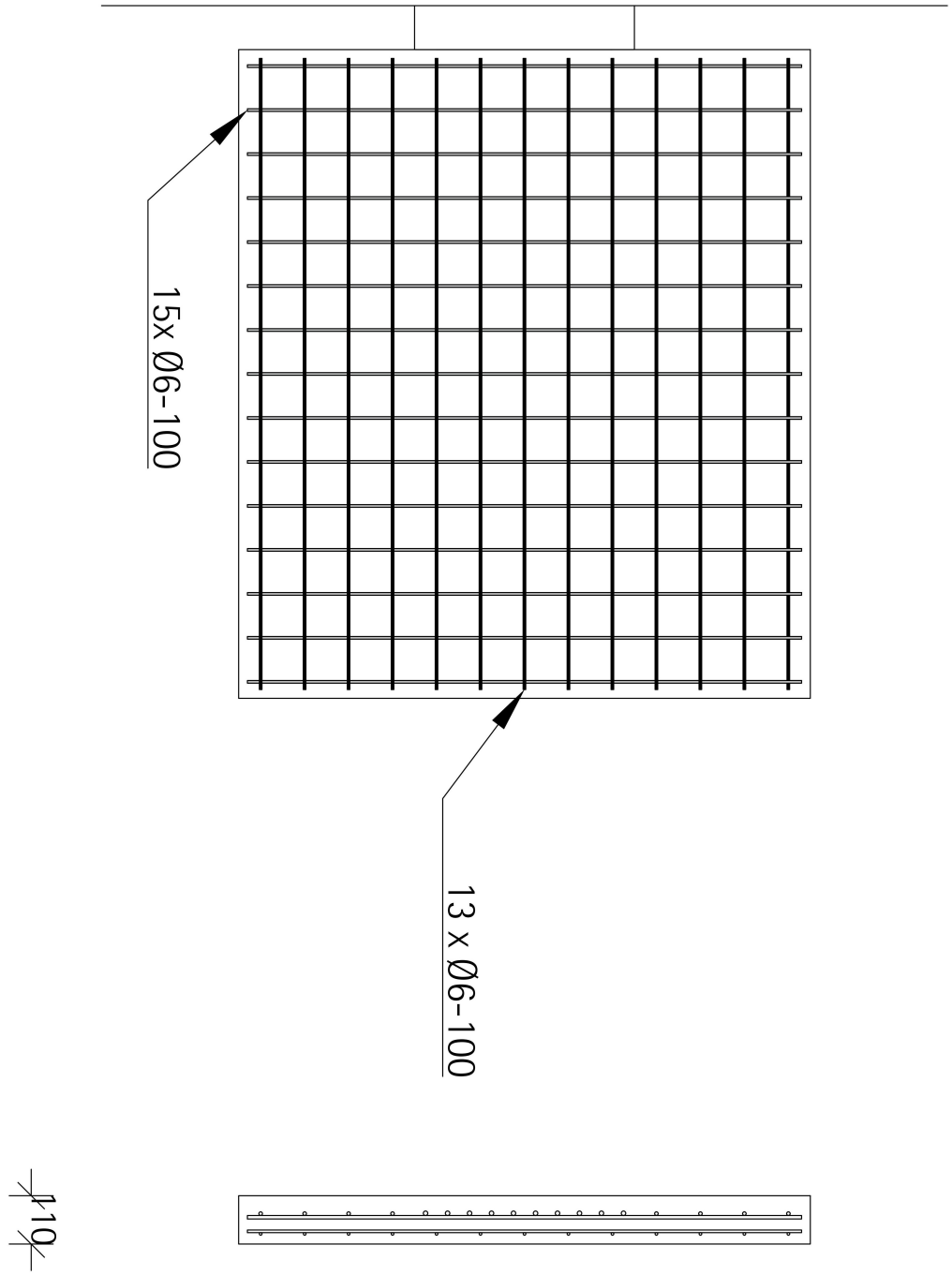

Figure H.2: Design of balcony with ridge, including bottom reinforcement configuration.

Results finite element analysis balcony with in-plane ridge

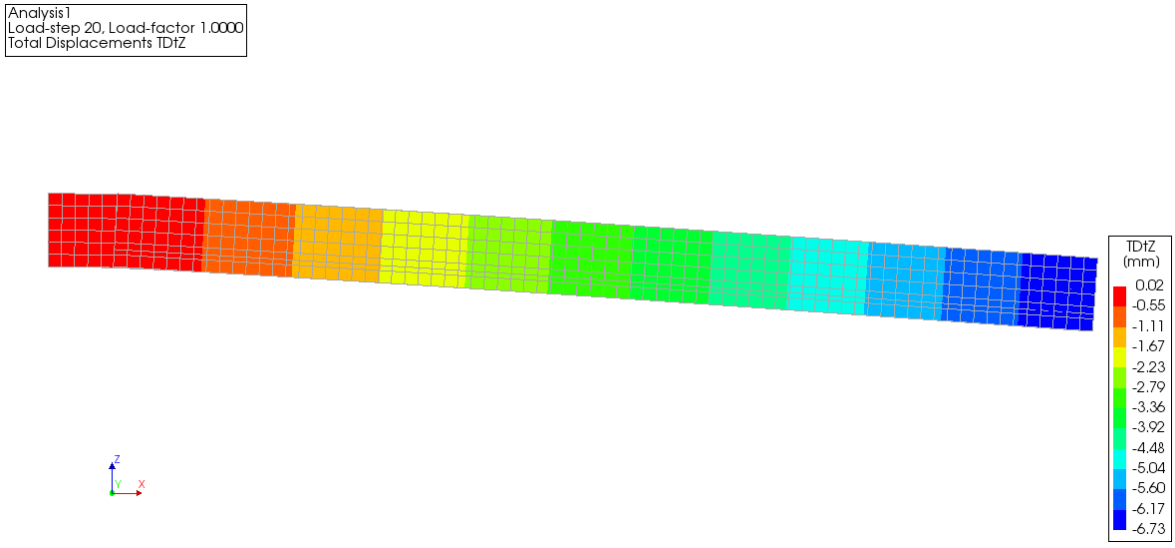

Figure I.1: Visualization of deformation following from the characteristic load combination.

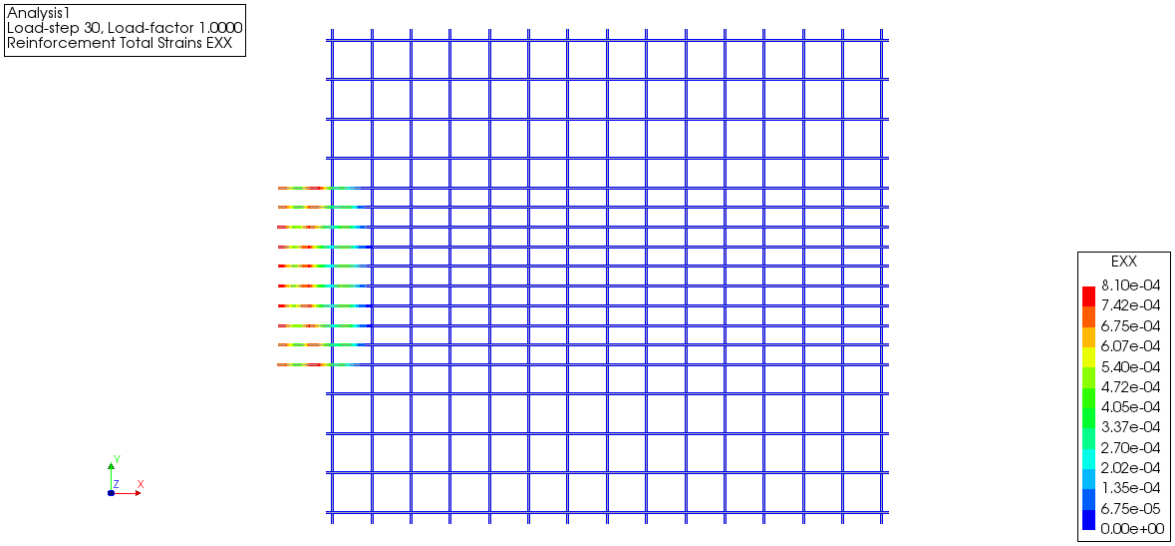

Figure I.2: Visualization of reinforcement strains in x-direction from the frequent load combination after the characteristic load combination has occurred.

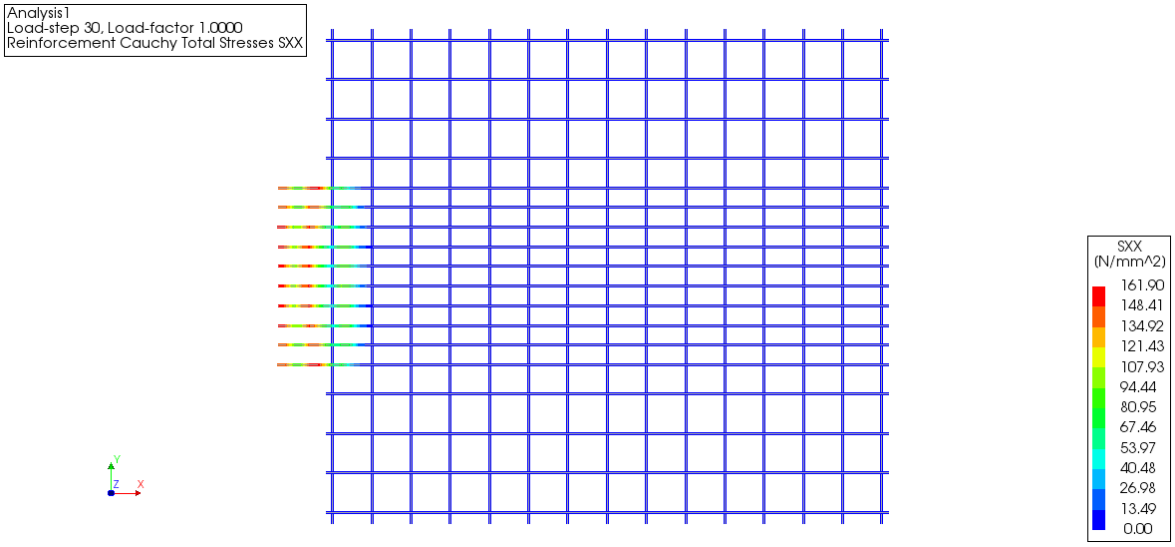

Figure I.3: Visualization of reinforcement stresses in x-direction from the frequent load combination after the characteristic load combination has occurred.

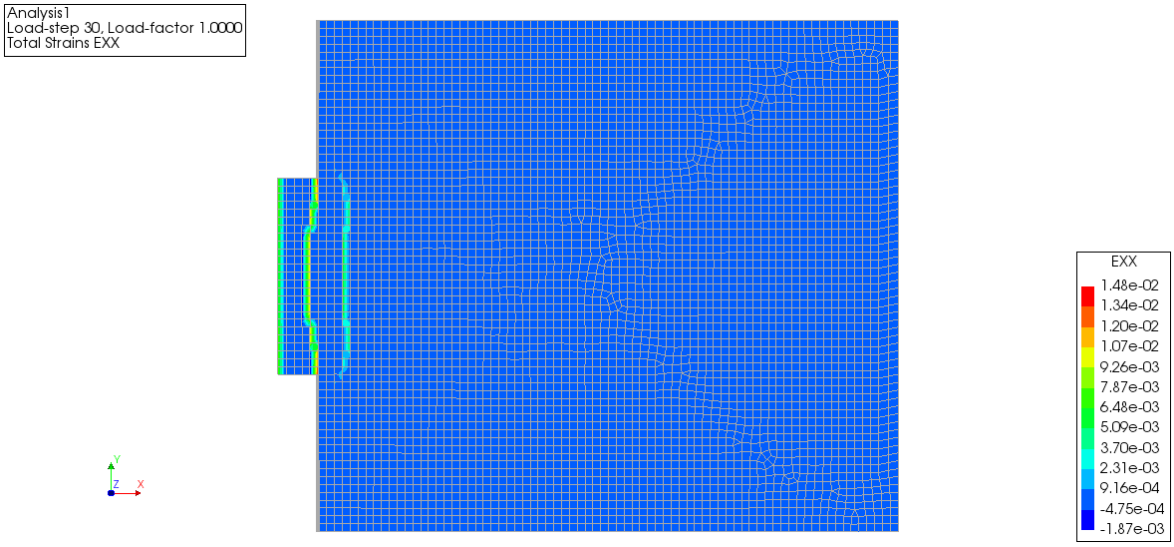

Figure I.4: Visualization of strains in x-direction after frequent load combination.

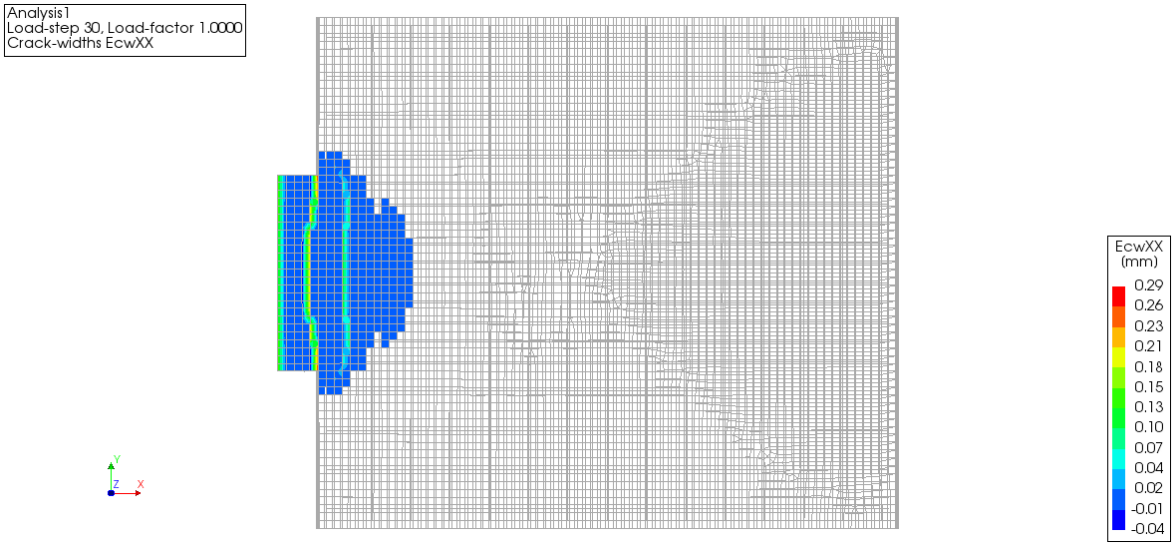

Figure I.5: Visualization of crack widths in x-direction determined by DIANA FEA. Maximum crack width occurs in corners between slab and ridge.

J

Script balcony with out-of-plane ridge

This appendix contains the script for the design and check process of the balcony with an out-of-plane ridge.

Dimensioning and checking of a cantilevering slab, supported by an out of plane ridge.

All units in N and mm

```
> restart;
```

Geometry

```
> lridge := 135 : lslab := 1575 − lridge : ltot := lridge + lslab : bslab := 1300 : bridge :=
      500 : hslab := 115 : hridge := 315 : supdist := 150 :
```

Material Properties Concrete: C90/105

```
> γc := 1.5 : Ecm := 43600 : fck := 90 : fcd := fck/γc : fctm := 5.05 : fctk := 3.54 : fctd :=
      fck/γc : fctmfl := max((1.6 − hslab/1000) fctm, fctm) : εc3 := 2.3·10^−3 : εcu3 := 2.6·10^−3 :
  fcmcube := 105 + 8 :
```

Material Properties Reinforcement: B500b

```
> γs := 1.15 : fyk := 500 : fyd := fyk/γs : Es := 200000 :
```

Loads

```
> G := 25000·10^−9 : g := 0.75·bslab : Q := 5000 :
```

Reinforcement configuration

```
> ϕtopbig := 12 : αe := Es/Ecm : sreb := 62.5 : n1 := ceil(bridge/sreb);
```

$$n1 := 8 \tag{5.1}$$

```
> ϕtopsmall := 8 : srebtopsmall := 100 : n2 := ceil((bslab − bridge)/srebtopsmall) :
> ϕtopcross := 8 : srebtopcross := 100 :
> ϕbottom := 6 : srebbottom := 100 :
> ϕbottomcross := 6 : srebbottomcross := 100 :
> ϕshear := 8 : srebshear := 50 : nshear := 8 : compangle := 62 :
> if ϕtopcross < 0.6·ϕtopbig then print(Top cross reinforcement should be at least '0.6
      ' times diameter main reinforcement) end if;
```

Concrete Cover

```
> cslab := 30 : cridge := 35 : cother := 20 :
```

Bending moments and shear forces slab

```
> Mks := (0.5·lslab)·lslab·bslab·hslab·G + Q·lslab + g·lslab;
```

$$Mks := 1.247904000\ 10^{7} \quad (7.1)$$

> $Vks := bslab \cdot hslab \cdot lslab \cdot G + Q + g;$

$$Vks := 11357.00 \quad (7.2)$$

> $Mfcs := (0.5 \cdot lslab) \cdot lslab \cdot bslab \cdot hslab \cdot G + 0.5 \cdot Q \cdot lslab + g \cdot lslab;$

$$Mfcs := 8.879040000\ 10^{6} \quad (7.3)$$

> $Vfcs := bslab \cdot hslab \cdot lslab \cdot G + 0.5 \cdot Q + g;$

$$Vfcs := 8857.00 \quad (7.4)$$

> $Mqbs := (0.5 \cdot lslab) \cdot lslab \cdot bslab \cdot hslab \cdot G + 0.3 \cdot Q \cdot lslab + g \cdot lslab;$

$$Mqbs := 7.439040000\ 10^{6} \quad (7.5)$$

> $Vqbs := bslab \cdot hslab \cdot lslab \cdot G + 0.3 \cdot Q + g;$

$$Vqbs := 7857.00 \quad (7.6)$$

> $Meds := 1.2 \cdot (0.5 \cdot lslab) \cdot lslab \cdot bslab \cdot hslab \cdot G + 1.5 \cdot 0.5 \cdot Q \cdot lslab + 1.2 \cdot g \cdot lslab;$

$$Meds := 1.173484800\ 10^{7} \quad (7.7)$$

> $Veds := 1.2 \cdot bslab \cdot hslab \cdot lslab \cdot G + 1.5 \cdot 0.5 \cdot Q + 1.2 \cdot g;$

$$Veds := 11378.400 \quad (7.8)$$

Bending moments and shear forces ridge

> $Mkr := (0.5 \cdot lslab + lridge) \cdot lslab \cdot bslab \cdot hslab \cdot G + Q \cdot (lslab + lridge) + g \cdot (lslab + lridge) + \frac{1}{2} \cdot lridge^{2} \cdot bridge \cdot hridge \cdot G;$

$$Mkr := 1.404811547\ 10^{7} \quad (8.1)$$

> $Vkr := bslab \cdot hslab \cdot lslab \cdot G + Q + g + lridge \cdot bridge \cdot hridge \cdot G;$

$$Vkr := 11888.56250 \quad (8.2)$$

> $Mfcr := (0.5 \cdot lslab + lridge) \cdot lslab \cdot bslab \cdot hslab \cdot G + 0.5 \cdot Q \cdot (lslab + lridge) + g \cdot (lslab + lridge) + \frac{1}{2} \cdot lridge^{2} \cdot bridge \cdot hridge \cdot G;$

$$Mfcr := 1.011061547\ 10^{7} \quad (8.3)$$

> $Vfcr := bslab \cdot hslab \cdot lslab \cdot G + 0.5 \cdot Q + g + lridge \cdot bridge \cdot hridge \cdot G;$

$$Vfcr := 9388.562500 \quad (8.4)$$

> $Mqbr := (0.5 \cdot lslab + lridge) \cdot lslab \cdot bslab \cdot hslab \cdot G + 0.3 \cdot Q \cdot (lslab + lridge) + g \cdot (lslab + lridge) + \frac{1}{2} \cdot lridge^{2} \cdot bridge \cdot hridge \cdot G;$

$$Mqbr := 8.535615469\ 10^{6} \quad (8.5)$$

> $Vqbr := bslab \cdot hslab \cdot lslab \cdot G + 0.3 \cdot Q + g + lridge \cdot bridge \cdot hridge \cdot G;$

$$Vqbr := 8388.562500 \quad (8.6)$$

> $Medr := 1.2 \cdot (0.5 \cdot lslab + lridge) \cdot lslab \cdot bslab \cdot hslab \cdot G + 1.5 \cdot Q \cdot (lslab + lridge) + 1.2 \cdot g \cdot (lslab + lridge) + 1.2 \cdot \frac{1}{2} \cdot lridge^{2} \cdot bridge \cdot hridge \cdot G;$

$$Medr := 1.922023856\ 10^{7} \quad (8.7)$$

> $Vedr := 1.2 \cdot bslab \cdot hslab \cdot lslab \cdot G + 1.5 \cdot 0.5 \cdot Q + 1.2 \cdot g + 1.2 \cdot lridge \cdot bridge \cdot hridge \cdot G;$

$$Vedr := 12016.27500 \quad (8.8)$$

Support reactions

> $Fsv := Vedr;$

$$Fsv := 12016.27500 \tag{9.1}$$

> $Fsh1 := \frac{Medr}{supdist};$

$$Fsh1 := 1.281349237\ 10^{5} \tag{9.2}$$

> $Fs21 := -\frac{Medr}{supdist}$

$$Fs21 := -1.281349237\ 10^{5} \tag{9.3}$$

Cracking moments

> $Mcrs := \frac{1}{6}\cdot bslab\cdot hslab^{2}\cdot fctm;\ Mcrsr := \frac{1}{6}\cdot bridge\cdot hslab^{2}\cdot fctm;$

$$Mcrs := 1.447035417\ 10^{7}$$
$$Mcrsr := 5.565520833\ 10^{6} \tag{10.1}$$

Check bending moment resistance slab

> $dslab := \frac{1}{n1\cdot\left(\frac{\phi topbig}{2}\right)^{2}\cdot\pi + n2\cdot\left(\frac{\phi topsmall}{2}\right)^{2}\cdot\pi}\left(n1\cdot\left(\frac{\phi topbig}{2}\right)^{2}\cdot\pi\cdot\left(hslab - cridge - \frac{\phi topbig}{2}\right) + n2\cdot\left(\frac{\phi topsmall}{2}\right)^{2}\cdot\pi\cdot\left(hslab - cridge - \phi topbig + 0.5\cdot\phi topsmall\right)\right);$

$$dslab := 73.38461538 \tag{11.1}$$

> $As := evalf\left(\mathrm{ceil}\left(\frac{bridge}{sreb}\right)\cdot\pi\cdot\left(\frac{\phi topbig}{2}\right)^{2} + \mathrm{ceil}\left(\frac{bslab - bridge}{srebtopsmall}\right)\cdot\pi\cdot\left(\frac{\phi topsmall}{2}\right)^{2}\right);$

$$As := 1306.902544 \tag{11.2}$$

> $\rho l := \frac{As}{bslab\cdot dslab};$

$$\rho l := 0.01369918809 \tag{11.3}$$

> $xu := \frac{As\cdot fyd}{\left(\frac{1}{2}\cdot\frac{\varepsilon c3}{\varepsilon cu3} + \left(1 - \frac{\varepsilon c3}{\varepsilon cu3}\right)\right)\cdot fcd\cdot bslab};$

$$xu := 13.06249419 \tag{11.4}$$

Determine a maximum reinforcement ratio for which yielding of steel occurs before crushing of concrete

> $eq2 := \left(\rho lmax2\cdot bslab\cdot dslab\right)\cdot fyk = \left(\frac{1}{2}\cdot\frac{\varepsilon c3}{\varepsilon cu3} + \left(1 - \frac{\varepsilon c3}{\varepsilon cu3}\right)\right)\cdot fck\cdot bslab\cdot xu:$

$\rho lmax := solve(eq2, \rho lmax2);$

$$\rho lmax := 0.01786850620 \quad (11.5)$$

> $\rho lmax := \min(0.04, \rho lmax);$

$$\rho lmax := 0.01786850620 \quad (11.6)$$

> **if** $\rho l > \rho lmax$ **then** $print(Reinforcement\ ratio\ is\ too\ high)$ **end if**

> $$\beta xu := \frac{1}{fcd\cdot\left(1-\frac{\varepsilon c3}{\varepsilon cu3}\right)xu+0.5\cdot fcd\cdot\left(\frac{\varepsilon c3}{\varepsilon cu3}\right)xu}\left(\left(1-\frac{\varepsilon c3}{\varepsilon cu3}\right)\cdot xu\cdot fcd\cdot 0.5\left(1-\frac{\varepsilon c3}{\varepsilon cu3}\right)xu+0.5\cdot\left(\frac{\varepsilon c3}{\varepsilon cu3}\right)\cdot xu\cdot fcd\cdot\left(\left(1-\frac{\varepsilon c3}{\varepsilon cu3}\right)xu+\frac{\left(\frac{\varepsilon c3}{\varepsilon cu3}\right)xu}{3}\right)\right);$$

$$\beta xu := 4.406137517 \quad (11.7)$$

> $zslab := dslab - \beta xu;$

$$zslab := 68.97847786 \quad (11.8)$$

> $Ns := fyd\cdot As : Mrd := Ns\cdot zslab;$

$$Mrd := 3.919484704\ 10^{7} \quad (11.9)$$

> $UC := \frac{Meds}{Mrd};$

$$UC := 0.2993977241 \quad (11.10)$$

Check bending moment transition zone ridge and slab

> $dsr := hslab - cridge - \frac{\phi topbig}{2};$

$$dsr := 74 \quad (12.1)$$

> $Assr := evalf\left(\text{ceil}\left(\frac{bridge}{sreb}\right)\cdot\pi\cdot\left(\frac{\phi topbig}{2}\right)^2\right); n := \text{ceil}\left(\frac{bridge}{sreb}\right)$

$$Assr := 904.7786844$$

$$n := 8 \quad (12.2)$$

> $\rho lsr := \frac{Assr}{bridge\cdot dsr};$

$$\rho lsr := 0.02445347796 \quad (12.3)$$

> $xusr := \frac{Assr\cdot fyd}{\left(\frac{1}{2}\cdot\frac{\varepsilon c3}{\varepsilon cu3}+\left(1-\frac{\varepsilon c3}{\varepsilon cu3}\right)\right)\cdot fcd\cdot bridge};$

$$xusr := 23.51248956 \quad (12.4)$$

Determine a maximum reinforcement ratio for which yielding of steel occurs before crushing of concrete

> $eq1 := (\rho lmax3 \cdot bridge \cdot dsr) \cdot fyk = \left(\frac{1}{2} \cdot \frac{\varepsilon c3}{\varepsilon cu3} + \left(1 - \frac{\varepsilon c3}{\varepsilon cu3}\right)\right) \cdot fck \cdot bridge \cdot xusr$:
> $\rho lmax := solve(eq1, \rho lmax3)$;

$$\rho lmax := 0.03189584082 \quad \textbf{(12.5)}$$

> $\rho lmax := \min(0.04, \rho lmax)$;

$$\rho lmax := 0.03189584082 \quad \textbf{(12.6)}$$

> **if** $\rho lsr > \rho lmax$ **then** $print(Reinforcement\ ratio\ is\ too\ high)$ **end if**

center of gravity compression zone on maximum capacity, β≠0.39 because of HSC:

> $\beta xusr := \left(\left(1 - \frac{\varepsilon c3}{\varepsilon cu3}\right) \cdot xusr \cdot fcd \cdot 0.5\left(1 - \frac{\varepsilon c3}{\varepsilon cu3}\right) xusr + 0.5 \cdot \left(\frac{\varepsilon c3}{\varepsilon cu3}\right) \cdot xusr \cdot fcd \cdot \left(\left(1 - \frac{\varepsilon c3}{\varepsilon cu3}\right) xusr + \frac{\left(\frac{\varepsilon c3}{\varepsilon cu3}\right) xusr}{3}\right)\right) \Big/ \left(fcd \cdot \left(1 - \frac{\varepsilon c3}{\varepsilon cu3}\right) xusr + 0.5 \cdot fcd \cdot \left(\frac{\varepsilon c3}{\varepsilon cu3}\right) xusr\right)$;

$$\beta xusr := 7.931047541 \quad \textbf{(12.7)}$$

> $\beta := \frac{\beta xusr}{xusr}$; $zsr := dsr - \beta xusr$

$$\beta := 0.3373121132$$
$$zsr := 66.06895246 \quad \textbf{(12.8)}$$

> $Ns := fyd \cdot Assr$: $Mrdsr := Ns \cdot zsr$;

$$Mrdsr := 2.599033908\ 10^{7} \quad \textbf{(12.9)}$$

> $UC := \frac{Meds}{Mrdsr}$;

$$UC := 0.4515080763 \quad \textbf{(12.10)}$$

Check bending moment ridge

> $dr := lridge - cother - \phi shear - \frac{\phi topbig}{2}$;

$$dr := 101 \quad \textbf{(13.1)}$$

> $Asr := evalf\left(\text{ceil}\left(\frac{bridge}{sreb}\right) \cdot \pi \cdot \left(\frac{\phi topbig}{2}\right)^2\right)$; $n := \text{ceil}\left(\frac{bridge}{sreb}\right)$

$$Asr := 904.7786844$$
$$n := 8 \quad \textbf{(13.2)}$$

> $\rho lr := \frac{Asr}{bridge \cdot dr}$;

$$\rho lr := 0.01791640959 \quad \textbf{(13.3)}$$

$$> xur := \frac{Asr \cdot fyd}{\left(\frac{1}{2} \cdot \frac{\varepsilon c3}{\varepsilon cu3} + \left(1 - \frac{\varepsilon c3}{\varepsilon cu3}\right)\right) \cdot fcd \cdot bridge};$$

$$xur := 23.51248956 \quad (13.4)$$

Determine a maximum reinforcement ratio for which yielding of steel occurs before crushing of concrete

$$> eq1 := (\rho lmax4 \cdot bridge \cdot dr) \cdot fyk = \left(\frac{1}{2} \cdot \frac{\varepsilon c3}{\varepsilon cu3} + \left(1 - \frac{\varepsilon c3}{\varepsilon cu3}\right)\right) \cdot fck \cdot bridge \cdot xur :$$

$$\rho lmax := solve(eq1, \rho lmax4);$$

$$\rho lmax := 0.02336922991 \quad (13.5)$$

$$> \rho lmax := \min(0.04, \rho lmax);$$

$$\rho lmax := 0.02336922991 \quad (13.6)$$

$$> \textbf{if } \rho lr > \rho lmax \textbf{ then } print(Reinforcement\ ratio\ is\ too\ high) \textbf{ end if}$$

center of gravity compression zone on maximum capacity, β≠0.39 because of HSC:

$$> \beta xur := \left(\left(1 - \frac{\varepsilon c3}{\varepsilon cu3}\right) \cdot xusr \cdot fcd \cdot 0.5\left(1 - \frac{\varepsilon c3}{\varepsilon cu3}\right) xusr + 0.5 \cdot \left(\frac{\varepsilon c3}{\varepsilon cu3}\right) \cdot xusr \cdot fcd \cdot \left(\left(1 - \frac{\varepsilon c3}{\varepsilon cu3}\right) xusr + \frac{\left(\frac{\varepsilon c3}{\varepsilon cu3}\right) xusr}{3}\right)\right) \Big/ \left(fcd \cdot \left(1 - \frac{\varepsilon c3}{\varepsilon cu3}\right) xusr + 0.5 \cdot fcd \cdot \left(\frac{\varepsilon c3}{\varepsilon cu3}\right) xusr\right);$$

$$\beta xur := 7.931047541 \quad (13.7)$$

$$> \beta := \frac{\beta xur}{xur}; zr := dr - \beta xur$$

$$\beta := 0.3373121132$$

$$zr := 93.06895246 \quad (13.8)$$

$$> Nsr := fyd \cdot As; Mrdr := Ns \cdot zr;$$

$$Nsr := 5.682184974\ 10^5$$

$$Mrdr := 3.661165407\ 10^7 \quad (13.9)$$

$$> Medr := Fsh1 \cdot supdist$$

$$Medr := 1.922023856\ 10^7 \quad (13.10)$$

$$> UC := \frac{Medr}{Mrdsr};$$

$$UC := 0.7395147289 \quad (13.11)$$

Bending moment resistance cross direction

Take into account the possibility of point load Q at the side. Conservative approach by using a clamped beam, cantilevering 1300/2=650 mm.

> $Mkcross := 0.5 \cdot G \cdot hslab \cdot 1000 \cdot \left(\frac{bslab}{2} \right)^2 + Q \cdot \left(\frac{bslab}{2} \right)$; $Medcross := 1.2 \cdot 0.5 \cdot G \cdot hslab \cdot 1000 \cdot \left(\frac{bslab}{2} \right)^2 + 1.5 \cdot Q \cdot \left(\frac{bslab}{2} \right)$

$$Mkcross := 3.857343750\ 10^6$$

$$Medcross := 5.603812500\ 10^6 \quad (14.1)$$

> $dcross := hslab - cridge - \phi topbig - 0.5 \cdot \phi topcross$;

$$dcross := 64.0 \quad (14.2)$$

> $Ascross := evalf\left(\text{ceil}\left(\frac{1000}{srebtopcross} \right) \cdot \pi \cdot \left(\frac{\phi topcross}{2} \right)^2 \right)$; $n := \text{ceil}\left(\frac{1000}{srebtopcross} \right)$

$$Ascross := 502.6548246$$

$$n := 10 \quad (14.3)$$

> $\rho lcross := \frac{Ascross}{1000 \cdot dcross}$;

$$\rho lcross := 0.007853981634 \quad (14.4)$$

> $xucross := \frac{Ascross \cdot fyd}{\left(\frac{1}{2} \cdot \frac{\varepsilon c3}{\varepsilon cu3} + \left(1 - \frac{\varepsilon c3}{\varepsilon cu3} \right) \right) \cdot fcd \cdot 1000}$;

$$xucross := 6.531247095 \quad (14.5)$$

Determine a maximum reinforcement ratio for which yielding of steel occurs before crushing of concrete

> $eq1 := (\rho lmax3 \cdot 1000 \cdot dcross) \cdot fyk = \left(\frac{1}{2} \cdot \frac{\varepsilon c3}{\varepsilon cu3} + \left(1 - \frac{\varepsilon c3}{\varepsilon cu3} \right) \right) \cdot fck \cdot 1000 \cdot xucross$:
$\rho lmax := solve(eq1, \rho lmax3)$;

$$\rho lmax := 0.01024432387 \quad (14.6)$$

> $\rho lmax := \min(0.04, \rho lmax)$;

$$\rho lmax := 0.01024432387 \quad (14.7)$$

> **if** $\rho lcross > \rho lmax$ **then** $print(Reinforcement\ ratio\ is\ too\ high)$ **end if**

center of gravity compression zone on maximum capacity, β≠0.39 because of HSC:

> $\beta xucross := \beta \cdot xucross$; $zcross := dcross - \beta xucross$;

$$\beta xucross := 2.203068759$$

$$zcross := 61.79693124 \quad (14.8)$$

> $Ns := fyd \cdot Ascross$: $Mrdcross := Ns \cdot zcross$;

$$Mrdcross := 1.350544593\ 10^7 \quad (14.9)$$

> $UC := \frac{Medcross}{Mrdcross}$;

$$UC := 0.4149298386 \quad (14.10)$$

>

Check vertical shear force in ridge

> $dridge := hridge - cridge - 0.5 \cdot \phi topbig;$

$$dridge := 274.0 \quad (15.1)$$

> $\rho lridge := \dfrac{evalf\left(n1 \cdot \pi \cdot \left(\dfrac{\phi topbig}{2}\right)^2\right)}{dridge \cdot bridge};$

$$\rho lridge := 0.006604223974 \quad (15.2)$$

> $Ved := Fsv;$

$$Ved := 12016.27500 \quad (15.3)$$

> $k := 1 + \sqrt{\dfrac{200}{dridge}}\ :$

> **if** $k \le 2$ **then** $k := k$ **else** $k := 2$ **end if**;

$$k := 1.854357658 \quad (15.4)$$

> $Crdc := \dfrac{0.18}{\gamma c}\ : vmin := evalf\left(0.035 \cdot k^{\frac{3}{2}} \cdot fck^{\frac{1}{2}}\right)\ :$

> $Vrdcmin := vmin \cdot bridge \cdot dridge;$

$$Vrdcmin := 1.148682804\ 10^5 \quad (15.5)$$

> $Vrdc := evalf\left(\left(Crdc \cdot k \cdot (100 \cdot \rho lridge \cdot fck)^{\frac{1}{3}}\right) \cdot bridge \cdot dridge\right);$

$$Vrdc := 1.189734575\ 10^5 \quad (15.6)$$

> $Vrdcridge := \max(Vrdcmin, Vrdc);$

$$Vrdcridge := 1.189734575\ 10^5 \quad (15.7)$$

> $UC := \dfrac{Vedr}{Vrdcridge};$

$$UC := 0.1009996284 \quad (15.8)$$

Check vertical shear force transition zone ridge and slab

> $dsr := hslab - cridge - 0.5 \cdot \phi topbig;$

$$dsr := 74.0 \quad (16.1)$$

> $\rho lsr := \dfrac{evalf\left(n1 \cdot \pi \cdot \left(\dfrac{\phi topbig}{2}\right)^2\right)}{dsr \cdot bridge};$

$$\rho lsr := 0.02445347796 \quad (16.2)$$

> $Ved := Fsv;$

$$Ved := 12016.27500 \quad (16.3)$$

> $k := 1 + \sqrt{\dfrac{200}{dsr}}\ :$

> **if** $k \le 2$ **then** $k := k$ **else** $k := 2$ **end if**;

$$k := 2 \quad (16.4)$$

> $Crdc := \frac{0.18}{\gamma c}$: $vmin := evalf\left(0.035 \cdot k^{\frac{3}{2}} \cdot fck^{\frac{1}{2}}\right)$:

> $Vrdcmin := vmin \cdot bridge \cdot dsr$;

$$Vrdcmin := 34748.49636 \quad \textbf{(16.5)}$$

> $Vrdc := evalf\left(\left(Crdc \cdot k \cdot (100 \cdot \rho lsr \cdot fck)^{\frac{1}{3}}\right) \cdot bridge \cdot dsr\right)$;

$$Vrdc := 53613.48206 \quad \textbf{(16.6)}$$

> $Vrdcsr := \max(Vrdcmin, Vrdc)$;

$$Vrdcsr := 53613.48206 \quad \textbf{(16.7)}$$

> $UC := \frac{Veds}{Vrdcsr}$;

$$UC := 0.2122301996 \quad \textbf{(16.8)}$$

Console analogy for ridge

> $dconsole := lridge - cother - \frac{\phi topbig}{2}$;

$$dconsole := 109 \quad \textbf{(17.1)}$$

> $av := hridge - hslab - 25$;

$$av := 175 \quad \textbf{(17.2)}$$

> **if** $2 \cdot (av + \beta xusr) \leq 3 \cdot lridge$ **then** $print(Console\ is\ deep\ beam)$ **end if**;

$$Console\ is\ deep\ beam \quad \textbf{(17.3)}$$

> $zrconsole := \min(0.2 \cdot (hridge - hslab) + 0.4 \cdot lridge, 0.8 \cdot (hridge - hslab))$;

$$zrconsole := 94.0 \quad \textbf{(17.4)}$$

>

Check horizontal shear force in ridge

> $dridgeh := lridge - cother - 0.5 \cdot \phi topbig$; $av := hridge - hslab - 25$;

$$dridgeh := 109.0$$
$$av := 175 \quad \textbf{(18.1)}$$

> $\rho lridge := \frac{evalf\left(n1 \cdot \pi \cdot \left(\frac{\phi topbig}{2}\right)^2\right)}{bridge \cdot dridgeh}$;

$$\rho lridge := 0.01660144375 \quad \textbf{(18.2)}$$

> $Ved := Fsh1$;

$$Ved := 1.281349237\ 10^5 \quad \textbf{(18.3)}$$

> **if** $Ved \leq 0.5 \cdot bridge \cdot dridgeh \cdot \left(0.6 \cdot \left(1 - \frac{fck}{250}\right)\right) \cdot fcd$ **and** $0.5 \leq \frac{av}{dridgeh} \leq 2$ **then** $Ved := \frac{av}{2 \cdot dridgeh} \cdot Ved$ **end if**;

$$Ved := 1.028606039\ 10^{5} \tag{18.4}$$

> **if** $Ved > 0.5 \cdot bridge \cdot dridgeh \cdot \left(0.6 \cdot \left(1 - \frac{fck}{250}\right)\right) \cdot fcd$ **then** $Ved := Ved$ **end if**;

>

> $k := 1 + \sqrt{\frac{200}{dridgeh}}$:

> **if** $k \le 2$ **then** $k := k$ **else** $k := 2$ **end if**;

$$k := 2 \tag{18.5}$$

> $Crdc := \frac{0.18}{\gamma c}$: $vmin := evalf\left(0.035 \cdot k^{\frac{3}{2}} \cdot fck^{\frac{1}{2}}\right)$;

$$vmin := 0.9391485502 \tag{18.6}$$

> $Vrdcmin := vmin \cdot bridge \cdot dridgeh$;

$$Vrdcmin := 51183.59599 \tag{18.7}$$

> $Vrdc := evalf\left(\left(Crdc \cdot k \cdot \left(100 \cdot \rho lridge \cdot fck\right)^{\frac{1}{3}}\right) \cdot bridge \cdot dridgeh\right)$;

$$Vrdc := 69407.09487 \tag{18.8}$$

> $Vrdcridge := \max(Vrdcmin, Vrdc)$;

$$Vrdcridge := 69407.09487 \tag{18.9}$$

> $UC := \frac{Ved}{Vrdcridge}$;

$$UC := 1.481989760 \tag{18.10}$$

> **if** $UC > 1$ **then** $print(Horizontal\ shear\ reinforcement\ necessary)$
> **else** $print(No\ horizontal\ shear\ reinforcement\ required)$ **end if**:

$$Horizontal\ shear\ reinforcement\ necessary \tag{18.11}$$

> **if** $UC > 1$ **then** $Ved := Fsh1$ **end if**;

$$Ved := 1.281349237\ 10^{5} \tag{18.12}$$

> $tausr := \frac{Ved}{bridge \cdot dridgeh}$; $Asrsreq := \frac{tausr \cdot bridge}{0.9 \cdot fyd} srebshear$; $Asshear := evalf\left(nshear \cdot \pi \cdot \left(\frac{\phi shear}{2}\right)^{2}\right)$;

$$tausr := 2.351099517$$
$$Asrsreq := 150.2091358$$
$$Asshear := 402.1238597 \tag{18.13}$$

> $Vrdsr := evalf\left(\frac{Asshear}{srebshear} \cdot zr \cdot (0.9 \cdot fyd) \cdot \cot\left(\left(\frac{compangle}{180}\right)\pi\right)\right)$;

$$Vrdsr := 1.557340943\ 10^{5} \tag{18.14}$$

> $Vrdsrmax := evalf\left(1 \cdot bridge \cdot zr \cdot \left(0.6 \cdot \left(1 - \frac{fck}{250}\right)\right) \cdot \left(\frac{fcd}{\cot\left(\left(\frac{compangle}{180}\right)\pi\right) + \tan\left(\left(\frac{compangle}{180}\right)\pi\right)}\right)\right)$;

$$Vrdsrmax := 4.444281125\ 10^{5} \tag{18.15}$$

> $Vrdsr := \min(Vrdsr, Vrdsrmax)$;

$$Vrdsr := 1.557340943\ 10^{5} \tag{18.16}$$

> $UC := \frac{Ved}{Vrdsr}$;

$$UC := 0.8227801643 \tag{18.17}$$

> $\rho w := \frac{Asshear}{srebshear \cdot bridge \cdot \sin(0.5\,\pi)} : \rho wmin := evalf\left(\frac{0.08 \cdot \mathrm{sqrt}(fck)}{fyk}\right)$:**if** $\rho w < \rho wmin$ **then** $print(Shear\ reinforcement\ ratio\ too\ low,\ increase\ area\ of\ shear\ reinforcement)$ **end if**;

> $slmax := 0.75 \cdot dridgeh\left(1 + \frac{\cos(0.5\,\pi)}{\sin(0.5\,\pi)}\right)$:**if** $srebshear > slmax$ **then** $print(Shear\ reinforcement\ spacing\ is\ too\ big)$ **end if**;

> $stmax := 0.75 \cdot dridgeh$;

$$stmax := 81.750 \tag{18.18}$$

Check vertical shear force in slab

> $dslab := hslab - cridge - 0.5 \cdot \phi topbig$;

$$dslab := 74.0 \tag{19.1}$$

> $\rho lridge := \frac{evalf\left(n1 \cdot \pi \cdot \left(\frac{\phi topbig}{2}\right)^{2}\right)}{bslab \cdot dslab}$;

$$\rho lridge := 0.009405183830 \tag{19.2}$$

> $Ved := Veds$;

$$Ved := 11378.400 \tag{19.3}$$

> $k := 1 + \sqrt{\frac{200}{dslab}}$:

> **if** $k \le 2$ **then** $k := k$ **else** $k := 2$ **end if**;

$$k := 2 \tag{19.4}$$

> $Crdc := \frac{0.18}{\gamma c}$: $vmin := evalf\left(0.035 \cdot k^{\frac{3}{2}} \cdot fck^{\frac{1}{2}}\right)$;

$$vmin := 0.9391485502 \tag{19.5}$$

> $Vrdcmin := vmin \cdot bslab \cdot dslab$;

$$Vrdcmin := 90346.09051 \tag{19.6}$$

> $Vrdc := evalf\left(\left(Crdc \cdot k \cdot (100 \cdot \rho lridge \cdot fck)^{\frac{1}{3}}\right) \cdot bslab \cdot dslab\right)$;

$$Vrdc := 1.013731433\ 10^{5} \tag{19.7}$$

> $Vrdc := \max(Vrdcmin, Vrdc)$;

$$Vrdc := 1.013731433\ 10^{5} \tag{19.8}$$

> $UC := \frac{Ved}{Vrdc}$;

$$UC := 0.1122427463 \quad (19.9)$$

Check detailing and element specific rules

>

> **if** $\min\left(\frac{fctm \cdot \frac{1}{6} \cdot bridge \cdot hslab^2}{fyd \cdot zsr}, 0.26 \cdot \frac{fctm}{fyk} \cdot bridge \cdot dsr\right) < Assr$
> **then** *print*(*Area of ridge reinforcement sufficient*)
> **else** *print*(*Area of ridge reinforcement should be increased*) **end if**;

Area of ridge reinforcement sufficient (20.1)

> **if** $\min\left(\frac{fctm \cdot \frac{1}{6} \cdot bslab \cdot hslab^2}{fyd \cdot zslab}, 0.26 \cdot \frac{fctm}{fyk} \cdot bslab \cdot dslab\right) < As$
> **then** *print*(*Area of slab reinforcement sufficient*)
> **else** *print*(*Area of slab reinforcement should be increased*) **end if**;

Area of slab reinforcement sufficient (20.2)

Crack width EC2 transition zone ridge and slab

Uses effective height. For long term kt=0.4 this method is verified with technosoft results.

> $xesr := dsr \cdot \left(-\alpha e \cdot \rho lsr + \sqrt{(\alpha e \cdot \rho lsr)^2 + 2\,\alpha e \cdot \rho lsr}\right)$;

$$xesr := 27.71883978 \quad (21.1)$$

> $xecross := dcross \cdot \left(-\alpha e \cdot \rho lcross + \sqrt{(\alpha e \cdot \rho lcross)^2 + 2\,\alpha e \cdot \rho lcross}\right)$;

$$xecross := 15.02783238 \quad (21.2)$$

> $wmax := 0.2$;

$$wmax := 0.2 \quad (21.3)$$

> $Mlin := fyd \cdot Assr \cdot \left(dsr - \frac{1}{3} xesr\right)$;

$$Mlin := 2.547557283\ 10^7 \quad (21.4)$$

> **if** $Mfcr \le Mlin$ **then** $z := dsr - \frac{1}{3} xers$ **else** $z := dsr - \beta xesr$ **end if**;

$$z := 74.0 - \frac{1}{3}\ xers \quad (21.5)$$

> $hceff := \min\left((hslab - dsr) \cdot 2.5, \frac{(hslab - xesr)}{3}\right)$;

$$hceff := 29.09372007 \quad (21.6)$$

> $hceffcross := \min\left((hslab - dcross) \cdot 2.5, \frac{(hslab - xecross)}{3}\right)$;

$$hceffcross := 33.32405587 \quad (21.7)$$

> **if** $hceff < cridge + 0.5 \cdot \phi topbig$
> **then** *print*(*Reinforcement isnt located wihtin hidden tensile member*) **end if**;

Reinforcement isnt located wihtin hidden tensile member (21.8)

> $\rho peff := \frac{Assr}{hceff \cdot bridge}$;

$$\rho peff := 0.06219752456 \quad (21.9)$$

> $\rho peffcross := \frac{Ascross}{hceffcross \cdot 1000}$;

$$\rho peffcross := 0.01508384293 \quad (21.10)$$

k1=0.8 for good bonding, k2=0.5 for pure bending, k3 en k4 follow from national annex. kt=0.6 because of short term loading.

> $k1 := 0.8 : k2 := 0.5 : k3 := 3.4 : k4 := 0.425 : kt := 0.6 :$

> $fcteff := fctm :$

> **if** $sreb \le (5 \cdot (hslab - dsr))$ **then** $srmaxx := k3 \cdot cridge + \frac{k1 \cdot k2 \cdot k4 \cdot \phi topbig}{\rho peff}$ **else** $srmaxx := 1.3(hslab - xesr)$ **end if**;

$$srmaxx := 151.7987330 \quad (21.11)$$

> **if** $srmaxx > \max((50 - 0.8\,fck) \cdot \phi topbig, 15 \cdot \phi topbig)$ **then** $srmaxx := \max((50 - 0.8\,fck) \cdot \phi topbig, 15 \cdot \phi topbig)$ **end if**;

> **if** $srebtopcross \le (5 \cdot (hslab - dcross))$ **then** $srmaxy := k3 \cdot cridge + \frac{k1 \cdot k2 \cdot k4 \cdot \phi topcross}{\rho peffcross}$ **else** $srmaxy := 1.3(hslab - xecross)$ **end if**;

$$srmaxy := 209.1626997 \quad (21.12)$$

> **if** $srmaxy > \max((50 - 0.8\,fck) \cdot \phi topcross, 15 \cdot \phi topcross)$ **then** $srmaxy := \max((50 - 0.8\,fck) \cdot \phi topcross, 15 \cdot \phi topcross)$ **end if**;

$$srmaxy := 120 \quad (21.13)$$

> $srmax := \frac{1}{\frac{\cos(0.5\,\pi)}{srmaxy} + \frac{\sin(0.5\,\pi)}{srmaxx}}$;

$$srmax := 151.7987331 \quad (21.14)$$

>

> $\sigma sr := \frac{fcteff}{\rho peff} \cdot (1 + \alpha e \cdot \rho peff) : \sigma s := \frac{Mfcr}{Assr \cdot zsr}$;

$$\sigma s := 169.1366841 \quad (21.15)$$

> $straindifference := \frac{(\sigma s - kt \cdot \sigma sr)}{Es}$; $minstraindifference := \left(0.6 \cdot \frac{\sigma s}{Es}\right)$;

$$straindifference := 0.0005326091815$$
$$minstraindifference := 0.0005074100523 \quad (21.16)$$

> **if** $straindifference \le minstraindifference$ **then** $straindifference := minstraindifference$ **end if**;

> $wk := straindifference \cdot srmax$;

$$wk := 0.08084939899 \quad (21.17)$$

> **if** $wk \le wmax$ **then** $print(Crack\ width\ is\ small\ enough)$ **else** $print(Crack\ width\ is\ too\ big)$ **end if**;

$$Crack\ width\ is\ small\ enough \quad (21.18)$$

>

Crack width EC2 ridge

Uses effective height. For long term kt=0.4 this method is verified with technosoft results.

> $xer := dr \cdot \left(-\alpha e \cdot \rho lr + \sqrt{(\alpha e \cdot \rho lr)^2 + 2\,\alpha e \cdot \rho lr} \right)$;

$$xer := 33.48022835 \qquad (22.1)$$

> $wmax := 0.3$;

$$wmax := 0.3 \qquad (22.2)$$

> $Mlin := fyd \cdot Asr \cdot \left(dr - \frac{1}{3} xer \right)$;

$$Mlin := 3.534141223\ 10^{7} \qquad (22.3)$$

> **if** $Mfcr \le Mlin$ **then** $zr := dr - \frac{1}{3} xer$ **else** $zr := dr - \beta xer$ **end if**;

$$zr := 89.83992388 \qquad (22.4)$$

> $hceff := \min\left((lridge - dr) \cdot 2.5, \frac{(lridge - xer)}{3} \right)$;

$$hceff := 33.83992388 \qquad (22.5)$$

> **if** $hceff < cother + 0.5 \cdot \phi topbig$
> **then** $print(Reinforcement\ isnt\ located\ wihtin\ hidden\ tensile\ member)$ **end if**;

> $\rho peff := \frac{Asr}{hceff \cdot bridge}$;

$$\rho peff := 0.05347403780 \qquad (22.6)$$

k1=0.8 for good bonding, k2=0.5 for pure bending, k3 en k4 follow from national annex. kt=0.6 because of short term loading.

> $k1 := 0.8 : k2 := 0.5 : k3 := 3.4 : k4 := 0.425 : kt := 0.6$:

> $fcteff := fctm$:

> **if** $sreb \le \left(5 \cdot \left(cother + \frac{\phi topbig}{2} \right) \right)$ **then** $srmax := k3 \cdot cother + \frac{k1 \cdot k2 \cdot k4 \cdot \phi topbig}{\rho peff}$
> **else** $srmax := 1.3\,(lridge - xer)$ **end if**;

$$srmax := 106.1493540 \qquad (22.7)$$

> **if** $srmax > \max\left((50 - 0.8\,fck) \cdot \phi topbig, 15 \cdot \phi topbig \right)$ **then** $srmax := \max\left((50 - 0.8\,fck) \cdot \phi topbig, 15 \cdot \phi topbig \right)$ **end if**;

> $\sigma sr := \frac{fcteff}{\rho peff} \cdot (1 + \alpha e \cdot \rho peff)$: $\sigma s := \frac{Mfcr}{Asr \cdot zr}$;

$$\sigma s := 124.3843834 \qquad (22.8)$$

> $straindifference := \frac{(\sigma s - kt \cdot \sigma sr)}{Es}$; $minstraindifference := \left(0.6 \cdot \frac{\sigma s}{Es} \right)$;

$$straindifference := 0.0002691114485$$
$$minstraindifference := 0.0003731531502 \qquad (22.9)$$

> **if** $straindifference \le minstraindifference$ **then** $straindifference := minstraindifference$ **end if**;

$$straindifference := 0.0003731531502 \qquad (22.10)$$

> $wk := straindifference \cdot srmax$;

$$wk := 0.03960996584 \qquad (22.11)$$

> **if** $wk \le wmax$ **then** $print(Crack\ width\ is\ small\ enough)$ **else** $print(Crack\ width\ is\ too\ big)$ **end**

if;

Crack width is small enough **(22.12)**

>

Stiffness determination ridge

> $\varphi := 0.9 : Einf := \frac{Ecm}{1+\varphi}; \alpha einf := \frac{Es}{Einf};$

$$Einf := 22947.36842$$

$$\alpha einf := 8.715596331 \quad \textbf{(23.1)}$$

> $xeinfsr := dsr \cdot \left(-\alpha einf \cdot \rho lsr + \sqrt{(\alpha einf \cdot \rho lsr)^2 + 2\,\alpha einf \cdot \rho lsr} \right);$

$$xeinfsr := 35.05085932 \quad \textbf{(23.2)}$$

> $Icsr := \frac{1}{12} \cdot bridge \cdot hslab^3;$

$$Icsr := \frac{190109375}{3} \quad \textbf{(23.3)}$$

> $EI0sr := evalf(Icsr \cdot Ecm);$

$$EI0sr := 2.762922917\ 10^{12} \quad \textbf{(23.4)}$$

> $\delta i0sr := \frac{1+3\cdot\alpha e\cdot\rho lsr}{1+\alpha e\cdot\rho lsr} : \delta iinfsr := \frac{1}{1+\varphi} \cdot \frac{1+3\cdot\alpha e\cdot\rho lsr}{1+\alpha e\cdot\rho lsr} :$

> $\delta ii0sr := \left(6 \cdot \left(\frac{dsr}{hslab}\right)^3 \left(\frac{xesr}{dsr}\right)^2 \left(1 - \frac{1}{3}\frac{xesr}{dsr}\right)\right) : \delta iiinfsr := \frac{1}{1+\varphi} \cdot \left(6 \cdot \left(\frac{dsr}{hslab}\right)^3 \left(\frac{xeinfsr}{dsr}\right)^2 \left(1 - \frac{1}{3}\frac{xeinfsr}{dsr}\right)\right) :$

>

Determine loading ratios:

> $\lambda := \frac{Mqbr}{Mfcr}; \mu 2 := \frac{Mcrsr}{Mqbr}; \mu 3 := \frac{Mcrsr}{Mfcr};$

$$\lambda := 0.8442231330$$

$$\mu 2 := 0.6520350938$$

$$\mu 3 := 0.5504631097 \quad \textbf{(23.5)}$$

> **if** $\mu 2 > 1$ **and** $\mu 3 > 1$ **then** *print*(*Cross section isnt always cracked*) **end if**;

> **if** $\mu 2 < 1$ **and** $\mu 3 > 1$
then *print*(*Cross section isnt always cracked with quasi static load combination*) **end if**;

> **if** $\mu 2 < 1$ **and** $\mu 3 < 1$ **then** *print*(*Cross section is always cracked*) **end if**;

Cross section is always cracked **(23.6)**

> $\delta csstarsr := \frac{\delta i0sr \cdot \delta ii0sr}{\mu 3^2 \cdot \delta ii0sr + (1-\mu 3^2) \cdot \delta i0sr} : \delta csstarstarsr := \frac{\delta iinfsr \cdot \delta iiinfsr}{\mu 2^2 \cdot \delta iiinfsr + \left(1 - \frac{1}{2}\,\mu 2^2\right) \cdot \delta iinfsr} :$

> $\delta cssr := \frac{\delta csstarsr \cdot \delta csstarstarsr}{\lambda \cdot \delta csstarsr + (1-\lambda) \cdot \delta csstarstarsr}$: $EIfsr := \delta cssr \cdot EI0sr$;

$$EIfsr := 7.219664006\ 10^{11} \quad (23.7)$$

>

Stiffness determination slab

> $xeslab := dslab \cdot \left(-\alpha e \cdot \rho l + \sqrt{(\alpha e \cdot \rho l)^2 + 2\ \alpha e \cdot \rho l} \right)$:

> $xeinfslab := dslab \cdot \left(-\alpha einf \cdot \rho l + \sqrt{(\alpha einf \cdot \rho l)^2 + 2\ \alpha einf \cdot \rho l} \right)$:

> $Ic := \frac{1}{12} \cdot bslab \cdot hslab^3$;

$$Ic := \frac{494284375}{3} \quad (24.1)$$

> $EI0 := evalf(Ic \cdot Ecm)$;

$$EI0 := 7.183599583\ 10^{12} \quad (24.2)$$

> $\delta i0 := \frac{1+3\cdot\alpha e\cdot\rho l}{1+\alpha e\cdot\rho l}$: $\delta iinf := \frac{1}{1+\varphi} \cdot \frac{1+3\cdot\alpha e\cdot\rho l}{1+\alpha e\cdot\rho l}$:

> $\delta ii0 := \left(6 \cdot \left(\frac{dslab}{h}\right)^3 \left(\frac{xeslab}{dslab}\right)^2 \left(1 - \frac{1}{3}\frac{xeslab}{dslab}\right)\right)$: $\delta iiinf := \frac{1}{1+\varphi} \cdot \left(6 \cdot \left(\frac{dslab}{h}\right)^3 \left(\frac{xeinfslab}{dslab}\right)^2 \left(1 - \frac{1}{3}\frac{xeinfslab}{dslab}\right)\right)$:

Determine loading ratios:

>

> $\lambda := \frac{Mqbs}{Mfcs}$; $\mu 2 := \frac{Mcrs}{Mqbs}$; $\mu 3 := \frac{Mcrs}{Mfcs}$;

$$\lambda := 0.8378203049$$
$$\mu 2 := 1.945191069$$
$$\mu 3 := 1.629720575 \quad (24.3)$$

> $\delta cs := \frac{\delta i0 \cdot \delta iinf}{\lambda \cdot \delta i0 + (1-\lambda)\,\delta iinf}$: $EIfslab := \delta cs \cdot EI0$;

$$EIfslab := 4.579751032\ 10^{12} \quad (24.4)$$

>

Eigen frequency

For the determination of the eigen frequency the characteristic load combination is applied since this load combination determines to which extend the member is cracked.

> $Feq := evalf\left(\frac{1}{4} \cdot G \cdot lslab + \left(\frac{ltot - 100}{ltot}\right)^3 \cdot Q + g\right)$;

$$Feq := 5081.816920 \quad (25.1)$$

> $wr := \frac{Feq \cdot lridge^3}{3 \cdot EIfsr} + \frac{Feq \cdot lslab \cdot lridge^2}{2 \cdot EIfsr}$; $\varphi r := \frac{Feq \cdot lridge^2}{2 \cdot EIfsr} + \frac{Feq \cdot lslab \cdot lridge}{EIfsr}$;

$$wr := 0.09813659843$$
$$\varphi r := 0.001432495010 \quad (25.2)$$

> $ws := wr + \varphi r \cdot lslab + \frac{Feq \cdot lslab^3}{3 \cdot EIfslab};$

$$ws := 3.265372565 \quad (25.3)$$

> $k := \frac{Feq}{ws}; m := \frac{Feq}{10};$

$$k := 1556.274765$$
$$m := 508.1816920 \quad (25.4)$$

> $\omega n := \sqrt{\frac{k \cdot 10^3}{m}};$

$$\omega n := 55.33929604 \quad (25.5)$$

> $f := \frac{\omega n}{2\,\pi};$

$$f := 8.807522510 \quad (25.6)$$

> **if** $f \geq 5$ **then** $print(Eigen\,frequency\,is\,OK)$ **else** $print(Eigen\,frequency\,is\,too\,low)$ **end if**;

Eigen frequency is OK (25.7)

>

Deflection

Deflection at t=∞, creep coefficient equals about 0.9. For this calculation the deflection and rotation of the structure behind the ridge and the connection is neglected. In reality this contributes significantly to the total deflection.

> **if** $\frac{Mqbr}{Mcrsr} > 1$ **and** $\frac{Mkr}{Mcrsr} > 1$ **then** $print(Always\,cracked)$ **end if**;

Always cracked (26.1)

> $qr := bridge \cdot hridge \cdot G : qs := bslab \cdot hslab \cdot G : Fs := 0.3 \cdot Q + g + qs \cdot lslab : Ms := 0.5 \cdot qs \cdot lslab^2 + 0.3 \cdot Q \cdot (lslab - 100) + g \cdot lslab :$

> $wr := \frac{qr \cdot lridge^4}{8 \cdot EIfsr} + \frac{Fs \cdot lridge^3}{3 \cdot EIfsr} + \frac{Ms \cdot lridge^2}{2 \cdot EIfsr}; \varphi r := \frac{qr \cdot lridge^3}{6 \cdot EIfsr} + \frac{Fs \cdot lridge^2}{2 \cdot EIfsr} + \frac{Ms \cdot lridge}{EIfsr};$

$$wr := 0.1011523244$$
$$\varphi r := 0.001464378304 \quad (26.2)$$

> $ws := wr + \varphi r \cdot lslab + \frac{qs \cdot lslab^4}{8 \cdot EIfslab} + \frac{g \cdot lslab^3}{3 \cdot EIfslab} + \frac{Q \cdot lslab^3}{3 \cdot EIfslab} - \frac{(Q \cdot 100) \cdot lslab^2}{2 \cdot EIfslab};$

$$ws := 3.833854869 \quad (26.3)$$

> $lrep := 2\,ltot;$

$$lrep := 3150 \quad (26.4)$$

> $UC := \frac{ws}{0.004 \cdot lrep};$

$$UC := 0.3042741960 \quad (26.5)$$

>

Anchorage of main reinforcement

Under the assumption bonding will be good

> $\eta 1 := 1 : \eta 2 := 1 : fctd := \frac{3.1}{\gamma c} :$

> $fbd := 2.25 \cdot \eta 1 \cdot \eta 2 \cdot fctd; Nsstm := 273.7 \cdot 10^3 :$

$$fbd := 4.650000001 \quad \textbf{(27.1)}$$

> $lbreq := \frac{\phi topbig}{4} \cdot \left(\frac{Nsstm}{Asr \cdot fbd} \right);$

$$lbreq := 195.1644620 \quad \textbf{(27.2)}$$

>

K

Normal forces strut-and-tie model

For the ridge and the beginning of the slab the strut-and-tie model in figure K.1 has been developed. During the determination of the normal forces the model has been supported fictitiously at the intersection of bars 9-10 and 10-11. At the intersection of 9-10 only horizontal movement is restrained, at 10-11 both vertical and horizontal movement is restrained.

The point loads in the model represent the actual supporting force. The two horizontal forces have a magnitude of 128 kN and the vertical force is 12 kN.

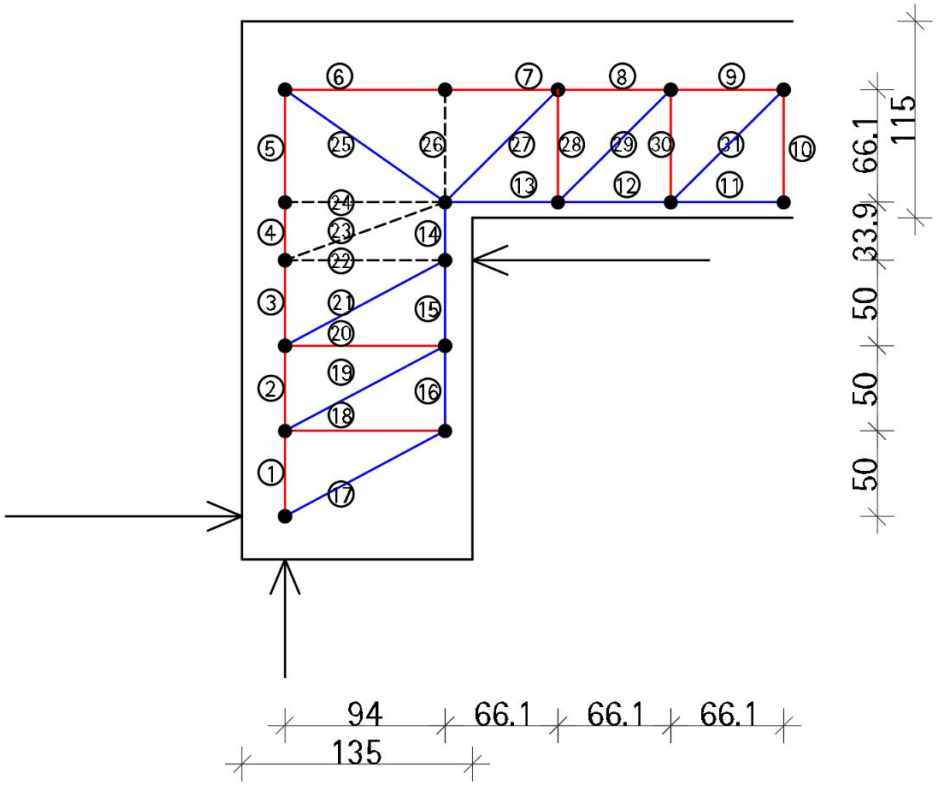

Figure K.1: Strut-and-tie model for ridge and slab with bar numbers.

Bar	Force type	Force magnitude [kN]	Bar	Force type	Force magnitude [kN]
S1	T	56.2	S17	C	-145.1
S2	T	124.3	S18	T	128.1
S3	T	192.5	S19	C	-145.1
S4	T	192.5	S20	T	128.1
S5	T	192.5	S21	C	-145.1
S6	T	273.7	S22	-	0
S7	T	273.7	S23	-	0
S8	T	261.7	S24	-	0
S9	T	249.7	S25	C	-334.6
S10	T	12	S26	-	0
S11	C	-237.7	S27	C	-17
S12	C	-249.7	S28	T	12
S13	C	-261.7	S29	C	-17
S14	C	-204.5	S30	T	12
S15	C	-136.3	S31	C	-17
S16	C	-68.2			

Table K.1: Normal forces in strut-and-tie model.

Force	Working force [kN]	Capacity [kN]	UC [-]
Horizontal tensile force slab Bars 6, 7	273	394	0.7
Vertical shear force slab Bars 10, 28, 30	12	53.6	0.22
Horizontal shear force ridge Bars 18, 20	155.7	128	0.82

Table K.2: Design checks tensile forces in reinforcement resulting from strut-and-tie model.

Final design result balcony with out-of-plane ridge

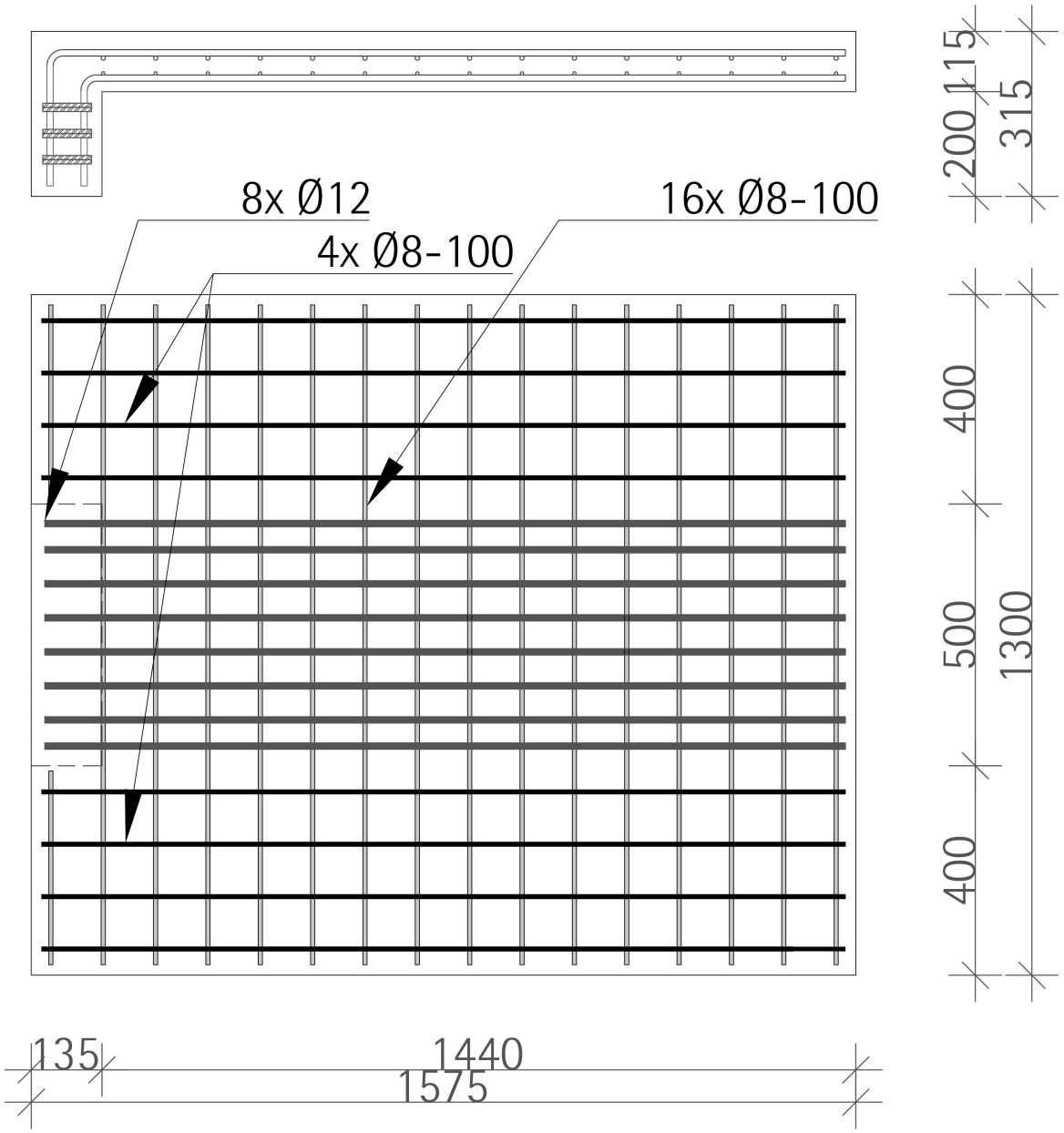

Figure L.1: Top reinforcement configuration and side view of final design remake Hi-Con balcony.

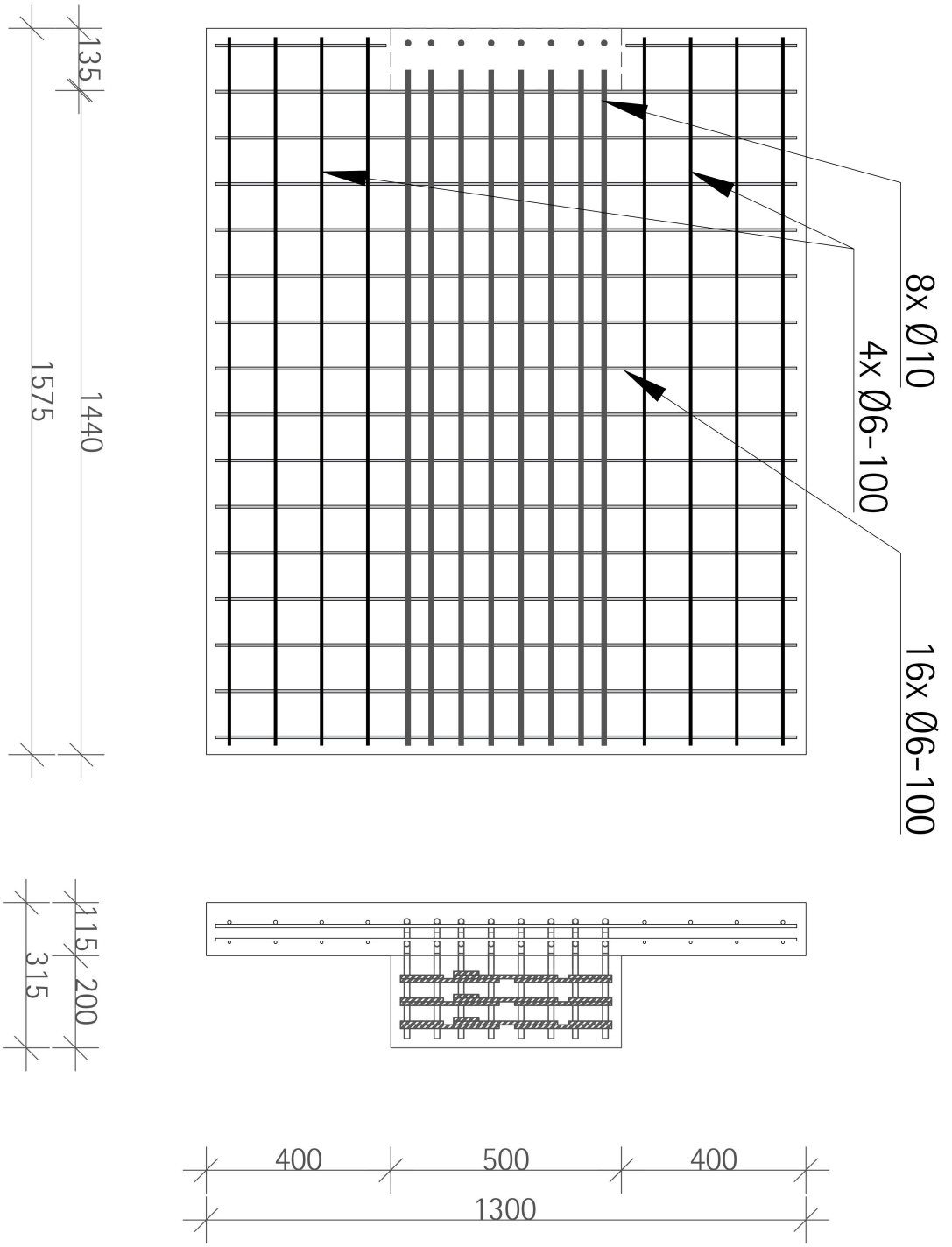

Figure L.2: Bottom reinforcement configuration and front view of final design remake Hi-Con balcony.

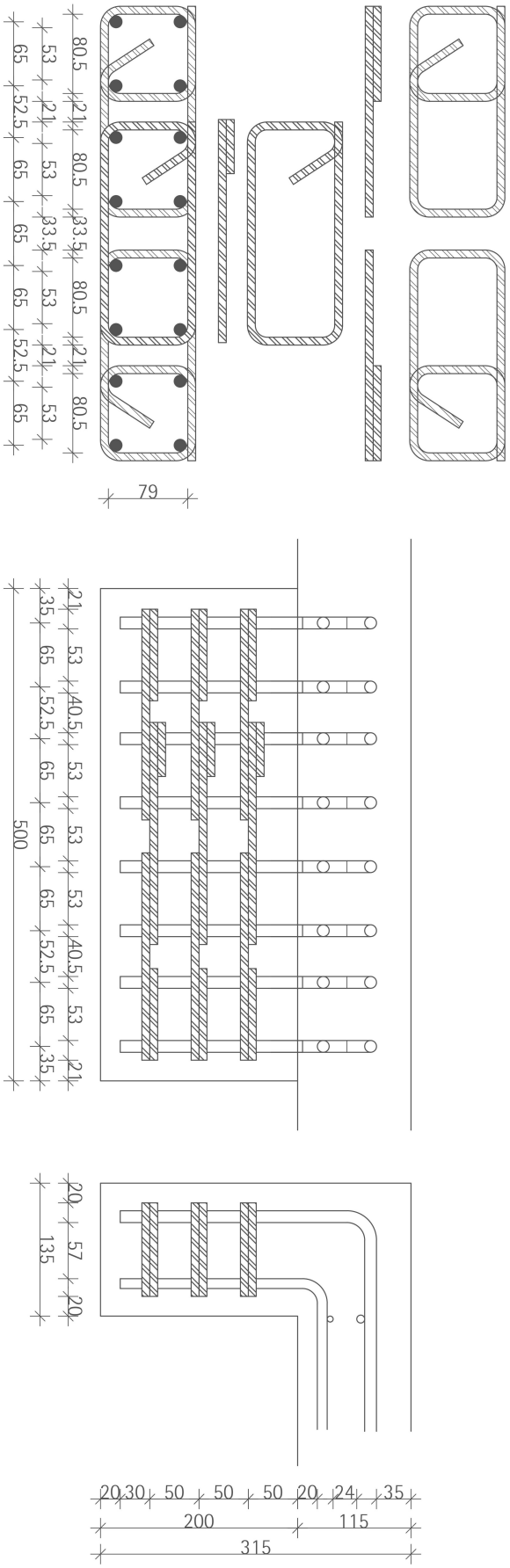

Figure L.3: Lay-out shear reinforcement.

M

Results finite element analysis balcony with out-of-plane ridge

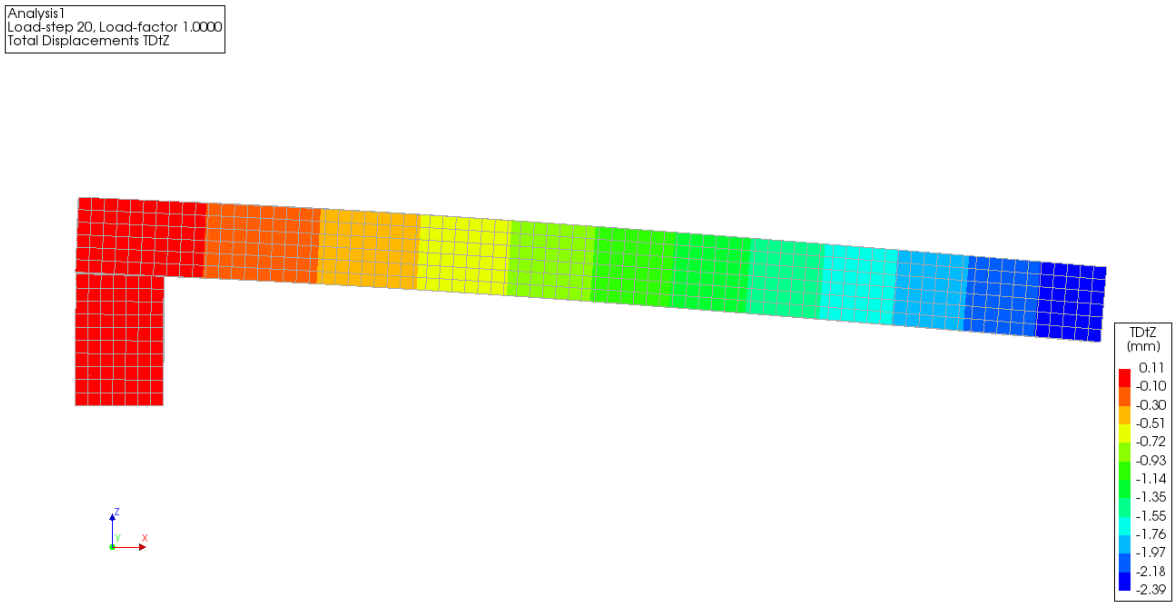

Figure M.1: Deformation of balcony with out-of-plane ridge resulting from frequent load combination after characteristic load combination has occurred.

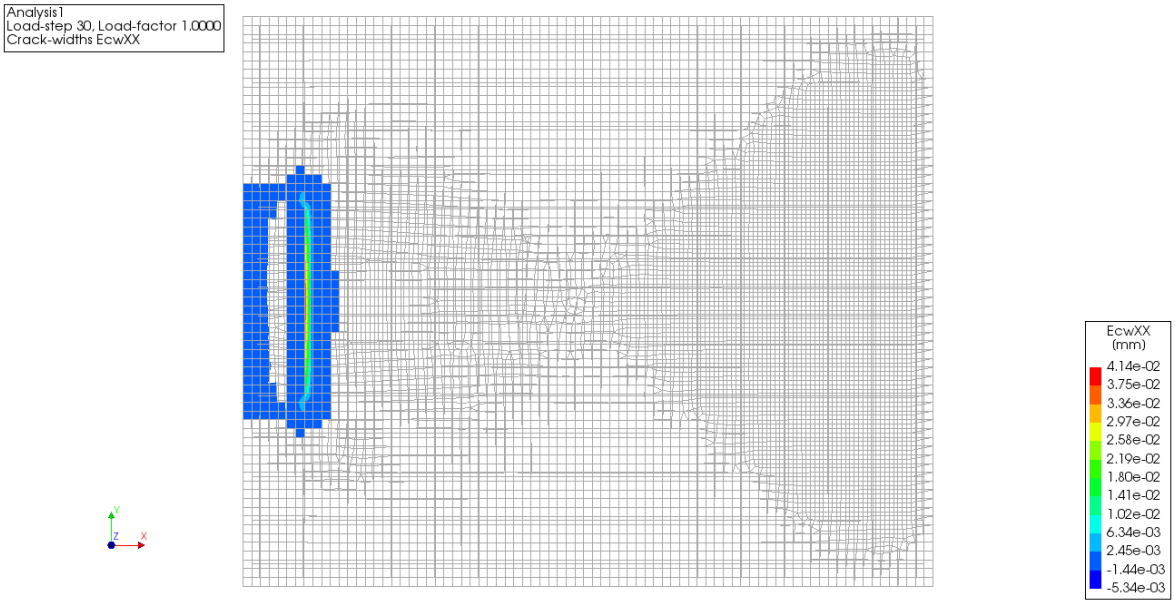

Figure M.2: Crack width in x-direction from frequent load combination after characteristic load combination has occurred.

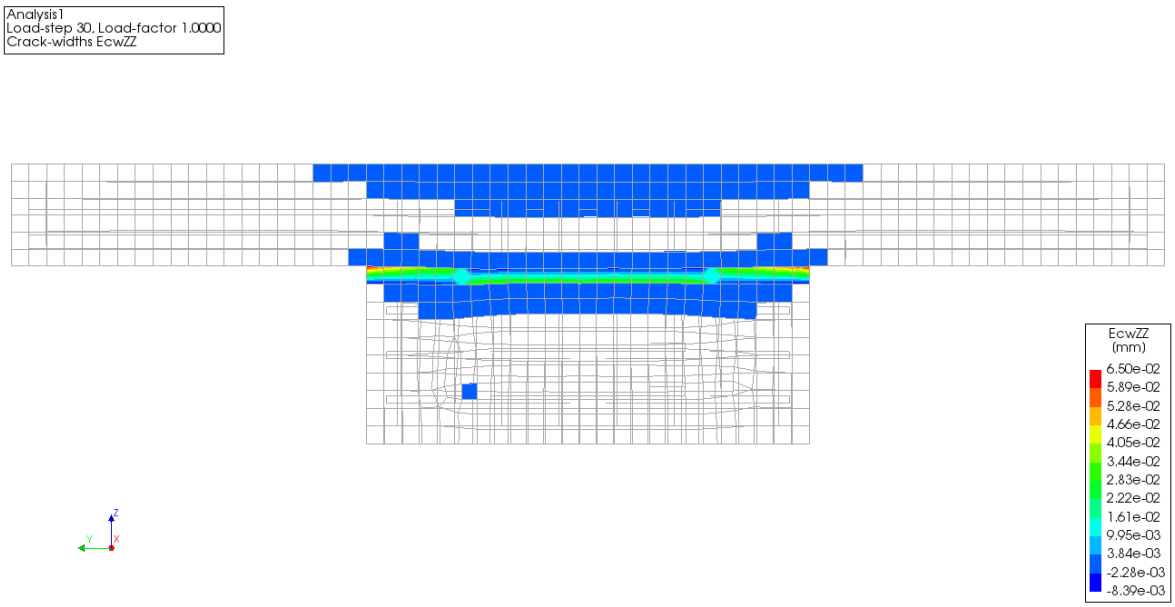

Figure M.3: Crack width in z-direction from frequent load combination after characteristic load combination has occurred.

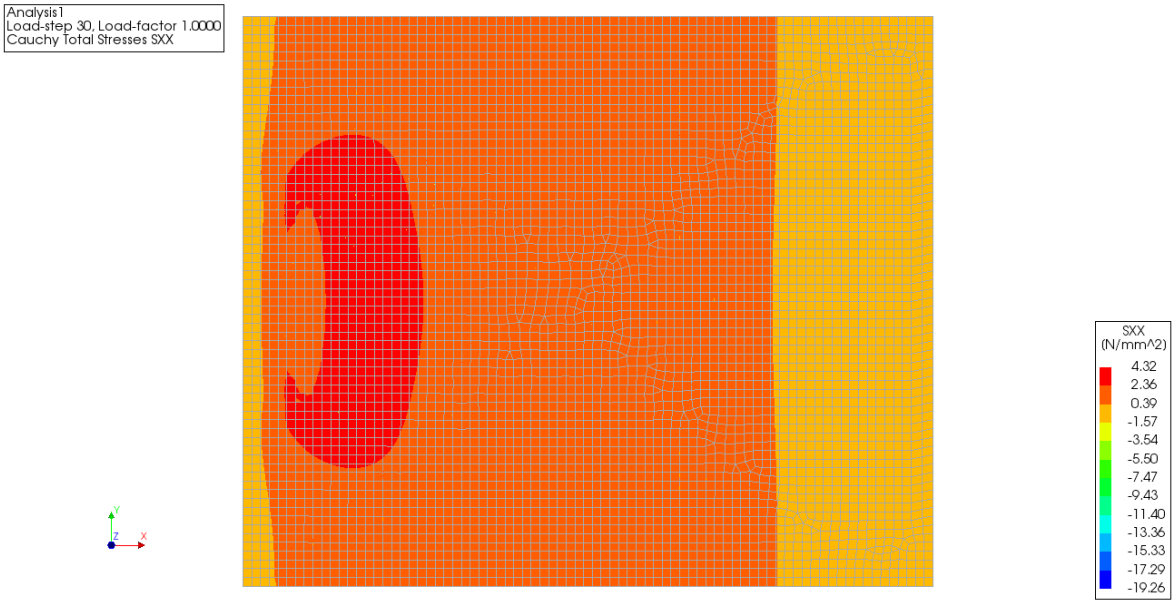

Figure M.4: Stresses in concrete in x-direction from frequent load combination after characteristic load combination has occurred.

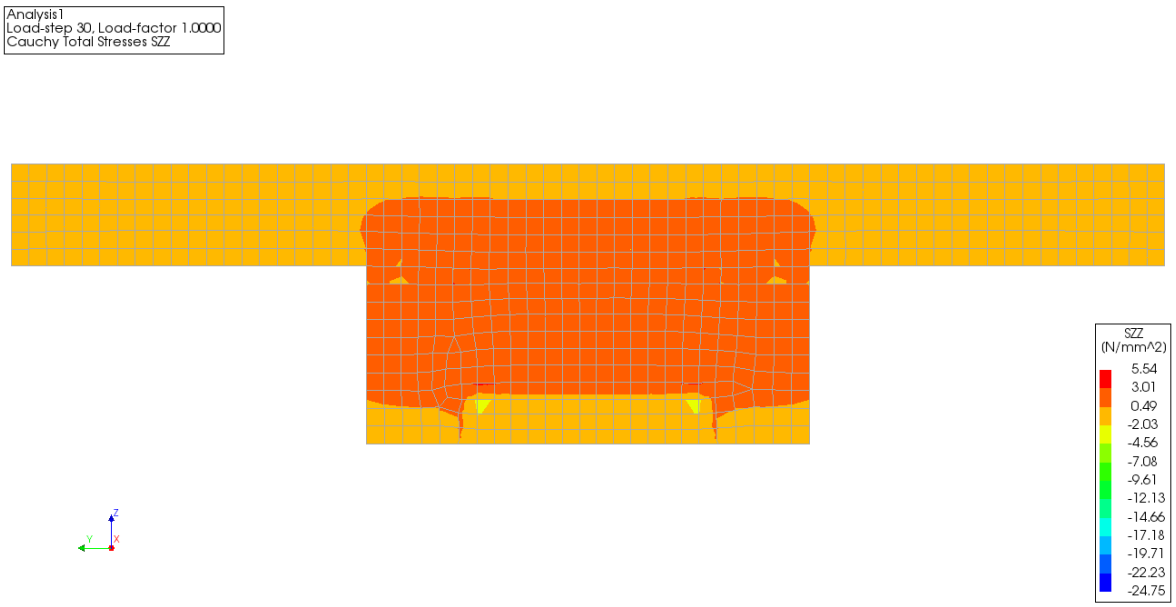

Figure M.5: Stresses in concrete in z-direction from frequent load combination after characteristic load combination has occurred.

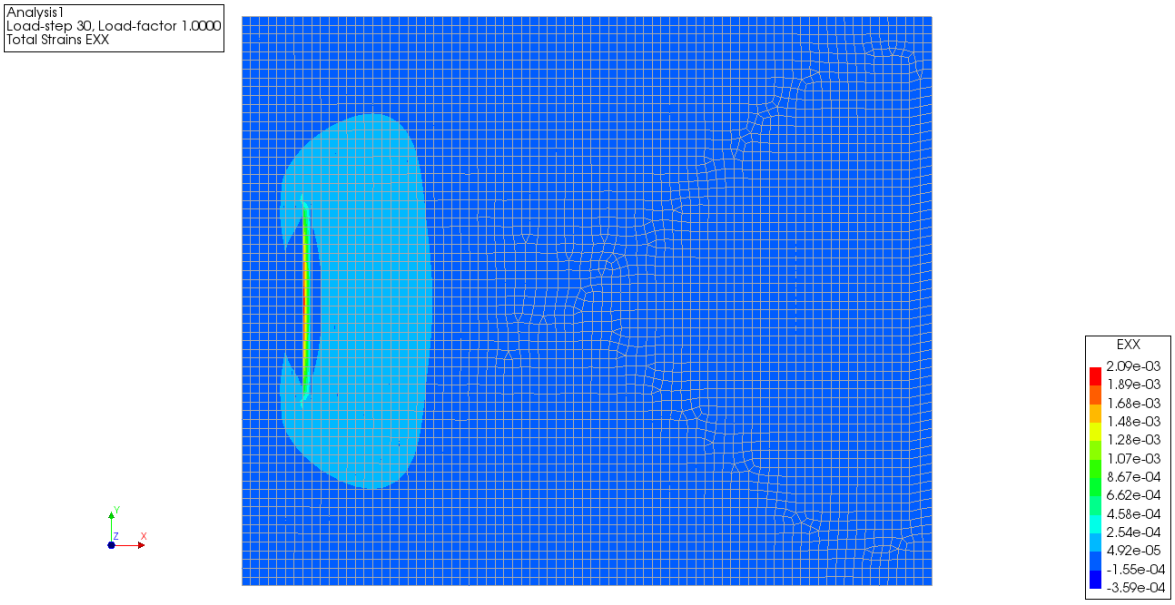

Figure M.6: Strains in concrete in x-direction from frequent load combination after characteristic load combination has occurred.

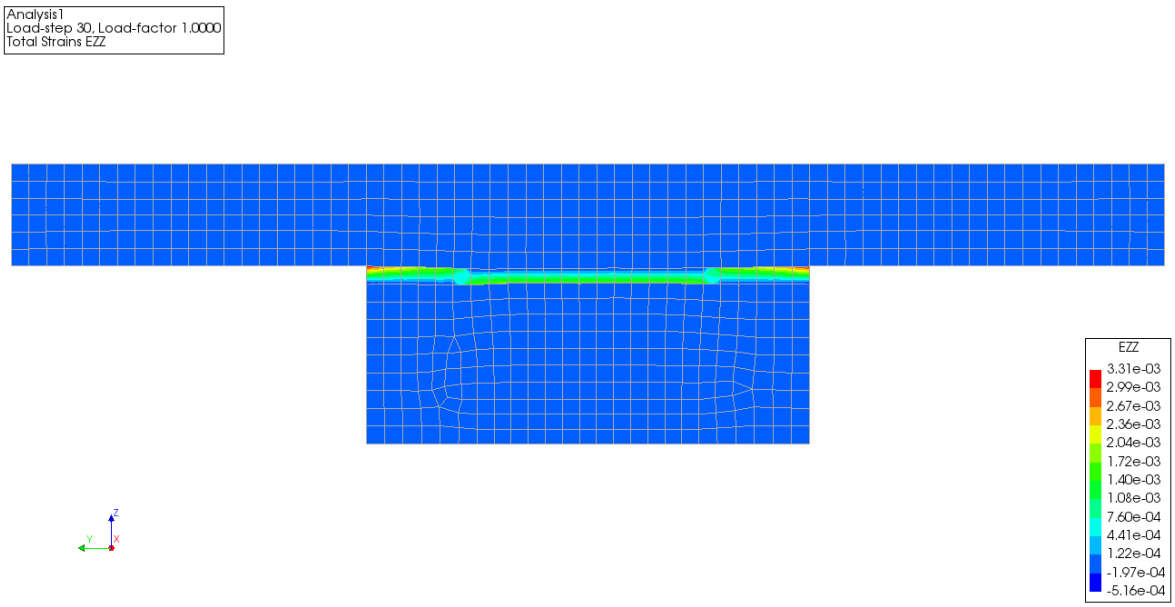

Figure M.7: Strains in concrete in z-direction from frequent load combination after characteristic load combination has occurred.

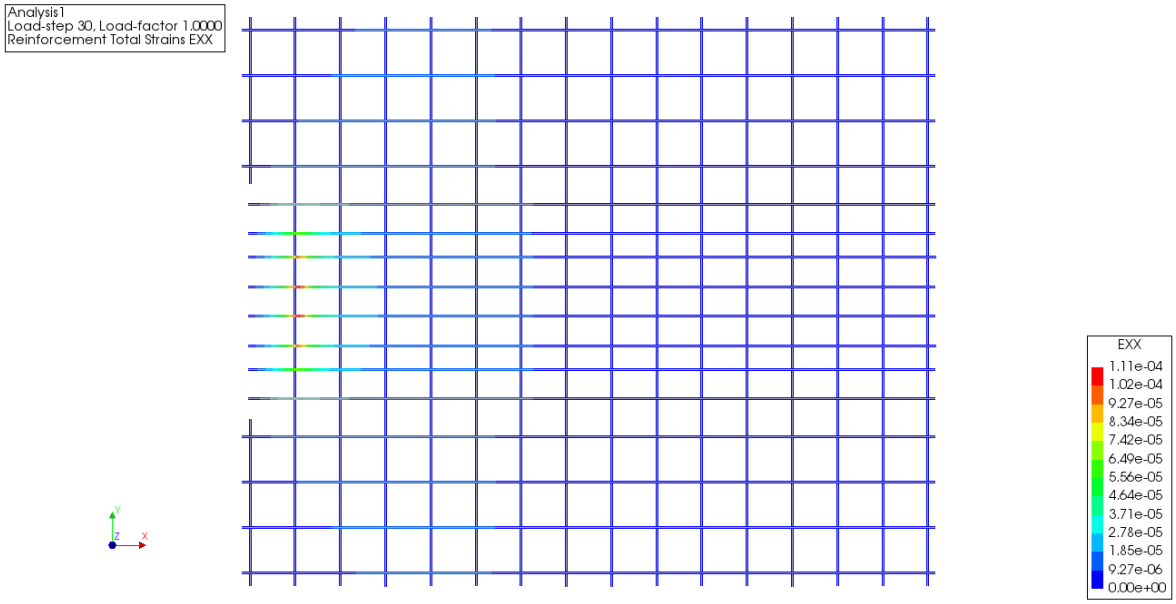

Figure M.8: Reinforcement strain in x-direction from frequent load combination after characteristic load combination has occurred.

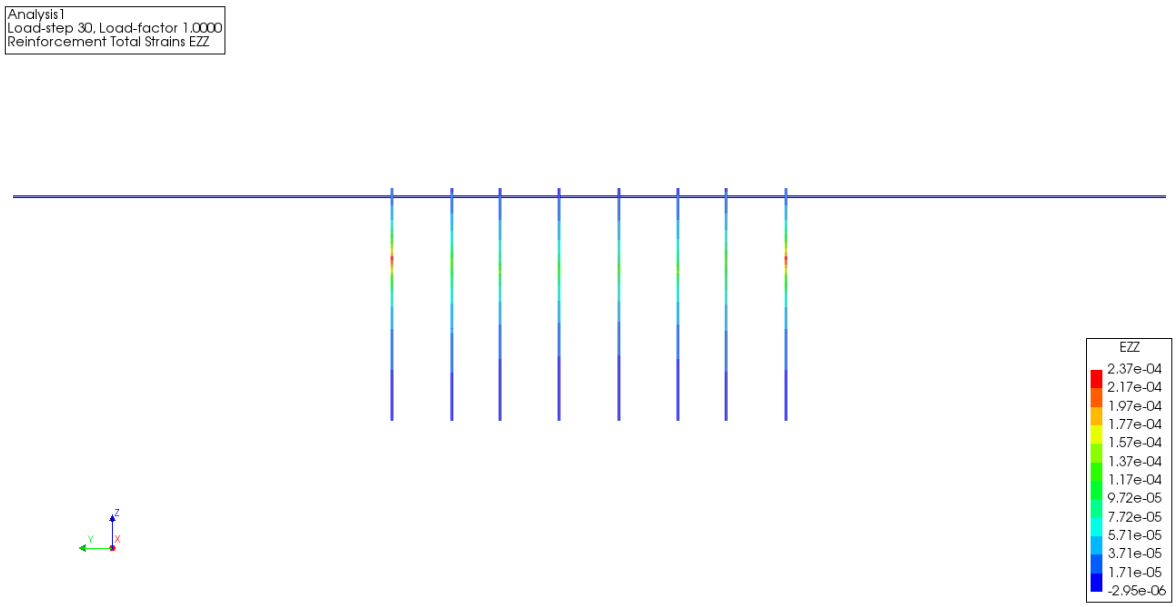

Figure M.9: Reinforcement strain in z-direction from frequent load combination after characteristic load combination has occurred.

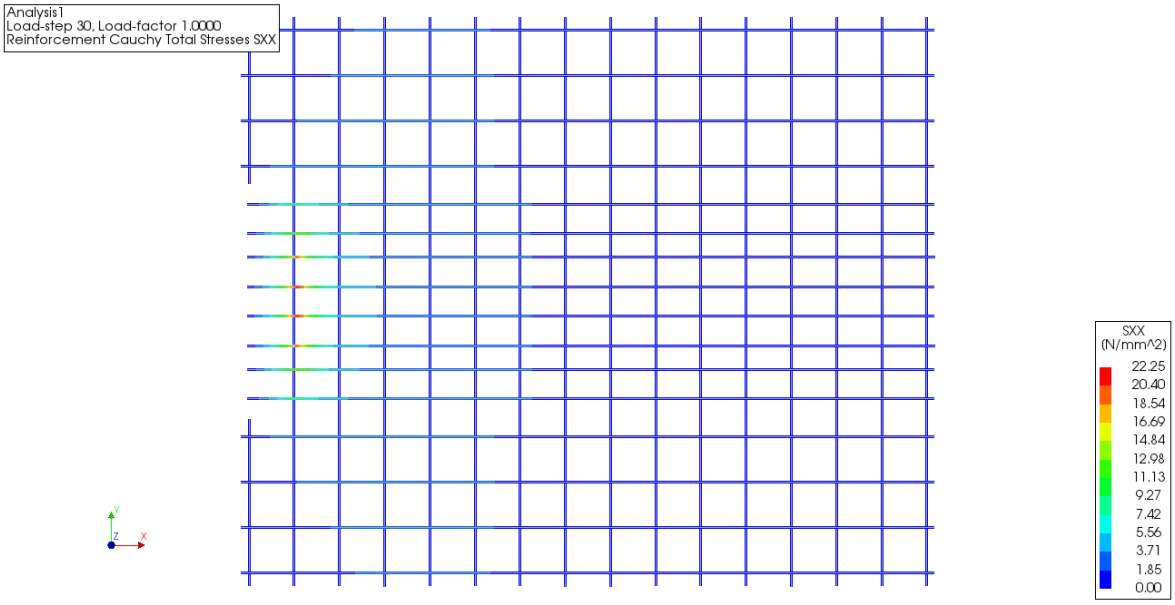

Figure M.10: Reinforcement stress in x-direction from frequent load combination after characteristic load combination has occurred.

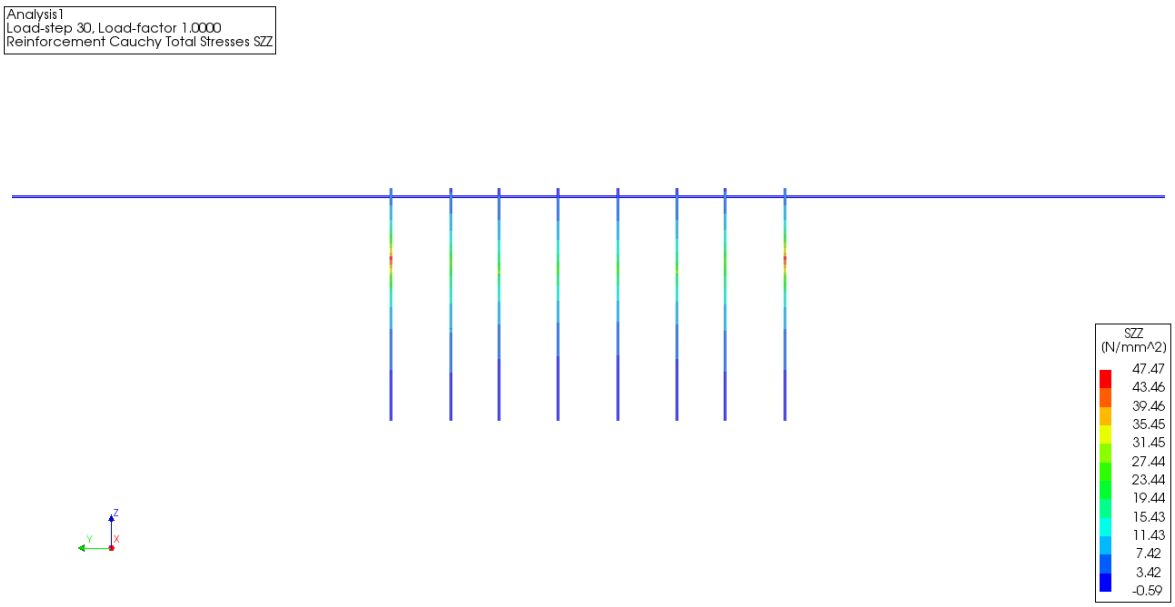

Figure M.11: Reinforcement stress in z-direction from frequent load combination after characteristic load combination has occurred.

N

Comparison of numerical results part III and IV

Two important differences occur in the numerical results of the balcony with an in-plane ridge and the one with the out-of-plane ridge. The crack width at the peak stress concentrations near the geometric disturbance are smaller in part IV compared to part III and contrary to part III no peak stress concentrations occur in the topside slab of the balcony from part IV.

Difference in peak stress concentrations in ridges

On the ridge in part IV a moment with a more or less similar magnitude is working as is on the ridge in part III. However, crack widths and steel stresses both in the middle of the ridge and at the location of the geometric disturbance are smaller.

The smaller crack widths and steel stresses in the out-of-plane ridge can be attributed to the following points:

- The eccentric normal compressive supporting force following from the shear force reduces, although marginally (substantiated in appendix N), the tensional stresses in the outer fibre of the ridge in part IV.
- The height of the ridge in part IV to take up the bending moment (135 mm) is bigger than the height of the ridge in part III (110 mm), resulting in a bigger internal lever arm.
- The concrete cover in the ridge in part IV equals 20 mm and the ridge in part III possesses a concrete cover of 35 mm, resulting in an increase of the internal lever arm.

The last two points are substantiated by the analysis results presented in figure N.1. For this analysis the out-of-plane ridge is reduced to a width of 100 mm (instead of 135 mm) and the concrete cover is increased to 35 mm to result in a similar cross section as the balcony with the in-plane ridge. Detailing rules for the shear reinforcement are neglected for this analysis. The higher amount of reinforcement for figure N.1 results in a smaller strain to reach equilibrium with the bending moment. The difference in peak strain between figure 12.7 and figure N.1 is thus induced by different reinforcement bars (in figure 12.7 10⌀10, in figure N.1 ⌀Ø12).

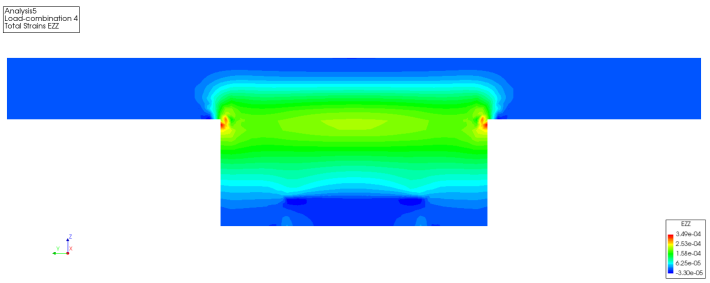

Figure N.1: Strain in z-direction at the backside of the slab and ridge for the ridge with a length of 100 mm (instead of 135 mm) following from linear analysis.

Absence of peak stress concentrations in slab part IV

In figure N.3 it is observed that in the slab of part IV no tensile peak stress concentrations occur, despite the fact that the slab is connected only locally. From the difference with the strain distribution in part III, figure N.4, the hypothesis emerged that the peak stress concentrations do not occur because the width of the slab on the top of the slab in the tensile region is undisturbed. This hypothesis is tested by linearly analysing the slab shape from part III with the out-of-plane ridge from part IV. The result is presented in figure N.5. It is observed that here the peak stress concentrations do occur, confirming the hypothesis. It can thus be concluded that the peak stresses are induced by a geometric disturbance of an area loaded in tension. The more slender the cross sections suffering from this effect become, the more pronounced the effect is.

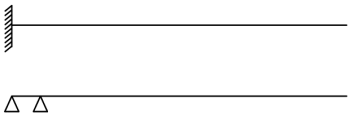

Figure N.2: Visualization of supports of slabs. Top figure: slab in part III. Bottom figure: slab in part IV.

The reason that the strains are smaller in figure N.5 compared to figure N.4, can be contributed to the fact that the maximum moment is smaller because of the ridge and its supports, see figure N.2. Furthermore, the slab in figure N.5 is 5 mm higher, and contains more reinforcement.

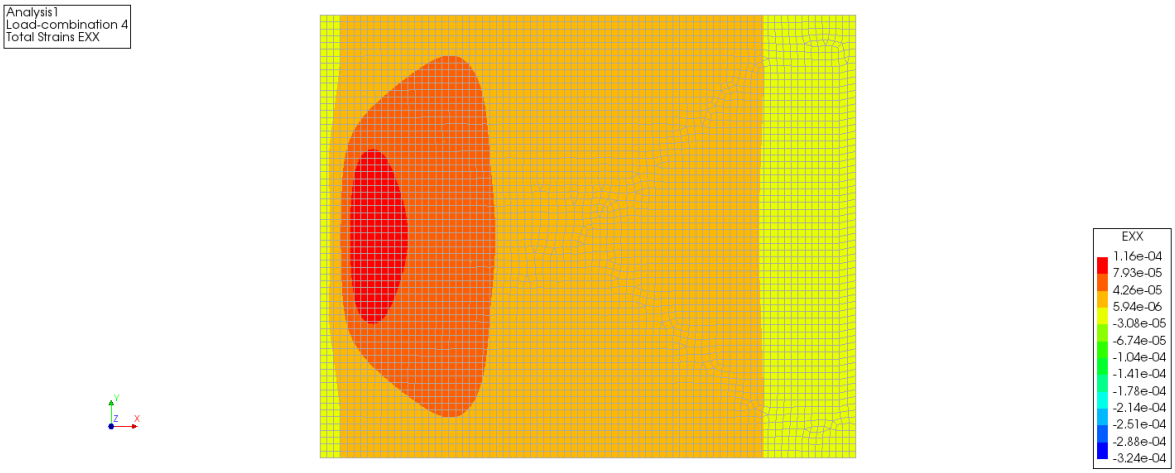

Figure N.3: Strain in x-direction of slab with out-of-plane ridge following from linear analysis.

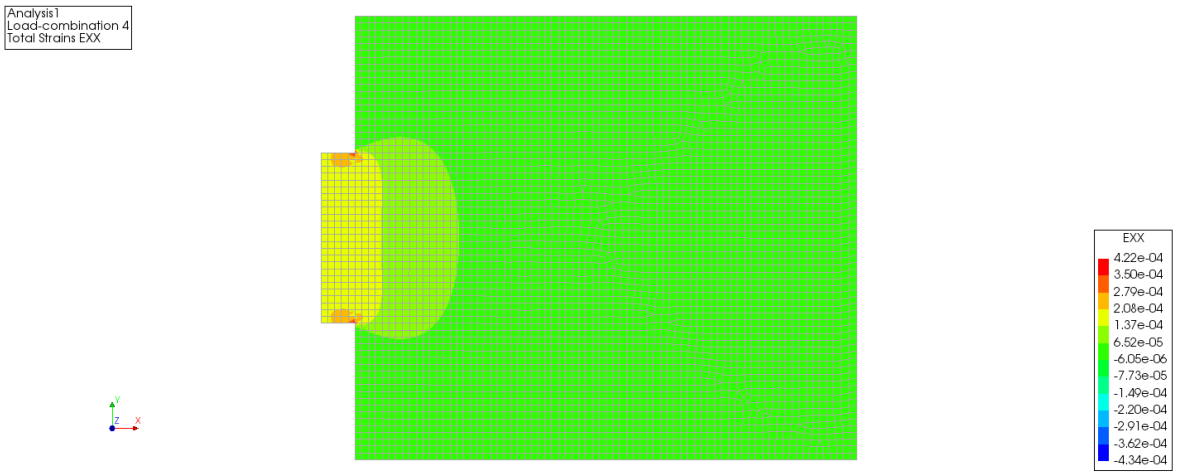

Figure N.4: Strain in x-direction of slab with in-plane ridge following from linear analysis.

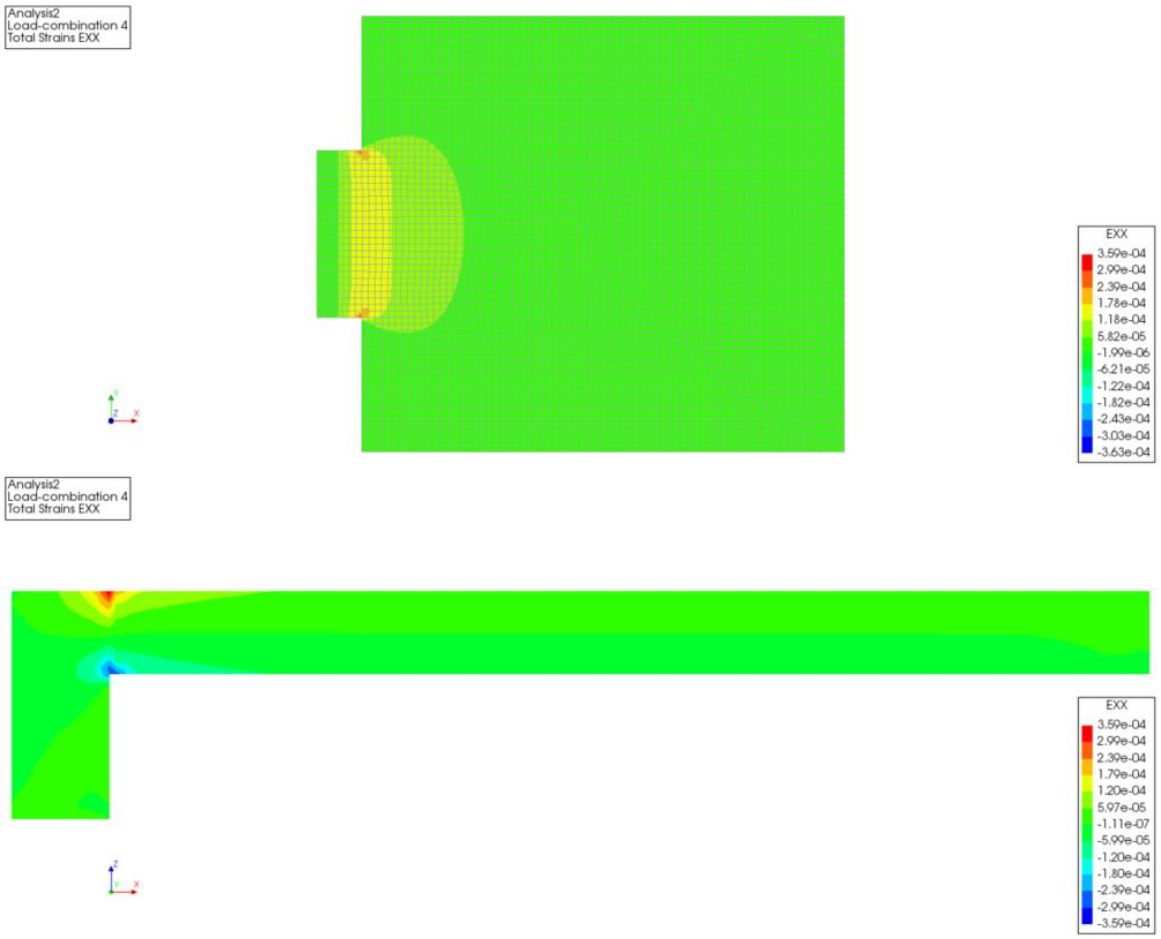

Figure N.5: Strain in x-direction of modified slab with out-of-plane ridge following from linear analysis. Top figure gives a top view of the slab whereas the bottom figure displays a longitudinal cross section.

Analytical reduction of stress in ridge part IV

In this appendix the statement that the tensile stress at the backside of the slab is reduced because of the eccentric vertical support force, made in the first paragraph of this appendix is substantiated.

Under the assumption of full linear behaviour with the help of the schematization in figure N.6:

$$F_{h,fc} = 58.4kN \qquad F_{v,fc} = 8.725kN \tag{N.1}$$

Stress at point A:

$$\sigma = \frac{F_{h,fc} * 10^3 * 150}{W_c} - \frac{F_{v,fc} * 10^3}{A_c} - \frac{F_{v,fc} * 10^3 * 42.5}{W_c} \tag{N.2}$$

$$= \frac{58.4*10^3*150}{1/6*500*135^2} - \frac{8.725*10^3}{500*135} - \frac{8.725*10^3*42.5}{1/*500*135^3} = 5.77 - 0.13 - 0.25 = 5.39N/mm^2$$

It appears that a reduction of tensile stress in the outer fibre of (5.77-5.39)/5.77*100 = 6.5% is induced by the eccentric vertical support.

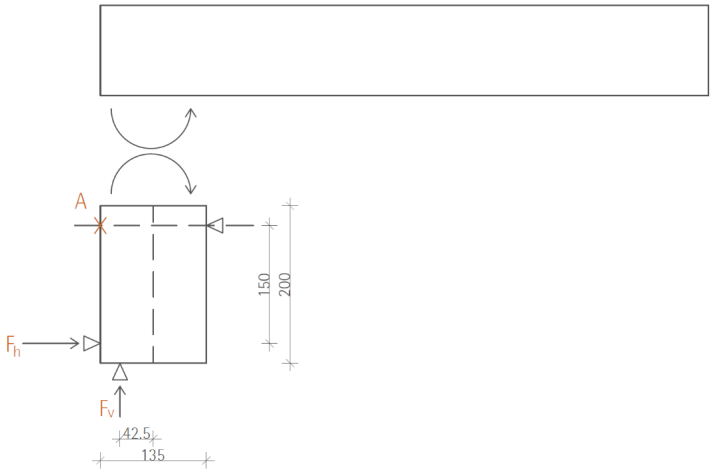

Figure N.6: Schematization of moment working on ridge. Maximum bending moment in ridge occurs at location A.

0

List of parameters used in scripts

This appendix presents the parameters used in the scripts and gives their actual definition/meaning.

Maple Parameter	Definition
ε_{c3}	Ultimate linear concrete strain
ε_{cu3}	Ultimate concrete strain
ϕ_r	Rotation of ridge
As	Reinforcement area in slab
Ascross	Reinforcement area in slab in cross direction
Asr	Reinforcement area in ridge, horizontally seen
Asrsreq	Requirend shear reinforcement area in transition zone ridge to slab
Asshear	Shear reinforcement area
Assr	Reinforcement area in transition zone ridge to slab
av	Parameter for console analogy
bridge	Width of ridge
bslab	Width of slab
compangle	Angle between compressive diagonal and tensile tie in strut-and-tie model
cother	Required minimum concrete cover on sides other than top side
Crdc	Parameter for determining shear resistance
cridge	Required minimum concrete cover in top of ridge
cslab	Required minimum concrete cover in top of slab
dconsole	Reinforcement height in console analogy
dcross	Reinforcement height in slab in cross direction
dr	Reinforcement height in ridge, horizontally seen
dridge	Reinforcement height in ridge, vertically seen
dridgeh	Reinforcement height in ridge, horizontally seen
dslab	Reinforcement height in slab
dsr	Reinforcement height in transition zone ridge to slab
Ecm	Secans modulus of elasticity of concrete
EI0	Initial bending moment stiffness
EI0sr	Initial bending moment stiffness fictitious ridge
EIfslab	Ficititous bending moment stiffness slab
EIfsr	Ficititous bending moment stiffness fictitious ridge
Einf	Eventual bending moment stiffness
Es	Design value modulus of elasticity reinforcing steel
η_1	Coefficient representing the quality of concrete-reinforcement bond
η_2	Coefficient representing the diameter of the reinforcement
f	Frequency
fbd	Bond force
fcd	Design value compressive strength concrete
fck	Characteristic value cube compressive strength of concrete
fcmcube	Mean cube compressive strength of concrete
fctd	Design value of tensile strength of concrete
fcteff	Effective tensile strength of concrete
fctk	Characteristic value of tensile strength of concrete
fctm	Mean tensile strength of concrete
fctmfl	Mean flexural tensile strength of concrete
Feq	Equivalent point load
Fsh1	Horizontal support force
Fsh2	Horizontal support force
Fsv	Vertical support force
fyd	Design value of yield strength of reinforcing steel
fyk	Characteristic value of yield strength of reinforcing steel
G	Dead weight of concrete
g	Dead weight of balustrade
hceff	Effective height of hidden tensile member
hridge	Height of ridge including height of slab
hslab	Height of slab
Ic	Moment of inertia of concrete slab
Icsr	Moment of inertia of concrete in transition zone from ridge to slab

k	Spring stiffness single-mass-spring system
k1	Coefficient for predicting crack width describing quality of bond
k2	Coefficient for predicting crack width describing load type
k3	Coefficient for predicting crack width
k4	Coefficient for predicting crack width
kt	Coefficient for predicting crack width describing time of loading
lbreq	Requirent anchorage length
lrep	Representative length for determining maximum allowable deflection
lridge	Length of ridge in sideview
lslab	Length of slab in sideview
ltot	Total cantilevering length of balcony
Mcrs	Cracking moment in slab
Mcrsr	Cracking moment transition zone slab to ridge
Medcross	Bending moment resistance slab cross direction
Medr	Bending moment resistance ridge
Meds	Bending moment resistance slab
Mfcr	Bending moment in ridge, frequent load combination
Mfcs	Bending moment in slab, frequent load combination
minstraindifference	Minimum strain difference between concrete and reinforcement
Mkcross	Bending moment in slab in cross direction, characteristic load combination
Mkr	Bending moment in ridge, characteristic load combination
Mks	Bending moment in slab, characteristic load combination
Mlin	Bending moment limit resulting in linear stress distribution over height
Mqbr	Bending moment in ridge, quasi-static load combination
Mqbs	Bending moment in slab, quasi-static load combination
Mrd	Bending moment resistance
Mrdcross	Bending moment resistance slab cross direction
Mrdr	Bending moment resistance ridge
Mrdsr	Bending moment resistance transition zone ridge to slab
$\mu 2$	Loading ratio
$\mu 3$	Loading ratio
n	Number of bars
n1	Number of bars
n2	Number of bars
Ns	Total normal force in reinforcement
nshear	Number of sections in shear reinforcement
Nsr	Total normal force in reinforcement in ridge
Nsstm	Maximum normal force in reinforcement following from strut-and-tie model
⌀bottom	Diameter longitudinal reinforcement in bottom of slab
⌀bottomcross	Diameter cross reinforcement in bottom of slab
⌀shear	Diameter shear reinforcement in ridge
⌀topbig	Diameter main reinforcement in top of ridge/slab
⌀topcross	Diameter cross reinforcement in top of slab
⌀topsmall	Diameter longitudinal reinforcement in top of slab
Q	Point load
sreb	Average spacing top reinforcement in ridge
srebbottom	Average spacing longitudinal reinforcement bottom slab
srebbottomcross	Average spacing cross reinforcement bottom slab
srebshear	Average spacing shear reinforcement stirrups
srebtopcross	Average spacing cross reinforcement in top slab
srebtopsmall	Average spacing small longitudinal reinforcement in top slab
srmax	Maximum crack spacing
straindifference	Strain difference between concrete and reinforcement
supdist	Vertical distance between horizontal supports
tausr	Shear stress

Ved	Shear force, fundamental load combination
Vedr	Shear force in slab, fundamental load combination
Veds	Shear force in ridge, fundamental load combination
Vfcr	Shear force in ridge, frequent load combination
Vfcs	Shear force in slab, frequent load combination
Vkr	Shear force in ridge, characteristic load combination
Vks	Shear force in slab, characteristic load combination
Vqbr	Shear force in ridge, quasi-static load combination
Vqbs	Shear force in slab, quasi-static load combination
Vrdc	Shear force resistance
wk	Value of crack width prediction
wmax	Maximum allowable crack width
wr	Maximum deflection of ridge
ws	Maximum deflection of slab
xeinfslab	Height of compressive zone in slab at t=inf
xeinfsr	Height of compressive zone in fictitious cross section at t=inf
xer	Height of compressive zone in ridge
xeslab	Height of compressive zone in slab at t=inf
xesr	Height of compressive zone in fictitious cross section
xu	Ultimate height of compression zone in slab
xucross	Ultimate height of compression zone in cross direction of slab
xur	Ultimate height of compression zone in ridge
xusr	Ultimate height of compression zone in transition zone ridge to slab
z	Internal lever arm
zcross	Internal lever arm in cross direction of slab
zr	Internal lever arm of ridge
zrconsole	Internal lever arm of ridge according to console analogy
zslab	Internal lever arm slab
zsr	Internal lever arm of fictitious cross section in transition zone from ridge to slab
αe	Ratio between Es and Ec at t=0
αeinf	Ratio between Es and Ec at t=inf
γc	Material factor concrete
γs	Material factor steel
ρl	Longitudinal reinforcement ratio in slab
ρl,cross	Reinforcement ratio in cross direction of slab
ρmax	Maximum allowable reinforcement ratio
ρl,r	Longitudinal reinforcement ratio in ridge, horizontally seen
ρlridge	Reinforcement ratio in ridge
ρlsr	Longitudinal reinforcement ratio in transition zone ridge to slab
ρpeff	Reinforcement ratio in hidden tensile member
ρw	Shear reinforcement ratio in ridge
ρwmin	Minimum shear reinforcement ratio in ridge
σs	Steel stress
σsr	Steel stress at the onset of cracking
ωn	First natural eigen frequency